Cellular Auxin Transport and its Regulation in *Arabidopsis*

Dissertation
zur
Erlangung der naturwissenschaftlichen Doktorwürde
(Dr. sc. nat.)

vorgelegt der
Mathematisch-naturwissenschaftlichen Fakultät
der
Universität Zürich

von
Aurélien Bailly
aus
Frankreich

Promotionskomitee
Prof. Dr. Enrico Martinoia (vorsitz)
Dr. Markus Geisler (Leitung der Dissertation)
Prof. Dr. Ueli Grossniklaus
Dr. Jean-Denis Faure

Zürich, 2008

ZUSAMMENFASSUNG

Auxin (Altgriechisch für wachsen) ist ein essentielles und das wahrscheinlich best untersuchteste Pflanzenhormon. Lokale Auxinverteilungsmuster, Auxingradienten genannt, determinieren die gesamte Pflanzenentwicklung, ihre Physiologie und ihre Erhaltung. Man nimmt an, dass diese Gradienten direkt durch fein regulierte, integrale Membrantransporter aufgebaut werden, die spezifisch für Auxin sind. Die Analyse zellulären Auxintransports wurde wesentlich durch chemische Inhibitoren, so genannte Auxintransport-Inhibitoren (ATI) erleichtert, die die Identifizierung von Kandidaten des Auxintransport-Netzwerkes erlaubte. Die ersten Proteine, für die eine Beteiligung an diesem Prozess belegt werden konnte, gehören zur pflanzenspezifischen Familie der AUX1/LIKE AUX1 (LAX)- und PIN-formed (PIN)-Familie. AUX1 und PIN1 zeigen eine gespiegelt asymmetrische zelluläre Verteilung auf der Plasmamembran auxinführenden Gewebes, das in Übereinstimmung mit dem ursprünglich prognostizierten Chemiosmotischen Modell des Auxintransports steht. Obwohl AUX1 and PIN-Proteine gezeigt wurden, am zellulären Auxininflux und –efflux teilzuhaben, blieb es lange unklar, ob sie direkt in der Lage sind, das Phytohormon Auxin zu transportieren. Es wurde spekuliert, dass PIN efflux facilitators für eine volle Funktionalität interagierende Proteine als Partner benötigen. Im Rahmen dieser Arbeit haben wir erstmalig einen ER-gebundenen Vertreter der PINs, PIN5, charakterisiert, der anscheinend für die zelluläre Auxin Homöostase verantwortlich ist. Dies weisst darauf hin, dass die Funktionalität der PIN-Proteine im Kontext Auxin-regulierter Prozesse sich nicht auf den polaren Auxintransport (PAT) beschränkt.

In dieser Arbeit haben wir die Beteiligung einer dritten Gruppe von Membranproteinen am Auxintransport nachgewiesen. Es gelang uns, ABCB1 (PGP1) und ABCB19 PGP19/MDR1), Mitglieder der Subfamilie der ABCB/Multidrug resistance (MDR)-/P-Glycoproteine (PGP) der ubiquitären ATP-Binding Cassette (ABC) Transporter Superfamilie, als primär aktive Auxinexporter zu etablieren.

Der ABCB1, 19-vermittelte Auxintransport soll zumindest teilweise durch Protein-Proteininteraktion reguliert werden. Obwohl kürzlich PIN-ABCB Interaktionen belegt wurden, bleibt deren Relevanz für den PAT unklar. ABCB- und PIN-Auxineffluxsysteme scheinen in spezifischen Geweben synergistisch zu kooperieren, wo sie einen funktionellen Auxinefflux-Komplex bilden.

Interessanterweise konnte in Pionierarbeiten gezeigt werden, dass Plasmamembran-extrakte den synthetischen ATI, 1-Naphtylphtalamsäure (NPA), binden. Dies führte zu dem Konzept, dass die Auxinefflux-Maschinerie ein NPA-sensitiver Multiprotein-Komplex sei. Gemäss dieser Hypothese besteht dieser NBP (NPA-bindendes Protein)-Komplex aus mindestens zwei Komponenten: dem Membran-integralen Auxincarrier und einer membranassoziierten,

regulatorischen Untereinheit. Unsere phänotypische und biochemische Analyse legte nahe, dass das membranverankerte, Multidomän- Immunophilin FKBP42, TWISTED DWARF1 (TWD1), als positiver Regulator des NPA-sensitiven ABCB1, 19-vermittelten Auxintransports fungiert. Darüber hinaus konnten wir zeigen, dass der ABCB1-TWD1 Komplex ein relevantes Ziel synthetischer und natürlicher Inhibitoren des Auxintransportes ist. Des Weiteren konnten wir durch Biolumineszenz Resonanzenergie Transfer (BRET)-Experimente demonstrieren, dass TWD1 für den inhibitorischen Effekt der ATIs auf ABCB1 verantwortlich ist, indem es wahrscheinlich den katalytischen Zyklus des Transporters kontrolliert.

Unter Hilfenahme eines strukturbasierenden Vergleichs pflanzlicher und tierischer ABCB1 Orthologe war es uns möglich, pflanzenspezifische Aminosäurecluster in so genannten intrazellulären Loops (ICL) der Proteine zu identifizieren; von diesen Regionen nimmt man an, dass sie die ATP-Bindungsenergie zur Substratbindung/-freisetzung übertragen. Diese Regionen scheinen daher eine Auxin-spezifische Bindungsstelle in pflanzlichen ABCB1 Orthologen zu bilden.

Die hohe Substratspezifität pflanzlicher ABCB-Proteine gegenüber Auxin steht im Gegensatz zu der eines phylogenetisch lose verwandten Transporters, ABCG37/PDR9/PIS1, für den im Rahmen dieser Arbeit gezeigt wurde, dass er ein breites Spektrum auxinogener Verbindungen und ATIs transportiert. Die Tatsache, dass die Substratspezifität pflanzlicher ABCB-Proteine in heterologen Expressionssystemen abnimmt, legt nahe, dass die Substratspezifität von ABCB-Proteinen auf pflanzenspezifischen Partnerproteinen basiert. Das Verständnis der molekularen Zusammenhänge dieser Regulation ist daher die Basis um die Entwicklung von Pflanzen zu begreifen.

Neben dem nahe liegenden agronomischen Potential, dürfte der Transfer dieser Erkenntnisse auch direkt dem menschlichen Wohle dienen. In der Tat ist es so, dass die promiskuitive Substratselektivität humaner ABCB1-Orthologe in Tumorzellen die Grundlage für Multidrug Resistance gegenüber Anti-Krebs Therapeutika bildet, was final zu einem Scheitern der Chemotherapie führt.

SUMMARY

Auxin (*to grow* in ancient Greek) is the most important and scientifically investigated hormone in the plant kingdom. Localised auxin distribution patterns, termed *auxin gradients*, are determinant for virtually all plant development, physiology and maintenance. The establishment of these gradients is thought to be directionally driven by finely regulated integral membrane transporters that are auxin-specific. In an effort to analyze cellular auxin movements, the use of chemical inhibitors, referred to as *auxin transport inhibitors (ATIs)* facilitated the identification of putative components of the auxin transport network. The first proteins demonstrated to be involved in this process belong to the plant-specific AUX1/LIKE AUX1(LAX) and PIN protein families. AUX1 and PIN1 proteins exhibit a mirrored asymmetric cellular distribution at the plasma membrane of auxin-conducting cells, consistent with the early proposed *chemiosmotic model* for auxin transport. Although AUX1 and PINs have been demonstrated to participate in cellular auxin influx and efflux respectively, their ability to transport the phytohormone remained uncertain and it was speculated that PIN auxin efflux facilitators require interacting protein partners for complete functionality. We have characterized the novel endoplasmic reticulum-localized PIN5 controlling auxin homeostasis, suggesting that the involvement of PIN proteins in auxin-related processes may not be limited to polar auxin transport (PAT).

In this work, we demonstrated that a third group of membrane proteins is involved in auxin transport. We have characterized ABCB1 and ABCB19, members of the ubiquitous ATP-binding cassette (ABC), belonging to a subset of ABCB/Multidrug resistance (MDR)/P-glycoprotein (PGP) transporter superfamily as primary-active auxin efflux transporters. Moreover, ABCB1/ABCB19-mediated auxin efflux was suggested to be regulated in part *via* protein-protein interactions. Although PIN-ABCB interactions have recently been elucidated, their significance in PAT is unclear. ABCB- and PIN-auxin efflux systems might synergistically cooperate in specific tissues, thus forming a functional auxin-efflux complex.

Interestingly, pioneer work suggested the auxin-efflux machinery to be an ATI-sensitive multi-component protein complex for its ability to bind the synthetic ATI NPA (1-N-naphtylphtalamic acid) in plasma membrane extracts. In this hypothesis the NBP (NPA-binding protein) complex comprises at least two components: the integral membrane auxin carrier and a membrane-attached regulatory subunit. We inferred from phenotypic and biochemical evidence that the membrane-anchored multi-domain immunophilin-like FKBP42/TWISTED DWARF1(TWD1) acts as a positive regulator of the NPA-sensitive ABCB1/19-driven auxin transport. We demonstrated that the TWD1-ABCB1 complex is a functional target of synthetic and natural ATI inhibition of auxin efflux. Moreover,

bioluminescent resonance energy transfer (BRET) assays revealed that TWD1 mediates the ATI inhibitory effects to ABCB1 transport activity, probably by controlling the catalytic cycle of the transporter.

The high degree of plant ABCB substrate-specificity towards auxin, observed from structure-based comparison of plant and animal ABCB1 orthologs, is in contrast to the non-specific auxinic compounds transport activity of the genetically distant ABCG37/PDR9/PIS1 protein analyzed in this work. As *Arabidopsis* ABCB1 auxin selectivity decreases in heterologous expression systems and in the absence of TWD1, one might expect that ABCB1 auxin-specificity requires plant-specific partner-proteins. TWD1- and PIN-ABCB1 interactions may therefore influence ABCB1 substrate-specificity towards auxin, thus underlining the complexities of auxin-transport regulation. Understanding the molecular aspects of this regulation is therefore an essential step to comprehend plant development.

Beyond the evident agronomical applications, transfer of this knowledge might be beneficial for human health. Indeed, the promiscuous substrate-selectivity of the human ABCB1 ortholog confers multi-drug resistance to tumor cells against anti-cancer therapeuticals, thus leading to the failure of chemotherapy.

Table of Contents

"Does one need to be a gambler, and welcome chance as an opportunity for discoveries to be a good scientist?

"Yes! It is even the approach that theoretically defines science. To be a good scientist, one needs to build hypotheses. Then one gambles: one bets that the world functions in a certain way. Either one loses or wins. Every scientific approach should be a game […] where one accepts the risk to be mistaken. But even in the scientific community, when the reassuring effect sets in, the one that consists in establishing a school of thinking, or to enroll in one of them, then science turns rapidly into ideology. Until the very moment when this ideology becomes delirious, cut off from sensible reality, and then collapses. Indeed, the history of scientific ideas is a graveyard of theories."

Boris Cyrulnik
(Science&Vie n°1079)

Introduction

The phytohormone auxin is essential for plant development and viability. As a consequence, auxin-related biological events have been extensively studied for over a century. Nowadays, the cellular and molecular mechanisms involved in the hormone signaling pathway are better understood, and the precise cellular distribution of auxin gradients seems to be the prevalent signal for virtually all developmental processes. Beside auxin synthesis and homeostasis, the specific transport of auxin is a key component of the hormonal pathway. Therefore, the proteins participating in this transport or in its control are of prime interest for comprehending auxin-related plant physiology. The chemiosmotic model for polar auxin transport, formulated in the 1970s, postulates the existence of asymmetrically-distributed membrane carrier-proteins to drive auxin transport in a cell-to-cell manner. Recent reports propose that a subset of ABC-transporters could be implicated in the primary-active efflux of the hormone. Furthermore, phenotypic and biochemical evidences suggest that ABC-mediated cellular auxin-efflux could be under the control of plant immunophilins. The present work will attempt to tackle these issues at the cellular and molecular levels.

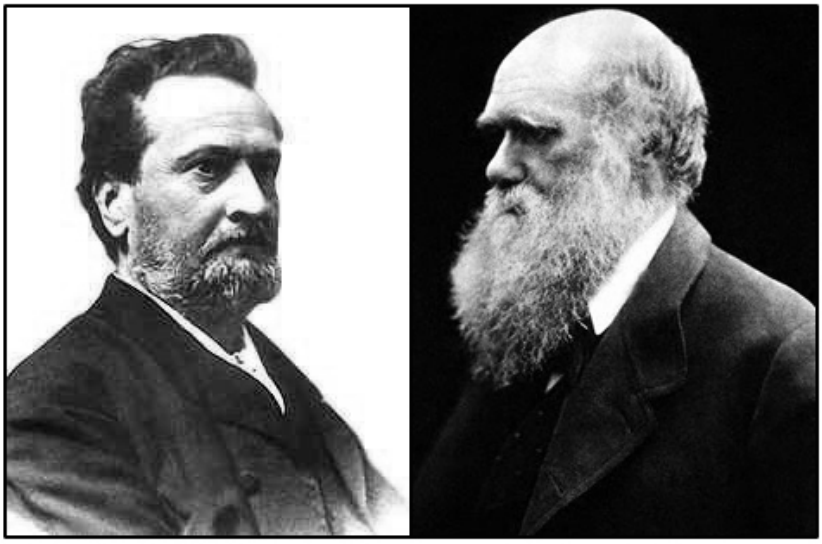

Julius von Sachs
(1832-1897)

Charles Darwin
(1809-1882)

Auxin: history and general concepts

One of the major improvements life acquired through evolution is communication. Without accurate mechanisms of communication between cells, tissues and organs, multicellular and social organisms would not exist. The shape, the function, the regulation and the coordination of the different parts of such life forms are only based on the ability to send and receive information remotely.

In contrast to animals, higher plants do not possess nervous systems. These electric networks are rapid and efficient means of communication but are greedy for energy. On the other hand, plants are sessile organisms with restricted access to resources; therefore, evolution favored chemical signals to coordinate and regulate metabolism, growth and morphogenesis from one tissue or organ to another.

This concept emerged in the XIX century, when Julius von Sachs, before Charles Darwin, suggested that the formation and growth of different plant organs are under the control of mobile chemical messengers (Sachs, 1865). From then until today, plant biology benefited from the discoveries and concepts initiated in animal biology. Animals synthesize and secrete chemicals that travel through the bloodstream from one organ to a distant and specific target to achieve important developmental and physiological effects. Such active signaling molecules are termed *hormones*. In analogy, plants produce a set of chemically distinct *phytohormones*, principally dissimilar to animal ones: auxins, cytokinins, ethylene, gibberellins, brassinosteroids, abscisic and jasmonic acids. The list of discovered signaling molecules in plants has not been closed yet, and their diversity and interaction reflect the need for plants to establish subtle mechanisms of communication (see Box 1).

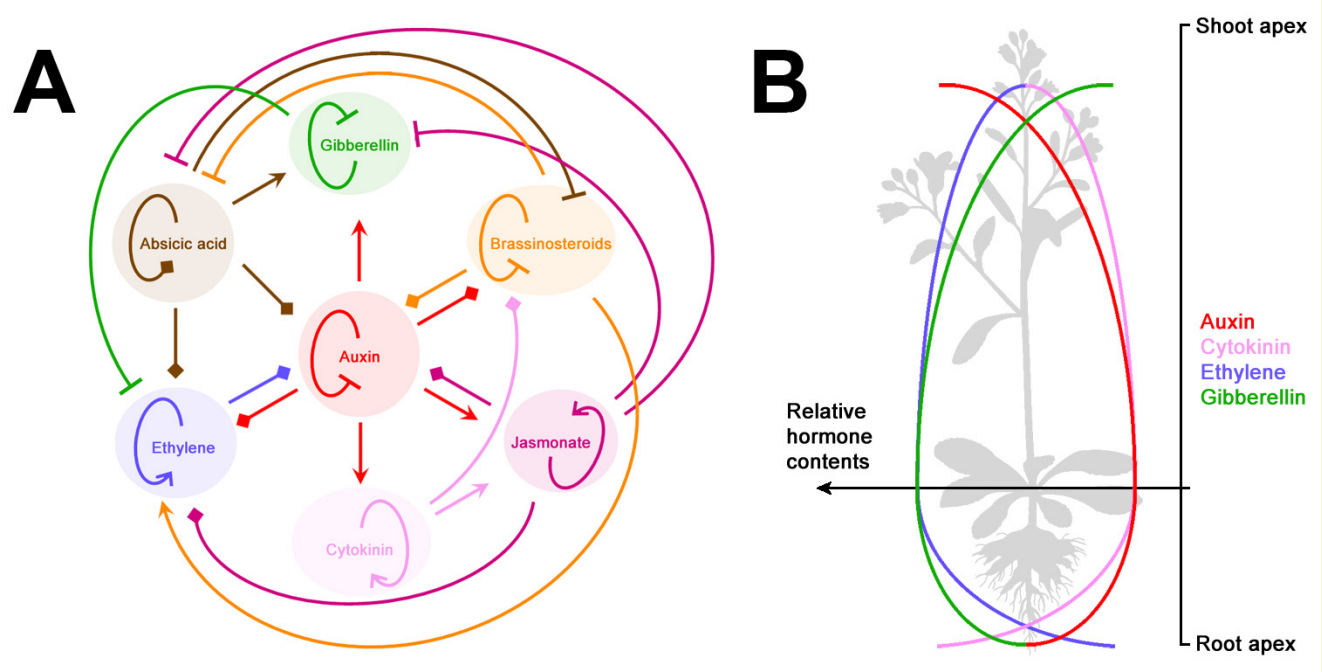

BOX 1. **Genes involved in hormone metabolism are highly interconnected**

A, Genes assigned to hormone biosynthetic pathways by GO annotation were identified within lists of hormone-responsive genes. Lines with arrowheads represent upregulation of hormone biosynthetic genes or downregulation of genes involved in hormone inactivation. Blocked arrows represent downregulation of genes involved in hormone biosynthesis or upregulation of genes involved in inactivation of a hormone. Diamond arrowheads indicate changes in gene expression with ambiguous outcomes (i.e., genes affected include those linked to both increased and decreased hormone levels). (taken and adapted from Nemhauser *et al.*, 2006).
B, This genetic control directs plant physiology, where the balance between the different phytohormones levels in tissues determines the fate of cells and organs.

Auxin was the first growth hormone to be discovered in plants and has rapidly been identified as an indispensable molecule for plant life. Indeed, auxin shares with cytokinins the particularity to be required continuously through all the plant's life cycle, whereas other hormones are only requested during specific regulatory or developmental processes. It is then not surprising that most of the early studies aiming to characterize plant growth physiology focused on auxin action and perception.

Historically, the first demonstration of the existence of a growth-promoting chemical in plant tissues was established in 1926, five decades after the outstanding experiments carried out by Charles and Francis Darwin placing the synthesis of auxin in the aerial tip of the growing plant (Darwin and Darwin, 1880; Went, 1926). Frits Went, unlike generations of pioneer scientists before him, did no try to extract the compound by just grinding the tissues, but rather let it diffuse out of an excised coleoptile tip into a block of gelatin (Went, 1926). The elegance of this experiment is more apparent nowadays, since we understand that grinded-tissues extracts freed the desired compound, but as well internal inhibitors, resulting in an inactive extract on cellular growth.

In the decade following Went's pioneer experiments, the growth substance was finally identified as indole-3-acetic acid (IAA), and numerous related analogs were then synthesized and tested for their agricultural potential. Some of these compounds are still in use in modern agriculture, like 2,4-D (2,4-dichlorophenoxyacetic acid) and NAA (1-naphthalene acetic acid) and favored for their stability. Even if several other auxins were isolated later in higher

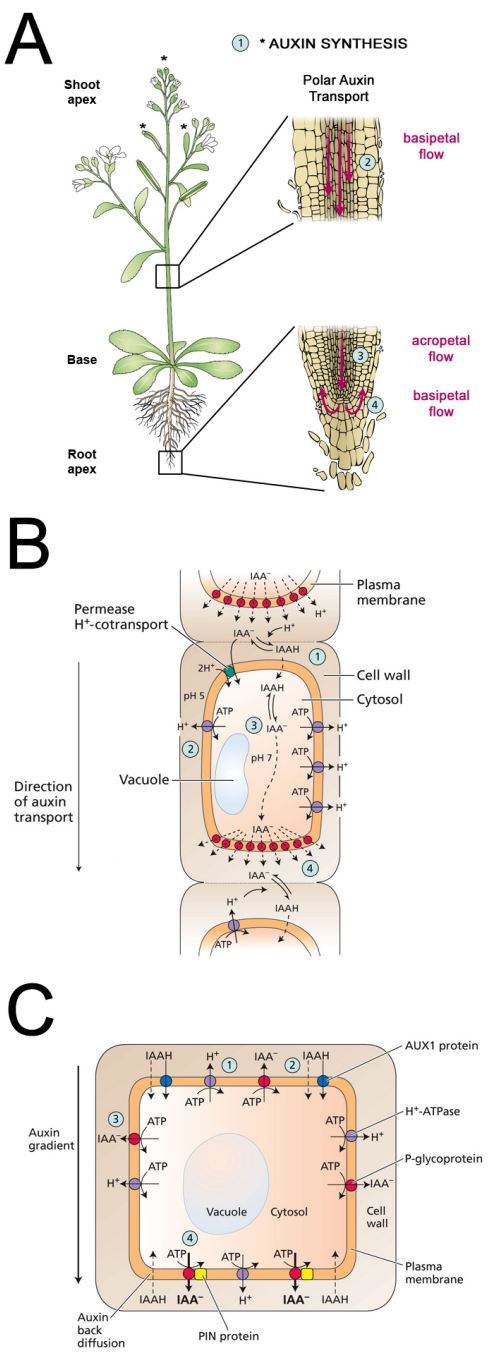

FIGURE 1. **Mechanisms of polar auxin transport**

***A*, Polar auxin fluxes**
Movement of auxin basipetally (from the apex toward the base) through the center of shoots and roots occurs by an iterated movement through cells - inward at the apical membrane and outward at the basal membrane. After auxin reaches the root tip, it moves acropetally (from the base toward the apex) in the cortical tissues.

***B*, A simplified chemiosmotic model of polar auxin transport**
Shown here is one elongated cell in a column of auxin-transporting cells (From Jacobs and Gilbert, 1983). (1) IAA enters the cell either passively in the undissociated form (IAAH) or by secondary active co-transport in the anionic form (IAA^-). (2) The cell wall is maintained at an acidic pH by the activity of the plasma membrane H^+-ATPase. (3) In the cytosol, wich has a neutral pH, the anionic form (IAA^-) predominates. (4) The anions exit the cell via auxin anion efflux carriers, concentrated at the basal ends of each cell in the longitudinal pathway.

***C*, Model for polar auxin transport in small meristematic cells**
In smaller cells near the meristems, because of high surface to volume ratio, back-diffusion of IAA into cells requires an additional energy-dependant efflux mechanism. (1) The plasma membrane H^+-ATPase (purple) pumps protons into the apoplast. The apoplastic acidity affects the rate of auxin transport by altering the ratio of IAAH and IAA^- present in the apoplast. (2) IAA can enter the cell via proton symporters such as AUX1 (dashed arrows). Once inside the cytosol, IAA is an anion, and may only exit the cell via active transport. (3) P-glycoproteins (red) are localized on the plasma membrane and may drive active (ATP-dependent) auxin efflux. (4) PIN proteins (yellow) are described as auxin efflux carrier protein and may associate with PGP proteins to overcome the effects of IAA back-diffusion.
(Adapted from Jones (1998) and Taiz and Zeiger, chapter 19 (2006))

plants, IAA is the most abundant and physiologically relevant. Therefore, the term *auxins* refers today to natural and synthetic substances which mimic the physiological activity of IAA.

Auxin biosynthesis, homeostasis and metabolism

Even though virtually all plant tissues seem to be capable of generating low levels of IAA, shoot apical meristems, young leaves and developing fruits and seeds are the primary sites of IAA synthesis (Ljung *et al.*, 2001; Ljung *et al.*, 2002). (Figure 1A and Box 1) IAA is structurally related to the amino acid tryptophan. The latter appears to be an evident precursor for IAA production, but different pathways of biosynthesis exist independently from tryptophan (Delker *et al.*, 2008). In the same extent, IAA is degraded in many ways and IAA breakdown products are supposed to be inactive (Bartel, 1997). A narrow description of these

mechanisms is not relevant for the understanding of the present work, but both IAA synthesis and degradation participate to the steady-state levels of auxin in plant (Taiz and Zeiger, 2006).

The biologically active form of the hormone is described as *free* IAA, since IAA conjugates are considered hormonally inactive (Ljung *et al.*, 2002; Woodward and Bartel, 2005). Revealing again the fine hormonal control within plants, most IAA is found in a covalently bound form - the highest free IAA contents are located in synthetic and target tissues (Ljung *et al.*, 2002). Auxin can be conjugated to a large panel of substances ranging from low molecular weight sugars or amino acids, to high molecular weight glucans, peptides or glycoproteins (Cohen and Bandurski, 1982; Seidel *et al.*, 2006; Woodward and Bartel, 2005). Conjugation of auxin is a reversible mechanism and the metabolism of conjugated IAA is a key factor in the time- and space-regulation of free auxin levels, protection against photo- or oxidative-degradation and storage (Figure 2, Woodward

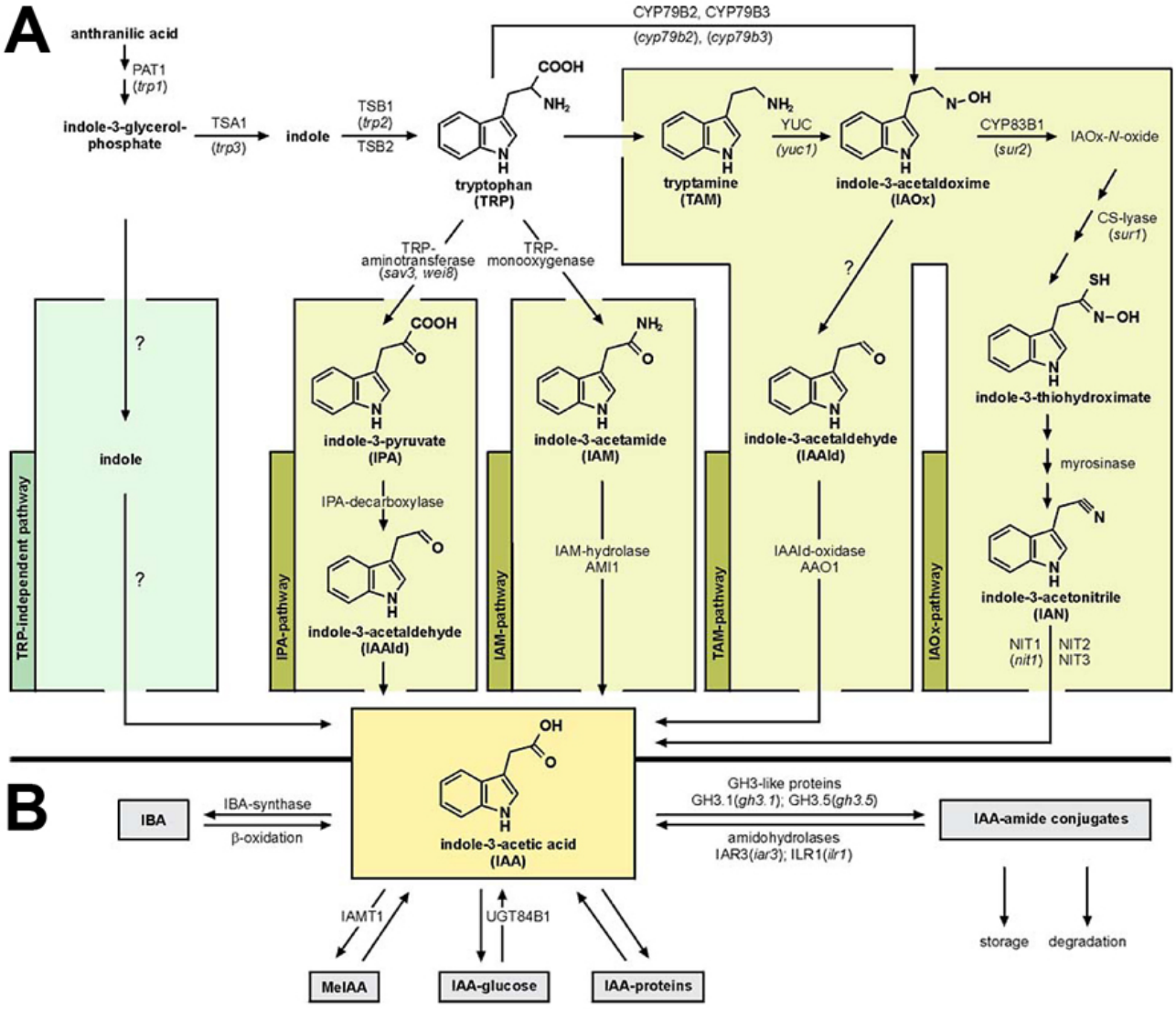

FIGURE 2. **Auxin synthesis and conjugation processes**

***A*, Tryptophan-dependent and independent auxin biosynthesis pathways**
A more comprehensive description of these mechanisms is given in Taiz and Zeiger (2006)
***B*, Auxin-conjugation mechanisms**
Both reversible (storage) and irreversible (degradation) conjugation events participate in the steady states of available free auxin in the cell.
Adapted from Bartel (1997)

and Bartel, 2005). For example, seeds and storage organs such as cotyledons contain large amounts of covalently bound auxin which might consequently be mobilized upon hydrolysis or ß-oxidation when needed (Woodward and Bartel, 2005).

Cellular IAA distribution is for the most part regulated by pH. As we will see later on, the anionic form of auxin, IAA^-, does not cross the lipid bilayers while the protonated form IAAH can diffuse through. As a result, auxin tends to accumulate in the more alkaline compartments of the cell. 1/3 of IAA is found in compartments such as chloroplasts (Ljung *et al.*, 2002; Sitbon *et al.*, 1993), while the rest is in the cytosol. Cytosolic IAA is metabolized by degradation or conjugation, whereas, in the chloroplast, IAA is protected from these mechanisms but stays in equilibrium with the amount of cytosolic IAA (Sitbon *et al.*, 1993).

Whereas auxin metabolism has been widely documented, the hormone homeostasis and the implication of the different cellular compartments in its mechanisms need to be further investigated. They indeed, directly or indirectly, are components of a broader process demonstrated to be crucial for plant development: the directional transport of the hormone.

Auxin transport

Since the shoot apex is the most important source of auxin in the plant, directional transport is thought to be required for the formation and maintenance of local auxin distribution patterns from the shoot tip to the root tip, called *auxin gradients*. These gradients determine, through cell division and elongation, a variety of developmental processes such as apical dominance, stem elongation, tropic responses, leaf and flower development, lateral root formation, wound healing, and leaf senescence (Davies, 2004; Teale *et al.*, 2006; Vieten *et al.*, 2007). In this respect, the hormone could be defined as a *morphogen*. Morphogen gradients found in other organisms are principally established by diffusion; but in plants, spatial gradients of auxin in tissues are maintained by an active cellular process termed *polar auxin transport* (PAT; Goldsmith *et al.*, 1981; Lomax *et al.*, 1985; Lomax *et al.*, 1995).

From the very first mitotic division of the zygote, gradients of IAA guide the patterning of the embryo into the parts that will become the organs of the plant and the overall apex-base structural polarity of plants directly derives from the polarity of auxin transport (Morris, 2004; Taiz and Zeiger, 2006). Indeed, auxin is the only phytohormone transported unidirectionally from the above-ground apical regions to the basal parts (nomenclature defines the shoot and root apices as *apical* and the root-shoot junction as *basal*, see Figure 1A). Nevertheless, the sole presence of auxin is not sufficient for the establishment of the shoot-root axis. In fact, the entire development virtually depends on the directed flow of auxin *via* PAT. As a simple illustration, roots form at the base because root differentiation is stimulated by auxin accumulation due to *acropetal* (i.e. towards the apex) transport, while shoots tend to form at the aerial apex where the auxin concentration is lowest.

Two distinct types of PAT can be recognized: a long-distance transport, down the whole plant body, and a short-distance transport that drives the hormone to definite places within specific tissues. In general, the major polar stream of auxin occurs from apical tissues towards the base of the plant and follows in the direction of the root tip (Kepinski and Leyser, 2005; Kramer and Bennett, 2006; Marchant *et al.*, 1999). The principal site of basipetal polar auxin transport in stems, leaves and roots is the vascular parenchyma tissue, most likely the xylem (Palme and

Galweiler, 1999). In vascular parenchyma, the overall direction of auxin transport in the plant is downward, in direction of the root tip. To summarize, auxin is transported basipetally in the shoot and continues *acropetally* (i.e. towards the root tip), mainly through the vascular tissues, in the root (Figure 1A). Most of the auxin that reaches the root tip is then translocated *via* the phloem. Auxin translocated in the phloem sieve tubes contributes to transport from shoot tissues to the growing root tip.

Basipetal auxin transport from the apex occurs in roots as well, in the epidermal and cortical tissues, and plays a central role in gravitropism. Once auxin reaches the root tip, a part of it is redirected back upwards (basipetally) through the root epidermis into the root elongation zone (Rashotte *et al.*, 2000) where it can be recycled back into the vascular stream (Figure 3, Blilou *et al.*, 2005)). As an increase in auxin concentration will inhibit cell expansion, the redistribution of auxin in the root initiates differential growth in the elongation zone resulting in root curvature.

In meristematic and differentiating tissues, such as the shoot and root apical meristems and during lateral organ formation, a short distance PAT is required. This short distance PAT in meristematic tissues is decisive for many auxin-mediated developmental processes and therefore needs a permanent fine-tuning to control organogenesis and various physiological events (Reinhardt *et al.*, 2003).

To achieve this vectorial movement, IAA is transported in a cell-to-cell mechanism. The hormone exits the cell through the plasma membrane, circulates across the compound middle lamella, and enters the next cell through its plasma membrane. The loss of auxin from cells is termed *auxin efflux* while the entry of auxin into cells is called *auxin influx* or *uptake*.

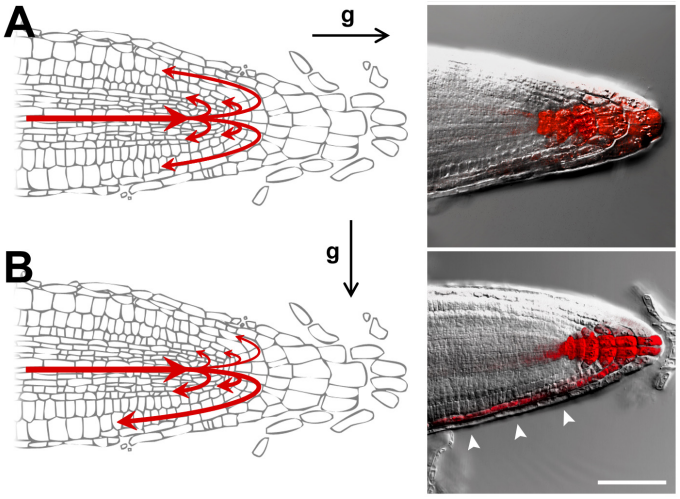

FIGURE 3. **Auxin gradients are laterally redirected in the root tip in response to gravity**

Expression of the DR5-GFP auxin-responsive reporter (in red) in *Arabidopsis* root tips is evenly distributed in vertically grown wild-type seedlings roots (***A***) whereas expression is elevated on the lower side of gravi-stimulated roots (***B***). Auxin accumulation inhibits cellular growth in these tissues while lower contents stimulate growth at the opposite side of the root, resulting in root bending. Arrowheads indicate elevated DR5-GFP expression in the lateral root cap. Scale bar 50µm

Polar transport is sensitive to oxygen deficiency and metabolic inhibitors (Cleland, 1967; Wilkins and Martin, 1967), suggesting that the overall mechanism requires metabolic energy. This allows a refined control of auxin distribution that could not be achieved solely *via* symplastic diffusion. As a matter of fact, PAT is faster than the rate of diffusion, but is slower than phloem translocation rates. The highest rates of PAT are detected in tissues neighboring the shoot and root apical meristems. Interestingly, the transport has be demonstrated to be specific for the active forms of auxin (either natural or synthetic ones) since no inactive analogs, IAA-conjugates, IAA metabolites or weak organic acids are polarly transported (Bartel, 1997; Bartel *et al.*, 2001; Campanella *et al.*, 1996). Such specificity would involve plasma membrane proteins able to recognize and specifically transport the active forms of the hormone.

The chemiosmotic model predicts auxin-transporting proteins

In accordance with chemiosmotic mechanisms of solute transport in cells, polar auxin transport has been described to result from two main proceedings: the proton motive force drives auxin into the cell, while the membrane potential makes auxin efflux possible (Mitchell and Moyle, 1967; Nobel, 1991; Taiz and Zeiger, 2006).

This hypothesis, termed *chemiosmotic model of polar auxin transport* (Jones, 1998; Raven, 1975; Rubery and Sheldrake, 1973; Rubery and Sheldrake, 1974), is based on the weak acid properties of IAA (pKa 4.75) (Figure 1B). Outside of the cell, the alkaline pH (about 5) displaces the acido-basic equilibrium in favor of the lipophilic, protonated form of IAA, IAAH, which is able to enter the cell by passive diffusion through the plasma membrane. When the hormone reaches the cytosol, the local neutral pH turns the molecule into its anionic form IAA^- and consequently prevents it from back-diffusion. This ion-trapping mechanism tends to concentrate IAA in the cytoplasm of the cell while lowering the extracellular concentration. The continuity of the hormone flow presupposes that IAA, following its chemical concentration gradient, must then exit the cell through dedicated anion carriers. The key characteristic of the chemiosmotic hypothesis is consequently these proteins' localization. According to the model, efflux carriers are expected to be found in the basal parts of conducting cells and this polarity would generate subsequently the polarity of auxin transport along the whole plant. These assumptions are often referred to as the *Cholodny-Went* (CW) hypothesis (Figure 1C, Cholodny, 1927; Evans, 1991; Went, 1926).

Although auxin uptake is pH dependent and can occur by IAAH passive diffusion through lipid bilayers, the fact that auxin influx is saturable (Marchant *et al.*, 1999) implies protein involvement. The amino acid permease-type carrier AUX1 (and homologous LIKE-AUX1/LAX genes) is likely to participate in the uptake of IAA (Bennett *et al.*, 1996; Marchant *et al.*, 1999; Pickett *et al.*, 1990). Indeed, *aux1* loss-of-function mutants display an agravitropic root phenotype that can be rescued by the membrane permeable 1-NAA, but not by hydrophilic IAA nor 2,4-D (Marchant *et al.*, 1999; Pickett *et al.*, 1990; Yamamoto and Yamamoto, 1998). Additionally, *aux1* roots show a reduced 2,4-D uptake (Marchant *et al.*, 1999). Initially localized in *Arabidopsis* roots (Bennett *et al.*, 1996), AUX1 displays a polar localization at the apical side of root apex cells (Figure 4A). In addition, *aux1* mutants show resistance towards cytotoxic concentrations of auxin, probably by preventing its entrance into the cell (Bennett *et al.*, 1996; Maher and Martindale, 1980). AUX1 may therefore greatly contribute to IAA accumulation in the cytosol by co-transporting two protons outside of the cell while letting IAA^- in (Bennett *et al.*, 1996; Parry *et al.*, 2001). Altogether, these data fit entirely to the chemiosmostic model hypothesis and define AUX1 as an apparent IAA influx carrier (Figure 1B and C).

Once IAA enters the cytosol, it accumulates in its anionic form. Consistent with the model, IAA^- is trapped in the cytosolic compartment and the sole way it can leave the cell is through an active transport. Although auxin influx represents the first step in its polar transport, the polarity of IAA transport is rather granted by the hormone efflux. PIN-FORMED (PIN) proteins belong to a family of 8 putative transmembrane carriers related to bacterial transporters and named after the unique pin-shaped loss-of-function phenotype of *pin1* mutants (Figure 4B; Galweiler *et al.*, 1998). PINs seem to be necessary for *Arabidopsis* auxin-related polarized organ development according to three main findings: 1. *pin1* morphological defects can be phenocopied by early NPA (1-N-naphthylphthalamic acid) applications on wild type seedlings (Galweiler

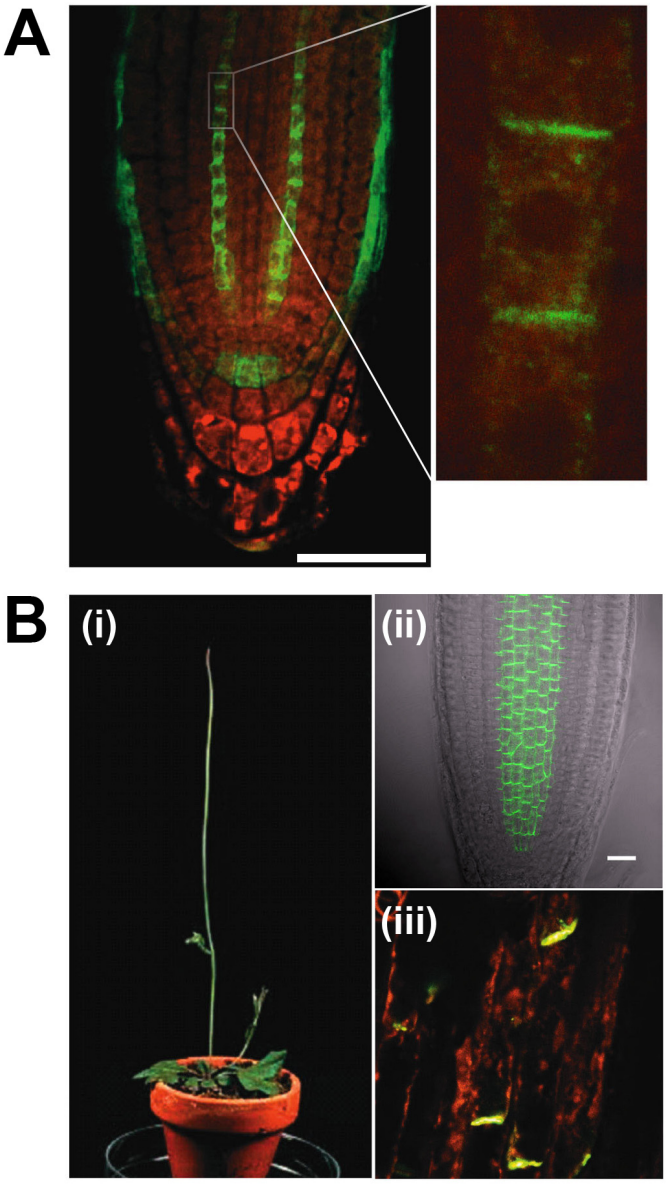

FIGURE 4. **AUX1 and PIN1 proteins cellular localizations are congruent with the chemiosmotic model for PAT**

A, immunolocalization of AUX1 in protophloem cells of the stele, in the columella and lateral root cap cells; asymmetric distribution of AUX1 in a file of protophloem cells (inset). (Swarup *et al*., 2001)

B, **(i)** needle-like phenotype of *pin1* loss-of-function mutants; **(ii)** immunolocalization of PIN1 in the vascular parenchyma; **(iii)** asymmetric distribution of PIN1 in vascular tissues. (Galweiler *et al*., 1998)

et al., 1998); 2. PIN1 basal localization on the plasma membrane is aligned with the polar auxin flow (Figure 4B; Friml and Palme, 2002; Galweiler *et al.*, 1998); 3. *pin2* (*eir1*/*agr1*) mutants are agravitropic (Maher and Martindale, 1980) and show a great sensitivity towards 1-NAA (Muller *et al.*, 1998). The sum of data accumulated also includes the relative homology and topology of PIN proteins with prokaryotic or eukaryotic amino acids transporters (Chen and Bush, 1997; Chen *et al.*, 1998; Luschnig *et al.*, 1998; Muller *et al.*, 1998), but attempts to demonstrate a direct transport activity have been unsuccessful until the starting point of this work. Despite the fact that PIN proteins seem to be essential to the auxin flow, it remains unclear whether they directly transport the hormone or rather participate in a presumed auxin efflux carrier complex – the term *efflux facilitators* is then favored to refer to these proteins (Figure 1C).

ABC transporters participate in auxin transport

The most remarkable feature of the auxin transport mechanism is its low energy cost to conduct the hormone from synthesis sites to remote targets. Indeed, according to the model, the maintenance of the membrane potential and the chemical gradients is sufficient to generate a polarized stream of auxin. Thus, the plasma membrane H^+-ATPase that maintains the apoplast at alkaline pH is a key player in PAT (Figure 1C). Nevertheless, this hypothesis is not satisfactory when auxin reaches the small cells of the apical meristems, where the polar transport of the hormone then requires an energy-dependent process to counter back-diffusion and drive the accurate signal.

ATP-binding cassette (ABC) transporters are members of one of the largest and most ancient protein superfamily present in all existing phyla from prokaryotes to humans (Martinoia *et al.*, 2002; Verrier *et al.*, 2008). However, plant genomes display

a remarkable feature: they possess an uncommonly large number of ABC transporters (*Arabidopsis thaliana* and *Oryza sativa* show over 120 putative ABC transporters (Jasinski *et al.*, 2003; Kolukisaoglu *et al.*, 2002; Martinoia *et al.*, 2002)) compared to the number (~50-60) found in other multicellular organisms of similar genome size (Figure 5; Jasinski *et al.*, 2003; Martinoia *et al.*, 2002; Sanchez-Fernandez *et al.*, 2001a; Sanchez-Fernandez *et al.*, 2001b; Theodoulou, 2000). It was proposed that the increase in ABC genes in plants would reflect the need for refined detoxification processes in these sessile organisms (Martinoia *et al.*, 2002; Theodoulou, 2000). In fact, these transmembrane proteins function in the energy-dependent transport of a wide variety of substrates across extra- and intracellular membranes, including metabolic products, sugars, vitamins, metal ions, peptides, lipids, sterols, and various drugs against their concentration gradients (Linton, 2007). ABC transporters require a minimum of four domains to achieve export or import: two transmembrane domains (TMDs), which probably define the ligand binding sites and provide specificity, and two nucleotide-binding domains (NBDs), that bind and hydrolyze ATP to release the translocation of the bound ligand through the TMDs. The consensus model of ABC transporters mechanism is then described as the coupling of two distinct cycles: an ATP catalytic cycle at the NBDs and a ligand transport cycle at the TMDs (Figure 6).

Recent evidences indicate that ABC transporters of the ABCB/p-glycoprotein/multidrug resistance-like (PGP/MDR) subclass may function in auxin transport. *Arabidopsis abcb1* and *19* mutants display phenotypic traits, such as epinastic cotyledons and first true leaves or curled and wrinkled adult rosette leaves, consistent with reduced levels of IAA transport (Figure 7; Noh *et al.*, 2001; Sidler *et al.*, 1998). This phenotype is even more pronounced in the *abcb1 abcb19* double mutant, added of reduced apical dominance, suggesting an overlapping function of the two proteins (Figure 7C; Noh *et al.*, 2001). Furthermore, polar auxin transport rates have been measured to be reduced in *abcb19*

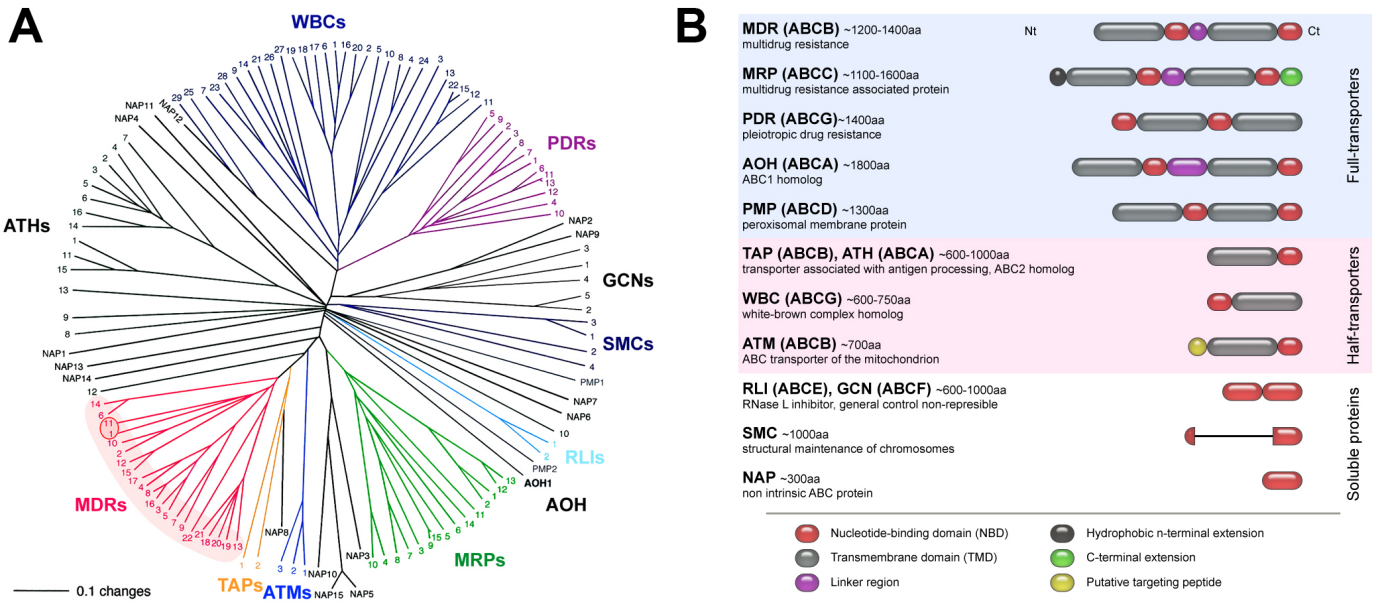

FIGURE 5. **ABC proteins in *Arabidopsis thaliana*: a large and diverse family**

A, Phylogeny of ABC proteins in the model plant *A. thaliana*. Relevant MDR proteins for this work, ABCB1/MDR11 and ABCB19/MDR1, are circled in red (adapted from Sanchez-Fernandez *et al.*, 2001)
B, Linear organization of the different typical ABC-protein domains in *Arabidopsis* ABC families. The actualized nomenclature (Verrier *et al.*, 2008) is indicated in brackets. (adapted from Sanchez-Fernandez *et al.*, 2001)

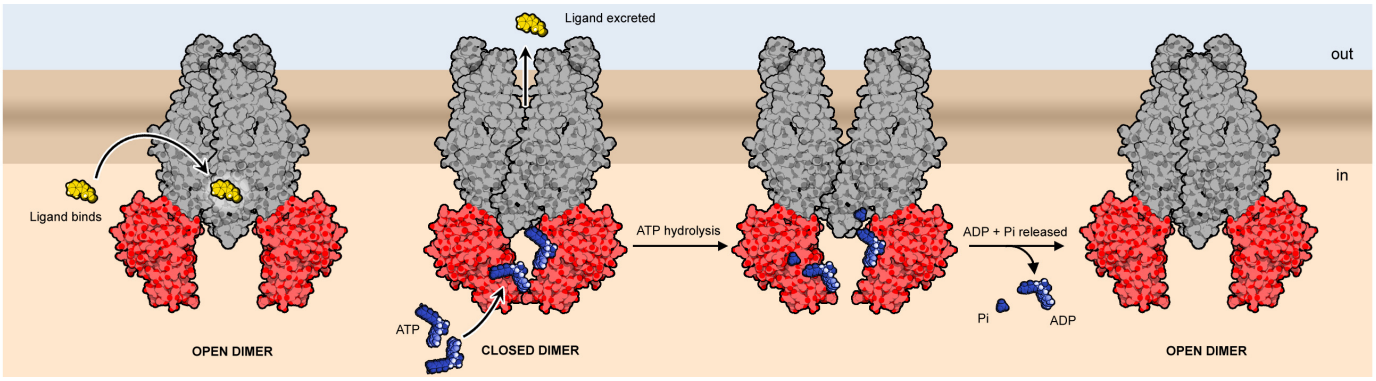

FIGURE 6. **Schematic model of the primary-energized ABC-transport mechanism**

In the established model for ABC-mediated transport, helices from each TMD (in grey) form the binding site(s) and the translocation pathway for the substrate (in yellow), while both NBDs (in red) transform the ATP-binding energy to perform a complete transport cycle (Hollenstein *et al.*, 2007). ABC proteins cycle between substrate- and ATP-bound or -release states to drive a broad range of compounds through biological membranes (after Linton *et al.*, 2007).

and *abcb1 abcb19* double mutant plants (Geisler *et al.*, 2003; Noh *et al.*, 2001). Interestingly, ABCB1 and 19 bind NPA (1-N-naphthylphthalamic acid), an efficient auxin transport inhibitor (ATI) (Geisler *et al.*, 2003; Murphy *et al.*, 2000; Murphy *et al.*, 2002; Noh *et al.*, 2001). NPA is known to bind to plasma membrane extracts, involving a putative membrane-attached receptor (Muday, 2000; Muday and Murphy, 2002), and this NPA-binding activity appears to be decreased in *abcb19* membrane extracts compared to wild type (Noh *et al.*, 2001). In support of these data, ABCB19 expressed in the heterologous yeast system exhibits specific NPA-binding activity (Noh *et al.*, 2001). In summary, ABCB1 and ABCB19 are likely to be implicated in polar auxin transport, whether by direct ATP-driven export of the hormone, or through interactions with auxin efflux carriers such as PINs. This is supported by the fact that some ABC transporters have been shown to cooperate with ion channels (Figure 1C; Kunzelmann and Schreiber, 1999; Noh *et al.*, 2001).

The involvement of ABCB-like proteins in IAA transport seems not to be restricted to *Arabidopsis* since other plant orthologs have been implicated in the hormone transport in the monocots maize (BRACHYTIC2/*Zm*ABCB1) and sorghum (DWARF3/*Sb*ABCB1) (Figure 7A and B; Multani *et al.*, 2003).

Regulation of auxin transport

Auxin transport, perception and signal transduction are vital to the proper growth and the maintenance of the plant and, therefore, the levels of expression and regulation of genes involved in these mechanisms are dependent on the tissues, the development stage or external stimuli. Although some auxin transporters may be genetically regulated by the hormone itself (Noh *et al.*, 2001; Peer *et al.*, 2004), the need for fast and accurate signal/responses processes would favor post-transcriptional mechanisms for auxin transport regulation.

The first attempts to understand and master auxin-related plant development arose together with modern agriculture. Owing to the evident agronomical interest, a broad spectrum of chemically distinct auxin transport inhibitors (ATIs) has been obtained during the last century. Amongst these compounds, NPA (1-N-naphthylphthalamic acid), CPD (2-carboxyphenyl-3-phenylpropane-1,3-dione) and TIBA (2,3,5-triiodobenzoic acid) efficiently and specifically block the hormone efflux, while NOA (1-naphthoxyacetic acid) has been shown to only prevent auxin influx (Parry *et al.*, 2001). In spite of this specificity, there

FIGURE 7. **Loss of ABCB1 function has severe developmental consequences in plants**

A* and *B, *abcb1* mutants in maize (*brachytic2*/*br2*) and sorghum (*dwarf3*/*dw3*) display compact stalks and subsequent auxin-defective phenotypes (Multani *et al.*, 2003).
C, in *Arabidopsis*, single *abcb1* and *abcb19* loss-of-function mutants display only mild growth phenotypes whereas *abcb1 abcb19* double mutant show radical auxin-related development defects. Mature plants grown in short-day conditions.

is no clear evidence regarding the mechanism by which these inhibitors block the auxin flow. NOA applications on *Arabidopsis* seedlings lead to a weak phenotype similar to *aux1* mutants without affecting auxin efflux (Parry *et al.*, 2001), whereas auxin efflux inhibitors (AEIs) applications show more profound effects on development, in accordance with the model (Hadfi *et al.*, 1998; Marchant *et al.*, 1999; Reinhardt *et al.*, 2000; Sabatini *et al.*, 1999). However, ATIs may be classified in, at least, two categories: 1. competitive inhibitors, such as TIBA, display weak auxin activities and may therefore act on a large set of auxin-related proteins; 2. non-competitive inhibitors, such as CPD and NPA, have been shown to rather bind to regulatory sites of distinct plasma membrane proteins (Petrasek *et al.*, 2003). Interestingly, AtABCB19 was shown to bind NPA (Murphy *et al.*, 2002; Noh *et al.*, 2001) and the typical ABCB plasma membrane localization observed in mammalian cells may correlate with the early described NPA-binding proteins (NBPs) in some tissues (Jacobs and Gilbert, 1983; Noh *et al.*, 2001). Until the beginning of this work, it remains unclear whether NBPs are integral proteins (Bernasconi *et al.*, 1996) or peripheral membrane proteins associated with the cytoskeleton (Cox and Muday, 1994). Nonetheless, NBPs were proposed to be a multi-component auxin transport complex and, for this reason, one can easily assume that both ABCB transporters may be physiologically relevant targets for synthetic AEIs action. In this scenario, given the fact that ABCBs are transmembrane proteins, the peripheral component of NBPs would await for identification.

There is increasing evidence that secondary metabolites, like flavonoids, act as endogenous ATIs (Brown *et al.*, 2001; Murphy *et al.*, 2000). Aglycone flavonoids are able to compete with NPA for unidentified plasma membrane proteins binding and *Arabidopsis* flavonoid-deficient mutants, *transparent testa* (*tt*), display increased auxin transport and auxin-dependent growth (Brown *et al.*, 2001; Buer and Muday, 2004; Peer *et al.*, 2001; Shirley *et al.*, 1995). Congruent with a role for ABCBs in IAA transport and regulation, flavonoids have been extensively characterized as mammalian ABCBs non-competitive inhibitors (Conseil *et al.*, 1998; Di Pietro *et al.*, 2002;

Hadjeri *et al.*, 2003; Lania-Pietrzak *et al.*, 2005). Moreover, their accumulation at the basal ends of polar cells, *in planta*, is in line with the localization of the presumed efflux carriers (Peer *et al.*, 2001).

Interestingly, flavonoids that compete for plasma membrane NPA binding-sites are as well described as protein kinases or protein phosphatases inhibitors (Bernasconi *et al.*, 1996; Garbers *et al.*, 1996). Phosphatase and kinase activities are key processes in gene expression, protein regulation and signal transduction, and may consequently represent a second level of auxin transport control. The characterization of two *Arabidopsis* mutants with defects in auxin transport, *rcn1* (roots curl in NPA, Deruere *et al.*, 1999) and *pid* (*pinoid*, Benjamins *et al.*, 2001), additionally supports this concept. Indeed, RCN1 encodes for the regulatory A subunit of the protein phosphatase 2A (PP2A-A, Deruere *et al.*, 1999; Garbers *et al.*, 1996) and *rcn1* loss-of-function mutants display enhanced sensitivity in NPA-mediated IAA efflux inhibition (Garbers *et al.*, 1996). The *pin1*-like phenotype of *pid* loss-of-function mutants revealed that PINOID, a serine/threonine protein kinase, controls PIN proteins polarity and thus the direction of the auxin flow (Benjamins *et al.*, 2001; Friml *et al.*, 2004).

The role of PINOID in PIN proteins trafficking is of prime interest as it describes a third mechanism likely to be involved in auxin signaling regulation. Most notably, overexpression of PINOID provokes a basal-to-apical relocalization of PIN proteins, resulting in severe developmental phenotypes that can be rescued by NPA treatments (Benjamins *et al.*, 2001). Indeed, ATIs have been earlier shown to interfere with the polar localization of the plasma membrane proteins to which they bind (Bernasconi *et al.*, 1996; Brunn *et al.*, 1992; Jacobs and Rubery, 1988; Petrasek *et al.*, 2003). In this extent, AUX1 and PIN proteins are liable to actin-dependent trafficking mechanisms that deliver membrane proteins to specific sites in order to achieve polar localization (Geldner *et al.*, 2001; Murphy *et al.*, 2005). In fact, PINs are thought to be constitutively cycled between the plasma membrane and endosomal compartments (Friml *et al.*, 2004; Geldner *et al.*, 2003; Geldner *et al.*, 2001; Swarup and Bennett, 2003; Swarup *et al.*, 2001). The lactone antibiotic brefeldin A (BFA) prevents cellular trafficking and, as a result, auxin conducting cells treated with BFA accumulate PIN proteins in internal compartments (Geldner *et al.*, 2001). This effect is reversible as cells washed out from BFA rapidly retrieve their typical plasma membrane PIN localization. Further analysis showed that high levels of ATIs (namely TIBA and NPA) prevented PINs to return to the plasma membrane after BFA was washed out, supporting ATIs involvement in cellular polar trafficking machinery (Geldner *et al.*, 2001). The same effect can be obtained using flavonols, such as quercetin or kaempferol, but only in flavonoid-deficient *transparent testa* mutant lines (Peer *et al.*, 2004), which might reflect the complex mechanisms of flavonoid-mediated auxin transport regulation.
Nevertheless, neither ATIs nor flavonoids can directly alter PIN cycling. On the other hand, the NPA-binding plasma membrane aminopeptidase APM1, related to mammalian proteins that participate in cell surface signal transduction, is sensitive to flavonoids and is likely to take part in ABCB1 and ABCB19 cellular trafficking (Murphy *et al.*, 2002). Such as, protein trafficking and its regulation might play a general role in driving the auxin flows.

Taken together, these data suggest that efficient auxin transport inhibition may rather alter protein-protein interactions and trafficking than single protein activities. Thus, the involvement of partner proteins in controlling auxin transporters needs further investigation in order to understand the hormonal signaling.

Plant immunophilins are key players of plant development

The C-terminus domain of ABCB1 has been identified to interact with the *cis-trans* peptidyl-prolyl-isomerase-(PPIase-)domain of the multidomain FK506 binding protein-(FKBP-)type immunophilin TWISTED DWARF1 (TWD1/FKBP42, (Kamphausen *et al.*, 2002) by using a yeast two-hybrid screening (Geisler *et al.*, 2003) Additionally, other p-glycoproteins were found to interact with TWD1, ABCB2, ABCB4, ABCB10 and ABCB19, from NPA-binding chromatography assays (Geisler *et al.*, 2003; Murphy *et al.*, 2002). It is very noteworthy that TWD1, unlike common FKBPs, does not show *in vitro* PPIase activity or FK506 immunosuppressant drug binding (Geisler *et al.*, 2003; Kamphausen *et al.*, 2002).

The well characterized FKBP12 is found in many organisms (Harrar *et al.*, 2001; Heitman *et al.*, 1992) and represents the basic single FK506-binding/PPIase domain. Interestingly, activity studies using the murine MDR3 ABCB-type transporter suggested that yeast FKBP12 may be required for proper MDR3 function (Hemenway and Heitman, 1996). FKBP12 has been further characterized to be a regulatory subunit of integral membrane calcium release channels in mammalian cells (Cameron *et al.*, 1995a; Cameron *et al.*, 1995b; Timerman *et al.*, 1995). In both cases, the FKBP12-dependent regulation appeared to be independent of its PPIase activity (Hemenway and Heitman, 1996; Timerman *et al.*, 1995). However, the systematic deletion of all *Saccharomyces cerevisiae* FKBPs did not display any evident phenotype. Therefore Dolinski and coworkers (1997) early proposed that this organism might have only conserved FKBPs that functionally interact with partner proteins, independently of their enzymatic properties (Dolinski *et al.*, 1997). In the light of these observations, TWD1 was suggested to be a direct regulator of the ABC proteins described above (Geisler *et al.*, 2003).

FIGURE 8. ***Arabidopsis twd1* and *abcb1 abcb19* mutants exhibit similar auxin-related phenotypes**

Both mutants display pleiotropic developmental phenotypes such as epinastic leaf growth, reduced apical dominance and extreme dwarfing (Geisler *et al.*, 2003). Scale bar, 5 cm. Mature plants grown under short-day conditions.

Twd1 mutants (*ucu2*, Geisler *et al.*, 2003; Perez-Perez *et al.*, 2004) display a severe auxin-related phenotype resembling the *abcb1 abcb19* double mutant (Figure 8). *Twd1* mutants also show reduced auxin transport, thus suggesting a role for TWD1 in ABCB-mediated auxin transport (Geisler *et al.*, 2003). In mammals, immunophilins have been extensively characterized as proteins principally involved in the immunological process (Harrar *et al.*, 2001). However, other plant multidomain FKBP-type immunophilins, *Arabidopsis* FKBP72/PASTICCINO1(PAS1) and wheat FKBP77 have been shown to be key players in hormone-dependent plant development (Faure *et al.*, 1998; Kurek *et al.*, 2002a; Kurek *et al.*, 2002b; Vittorioso *et al.*, 1998). Interestingly, TWD1 is the only plant FKBP to possess a C-terminal membrane anchor (Geisler *et al.*, 2003; Kamphausen *et al.*, 2002). The latter has been shown to anchor TWD1 to the plasma membrane and the vacuolar membrane (Geisler *et al.*, 2003; Kamphausen *et al.*, 2002), where it interacts with another couple of close-related

Multidrug resistance-associated proteins (MRPs), ABCC1/MRP1 and ABCC2/MRP2. Interestingly this interaction does not occur *via* TWD1 PPIase domain, but its tetratricopepide repeat (TPR) domain (Geisler *et al.*, 2004).

Even though these interactions have not been fully characterized, the sum of data accumulated suggests that ABCB1 and 19 participate in auxin transport, eventually under the control of the immunophilin TWD1. Anyway, three points need to be clarified in order to validate this hypothesis. First, the suggested ABCB1/19-mediated active IAA transport has not yet been demonstrated to occur *in vitro* or *in vivo*. This demonstration would require to be consistent with the observed auxin flow to be pertinent. Second, although *in vitro* interaction between the immunophilin and ABC proteins has been proven, TWD1's direct participation in the regulation of auxin transport *via* ABCBs has to be investigated *in vivo* to characterize its role in the hormone signal. Finally, the observed inhibitory effects of flavonoids and synthetic auxin transport inhibitors on plant growth could partially be explained by their modulation of the ABCB-mediated auxin transport, either by direct inhibition of the ABC protein activities or by an indirect TWD1-driven mechanism. Such a demonstration would add more pieces to the complex auxin jigsaw puzzle.

Chapter 1

MODULATION OF P-GLYCOPROTEIN-MEDIATED AUXIN TRANSPORT

A subset of membrane proteins actively participates in the directional transport of the essential phytohormone auxin across biological membranes in plant cells. Amongst them, members of the *Arabidopsis thaliana* ABC-transporter superfamily were proposed to be involved in the primary-active cellular auxin export, thus participating in hormone-related physiological processes. Recent work suggested that ABCB1/PGP1-mediated auxin efflux might be regulated in part via protein–protein interactions. The carboxy terminus of ABCB1 was identified in a yeast two-hybrid screen as an interactor of the immunophilin-like protein TWISTED DWARF1 (TWD1). Mutations in *TWD1* result in severe auxin-related developmental phenotypes, remarkably similar to those of *abcb1 abcb19* double mutants. ABCB1/19-TWD1 interactions were verified using *in vitro* pull downs, co-immunoprecipitation, NPA- and TWD1-affinity chromatography and *in vivo* BRET assays. Assays of auxin transport in heterologous systems co-expressing TWD1 and ABCB1 indicate that TWD1 mediates the specific auxin transport regulation of ABCB1 activity. Additionally, TWD1-ABCB1 interaction might confer substrate-specificity to the transporter. We further propose that this regulation might be modulated by flavonoids, a subclass of secondary metabolites described *in planta* as polar auxin transport inhibitors.

Cellular efflux of auxin catalyzed by the Arabidopsis MDR/PGP transporter AtPGP1

Markus Geisler[1,†], Joshua J. Blakeslee[2,†], Rodolphe Bouchard[1], Ok Ran Lee[2], Vincent Vincenzetti[1], Anindita Bandyopadhyay[2], Boosaree Titapiwatanakun[2], Wendy Ann Peer[2], Aurélien Bailly[1], Elizabeth L. Richards[2], Karin F. K. Ejendal[3], Aaron P. Smith[2,‡], Célia Baroux[1], Ueli Grossniklaus[1], Axel Müller[4,§], Christine A. Hrycyna[3], Robert Dudler[1], Angus S. Murphy[2,*] and Enrico Martinoia[1]

[1]Basel-Zurich Plant Science Center, University of Zurich, Institute of Plant Biology, CH-8007 Zurich, Switzerland,
[2]Department of Horticulture and
[3]Department of Chemistry, Purdue University, West Lafayette, IN 47907 USA, and
[4]Lehrstul für Pflanzenphysiologie, Ruhr-Universität Bochum, D-44801 Bochum, Germany

[†]These authors contributed equally to this work.
[‡]Present address: Department of Genetics, University of Georgia, Athens, GA, USA.
[§]Present address: Carbogen AG, C11-5001 Aarau, Switzerland.

Summary

Directional transport of the phytohormone auxin is required for the establishment and maintenance of plant polarity, but the underlying molecular mechanisms have not been fully elucidated. Plant homologs of human multiple drug resistance/P-glycoproteins (MDR/PGPs) have been implicated in auxin transport, as defects in MDR1 (AtPGP19) and AtPGP1 result in reductions of growth and auxin transport in Arabidopsis (*atpgp1*, *atpgp19*), maize (*brachytic2*) and sorghum (*dwarf3*). Here we examine the localization, activity, substrate specificity and inhibitor sensitivity of AtPGP1. AtPGP1 exhibits non-polar plasma membrane localization at the shoot and root apices, as well as polar localization above the root apex. Protoplasts from Arabidopsis *pgp1* leaf mesophyll cells exhibit reduced efflux of natural and synthetic auxins with reduced sensitivity to auxin efflux inhibitors. Expression of AtPGP1 in yeast and in the standard mammalian expression system used to analyze human MDR-type proteins results in enhanced efflux of indole-3-acetic acid (IAA) and the synthetic auxin 1-naphthalene acetic acid (1-NAA), but not the inactive auxin 2-NAA. AtPGP1-mediated efflux is sensitive to auxin efflux and ABC transporter inhibitors. As is seen in planta, AtPGP1 also appears to mediate some efflux of IAA oxidative breakdown products associated with apical sites of high auxin accumulation. However, unlike what is seen *in planta*, some additional transport of the benzoic acid is observed in yeast and mammalian cells expressing AtPGP1, suggesting that other factors present in plant tissues confer enhanced auxin specificity to PGP-mediated transport.

Introduction

Transport of the plant auxin indole-3-acetic acid (IAA) is best described by a chemiosmotic model in which plasma membrane ATPases generate an H^+ gradient between the neutral cytoplasm and the acidic extracellular space (Lomax *et al*., 1995). Cellular IAA uptake is mediated by lipophilic diffusion of IAAH augmented by tissue-specific gradient-driven H^+ symport activity (Lomax *et al.*, 1985; Swarup *et al.*, 2004). The same gradient motivates carrier-mediated efflux of cytoplasmic anionic IAA^-. The bias of auxin transport is attributed to highly regulated, polar-localized efflux complexes characterized by the PIN-FORMED (PIN) family of facilitator proteins (Friml and Palme, 2002). PINs have been shown to align with the auxin transport vector and to be necessary for normal polarized organ development and auxin movement (Benkova *et al.*, 2003; Blilou *et al.*, 2005; Galweiler *et al.*, 1998; Palme and Galweiler, 1999). Treatment with auxin efflux inhibitors (AEIs) phenocopies some *pin* mutant phenotypes (Friml and Palme, 2002). Additionally, some members of the PIN family exhibit vectoral relocation during tropic growth, and function in the generation and maintenance of auxin sinks (Chen *et al.*, 1998; Friml et *al.*, 2002a,b; Muller *et al.*, 1998).

Plant homologs of human multiple drug resistance/P-glycoproteins (MDR/PGPs) are numerous. The Arabidopsis PGP sub-family of ABC transporters is large, containing 21 members (five of which are highly homologous) (Jasinski *et al.*, 2003; Martinoia *et al.*, 2002). Structural characteristics of mammalian MDR/PGPs are well conserved in plant homologs, except in the predicted pore-facing helical domains thought to confer substrate specificity (Ambudkar et *al.*, 2003). Analysis of expression patterns of the 21 members of the PGP subfamily, using both the AREX and AtGENEXPRESS microarray databases, shows that members of the PGP family exhibit distinct yet overlapping expression patterns (http://www.arexdb.org/index.jsp; Schmid *et al.*, 2005).

PGPs have been implicated in auxin transport, as defects in MDR1 (AtPGP19) and AtPGP1 result in reduced growth and auxin transport of varying severity in Arabidopsis (*atpgp1*, *atpgp19*), maize (*brachytic2*/*zmpgp1*) and sorghum (*dwarf3*/*sbpgp1*) (Geisler *et al.*, 2003; Multani *et al.*, 2003; Noh *et al.*, 2001). Further, auxin transport defects and dwarf phenotypes are more exaggerated in Arabidopsis double mutants, suggesting overlapping function (Noh *et al.*, 2001). As gradient-driven anion efflux is sufficient to drive polar transport, it is not clear where plasma membrane-localized MDR/PGP ATP-binding cassette transporters fit into this scheme.

A mechanistic explanation of PGP function in auxin transport was suggested when, after fixation and detergent treatment, PIN1 was found to be mislocalized from the plasma membrane in xylem parenchyma cells of hypertropic Arabidopsis *atpgp19* hypocotyls, but not in *atpgp1* hypocotyls which do not exhibit altered tropic responses (Noh *et al.*, 2003). These results suggest that PGPs might regulate transport by stabilizing plasma membrane efflux complexes, especially as PGPs are difficult to solubilize; are localized in detergent-resistant membrane microdomains (lipid rafts); bind the non-competitive AEI 1-N-naphthylphthalamic acid (NPA); and are components of membrane complexes that can be dissociated by NPA treatment (Geisler *et al.*, 2003; Murphy *et al.*, 2002; Noh *et al.*, 2001). It is important to characterize the transport activity of PGPs in order to understand their functional role in these complexes.

Here we characterize the AtPGP1 protein (hereafter referred to as PGP1) by examining PGP1 localization, activity, substrate specificity and inhibition of activity. We confirm that PGP1 has an intermediate dwarf phenotype under short-day conditions, and characterize other auxin-related phenotypes. We show that PGP1 exhibits non-polar subcellular localization at the shoot and root apices that is consistent with PGP1 expression. We show that *pgp1* mutant protoplasts exhibit reduced IAA transport, substrate specificity, and reduced sensitivity to AEIs. We show that PGP1 expressed in yeast and the standard mammalian cell expression system used to analyze human MDR-type proteins can mediate efflux of IAA and the synthetic auxin 1-NAA, but not the weak synthetic auxin 2-NAA. Further, PGP-mediated efflux is sensitive to auxin efflux and ABC-transporter inhibitors. PGP1 expression in yeast also results in increased resistance to toxic indolic IAA analogs. Expression of PGP1 in mammalian cells does not enhance the efflux of other classes of compounds that are common substrates for mammalian MDR-type transporters.

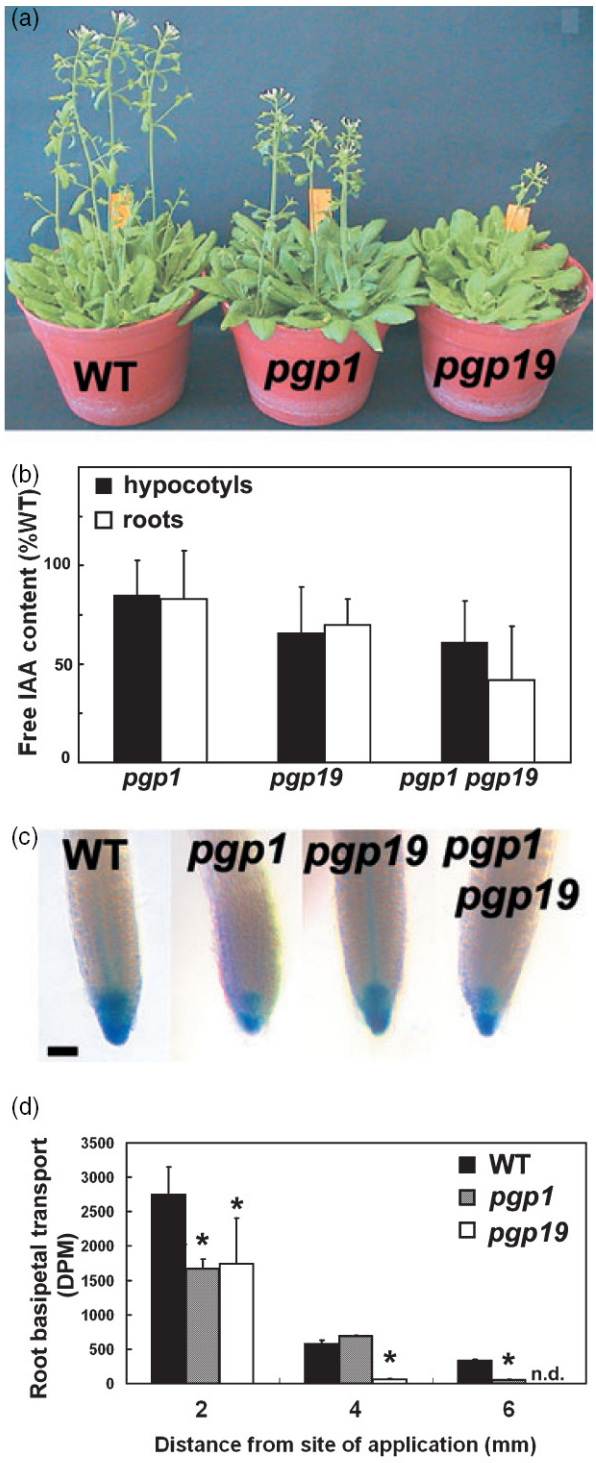

FIGURE 1. ***pgp1* mutants have a subtle phenotype.**
(a) *pgp1* and *pgp19* mutants have a dwarf phenotype under short-day conditions.
(b) Free IAA content in 5-day seedlings. Values are mean ± SD from 500 seedlings per replicate, n = 3. WT values = 100% ± 0.074 for hypocotyls, and 100% ± 11.114 for roots.
(c) Pro_{DR5}:GUS expression in 5-day seedling root tips. Bar, 0.1 mm.
(d) Basipetal ^{3}H-IAA transport from the root tip in 5-day seedlings. Values are mean ± SD from 10 seedlings per replicate, n = 3.

Results

pgp1 exhibits subtle auxin-related phenotypes

While the growth phenotypes of *atpgp19* (hereafter referred to as *pgp19*) and the double mutant *pgp1 pgp19* are clearly visible in both short- and long-day conditions (Geisler *et al.*, 2003; Noh *et al.*, 2001), those of *pgp1* are not. Enhanced tropic bending observed in *pgp19* hypocotyls is not observed in *pgp1* hypocotyls (Noh *et al.*, 2003), and gravitropic defects are difficult to quantify in *pgp1* roots, largely because of greater variability in root gravitropic bending and root nutation compared with the wild type (Noh *et al.*, 2003). Reduced hypocotyl growth reported in antisense *PGP1* transformants (Sidler *et al.*, 1998) was not observed in the *pgp1* mutant (Noh *et al.*, 2001) and, in our hands and under long-day conditions, shoot and hypocotyl growth of *pgp1* mutants was difficult to distinguish from wild type (not shown). However, under shorter-day conditions, mature *pgp1* exhibited an intermediate dwarf phenotype that is not as severe as *pgp19* (Figure 1a) and is consistent with intermediate reduction in the transport of ^{3}H-IAA from the shoot apex to the root–shoot transition zone previously observed in *pgp1* (Geisler *et al.*, 2003). However, as previous assays utilizing higher concentrations of ^{14}C-IAA indicated slight increases in *pgp1* auxin transport levels (Noh *et al.*, 2001), free IAA levels in hypocotyls and whole roots of 5-day *pgp1* and *pgp19* seedlings were determined (Figure 1b) and were found to be consistent with more recently published transport data (Geisler *et al.*, 2003).

Consistent with auxin levels observed in whole-root tissues, free IAA levels in *pgp19* primary root tips were severely reduced (62 ± 18.3% of wild type). However, levels in *pgp1* root tips were lower than expected (38 ± 29.7% of wild type). A small increase in IAA leakage from *pgp1* (and not *pgp19*) root tips is also apparently a factor as, like the flavonoid-deficient mutant *tt4* (Murphy *et al.*, 2000; Peer *et al.*, 2004), *pgp1* root tips exhibited enhanced leakage of radiolabeled IAA into the support media in assays of shoot-to-root polar ^{3}H-IAA transport (124 ± 9.4% of wild-type levels). Confirming these results, expression of the auxin reporter construct Pro_{DR5}:GUS was reduced in *pgp1*, *pgp19* and *pgp1 pgp19* compared with wild type, but was stronger in *pgp19* than in *pgp1* and *pgp1 pgp19* (Figure 1c). Additionally, a stelar Pro_{DR5}:GUS signal observed in *pgp19* was not visible in *pgp1*,

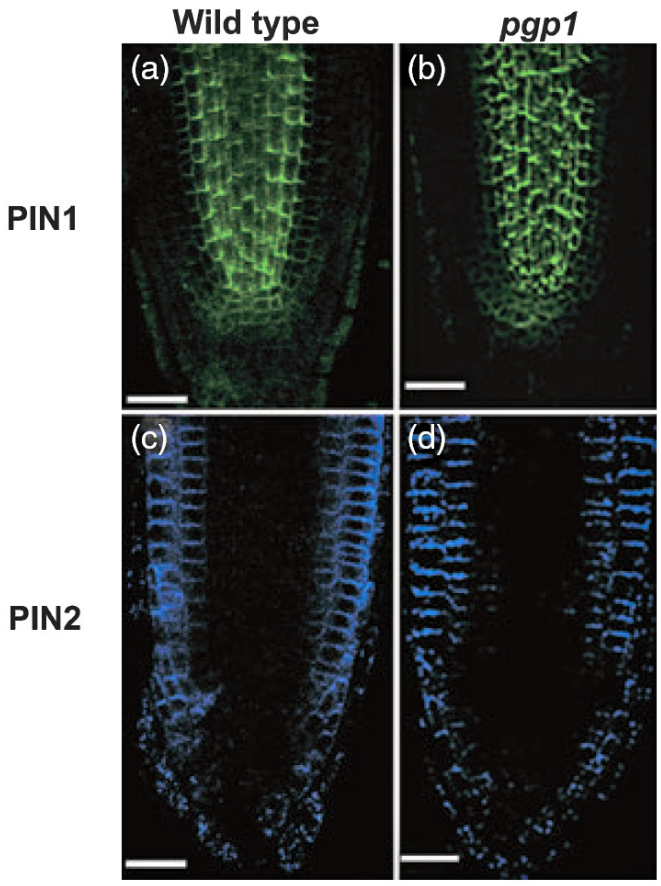

FIGURE 2. **PIN1 and PIN2 localization is unaltered in *pgp1* root tips**.
(a) PIN1 immunolocalization in 5-day wild type root tips.
(b) PIN1 immunolocalization in 5-day *pgp1* root tips.
(c) PIN2 immunolocalization in 5-day wild type root tips.
(d) PIN2 immunolocalization in 5-day *pgp1* root tips. Bar, 125 *μ*m.

Treatment	*AtPGP1*
Whole seedlings	
Light	1.00 ± 0.73
Light + NPA	0.60 ± 1.66
Dark	14.89 ± 0.98*
Dark + NPA	3.70 ± 1.69
Shoots	
Wild type	1.0 ± 0.8
Wild type + IAA	8.5 ± 1.4*
Roots	
Wild type	1.0 ± 0.9
Wild type + IAA	2.1 ± 0.9

TABLE 1. **Relative expression of AtPGP1 in 5-day wild-type seedlings**
NPA, 1-N-naphthylphthalamic acid; IAA, indole-3-acetic acid.
*Significantly different (P < 0.05), anova followed by Tukey's post-hoc analysis.

consistent with a lesser accumulation of auxin in *pgp1* root tips compared with *pgp19*. The reductions of Pro_{DR5}:GUS staining observed in *pgp* mutant root tips have been further confirmed in a recently published study showing reduced Pro_{DR5}:GUS expression in the root tips of independently generated *pgp1* and *pgp19* mutants (Lin and Wang, 2005).

IAA root basipetal transport in 5-day pgp1 seedlings

Pro_{DR5}:GUS results suggested that basipetal transport in *pgp1* and *pgp19* might be reduced at the root tip. Consistent with these results, export of radiolabeled IAA to the 2-mm segment proximal to the root tip in *pgp1* and *pgp19* was less than in the wild type (Figure 1d). Auxin transport to the next 2-mm segment was less than wild type in *pgp19* but not *pgp1*, consistent with stronger *PGP19* expression in non-apical tissues compared with *PGP1* (Noh *et al.*, 2001; Sidler *et al.*, 1998) and greater apparent auxin retention in *pgp19*, indicated by Pro_{DR5}:GUS (Figure 1c). As PIN1 and PIN2 were not mislocalized in *pgp1* root tips (Figure 2a–d), altered PIN localization cannot account for the altered auxin transport. Application of IAA ≥2 mm above root tips of both *pgp* mutants resulted in only marginal reductions in transport compared with wild type (approximately 5% in *pgp19* and 14% in *pgp1*), suggesting limited PGP function in root basipetal transport in non-apical tissues. However, wild-type rates of basipetal auxin transport in these tissues are also much lower than apical transport rates, and decrease with distance from the root tip (data not shown). These results are similar to Pro_{DR5}:GUS activity and root basipetal transport reported in *agr1-5*/*pin2* root tips (Shin *et al.*, 2005).

PGP1 localization is non-polar at shoot and root apices

Auxin transport profiles of *pgp1* and the strong expression of *PGP1* observed in light-grown root and shoot apices (Noh *et al.*, 2001; Sidler *et al.*, 1998) focused our attention on PGP1 function in these regions. Unlike *PGP19*, which is highly expressed in upper hypocotyls and throughout the root in light-grown seedlings (Noh *et al.*, 2001), *PGP1* is expressed at lower levels in non-apical tissues in both light- and dark-grown seedlings (Geisler *et al.*, 2003; Noh *et al.*, 2001). Pro_{PGP1}:GUS enzyme and quantitative real-time PCR assays confirmed that *PGP1* expression is

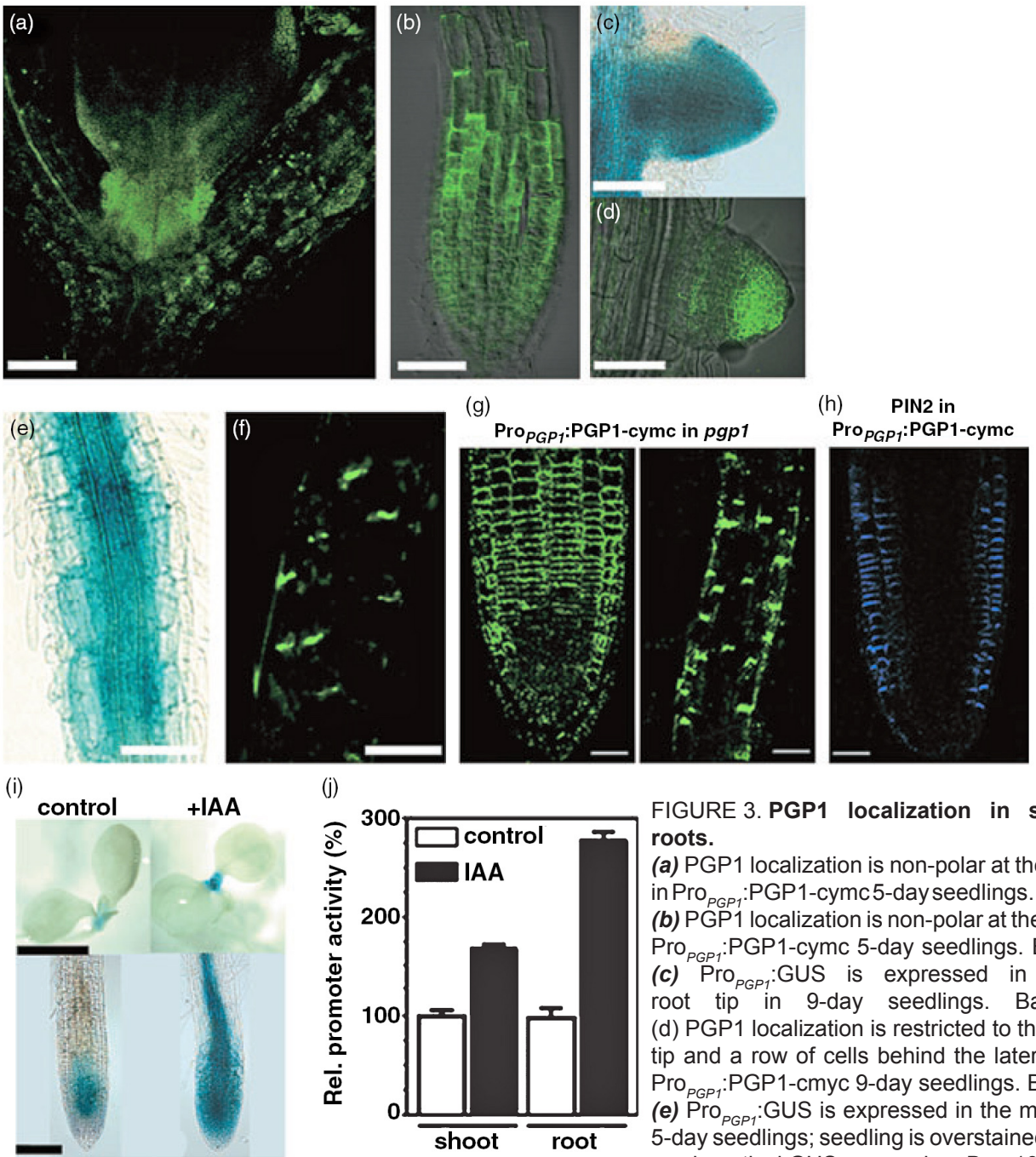

FIGURE 3. **PGP1 localization in shoots and roots.**
(a) PGP1 localization is non-polar at the shoot apex in Pro$_{PGP1}$:PGP1-cymc 5-day seedlings. Bar, 100 *μ*m.
(b) PGP1 localization is non-polar at the root apex in Pro$_{PGP1}$:PGP1-cymc 5-day seedlings. Bar, 100 *μ*m.
(c) Pro$_{PGP1}$:GUS is expressed in the lateral root tip in 9-day seedlings. Bar, 100 *μ*m.
(d) PGP1 localization is restricted to the lateral root tip and a row of cells behind the lateral root tip in Pro$_{PGP1}$:PGP1-cmyc 9-day seedlings. Bar, 100 *μ*m.
(e) Pro$_{PGP1}$:GUS is expressed in the mature root of 5-day seedlings; seedling is overstained to visualize weak cortical GUS expression. Bar, 100 *μ*m.
(f) PGP1 localization is polar in the mature root of Pro$_{PGP1}$:PGP1-cymc 5-day seedlings. Bar, 100 *μ*m.
(g) When *pgp1* is transformed with Pro$_{PGP1}$:PGP1-cmyc, the localization of the protein is consistent with the localization of the *in situ* hybridization and Pro$_{PGP1}$:GUS expression previously published (Sidler *et al.*, 1998) and that observed in wild type transformants. Bars, 125 and 70 *μ*m, respectively.
(h) PIN2 localization is not different from wild type in Pro$_{PGP1}$:PGP1-cmyc transformants. Bar, 125 *μ*m.
(i) Pro$_{PGP1}$:GUS expression increases at the shoot and root apices after 10-day seedlings are treated with 2 *μ*M auxin (+IAA). Bar, 5 mm shoots, 0.2 mm roots. The seedlings were stained for identical amounts of time.
(j) Relative promoter activities in Pro$_{PGP1}$:GUS transformants with and without 1 *μ*M IAA treatment.

strongest in root and shoot apices in dark-grown wild-type seedlings (Table 1). Pro$_{PGP1}$:GUS visualization also confirmed previous reports of *PGP1* expression in lateral root primordia and apices (Sidler *et al.*, 1998; Figure 3c), as well as previously unpublished weaker expression in cortical cells of the mature root and endodermal cells at the upper border of the distal elongation zone (Figure 3e). *PGP1* expression in these tissues was further confirmed by examination of original *in situ* hybridization materials from Sidler

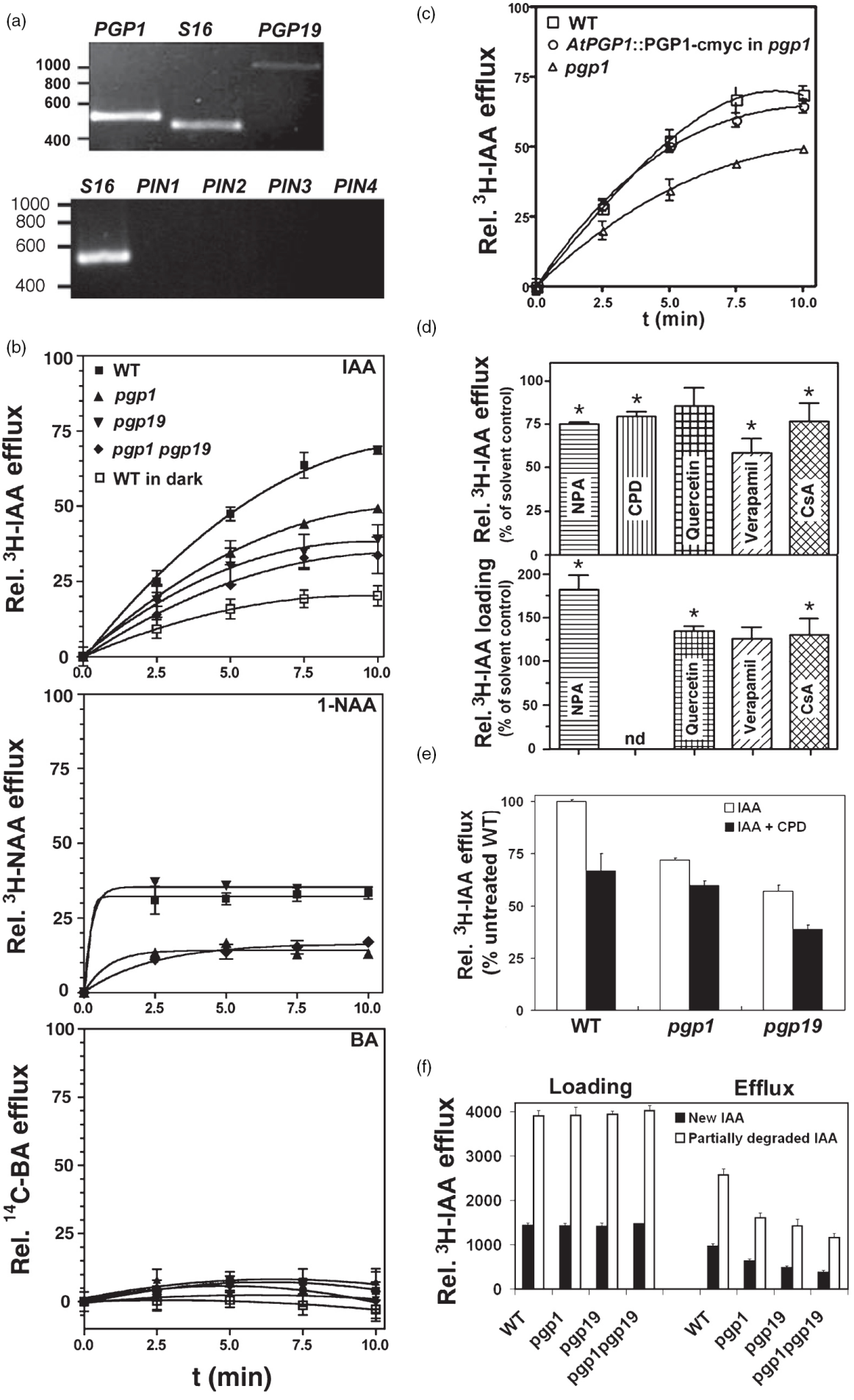
(a)
PGP1
S16
PGP19
1000
800
600
400
S16
PIN1
PIN2
PIN3
PIN4
(b)
IAA
WT
pgp1
pgp19
pgp1 pgp19
WT in dark
Rel. 3H-IAA efflux
1-NAA
Rel. 3H-NAA efflux
BA
Rel. 14C-BA efflux
t (min)
(c)
WT
AtPGP1::PGP1-cmyc in pgp1
pgp1
Rel. 3H-IAA efflux
t (min)
(d)
Rel. 3H-IAA efflux (% of solvent control)
Rel. 3H-IAA loading (% of solvent control)
NPA
CPD
Quercetin
Verapamil
CsA
nd
(e)
IAA
IAA + CPD
Rel. 3H-IAA efflux (% untreated WT)
WT
pgp1
pgp19
(f)
Loading
Efflux
New IAA
Partially degraded IAA
Rel. 3H-IAA efflux
WT
pgp1
pgp19
pgp1pgp19

◂ FIGURE 4. **Cellular auxin efflux by PGPs reflects *in planta* auxin transport.**
(a) RT-PCR of 40S ribosomal protein *S16* (At2g09990), *PGP1* and *PGP19* (top) and *PIN1*, *PIN2*, *PIN3* and *PIN4* (bottom) in wild type leaf mesophyll protoplasts.
(b) ^{3}H-IAA efflux from wild type (WT) leaf mesophyll protoplasts and reduced efflux from *pgp1*, *pgp19*, *pgp1 pgp19* and dark-treated wild type leaf mesophyll protoplasts. ^{3}H-1-NAA efflux was reduced in *pgp1* and *pgp1 pgp19* compared with wild type. No efflux of ^{14}C-BA was observed. Maximum loading of the cells is set at 100%. Values are mean activities ± standard errors from three to five individual measurements, $n = 4$.
(c) Pro_{PGP1}:PGP1-cmyc functionally complements *pgp1*. When *pgp1* is transformed with Pro_{PGP1}:PGP1-cmyc, auxin efflux from in leaf mesophyll protoplasts is not different from wild type.
(d) ^{3}H-IAA efflux from Arabidopsis wild type protoplasts was significantly reduced by inhibitors of auxin efflux and mammalian MDRs. ^{3}H-IAA efflux from protoplasts (upper panel) and loading into cell suspension cultures (lower panel) in the absence (solvent control) or presence of 10 *μ*m of indicated inhibitors was determined after 10 min. Inhibitors assayed were: 1-*N*-naphthylphthalamic acid (NPA), 1-cyclopropyl propane dione (CPD), quercetin, verapamil, and cyclosporin A (CsA). Values are mean ± standard deviations (error bars) of three individual measurements, four samples each; export statistically different (Mann–Whitney *U*-test, $P < 0.05$) compared with solvent controls is indicated by an asterisk. n.d., not determined.
(e) ^{3}H-IAA efflux from wild-type, *pgp1* and *pgp19* protoplasts is reduced by the non-hydrolyzable inhibitor cyclopropyl propane dione (CPD). ^{3}H-IAA efflux in the absence and presence of 10 *μ*m CPD was determined after 10 min. Values are mean activities ± standard deviations (error bars) of three individual experiments, four samples each. $P > 0.05$ for *pgp1*.
(f) Inclusion of partially degraded ^{3}H-IAA resulted in increased loading of labeled IAA in wild type and *pgp* mutant protoplasts. Apparent rates of efflux appeared to increase as well. However, the relative reduction of efflux seen with fresh ^{3}H-IAA effluence observed in *pgp* mutant protoplasts remained the same.

et al. (1998) and microarray expression data in AREX (http://www.arexdb.org/index.jsp).

PGP1 proteins were immunolocalized utilizing a functional Pro_{PGP1}:PGP1-cmyc transformant (see Experimental procedures), and the localization patterns were compared with Pro_{PGP1}:GUS expression. PGP1 exhibits a strong non-polar localization in shoot and root apical cells as well as lateral root tips (Figure 3a,b,d). This suggests a role for PGP1 in non-directional auxin export from apical cells, and suggests that PGP function may be additive to, or synergistic with, PIN protein function.

Interestingly, in root tissues above the distal elongation zone, an apparent polar PGP1 localization was observed in mature cortical and endodermal cells at the upper boundary of the distal elongation zone (Figure 3f), suggesting that PGP1 may function in polar or reflux auxin movement (Blilou *et al.*, 2005) in these tissues. In endodermal cells, the localization was always basal. In cortical cells, the localization was predominantly basal, although an apical localization without any obvious pattern was observed in some cortical cells flanking the stele. No reorientation of the basal signals was observed after microdeposition of IAA at the shoot or root tip or along the root surface (see Experimental procedures), suggesting a developmental basis for apical or basal localization. Transformation of *pgp1* with Pro_{PGP1}:PGP1-cmyc complemented the mutant phenotype and restored wild-type auxin transport profiles (Figure 4c), and PGP1 protein localization was similar to that seen in transformed wild type (Figure 3g); PIN2 localization was not altered in transformants (Figure 3h). No signal was observed in wild-type immunolocalizations utilizing only primary or secondary antibodies under any detergent-solubilization conditions; no signal was observed in transformant immunolocalizations utilizing secondary antibodies only (Supplemental Figure 1).

PGP1 expression is auxin responsive

As is the case for *PGP19* (Noh *et al.*, 2001), *PGP1* expression appears to be auxin-responsive (Figure 3i,j; Table 1) and the *PGP1* promoter contains auxin response element motifs (ARFAT, ASF-1 and NtBBF1). However, *PGP1* expression in shoot tips did not expand spatially with auxin treatment (Figure 3i). *PGP1* expression was also NPA-sensitive, and NPA treatment reversed increased *PGP1* expression observed in dark-grown wild-type seedlings (Table 1).

PGP1 mediates cellular efflux in Arabidopsis protoplasts

In order to determine whether differences in auxin transport could be observed at the cellular level, efflux from protoplasts under conditions that minimize IAA catabolism was quantified. Protoplasts were isolated from leaf mesophyll cells of wild-type, *pgp1*, *pgp19* and *pgp1 pgp19* plants, but not from *pin1*, *pin2*, *pin3* or *pin4* mutants, as *PIN1*, *PIN2*, *PIN3* and *PIN4*

Line	Protoplast characteristics			
	Vacuolar pH	Relative volume	Relative surface area	Number of chloroplasts
Wild type	6.40	1	1	37 ± 9
pgp1	6.31	0.976 ± 0.031	0.949 ± 0.015	40 ± 9
pgp19	6.19	0.998 ± 0.028	0.919 ± 0.020	36 ± 5
pgp1 pgp19	6.04	0.724 ± 0.053*	0.514 ± 0.058*	37 ± 9

TABLE 2. **Vacuolar pH and morphological features of leaf mesophyll protoplasts**
*Significantly different from wild type ($P < 0.05$), anova followed by Tukey's post-hoc analysis.

Time (min)	α-Naphthylamine formation (naphthylamine equivalents)	
	Wild type	pgp1/pgp19
0	ND	ND
5	0.4 ± 0.91	3.2 ± 0.51
10	2.6 ± 2.21	6.8 ± 1.20
15	4.7 ± 2.34	7.1 ± 2.03

TABLE 3. **1-N-naphthylphthalamic acid (NPA) hydrolysis in *pgp1/pgp19* protoplasts**
NPA hydrolysis is rapid in pgp mutant protoplasts compared with wild-type protoplasts. Chorophyll-normalized protoplast solutions were incubated with 20 μm NPA. α-Naphthylamine was determined as described previously (Murphy and Taiz, 1999a). ND, not determined.

expression is low in wild-type leaves (Figure 4a).

Wild-type protoplasts exhibited ^{3}H-IAA efflux into the media (Figure 4b), and reductions in ^{3}H-IAA efflux from *pgp* protoplasts compared well with transport reductions seen in whole plants: 72% in *pgp1*; 57% in *pgp19*; 49% in *pgp1 pgp19* (Figure 4b). *pgp1* mutants transformed with Pro_{PGP1}:PGP1-cmyc had efflux levels similar to wild type (Figure 4c). Vacuolar pH, relative protoplast volume and surface area, and chloroplast number per protoplast did not differ significantly between wild-type and *pgp* protoplasts, excluding indirect effects such as vacuolar trapping (Table 2). Consistent with ATP dependence of the process, auxin efflux was diminished in protoplasts isolated from plants kept in the dark for 24 h (ATP-depleted) (30% of light-grown wild type; Figure 4b).

The synthetic auxin 1-NAA was exported by wild-type and *pgp19* protoplasts, but not *pgp1* or *pgp1 pgp19* protoplasts (Figure 4b), suggesting that PGP1 transports this synthetic auxin better than PGP19. Substrate specificity in the protoplast system was investigated further using radiolabeled benzoic acid (^{14}C-BA), a weak acid commonly used as a poorly transported control in plant assays. Negligible efflux of ^{14}C-BA out of wild type, *pgp1*, *pgp19*, *pgp1 pgp19*, and ATP-depleted wild-type protoplasts was observed (Figure 4b), demonstrating that IAA efflux from protoplasts reflects the specific auxin transport observed in whole plants.

As the AEI NPA binds MDR/PGPs (Murphy *et al.*, 2002; Noh *et al.*, 2001), and NPA treatment disrupts membrane protein complexes containing PGPs (Geisler *et al.*, 2003), IAA efflux from wild-type protoplasts would be expected to be NPA-sensitive, and *pgp* mutant protoplasts would be expected to exhibit diminished NPA sensitivity. However, an inactivating NPA amidase activity associated with the membrane aminopeptidase AtAPM1 (Katekar and Geissler, 1979, 1980; Katekar *et al.*, 1981; Murphy and Taiz, 1999a,b; Murphy *et al.*, 2002) is present in Arabidopsis leaves and is particularly active in leaf protoplasts (Murphy *et al.*, 2002; Table 3). Treatment with NPA would be expected to increase initial ^{3}H-IAA loading, but to be less effective in inhibiting ^{3}H-IAA efflux. Treatment with NPA resulted in an 82% increase in ^{3}H-IAA loading of wild-type protoplasts (Figure 4d), but only a 24% decrease in efflux. Consistent with even higher levels of NPA amidase activity in protoplasts derived from *pgp1* and *pgp19* (Table 3), measurements of NPA efflux inhibition from *pgp* protoplasts were highly variable.

However, when the non-hydrolysable NPA analog cyclopropyl propane dione (CPD) was substituted for NPA in wild-type protoplast assays, mean ^{3}H-IAA efflux was reduced approximately 30% (Figure 4e). In contrast, CPD inhibited ^{3}H-IAA transport from the tips of intact young Arabidopsis rosette leaves approximately 40% (not shown), suggesting that structural characteristics of intact tissues not present in protoplasts contribute to NPA/CPD sensitivity. Low levels of *PIN* expression in leaf protoplasts (Figure 4a) suggest that lower abundance of PIN proteins in mesophyll tissues may be involved in this reduction of AEI sensitivity. As expected, ^{3}H-IAA efflux from CPD-treated protoplasts decreased approximately 12% in *pgp1* and approximately 20% in *pgp19* compared with the respective untreated protoplasts (Figure 4e). These results suggest that PGP19 is less sensitive than PGP1 to AEIs such as NPA and CPD, but also confirms that NPA/CPD inhibition requires

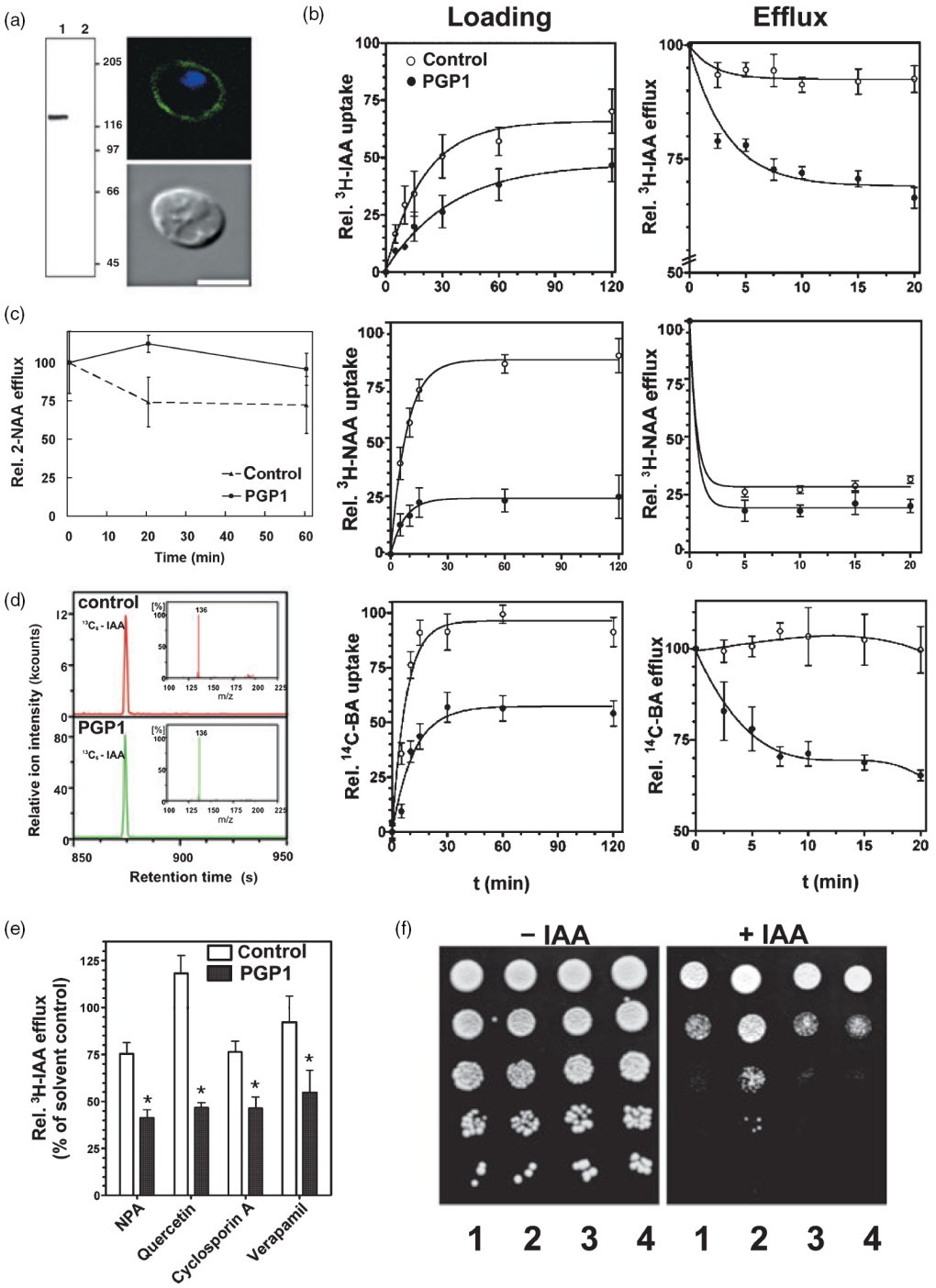

FIGURE 5. **Heterologous expression of *PGP1* in yeast cells results in auxin efflux.**
(a) PGP1-transformed yeast express and correctly target PGP1 to the plasma membrane. Western blot of microsomes from transformed yeast: lane 1, PGP1; lane 2, vector control. Confocal analysis with anti-AtPGP1 antibody (green) and DAPI-stained nucleus (blue) (top), DIC image (bottom). Several hundred yeast cells were examined and >90% showed the pattern. Bar, 5.6 *μ*m. ***(b)*** Yeast cells (strain JK93dα,with reduced endogenous ABC transporter activity) expressing *PGP1* effluxed ^{3}H-IAA, ^{3}H-1-NAA, and ^{14}C-BA compared with empty vector control. Mean activities ± standard errors, three to five individual measurements, $n = 4$. Values presented are relative to the total amount of radiolabeled IAA present in the media. ***(c)*** No efflux of 2-NAA was observed in yeast cells expressing *PGP1*. (d) MS/MS analysis of $^{13}C_6$-IAA effluent by yeast. ***(e)*** ^{3}H-IAA efflux by yeast cells expressing *PGP1* was significantly reduced by auxin transport inhibitors and inhibitors of mammalian MDRs. Inhibitor concentrations were 10 *μ*m. Solvent controls were set at 100%. Values presented are relative to total loading at time 0. Mean activities ± standard errors, three to five individual measurements, $n = 4$.
(f) AtPGP1, but not mouse MDR3, functionally rescued a *yap1-1* mutant strain. 10-fold dilutions of yeast cells transformed with AtPGP1 (lane 2), MmMDR3 (lane 4) or corresponding vector controls pNEV (lane 1) and pVT (lane 3) were spotted on control plates or plates supplemented by 10 *μ*m IAA.

factors that are altered in protoplasts.

The strong localization of PGP1 in apical tissues suggests that PGPs might also transport IAA breakdown products produced in these tissues (Kerk *et al.*, 2000). Unlabeled, presumably partially degraded IAA is often included in whole-plant radiolabeled auxin transport assays as it enhances measurable transport, possibly by enhancing uptake (Rashotte *et al.*, 2000). Protoplast assays were repeated using either >99% radiolabeled IAA or a 1:1 mixture of IAA and IAA oxidative breakdown products (primarily oxindoleacetic acid and indoleacetaldehyde, as determined by LC/MS and GC/MS). Increased loading and efflux was observed with the mixture (Figure 4f), but relative efflux from wild-type and *pgp* mutant protoplasts at 10 min was similar with both treatments. These results suggest that, in leaf cells, uptake and efflux of some IAA metabolites may be mediated by a PGP-dependent mechanism. However, it is not clear how far the specificity of IAA efflux might be enhanced in tissues where *PIN*s are strongly expressed.

Analysis of PGP1 and auxin efflux in yeast

Heterologous expression of *PIN2* in yeast was previously used to demonstrate a positive impact on net auxin efflux (Chen *et al.*, 1998). Although PGP19 was found to be mistargeted when expressed in a *Saccharomyces cereviseae* deletion strain (JK93dα) with reduced ABC transporter activity (Noh *et al.*, 2001), immunohistochemical analyses indicated that *PGP1* expressed in JK93dα strain was localized in the plasma membrane (Figure 5a). Yeast expressing *PGP1* exhibited time-dependent loading and efflux of radiolabeled IAA, 1-NAA and BA (Figure 5b). ^{3}H-IAA efflux was temperature- and glucose-dependent (Supplemental Figure 2*A*,*B*); membrane permeability was unaltered (Supplemental Figure 2*C*); and the effluent species was determined by GC-MS to be ^{3}H-IAA (Figure 5d). Efflux of ^{3}H-IAA was seven times greater in *PGP1*-transformed yeast than in vector controls, and efflux of ^{3}H-1-NAA was also slightly increased (Figure 5b). However, although no efflux of the weak synthetic auxin 2-NAA was seen (Figure 5c), a lack of specificity was indicated when efflux of ^{14}C-BA was seen to be almost equal to that of ^{3}H-IAA (Figure 5b).

Consistent with PGP1 mediation of auxin efflux, ^{3}H-IAA efflux in PGP1-transformed yeast was significantly reduced by treatment with NPA, the mammalian MDR/PGP inhibitors cyclosporin A and verapamil, and the inhibitor of both auxin transport and mammalian MDR/PGPs, quercetin (Figure 5e). Further, expression of PGP1 in the hypersensitive *gef1* yeast mutant exhibited increased resistance to the cytotoxic IAA analog 5-fluoroindole which could be reversed by both AEIs and ABC transport inhibitors (M.G., unpublished data). Additionally, yeast *yap1-1* mutants, which are hypersensitive to IAA due to increased expression of AUX1-like permeases (Prusty *et al.*, 2004), are rescued by AtPGP1 but not by mouse MDR3 (Raymond *et al.*, 1992) when grown on IAA (Figure 5f).

Analysis of PGP1-mediated auxin efflux in mammalian cell lines

Vaccinia virus/T7 RNA polymerase expression in human HeLa cells has become a standard system for assaying mammalian PGPs, as it provides efficient heterologous expression of functional eukaryotic plasma membrane proteins and suppression of host-protein synthesis (Elroy-Stein and Moss, 1991; Hrycyna *et al.*, 1998; Moss, 1991). Protocols to confirm protein functionality and to assay net accumulation of radiolabeled and fluorescent substrates are well established (Hrycyna *et al.*, 1998). These protocols were modified to allow loading of ^{3}H-IAA into HeLa cells while maintaining cell viability and substrate integrity.

HeLa cells expressing *PGP1* exhibited significant ^{3}H-IAA efflux compared with empty vector controls (Figure 6a). Although loading of ^{3}H-1-NAA was less than that seen with ^{3}H-IAA, cells expressing *PGP1* exhibited a small net efflux of ^{3}H-1-NAA (Figure 6a). Cells expressing *PGP1* exhibited significant ^{3}H-IAA efflux compared with cells transformed with empty vector alone over a sixfold concentration range (Figure 6a,b). No net efflux of 2-NAA could be detected in cells expressing *PGP1* (Figure 6c). However, as seen when PGP1 was expressed in yeast, PGP1-mediated net ^{3}H-BA efflux was also observed when ^{3}H-BA was supplied at higher concentrations (Figure 6b). Background efflux of ^{3}H-BA in empty vector controls was higher than with ^{3}H-IAA, presumably due to endogenous mammalian benzoate/monocarboxylic acid transport activity (Yan and Taylor, 2002). Expression of *PGP1* in HeLa cells resulted in more auxin substrate specificity than when *PGP1* was expressed in yeast, as PGP1-mediated

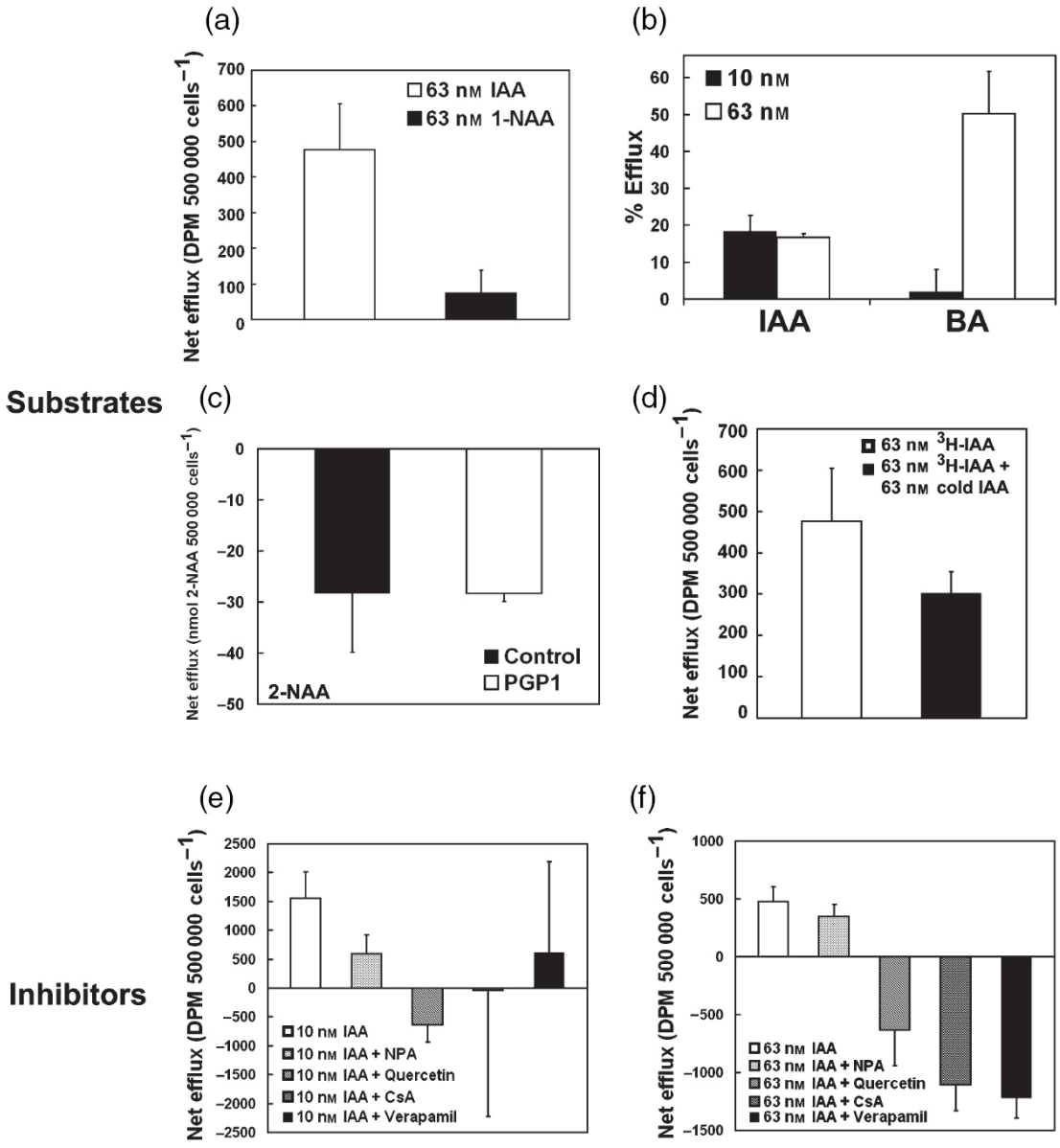

FIGURE 6. **Efflux of radiolabeled substrates from HeLa cells expressing *PGP1*.**
Net efflux is expressed as DPM/500 000 cells: the amount of auxin retained by cells transformed with empty vector minus the amount of auxin retained by cells transformed with gene of interest. Reductions in auxin retention (efflux) in transformed cells are presented as positive values, while increases of auxin retention are presented as negative values. In all cases, expression and localization of expressed Arabidopsis proteins were confirmed by RT-PCR (Blakeslee *et al.*, 2004) and Western blotting (Hrycyna *et al.*, 1998) using standard protocols for the system. Cell viability after treatment was confirmed visually and via cell counting. Data points were normalized to the average empty control vector value of 2851.885 DPM/500 000 cells for auxin treatments. Means with sum standard deviations, $n = 3$. ***(a)*** ^{3}H-IAA efflux was increased in HeLa cells expressing *PGP1*. PGP1 also modulated efflux of 1-napthalene acetic acid (^{3}H-1-NAA) and benzoic acid (^{3}H-BA). ***(b)*** ^{3}H-IAA efflux remained constant over a sixfold concentration range in cells expressing *PGP1*. Cells expressing *PGP1* transport BA only at high concentrations. Values are presented as percent efflux of empty vector control. ***(c)*** 2-NAA was retained in HeLa cells expressing *PGP1*. Cells were incubated with 62.59 nm cold 2-NAA. 2-NAA levels were measured via LC-MS. Data are presented in nanomoles 2-NAA/500 000 cells ± SD, and represent values obtained from two experiments, three replicates each. ***(d)*** Unlabelled auxin degradation products competitively inhibit PGP1-modulated efflux. HeLa cells expressing *PGP1* were incubated with a 1:1 mixture of 50.3%^{3}H-IAA and oxidative IAA breakdown products (20.4%^{3}H-oxindole-3-acetic acid, 16.8%^{3}H-oxindole-3-carbinol, 5.7%^{3}H-indole-3-aldehyde, and 6.8%^{3}H-methylene oxindole, by LC-MS/MS). ***(e)*** ^{3}H-IAA efflux by PGP1 was inhibited by treatment with 10 μm NPA, 200 nm quercetin and by the ABC transport inhibitors cyclosporin A (CsA) and verapamil. ***(f)*** ^{3}H-IAA efflux by PGP1 was inhibited by treatment with 10 μm NPA, 200 nm quercetin and by the ABC transport inhibitors cyclosporin A (CsA) and verapamil when cells were loaded with 10 nm radiolabeled substrate.

net efflux of ^{3}H-BA decreased to zero when ^{3}H-BA concentration was reduced to 10 nm, while ^{3}H-IAA efflux was unaffected (Figure 6b). Competition assays utilizing 10× more unlabeled BA than ^{3}H-IAA resulted in substantial inhibition of background ^{3}H-IAA efflux (data not shown), and ^{3}H-IAA efflux was reduced 22 ± 12.5% less in cells expressing *PGP1* than in empty vector controls. This suggests that background IAA efflux in HeLa cells is mediated by a monocarboxylic acid transporter, and that PGP1 is a functional IAA transporter when expressed in HeLa cells. Supporting this conclusion, the monocarboxylate transport inhibitor cardio green reduced background but not PGP1-mediated efflux (not shown).

All the assays were conducted in a buffer solution containing 1-2 mM citrate (see Experimental procedures), indicating that organic acids such as citrate and malate are not substrates for PGP1-mediated transport. Further, no efflux of mammalian MDR/PGP hydrophobic substrates (rhodamine 123, daunomycin, BODIPY-vinblastine) was seen in cells expressing *PGP1* (Supplemental Figure 3*A-D*). These results indicate that PGP1-mediated efflux is specific for active auxins and, to a lesser extent, a subset of aromatic carboxylic acids.

PGP1-mediated efflux of IAA oxidative degradation products in HeLa cells

As protoplast assays suggested that PGP1 may also be involved in efflux of IAA oxidative degradation products (Figure 4f), HeLa cells expressing PGP1 were incubated with a 1:1 mixture of ^{3}H-IAA and oxidative IAA breakdown products. Consistent with protoplast results, incubation of cells with 10 nm (indole equivalents) of the mixture resulted in net loading in transfected cells to levels twice those observed when cells were loaded with 63 nm fresh IAA. PGP1-mediated net ^{3}H-IAA efflux was also twice as high with this treatment (Figure 6d), but, NPA sensitivity observed at lower IAA concentrations was retained. When fresh ^{3}H-IAA was mixed with an equal amount (indole equivalents) of unlabeled oxidative breakdown products, net efflux was reduced (Figure 6d), suggesting competitive inhibition of IAA efflux. These data support a role for PGP1 in the transport of auxin breakdown products *in planta.*

Inhibitor studies of PGP1-mediated efflux in HeLA cells

The effects of inhibitor treatments on PGP1-mediated ^{3}H-IAA efflux were normalized to inhibitor-treated empty vector controls. PGP1-mediated ^{3}H-IAA net efflux was inhibited by treatment with 10 μm NPA (Figure 6e), and efflux was more NPA-sensitive at lower IAA concentrations (Figure 6e,f). Both mammalian and *Arabidopsis* PGPs have been shown to bind the aglycone flavonoid quercetin (Ferte *et al.*, 1999; Murphy *et al.*, 2002) which decreases mammalian PGP activity and negatively regulates auxin transport in plant tissues where PGPs are expressed (Brown *et al.*, 2001; Ferte *et al.*, 1999; Peer *et al.*, 2001, 2004). Treatment with flavonoids and mammalian MDR/PGP inhibitors has previously been shown to reverse efflux of human MDR substrates to the point of net retention in mammalian cells (Zhang and Morris, 2003). Net ^{3}H-IAA efflux by PGP1 was reversed when cells were treated with 200 nm quercetin (Figure 6e,f). Treatment with the MDR/PGP inhibitors verapamil and cyclosporin A increased net retention in cells expressing *PGP1* (Figure 6e,f), suggesting an additive cytotoxicity of these compounds in transfected cells. These data support the hypothesis that PGP1-mediated IAA transport can be regulated by endogenous flavonoids, as well as NPA. Apparently due to the background activities observed, PGP-mediated efflux exhibited reduced sensitivity to quercetin and standard MDR/PGP inhibitors at lower IAA concentrations (Figure 6e).

Discussion

Taken together, these results indicate that, in *Arabidopsis*, PGP1 can mediate cellular efflux of IAA and some IAA metabolites. Further, protoplast and whole-plant transport assays suggest that PGPs are capable of mediating auxin transport *in planta*, although other transport proteins may also function in auxin efflux. As PGP1-mediated auxin efflux in heterologous systems exhibits decreased specificity and AEI sensitivity, other factors present *in planta* are probably required for the high degree of specificity seen in polar auxin transport. Non-polar localization of PGP1 at root and shoot apices suggests that interactions with other proteins are also required to confer directionality to auxin transport in those tissues. In these tissues, where rediffusion of

IAA exported from small cells would be expected to impair gradient-driven transport, additional energy-dependent IAA efflux might be required.

PGP1 localization and inhibition by quercetin are also consistent with its proposed interaction with endogenous flavonoids (Murphy et al., 2000; Peer et al., 2004). Strong expression of PGP1 in apical tissues, localized reduction of IAA transport in the root tips of *pgp1* mutants, and PGP-mediated transport of IAA breakdown products suggest that PGP1 functions in regions exposed to high auxin concentrations. Further, the non-polar localization of PGP1 in root apices suggests that, where PIN–PGP interactions might take place, PIN proteins may confer an accelerated vectoral component to PGP-mediated transport. Specific interactions of the many PIN and PGP family members in discrete tissues would be predicted to provide tight control of transport mechanisms. To elucidate the role of PGP family members in auxin transport, further developmental and cell biological studies are required.

Experimental procedures

Plant growth conditions

Plants were grown as described previously (Geisler *et al.*, 2003). For phenotypes of adult plants, Col-0, *pgp1* (At2g36910) and *pgp19* (At3g28860) mutants were grown under short-day conditions: 8 h 100 μmol m^{-2} sec^{-1} white light, 22°C.

Expression and localization analysis

To construct the PGP1 (At2g36910) cmyc tag line (Pro_{PGP1}:PGP1-cmyc), a synthetic double-stranded oligonucleotide (forward primer: 5'-*ctag*agcagaagctt**t**atctccgaggaggacct*ctagt*gagct; reverse primer: 5'-c*actagt*aggtcctcctcggagat**a**agcttctgct) encoding the 9E10 c-myc epitope was introduced into *Spe*I and *Sac*I sites of construct p4kbPstI (Sidler *et al.*, 1998), leading to p4kbMyc2. The cmyc epitope is thereby inserted at amino acid residue Leu_{14}. In comparison with the original sequence, a base pair was changed (bold letter) leading to introduction of a diagnostic *Hin*dIII site (underlined) without changing the codon bias. The 5'*Spe*I site of the oligonucleotide (italic) was designed in such a way that it was destroyed upon ligation, allowing us to use the downstream *Spe*I site (italic) for further cloning. To add the 3'-terminal part of the *PGP1* gene, a 6.7-kb *Spe*I fragment was cut out from plasmid pOE and inserted in the correct orientation into p4kbMyc2 predigested with *Spe*I, leading to pBSKMdrMyc2. From this a 9-kb *Sal*I fragment encompassing *PGP1* was subcloned into the *Sal*I site of binary plant transformation vector pBI101 (Clontech, Palo Alto, CA, USA). The final construct, PGP1cmyc2b (Pro_{PGP1}:PGP1-cmyc), containing the full-length genomic fragment of *PGP1* (including the cmyc tag at base pair 980) flanked by the *PGP1* promoter and terminator sequences, was introduced into *Arabidopsis thaliana* (ecotype Columbia) by *Agrobacterium tumefaciens*-mediated vacuum infiltration. Homozygous plants were selected on 0.5× MS medium containing 50 μg ml^{-1} kanamycin, and insertion was verified by Southern analysis.

For complementation, *pgp1* mutant plants (Noh *et al.*, 2001) were transformed with the binary vector PGP1cmyc2b (Pro_{PGP1}:PGP1-cmyc) via vacuum infiltration, and homozygous lines were selected on 0.5× Murashige and Skoog (MS) medium containing kanamycin.

Arabidopsis seedlings were grown on 1% phytagar plates (0.5× MS basal salts, pH 4.85) under white light (photon flux rate 100 μmol m^{-2} sec^{-1}, 14 h light, 22°C) and 5- and 9-day seedlings were prepared for immunolocalization as described by Friml *et al.* (2003) with the following modifications: in some cases, in place of 2% driselase, 0.5 pectolyase was used for 5-day seedlings and 0.8% pectolyase for 9-day roots. Seedlings were incubated overnight (37°C) with mouse anti-cmyc antibody (Santa Cruz Biotechnology, Santa Cruz, CA, USA) at 1:250 dilution, for 3 h at 37°C with rabbit anti-mouse-FITC (whole IgG, Sigma F7506, St Louis, MO, USA) and for 3 h at 37°C with goat anti-rabbit-Alexa 488 at 1:250 in 3% BSA/MTSB, respectively. Immunofluorescence analysis was done using a confocal laser scanning microscope (Nikon, Melville, NY, USA, Eclipse 800) equipped with an argon laser (488 nm) (Bio-Rad). Images were captured with a SPOT camera and processed using Adobe photoshop 5.0.

For histochemical GUS staining, 10-day light-grown Pro_{PGP1}:GUS transgenic seedlings were incubated in 10 mm HEPES (pH 5.2), 500 mm sorbitol containing 2 μm benzoic acid or IAA for 3 h. For all comparisons between treatments, identical staining conditions were used. For promoter gene quantification, Pro_{PGP1}:GUS transgenic seedlings were transferred for 3 h onto 0.5×

MS plates supplemented with 1 μm IAA. Seedlings were washed in MS and separated manually into root and shoot, and GUS activity was assayed using 4-β-4-methylumbelliferone-glucuronide as substrate. For each sample, segments of 40 seedlings were pooled and analyzed.

Protoplast and cell culture efflux experiments

Arabidopsis mesophyll protoplasts were prepared from rosette leaves of plants grown on soil under white light (100 μmol m^{-2} sec^{-1}, 8 h light/16 h dark, 22°C). Intact protoplasts were isolated as described (Geisler *et al.*, 2003) and loaded by incubation with 1 μl ml^{-1} ^{3}H-IAA (specific activity 20 Ci $mmol^{-1}$, American Radiolabeled Chemicals, St Louis, MO, USA), 7-^{14}C-benzoic acid (53 mCi $mmol^{-1}$, Moravek Biochemicals, Brea, CA, USA) or 4-^{3}H-1-naphthalene acetic acid (25 Ci $mmol^{-1}$, American Radiolabeled Chemicals) on ice. External radioactivity was removed by separating protoplasts using a 50–30–5% percoll gradient. Samples were incubated at 25°C and efflux halted by silicon oil centrifugation. Retained and effluxed radioactivity was determined by scintillation counting of protoplast pellets and aqueous phases. For inhibitor studies, protoplasts were isolated and assayed in the presence of 10 μm of indicated inhibitors or the solvent alone.

Efflux experiments were performed with three to five independent protoplast preparations with four replicas for each time point. Protoplast volumes were determined by the addition of 0.05 μCi ^3H_2O in separate assays; protoplast surfaces were calculated by measuring protoplast diameters. Vacuolar pH was determined directly from homogenated whole leaves following centrifugation.

For inhibitor studies, 50 ml Arabidopsis cell suspension culture (May and Leaver, 1993) was grown in MS basal medium supplemented with 3% sucrose (w/v), 0.5 mg l^{-1} naphthalene acetic acid, and 0.05 mg l^{-1} kinetin in the presence of 10 μm of indicated inhibitors or the solvent alone for 12 h. Prior to measurements, the culture was centrifuged for 10 min at 115g and 4°C, washed with sterile water and resuspended in 10 ml MCP (500 mm sorbitol, 1 mm $CaCl_2$, 10 mm MES, pH 5.6). Then 1 μl ml^{-1} ^{3}H-IAA (specific activity 20 Ci $mmol^{-1}$, American Radiolabeled Chemicals) was added, and four 500 μl aliquots were collected after 0 and 10 min incubation at 25°C and filtered on Millipore Durapore 0.22 μm GV filters. Cylcopropyl propane dione (CPD) was obtained from Caisson Labs (Rexburg, ID, USA).

Transcript detection by RT-PCR

Total RNA from Arabidopsis wild-type protoplasts was prepared, and DNaseI (Qiagen, Valencia, CA, USA) treatment was performed with column-bound RNA. Oligo dT-primed cDNA from 1 μg total RNA was synthesized using the reverse transcription system (Promega, Madison, WI, USA). Transcripts specific for *PGP1* (At2g36910), *PIN1* (At1g73590), *PIN2* (At5g57090), *PIN3* (At1g70940), *PIN4* (At2g01420) and 40S ribosomal protein *S16* (At2g09990) were detected by conventional PCR for 30 and 35 cycles at 52°C annealing temperature. Intron-spanning PCR primers were: S16-S 5'-ggcgactcaaccagctactga; S16-AS 5'-cggtaactctt tggtaacga; PGP1-S 5'-gtccctcaagagccgtgcttg; PGP1-AS 5'-ccatcatcgatgacagcgatc, PIN1-S 5'-tggagctcaagtgcttcgccg; PIN1-AS 5'-gagaagagttatgggcaacgc; PIN2-S 5'-cacggggtcaacgagtggagc; PIN2-AS 5'-ctgagaatatcaggatggacg; PIN3-S 5'-tgatgacaaggctgatactg; PIN3-AS 5'-gtaaatcaccacgtaatccg; PIN4-S 5'-acaacgccgttaaatatgga; PIN4-AS 5'-agaccccattttattcagcc. Equal volumes of PCR products were separated on 2.5% agarose gels. Negative controls in the absence of enzyme in the reverse transcriptase reaction yielded no products.

RNA isolation and quantitative RT–PCR analysis

RNA isolation and quantitative RT–PCR analysis were carried out as described previously, with slight modification (Blakeslee et al., 2004), using the ABI Prism 7000 Sequence Detection System (Applied Biosystems, Foster City, CA, USA) in mixtures of 10 μl TaqMan Universal PCR Master Mix containing AmpliTaq Gold DNA polymerase, AmpErase uracil-*N*-glycosylase (UNG), deoxynucleoside triphosphates with dUTP, a passive reference dye, optimized buffer components (Applied Biosystems), 500 nm each primer and optimum amount of template DNA in a total volume of 20 μl. *β-tubulin* (At5g12250) forward and reverse primers were 5'-ttcccgggtcagctcaac and 5'-ggagacgagggaaaggaatga, respectively. Primers used for the *AtPGP1* transcript were 5'-tctggcgactagctaaaatgaactc and 5'-ccacaaatgacagagcctactga. The *AtPGP19* forward primer sequence was 5'-ggaagtttgaggaatctgagctattc, and the reverse primer sequence was 5'-

tcggtcagtctctgcatttga. Transcripts specific for *β-tubulin*, *AtPGP1* and *AtPGP19* were detected by PCR; activation of AmpErase UNG (2 min, 50°C) and *Taq* polymerase (10 min, 95°C), 40 cycles of denaturation (15 sec, 95°C) and elongation (1 min, 60°C).

Analysis of IAA contents and transport

pgp1 mutants expressing the maximal auxin-inducible reporter Pro_{DR5}:GUS (Ulmasov *et al.*, 1997) were generated via crossing with wild-type Pro_{DR5}:GUS plants. Seedlings were grown for 5 days as described above and stained for GUS expression (Ulmasov *et al.*, 1997).

For endogenous free auxin quantification, seedlings were grown as previously described (Geisler *et al.*, 2003). Nine days after planting seedlings were harvested, the cotyledons excised, and seedlings cut in half at the root–shoot transition zone. Roots and shoots were collected in lots of 500, and free auxin was quantified by GC-MS as described previously (Chen *et al.*, 1988). Data presented are the averages of three lots of 500 seedlings. Auxin quantifications were confirmed by GC-MS after pentafluorobenzyl derivatization (Prinsen *et al.*, 2000).

For additional free auxin quantifications, hypocotyl and root segments of 30–50 seedlings were collected and pooled. Samples were extracted and analyzed by GC-MS. Calculation of isotopic dilution factors was based on the addition of 100 pmol $^2H_2$-IAA to each sample. In some cases, roots of 40 seedlings were divided manually into 2-, 8- and 10-mm segments from the root tip, and analyzed as described above.

Auxin transport assays on intact, light-grown Arabidopsis seedlings treated with a 0.1 μl microdroplet of 1 μm auxin at the root apical meristem, using techniques described by Geisler *et al.* (2003), and root segments of 2 mm, were collected 2, 4 and 6 mm from the root tip.

2-NAA quantification

Triplicate samples were pooled and extracted in methanol/2% HCl with shaking at 4°C for 30 min. An equal volume of diethylether/hexane (1:1) was added, samples were shaken vigorously, and the upper phase was collected. This was repeated twice. Aminopropylsilyl solid phase extraction columns (Alltech, State College, PA, USA), were preconditioned with hexane before sample extracts were added. Eluate was collected from the application of three bed volumes of diethylether/2% formic acid to the column. Samples were dried prior to resuspension in methanol/1% phosphoric acid. Samples were analyzed by LC-MS using a Waters C18 MS column on a Q-TOF Micro equipped with a collision cell and phosphoric acid lock spray for internal calibration (Waters, Bedford, MA, USA), using naphthalene as an internal standard.

Auxin metabolite characterization

IAA oxidative breakdown products were determined by LC-MS and GC-MS (Ljung *et al.*, 2002, 2005).

Yeast assays

The PGP1 cDNA was cut out from plasmid pUCcMDR (Windsor *et al.*, 2003) with *Stu*I and *Hin*cII and cloned into the Klenow filled *Not*I site of yeast shuttle vector pNEV (pNEV-PGP1). pNEV and pNEV-PGP1 were introduced into *S. cerevisiae* strain JK93dα or *yap1-1* (Prusty *et al.*, 2004), and single colonies were grown in synthetic minimal medium without uracil (SD-URA), supplemented with 2% glucose. For detoxification assays, transformants grown in SD-URA to an OD_{600} of approximately 0.8 were washed and diluted to $OD_{600} = 1$ in water. Cells were 10-fold diluted five times, and 5 μl of each dilution were spotted onto minimal media plates supplemented with 10 μm IAA. Growth at 30°C was assessed after 3–5 days. Assays were performed with three independent transformants.

For loading experiments, cells were grown to $OD_{600} = 1$, washed and incubated at 30°C with combinations of 1 μl ml^{-1} 5-^{3}H-IAA (specific activity 20 Ci mmol^{-1}, American Radiolabeled Chemicals), 7-^{14}C-BA (53 mCi mmol^{-1}, Moravek Biochemicals), 4-^{3}H-1-NAA (25 Ci mmol^{-1}, American Radiolabeled Chemicals) or 1 μm 2-NAA (Sigma) in SD-URA (pH 4.5). Aliquots of 0.5 ml were taken after 0, 5, 10, 30, 60 and 120 min incubation at 30°C. For efflux experiments, cells were loaded for 10 min on ice, washed twice with cold water, and resuspended in 15 ml SD (pH 4.5). Then 0.5-ml aliquots were taken after 0, 2.5, 5, 7.5 10, 15 and 20 min incubation at 30°C.

For assaying permeabilities, yeast was grown to

logarithmic phase (OD_{600} = 1.25), washed with water followed by fluorescein diacetate (FDA) buffer, and resuspended in 5 ml FDA buffer [50 mm HEPES-NaOH (pH 7.0), 5 mm 2-deoxy-d-glucose]. Then 10 μl 5 mm FDA was added to a 990 μl cell suspension, and aliquots were measured at 485 nm excitation and 535 nm emission. To determine the temperature dependency of efflux, loaded yeast cells were washed, divided into two aliquots and incubated at 4 and 30°C, respectively. For assaying ATP dependency of transport, yeast were grown to logarithmic phase, washed with water and FDA buffer, resuspended in 50 ml FDA buffer, and incubated for 1 h at 30°C. Cells were harvested, washed and resuspended in 10.8 ml 20 mm sodium citrate (pH 4.5). After temperature equilibration at 30°C, 1 μl ml^{-1} 5-^{3}H-IAA was added, and resuspensions were divided into two aliquots followed by addition of 0.6 ml 20% glucose to one aliquot. For inhibitor studies, yeasts were grown for 12 h prior to measurement, and assayed in the presence of 10 μm of indicated inhibitors or the solvent alone.

All aliquots were filtered on Whatman GF/C filters and washed three times with cold water, and retained radioactivity was quantified by scintillation counting. All transport experiments were performed three to five times with independent transformants, with four replicas each.

To verify the identity of effluxed IAA, yeast cells transformed with pNEV and pNEV-PGP1 were loaded with 10 μm $^{2}H_{5}$-IAA and 1 μm $^{13}C_{6}$-IAA in 20 mm sodium citrate (pH 4.5). Effluxed IAA was extracted by ethyl acetate and analyzed by MS-MS.

Yeast PGP1 expression and immunolocalization

Yeast cells transformed with pNEV and pNEV-PGP1 were grown to mid-log phase and microsomes were separated via 7.5% PAGE. Western blots were immunoprobed using anti-PGP1 antibody (Sidler *et al.*, 1998). Yeast immunolocalization was performed using standard protocols. Fixed yeast cells were incubated overnight at 30°C with rabbit anti-PGP1 antibody (Sidler *et al.*, 1998) and for 3 h with goat anti-rabbit-Alexa 488 at 1:200 in 3% BSA. Stained cells were incubated in mounting media containing 4',6-diamidino-2-phenylindole (DAPI), and immunofluorescence analysis was done using a confocal laser scanning microscope (Leica, DMIRE2) equipped with argon (488 nm) and UV laser (410 nm). Fluorescence, differential interference contrast and DAPI images were processed using Adobe photoshop 7.0. Vector controls showed no detectable fluorescence with anti-PGP1 antibody.

HeLa cell assays

Radiolabeled substrate accumulation assay. PGP1 (At2g36910) was expressed in mammalian HeLa cells using a vaccinia virus co-transfection system providing several advantages over other heterologous expression systems, including proper glycosylation and suppression of host-protein synthesis following vaccinia infection (Elroy-Stein and Moss, 1991). The transient vaccinia expression system was used because stable cell lines develop mutations and express other endogenous drug-resistance mechanisms. Full-length, hemagglutinin (HA)-tagged PGP1 was cloned into the multiple cloning site of the pTM1 vector (Hrycyna *et al.*, 1998). For pTM1-PGP1, a *PGP1* PCR fragment containing *Xma*I/*Bam*HI restriction sites was generated using the following primers: PGP1-S 5'-tcc ccc cgg ggc atg gat aat gac ggt and PGP1-AS 5'-cgc gga tcc agc gta atc tgg tac gtc gta agc atc atc ttc ctt aac. Assays for accumulation of radiolabeled substrates were performed according to the method described by Hrycyna *et al.* (1998), with the following modifications: cells were transfected in six-well plates with 2 μg DNA (pTM1 control vector, PGP1) per well. For radiolabeled substrate accumulation assays, gradient conditions were developed wherein radiolabeled auxin was passively accumulated by empty vector control HeLa cells without induction of cellular damage. Confluent cells were transfected in six-well plates, and 16–24 h after transfection cells were washed with 3 ml pre-warmed Dulbecco's modified Eagle's medium, 5% fetal bovine serum. Each transfection utilized 600 000–1 000 000 cells, and equal loading of wells was verified by sampled cell counts. Cell counts were determined by Coulter counting and microscopic visualization (percentage confluence). Cells were then incubated with 2 ml PBS citrate buffer pH 5.5, 5% calf sera containing either 10 or 62.5 nm of the following radiolabeled substrates: ^{3}H-IAA (specific activity 26 Ci $mmol^{-1}$, Amersham Biosciences, Piscataway, NJ, USA); ^{3}H-benzoic acid (specific activity 20 Ci $mmol^{-1}$, American Radiolabeled Chemicals); or ^{3}H-1-NAA (specific activity 20 Ci $mmol^{-1}$, American Radiolabeled Chemicals). Possibly due to buffer compatibility issues, it was difficult to

maintain solubilization of 1-NAA in loading assays. For radiolabeled auxin degradation product assays, cells were loaded with 10 nm radiolabeled IAA breakdown products (specific activity 25 Ci $mmol^{-1}$, American Radiolabeled Chemicals). Cells were incubated with radiolabeled substrates for 40 min at 37°C, 5% CO_2. For inhibitor studies, cells were incubated with radiolabeled IAA in the presence of 10 μm NPA, 200 nm quercetin, 1 μm cyclosporin A or 5 μm verapamil. After incubation, cells were washed three times with 3 ml ice-cold PBS, removed from the wells by trypsinization, and added to 18 ml scintillation fluid. Samples were counted in a Perkin-Elmer scintillation counter. Components of the radiolabeled auxin breakdown product mixture were determined and quantified via LC-MS. For cold 2-NAA retention studies, cells were incubated with 62.59 nm cold 2-NAA, harvested and extracted. 2-NAA was quantified using LC-MS. As with 1-NAA, it proved difficult to keep 2-NAA solubilized for cell loading in the buffer system used. Fluorescent substrate accumulation assays were performed in the HeLa cell system as previously described (Hrycyna *et al.*, 1998).

Data points were normalized to the average empty control vector value of 2851.885 DPM/500 000 cells for auxin treatments. Cell viability after treatment was confirmed visually and via cell counting.

Western blotting of HeLa cells

HeLa cells expressing PGP1 were harvested using a rubber policeman. Proteins were isolated from cells as described previously (Hrycyna *et al.*, 1998). Proteins were separated via 7% SDS-PAGE, then transferred onto nylon membrane at 10 V, in an ice bath, overnight. After blocking with 5% non-fat dried milk in 1× PBS with 0.1% Tween 20, the nylon membrane was incubated with primary antibody for 2 h at 4°C (anti-HA, Sigma). Following washing, membranes were incubated with horseradish peroxidase-conjugated secondary antibody, and developed using the ECL chemiluminescence system according to the manufacturer's protocol (Amersham Pharmacia Biotech, Piscataway, NJ, USA).

Data analysis

Data were analyzed using prism 4.0b (Graphpad Software, San Diego, CA, USA). Statistical analysis was performed using spss 11.0 (SPSS Inc., Chicago, IL, USA) and sigmastat (Systat, Point Richmond, CA, USA).

Acknowledgements

We thank V. Croy, C. Gaillard, C. Ringli and A. Hopf for technical assistance, S. Plaza for help with statistical analysis, and I. Baxter for microarray data. This publication is dedicated to M.D.R. Louma (MG) and to the memory of Kenneth Thimann (ASM and WAP). This manuscript was written by ASM, MG, JJB, WAP and EM. Experiments were conceptualized by MG, JJB, WAP, ASM and EM. Auxin transport assays – whole plant: JJB; protoplast: MG, RB, VV, AB, JJB and ASM; yeast: MG, RB, JJB and ASM; HeLa cells: JJB. Implementation of HeLa cell system for auxin transport studies: JJB, ASM, ORL, KFKE and CAH. Immunolocalizations – yeast: JJB, MG and VV; Arabidopsis PIN and PGP-cmyc: AB, BT, CB and UG. Auxin determinations – ASM, AM and ELR. Cloning of PGP1 into the pTM1 expression vector by ORL. Real-time PCR analysis of PGP1 expression in HeLa cells and whole plants by ORL and WAP. DR5::GUS/PGP reporter constructs prepared by AS and ASM; DR5::GUS assays by JJB and WAP; PGP1::GUS reporter constructs created by RD; PGP1::GUS assays by MG; PGP1-cmyc transformants created by MG. Funding: National Science Foundation (US) to ASM, National Science Foundation (SWISS) to EM.

Supplemental data

The original on-line version of this article (available at http://www.blackwellpublishing.com) contains the following supplemental figures .

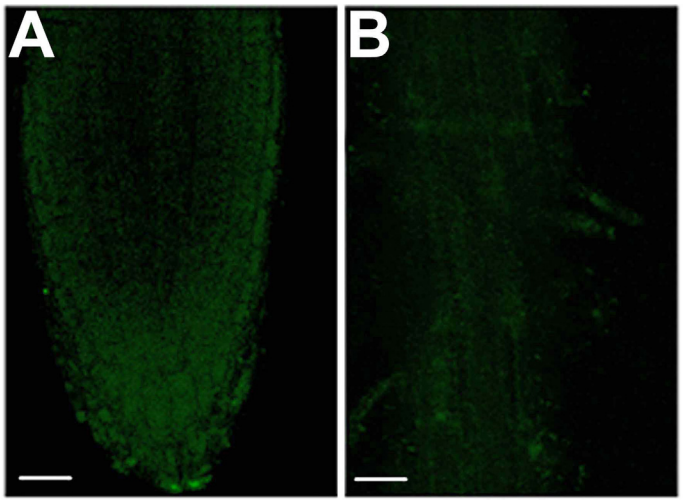

SUPPL. FIGURE 1. **Anti-c-myc antibody controls.** ***A,*** No immunolocalization signal was observed in wild type root tips with the anti-c-myc antibody. ***B,*** No immunolocalization signal was observed in wild type mature roots with the anti-c-myc antibody. Bar, 125 *μ*m.

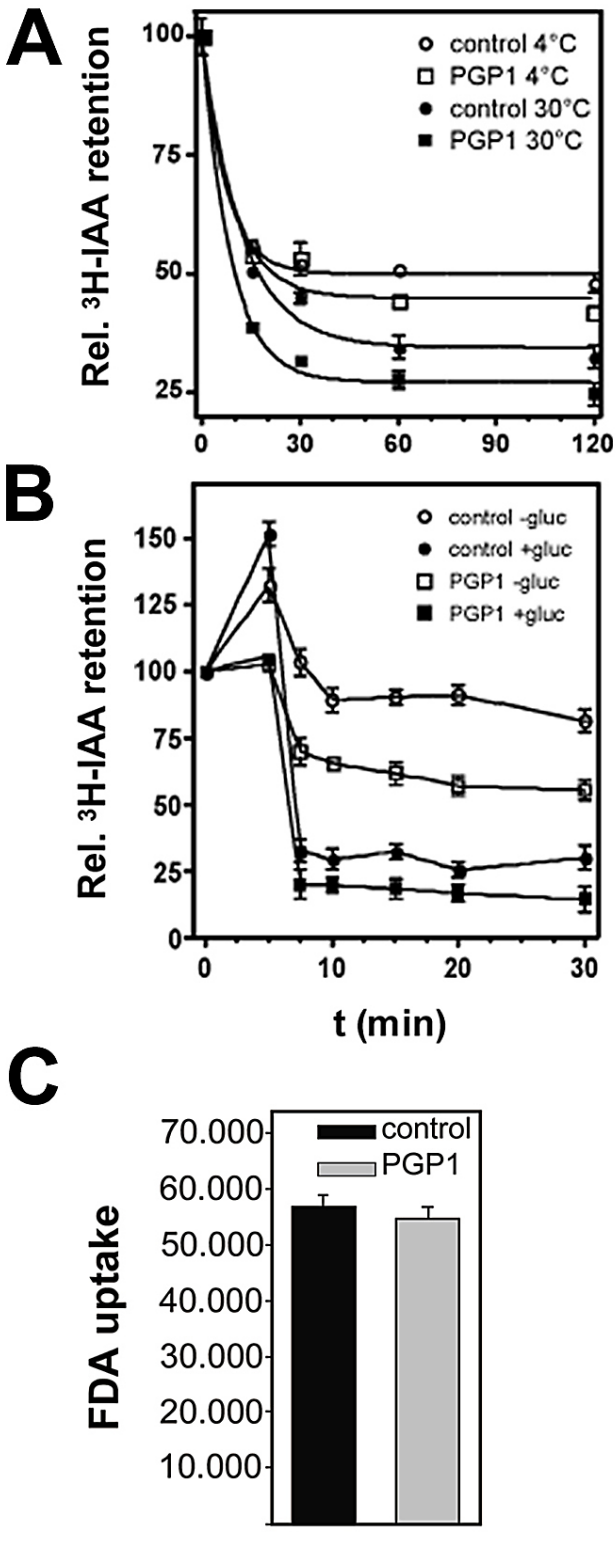

SUPPL. FIGURE 2. ***PGP1*** **expressed in yeast cells with reduced ABC transporter activity.**
As might be expected for an energized transport mechanism, PGP1-mediated IAA export in yeast was both temperature- and glucose-dependent ***(A, B)***. Yeast cell permeability was similar in cells transformed with either empty vector or *PGP1* ***(C)***. ***A,*** IAA efflux in yeast is temperature-dependent. Initial loading was at the same magnitude (±10%). Presented data represent relative mean activities plus standard deviations. ***B,*** IAA efflux in yeast is glucose-dependent. Initial loading was at the same magnitude (±10%). Presented data represent relative mean activities plus standard deviations. ***C,*** Yeast transformed with pNEV-PGP1 (PGP1) or empty plasmid pNEV (control) have similar permeabilities. Yeast cells were incubated with the dye FDA and internal fluorescence was measured. Presented data represent relative mean activities of three to five individual measurements of four samples plus standard deviations.

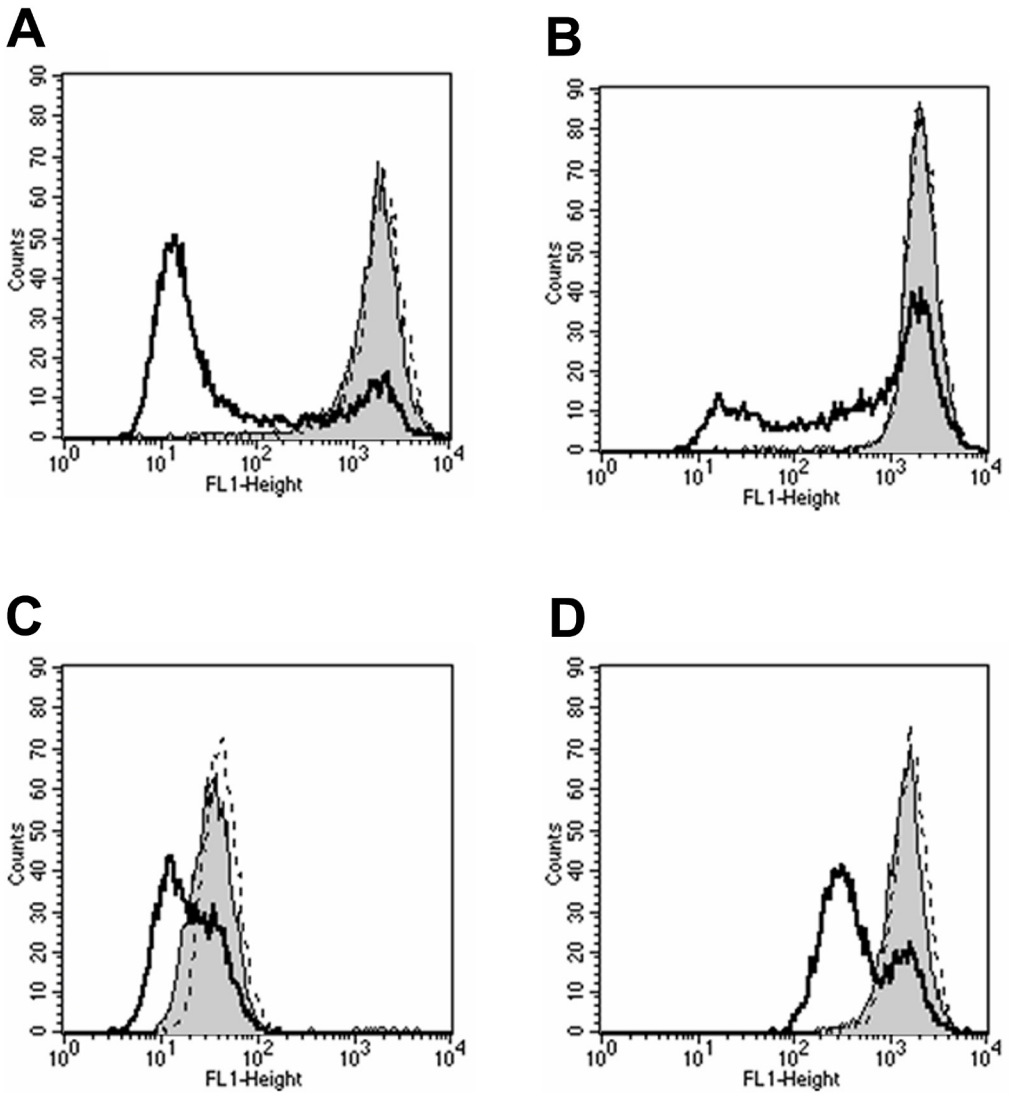

SUPPL. FIGURE 3. ***PGP1* expressed in HeLa cells did not transport HsMDR substrates.**
A-D, HeLa cells expressing PGP1 did not transport common mammalian MDR substrates. Grey peak represents cells transformed with pTM1 control vector (negative control). Solid line, *Homo sapiens* MDR1 (positive control); large dashes, PGP1. Shifting of observed peaks to the left indicates transport of the fluorescent substrate. Substrates tested: ***A,*** Rhodamine 123, ***B,*** Rhodamine 123 + cyclosporin A (1 μM), ***C,*** daunomycin, and ***D,*** BODIPY-tagged vinblastine. Assays were performed according previously described protocols (Hrycyna *et al.*, 1998), and substrate retention was analyzed by FACS.

Immunophilin-like TWISTED DWARF1 Modulates Auxin Efflux Activities of Arabidopsis P-glycoproteins

Rodolphe Bouchard[‡], Aurélien Bailly[‡], Joshua J. Blakeslee[§], Sophie C. Oehring[‡], Vincent Vincenzetti[‡], Ok Ran Lee[§1], Ivan Paponov[¶], Klaus Palme[¶], Stefano Mancuso[‖], Angus S. Murphy[§], Burkhard Schulz[§], and Markus Geisler[‡2]

From the [‡]Zurich-Basel Plant Science Center, University of Zurich, Institute of Plant Biology, and Molecular Plant Physiology, CH-8008 Zurich, Switzerland, the [§]Department of Horticulture and Landscape Architecture, Purdue University, West Lafayette, Indiana 47907, the [¶]Institut für Biologie II, Universität Freiburg, D-79104 Freiburg, Germany, and the [‖]Department of Horticulture, University of Firenze, I-50019 Sesto Fiorentino, Italy

[1] Present address: Department of Biology Chungnam National University, Daejeon 305–764, Korea.
[2] To whom correspondence should be addressed: Inst. of Plant Biology, University of Zurich, Zolliker Strasse 107, CH-8008 Zurich, Switzerland. Tel.: 41-1-634-8276; Fax: 41-1-634-8204; E-mail: markus.geisler@botinst.unizh.ch.

Summary

The immunophilin-like protein TWISTED DWARF1 (TWD1/FKBP42) has been shown to physically interact with the multidrug resistance/P-glycoprotein (PGP) ATP-binding cassette transporters PGP1 and PGP19 (MDR1). Overlapping phenotypes of *pgp1/pgp19* and *twd1* mutant plants suggested a positive regulatory role of TWD1 in PGP-mediated export of the plant hormone auxin, which controls plant development. Here, we provide evidence at the cellular and plant levels that TWD1 controls PGP-mediated auxin transport. *twd1* and *pgp1/pgp19* cells showed greatly reduced export of the native auxin indole-3-acetic acid (IAA). Constitutive overexpression of PGP1 and PGP19, but not TWD1, enhanced auxin export. Coexpression of TWD1 and PGP1 in yeast and mammalian cells verified the specificity of the regulatory effect. Employing an IAA-specific microelectrode demonstrated that IAA influx in the root elongation zone was perturbed and apically shifted in *pgp1/pgp19* and *twd1* roots. Mature roots of *pgp1/pgp19* and *twd1* plants revealed elevated levels of free IAA, which seemed to account for agravitropic root behavior. Our data suggest a novel mode of PGP regulation via FK506-binding protein-like immunophilins, implicating possible alternative strategies to overcome multidrug resistance.

Introduction

The plant signaling molecule auxin (indole-3-acetic acid (IAA))[3] plays a critical role in plant growth and development (Benkova *et al.*, 2003; Friml and Wisnieswska, 2005; Friml, 2003). Moreover, IAA has been shown to have potential value as a photoactivable cytotoxin with applications in cancer therapy (Folkes and Wardman, 2003). Although auxin signaling shares some similarities with mammalian neurotransmitter signaling (Baluska *et al.*, 2003; Schlicht *et al.*, 2006), auxin is generally classified as a phytohormone because of its transport from sites of synthesis to loci of activity. Auxin transport is polar from the shoot apex to the root apex and in reverse to the root-hypocotyl junction in a cell-to-cell manner (Blakeslee *et al.*, 2005; Friml, 2003). Polar auxin transport appears to provide essential directional and positional information for developmental and physiological processes (Blilou *et al.*, 2005). A chemiosmotic model of auxin transport (Goldsmith, 1977; Lomax *et al.*, 1995) was supported by the identification and characterization of candidate proteins for auxin influx (AUX1/LAX family) and efflux (PIN family) (reviewed in Friml *et al.* (2005) and Blakeslee *et al.* (2005)). Members of both families are essential components of auxin influx and efflux complexes, and most strikingly, the major proteins of both families (AUX1 and PIN1) reveal polar expression patterns that are congruent with known routes of auxin movement (Friml, 2003). Evidence has been provided for a model in which multiple PIN proteins interact to create an auxin reflux loop (Blilou *et al.*, 2005), and it has been shown recently that some members of the PIN family are rate-limiting factors in cellular auxin efflux (Petrášek *et al.*, 2006).

Recently, members of the large plant multidrug resistance (MDR)/P-glycoprotein (PGP)/ABCB family (hereafter referred to as PGP) have been shown to function in auxin transport (Blakeslee *et al.*, 2005; Martinoia *et al.*, 2002; Jasinski *et al.*, 2003; Geisler and Murphy, 2006). Mammalian members of this superfamily of ATP-binding cassette (ABC) transporters are widely studied because they catalyze ATP-dependent export of planar anionic chemotherapeutic agents (Krishna and Mayer, 2001). Loss-of-function mutations in *PGP1* and *PGP19* (*MDR1*) result in reduced auxin transport in intact tissues and impaired growth in *Arabidopsis* (Noh *et al.*, 2001; Geisler *et al.*, 2003; Geisler *et al.*, 2005; Lin and Wang, 2005), maize (*Zea mays pgp1*/*brachytic2*), and sorghum (*Sorghum bicolor pgp1*/*dwarf3*) (Multani *et al.*, 2003). Interestingly, the dwarf phenotype of *pgp1*/*pgp19* double mutants is more severe than those of the single knockouts, suggesting separate but overlapping functions (Geisler *et al.*, 2003; Lin and Wang, 2005). PGP1 has been shown to catalyze the primary active transport of native and synthetic auxins using plant and heterologous transport systems. PGP1 activity is inhibited by auxin efflux inhibitors such as *N*-1-naphthylphthalamic acid (NPA) and flavonols as well as anticancer drugs such as verapamil and cyclosporin A (Geisler *et al.*, 2005). Consistent with predictions from chemiosmotic models of sites requiring additional direct auxin efflux (Blakeslee *et al.*, 2005), PGP1 exhibits non-polar plasma membrane localization in small meristematic cells of the root and shoot apices and polar (mainly basal) expression in expanded cells of the elongation zone and above. Two recent studies showed that a related protein (PGP4) functions in root and root hair development and that it catalyzes substantial auxin influx (Santelia *et al.*, 2005; Terasaka *et al.*, 2005), suggesting that PGP1 and PGP4 might function cooperatively in auxin movement (Geisler and Murphy, 2006; Santelia *et al.*, 2005).

Plant PGPs seem to function as central catalytic elements of multiprotein auxin transport complexes (Blakeslee *et al.*, 2005; Geisler and Murphy, 2006; Geisler *et al.*, 2003; Murphy *et al.*, 2002). The C-terminus of PGP1 has been identified in a yeast two-hybrid screen using the soluble portion of the putative glycosylphosphatidylinositol-anchored immunophilin-like protein TWISTED DWARF1 (TWD1/FKBP42) as bait (Geisler *et al.*, 2003). Moreover, several PGPs (including PGP1, PGP19, and PGP4) have been co-purified with TWD1 from high affinity NPA-binding complexes with other proteins known to be involved in protein trafficking and cycling (Murphy *et al.*, 2002; Geisler *et al.*, 2003). *twd1* plants, which are allelic to *ultracurvata2* (*ucu2*) (Perez-Perez *et al.*, 2004), show a drastic pleiotropic auxin-related phenotype that includes dwarfism,

[3] The abbreviations used are: IAA, indole-3-acetic acid; MDR, multidrug resistance; PGP, P-glycoprotein; ABC, ATP-binding cassette; NPA, N-1-naphthylphthalamic acid; FKBP, FK506-binding protein; MRP, MDR-associated protein; GFP, green fluorescent protein; GC-MS, gas chromatography mass spectrometry; RT, reverse transcription; YFP, yellow fluorescent protein; CFP, cyan fluorescent protein; HA, hemagglutinin; NAA, naphthylacetic acid.

epinastically growing leaves, and disorientation of organ growth at both the epidermal and whole plant levels. Interestingly, *twd1* plants resemble those of *pgp1*/*pgp19* double mutants, and PGP1/PGP19-TWD1 interaction can be verified by a broad array of methods (Geisler *et al.*, 2003). Similar mutant phenotypes, together with reduced auxin transport in intact hypocotyls, suggested a regulatory role for PGP1 and PGP19 in auxin transport (Geisler and Murphy, 2006; Geisler *et al.*, 2003; Romano *et al.*, 2005).

TWD1 belongs to the FK506-binding protein (FKBP)-type subfamily of immunophilins, which are ubiquitous proteins known to mediate immunosuppression in mammals (Romano *et al.*, 2005; Harrar *et al.*, 2001; Schiene and Fischer, 2000). Based on drastic phenotypes of knock-out mutants and transgenic plants with altered gene expression levels, multidomain FKBPs such as PASTICCINO1 (FKBP52/PAS1) and wheat FKBP77 (Faure *et al.*, 1998; Vittorioso *et al.*, 1998; Kurek *et al.*, 2002) have been found to be key players in plant development (Harrar *et al.*, 2001). TWD1, which also belongs to the multidomain FKBP family, is distinguished by its unique C-terminal membrane anchor, which localizes the protein to both the plasma (Geisler *et al.*, 2003) and vacuolar (Kamphausen *et al.*, 2002) membranes. In the latter, TWD1 functionally interacts with the C termini of MDR-associated protein (MRP)-like ABC transporters MRP1 and MRP2 (Geisler *et al.*, 2004). Interestingly, both pairs of ABC transporters interact with independent domains of TWD1. PGP1 and PGP19 interact with the *cis,trans*-peptidylprolyl isomerase-like domain, and MRP1 and MRP2 interact with the tetratricopeptide repeat domain. This difference in binding to TWD1 domains might specify functional diversity of the interactions.

In both cases, regulatory roles of TWD1 in individual ABC transporter pairs have been suggested (Geisler *et al.*, 2003; Geisler *et al.*, 2004), but the final molecular proof is still lacking. Mammalian FKBPs are known to bind and modulate calcium release channels (Cameron *et al.*, 1995; Timerman *et al.*, 1995). Furthermore, FKBP12 has been shown to regulate murine MDR3 activity, but attempts to demonstrate interaction have been thus far unsuccessful (Hemenway and Heitman, 1996). Interestingly, FKBP12-dependent regulation of MDR3-mediated drug resistance does not require *cis,trans*-peptidylprolyl isomerase activity (Cameron *et al.*, 1995; Mealey *et al.*, 1999). Consistent with these observations, the PGP-interacting *cis,trans*-peptidylprolyl isomerase-like domain of TWD1 has been shown to lack any isomerase activity and not to bind FK506 (Kamphausen *et al.*, 2002; Weiergraber *et al.*, 2006). Here, we provide several lines of evidence that TWD1 functions as a positive regulator of PGP1-mediated auxin transport, suggesting a novel mode of PGP regulation via FKBP-type immunophilins.

Experimental procedures

Plant growth conditions

Arabidopsis thaliana plants were grown as described previously (Geisler *et al.*, 2003). For quantification of gravitropism, wild-type and *pgp1* (At2g36910), *pgp19* (At3g28860), *pgp1*/*pgp19*, and *twd1* (At3g21640) mutant seeds (all ecotype Wassilewskija) were surface-sterilized and grown on half-strength Murashige and Skoog medium and 0.7% Phytagar (Invitrogen, Paisley, UK) under continuous light conditions as described (Lariguet and Fankhauser, 2004). Each gravistimulated root was assigned to one of twelve 30° sectors in the circular histograms; the length of each bar represents the percentage of seedlings showing the same direction of root growth. The number of seedlings for each genotype was between 72 and 96.

Analysis of IAA contents and responses

A. thaliana wild-type, *pgp1, pgp19, pgp1*/*pgp19*, and *twd1* mutant plants (all ecotype Wassilewskija) expressing the maximal auxin-inducible reporter Pro_{DR5}-green fluorescent protein (GFP) construct were generated by *Agrobacterium*-mediated transformations using the *DR5-GFPm* construct (Ottenschläger *et al.*, 2003). Homozygous T3 was used for all experiments described. Seedlings were grown vertically for 5 days as described above, stained with 10 μM propidium iodide before microscopy, and analyzed by differential interference contrast (Leica DM R microscope equipped with a Leica DC300 F charge-coupled device). For histological signal localization, both images were electronically merged and further processed with Photoshop 7.0. (Adobe Systems Inc., Mountain View, CA).

For endogenous free auxin quantification, shoot and root segments of 30–50 seedlings were collected and pooled. The samples were extracted with MeOH and analyzed by gas chromatography-mass spectrometry

(GC-MS). Calculation of isotopic dilution factors was based on the addition of 100 pmol of [^{2}H]IAA to each sample. In some cases, roots of 40 seedlings were manually divided into root segments (see Figure 4*C*) and analyzed as described above. The data are presented the means of three independent lots of 30–50 seedlings each.

Expression and localization analysis

Immunolocalization in roots was performed as described (Ueda *et al.*, 2004). Labeling was performed with rabbit anti-PIN1 and guinea pig anti-PIN2 antibodies at 1:500 and 1:400 dilutions, respectively. Alexa Fluor 488-conjugated goat anti-rabbit and anti-guinea pig secondary antibodies were used at 1:400 dilution. During the immunolocalization procedures, solutions were changed using a pipetting robot (InsituPro, Intavis Bioanalytical Instruments AG). Plasma membranes and microsomal fractions were separated by aqueous two-phase partitioning or continuous sucrose gradient centrifugation and immunoprobed as described (Geisler *et al.*, 2003).

Transcript detection by reverse transcription (RT)-PCR

Semiquantitative RT-PCR was performed as described (Geisler *et al.*, 2000). Transcripts specific for *PGP1* (At2g36910), *TWD1* (At3g21640), and 40 S ribosomal protein *S16* (At2g09990) were detected by conventional PCR for 25 and 30 cycles at an annealing temperature of 52 °C. The intron-spanning PCR primers used were as follows: S16, 5'-ggcgactcaaccagctactga (sense) and 5'-cggtaactctttggtaacga (antisense); PGP1, 5'-gtccctcaagagccgtgcttg (sense) and 5'-ccatcatcgatgacagcgatc (antisense); TWD1, 5'-ccatagcatacatgggggacg (sense) and 5'-tctgtggcgtcgaaagatacg (antisense). Equal volumes of PCR products were separated on 2.5% agarose gels. Negative controls in the absence of enzyme in the RT reaction yielded no products.

Protoplast efflux experiments

Intact *Arabidopsis* mesophyll protoplasts were prepared from the rosette leaves of plants grown on soil under white light (100 µmol m^{-2} s^{-1}, 8-h light/16-h dark cycle, 22 °C), and auxin efflux experiments were performed as described (Geisler *et al.*, 2005). Briefly, intact protoplasts were isolated as described (Geisler *et al.*, 2003) and loaded by incubation with 1 µl/ml [^{3}H]IAA (specific activity of 20 Ci/mmol; American Radiolabeled Chemicals, Inc., St. Louis, MO) on ice. External radioactivity was removed by Percoll gradient centrifugation (Geilser *et al.*, 2005). Efflux was started by incubation at 25 °C and halted by silicon oil centrifugation. Effluxed radioactivity was determined by scintillation counting of the aqueous phases and is presented as relative efflux of the initial efflux (efflux prior to incubation), which was set to zero. Protoplast volumes, surfaces, and vacuolar pH were determined as described (Geilser *et al.*, 2005).

Yeast assays

cDNAs from *Arabidopsis* TWD1 (At3g21640), FKBP12 (At1g58450), and ROF1 (At3g25230) were cloned into the BamHI and SalI sites of the copper-inducible yeast shuttle vector pRS314CUP (Dünnwald *et al.*, 1999). pNEV, pNEV-PGP1 (Geilser *et al.*, 2005), pRS314CUP, pRS314CUP-FKBP12, and pRS314CUP-ROF1 were introduced into *Saccharomyces cerevisiae* strains JK93dα (Hemenway and Heitman, 1996) SMY87-4 (Arndt *et al.*, 1999), PJ69-4a (Cruz *et al.*, 1999), and *yap1-1* (Prusty *et al.*, 2004), and single colonies were grown in synthetic minimal medium without uracil and tryptophan and supplemented with 2% glucose and 100 µM $CuCl_2$. For detoxification assays, transformants grown in the same medium to $A_{600} \approx 0.8$ were washed and diluted to $A_{600} = 1.0$ in water. Cells were 10-fold diluted five times, and each 5 µl were spotted on minimal medium plates supplemented with 10 µM IAA or 750 µM 5-fluoroindole. Growth at 30 °C was assessed after 3–5 days. Assays were performed with three independent transformants.

IAA transport experiments were performed as described (Geisler *et al.*, 2003). For loading experiments (see Figure 6, *C* and *D*; and supplemental Figure 6*A*), cells were grown to $A_{600} = 1.0$, washed, and incubated at 30 °C with 1 µl/ml 5-[^{3}H]IAA (specific activity of 20 Ci/mmol; American Radiolabeled Chemicals, Inc.) in synthetic minimal medium (pH 4.5). Aliquots of 0.5 ml were taken after incubation at 30 °C. IAA retention is expressed as relative loading of the initial loading (t = 2.5 min), which was set to zero. For efflux experiments (see Figure 6*B*), cells were loaded for 10 min on ice, washed twice with cold water, and resuspended in 15 ml of synthetic minimal medium (pH 4.5). Aliquots of 0.5 ml were taken after incubation at 30 °C. IAA

retention is expressed as relative loading of the initial (maximal) loading (t = 0 min), which was set to 100%.

PGP1 and TWD1 expression in yeast and immunolocalization

Yellow fluorescent protein (YFP) and cyan fluorescent protein (CFP) were amplified by PCR from plasmids pEYFP and pECFP (Clontech) inserted in-frame into AscI sites generated in the coding regions of pNEV-PGP1 (bp 2,674) and pRS314CUP-TWD1 (bp 64) using the QuikChange XL site-directed mutagenesis kit (Stratagene, La Jolla, CA). YFP and CFP were inserted into the cytoplasmic loop between transmembrane domains 10 and 11 of PGP1 and into the very N terminus of TWD1. Cells coexpressing PGP1-YFP and TWD1-CFP were incubated in mounting medium containing 4',6-diamidino-2-phenylindole, and immunofluorescence analysis was performed using a Leica DM IRE2 confocal laser scanning microscope equipped with argon (488 nm) and UV (410 nm) lasers. Fluorescence and differential interference contrast images were processed using Photoshop 7.0. Vector controls showed no detectable fluorescence.

Yeast cells coexpressing PGP1 and TWD1 were grown to mid-log phase, and microsomes were separated via continuous sucrose gradient centrifugation (Geisler *et al.*, 2004). Plasma membrane fractions were subjected to 7.5% PAGE, and Western blots were immunoprobed using anti-PGP1 (Sidler *et al.*, 1998) and anti-TWD1 (Geisler *et al.*, 2003) antibodies.

HeLa cell assays

Radiolabeled substrate accumulation assays after transient coexpression of PGP1 (At2g36910) and TWD1 (At3g21640) at a 1:0.5 ratio were performed as described (Geisler *et al.*, 2005). Net efflux (the amount of auxin retained by cells transformed with empty vector minus the amount of auxin retained by cells transformed with PGP19) is expressed as disintegrations/min/500,000 cells. The average empty control vector value was 2852 disintegrations/min/500,000 cells.

In all cases, expression and localization of *PGP19* was confirmed by RT-PCR and Western blotting using standard protocols for the system (Hrycyna *et al.*, 1998; Blakeslee *et al.*, 2004). Cell viability after treatment was confirmed visually and via cell counting.

Recording Root Apex Auxin Fluxes Using an IAA-specific Microelectrode

A platinum microelectrode (Mancuso *et al.*, 2005) was used to monitor IAA fluxes in *Arabidopsis* roots as described (Santelia *et al.*, 2005). For measurements, plants were grown in hydroponic cultures and used 5 days after germination. Differential current from an IAA-selective microelectrode placed 2 µm from the root surface was recorded in a self-referencing mode. The sensor was vibrated between two positions 10 µm distant at a rate of 0.1 Hz.

Data analysis

Data were analyzed using Prism 4.0b (GraphPad Software, San Diego, CA), and statistical analysis was performed using SPSS 11.0 (SPSS, Inc., Chicago, IL).

Results

Cellular and polar transport of IAA is reduced in twd1 and pgp1/pgp19 mutants, indicating a regulatory role for TWD1

Recently, interactions between TWD1 and the MDR/PGP-type transporter PGP1 and its closest homolog, PGP19, were demonstrated (Geilser *et al.*, 2003). Indirect evidence suggests that TWD1 functions in part by regulating the overlapping auxin transport activities of PGP1 and PGP19 (Geisler and Murphy, 2006; Geisler *et al.*, 2003; Geisler *et al.*, 2005).

To demonstrate the physiological impact of TWD1 interaction, we measured PGP-mediated cellular efflux of radiolabeled auxin (IAA) in isolated leaf mesophyll protoplasts using silicon oil centrifugation (Geisler *et al.*, 2005). Protoplasts from *twd1* plants showed greatly reduced IAA efflux (48%) compared with those from wild-type plants (100%) (Figure 1*A*). This reduction of efflux in *twd1* protoplasts was slightly (but not significantly) less than that observed in *pgp1*/*pgp19* protoplasts (49%) (Geisler *et al.*, 2005). These measurements correlate well with auxin transport rates found in intact tissues (Geisler *et al.*, 2003). The presence of PGP1, PGP19, and TWD1 in the assayed cells was verified both by RT-PCR in

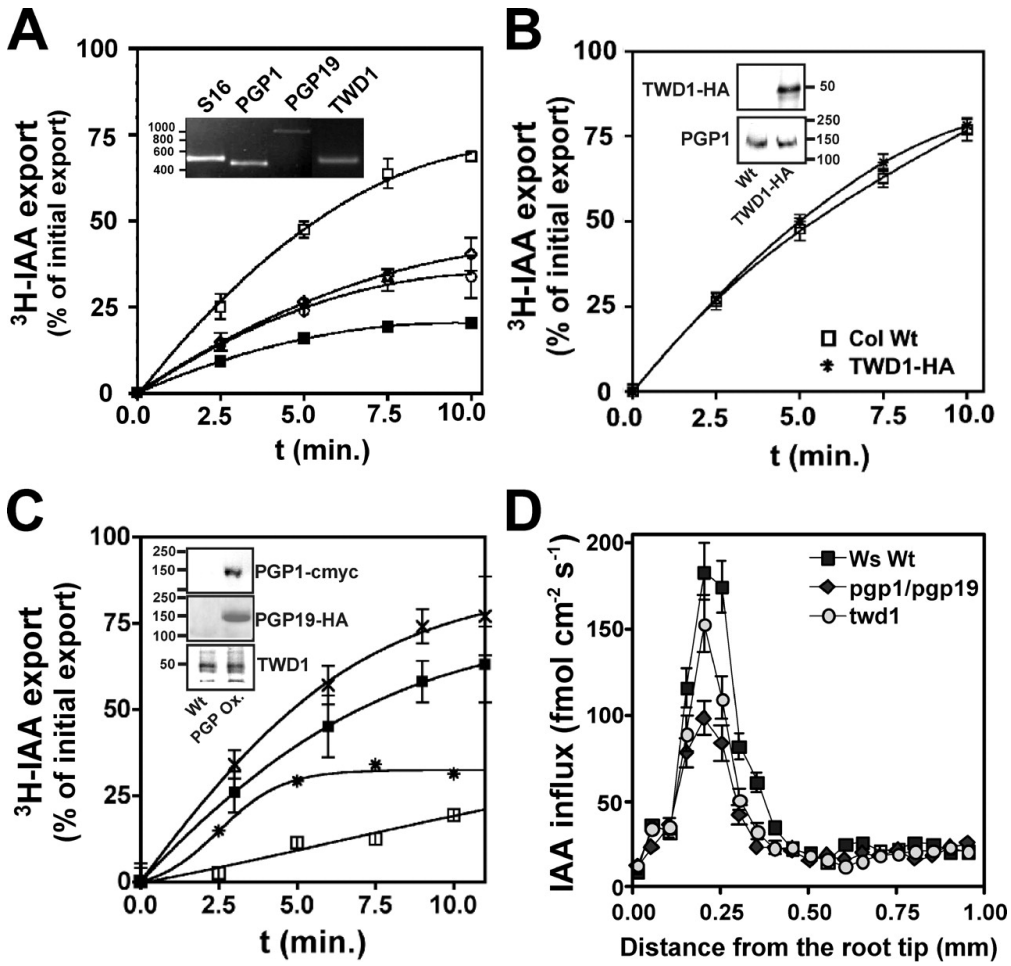

FIGURE 1. **Cellular IAA export is reduced in *twd1*, but is not affected by overexpression of TWD1.**
A, cellular [^{3}H]IAA export in wild-type mesophyll protoplasts (ecotype Wassilewskija;□) was reduced to a similar extent in *twd1* (○) and *pgp1*/*pgp19* (◊) plants. We used de-energized (dark-treated) plant material (■) as a negative control. The presence of PGP1, PGP19, and TWD1 in wild-type protoplasts was verified by semiquantitative RT-PCR (*inset*). Efflux is presented as relative export of the initial export. Data are the means ± S.D. of three to five individual experiments (n = 4). ***B,*** constitutive overexpression of TWD1 did not alter [^{3}H]IAA export, suggesting a regulatory role of TWD1. Overexpression of TWD1-HA in protoplasts was verified by Western blot analysis using anti-HA antibody (Geisler *et al.*, 2003); overexpression of TWD1 did not alter expression of PGP1 or PGP19 (*inset*) as shown using anti-PGP1 antibody, which does not differentiate between PGP1 and PGP19 (Geisler *et al.*, 2003). ***C,*** constitutive overexpression of PGP1-c-Myc (*) and PGP19 (x) enhanced [^{3}H]IAA export compared with their corresponding wild-type (*Wt*) ecotypes, RLD (□) and Columbia (*Col*;■), respectively. Overexpression (*Ox.*) of PGP1 and PGP19 in protoplasts was verified by Western blot analysis using anti-c-Myc and anti-HA antibodies. Overexpression of PGPs did not alter expression of TWD1 (*inset*) shown for PGP1. ***D,*** IAA influx was reduced in the transition zone of *pgp1*/*pgp19* and *twd1* roots. Shown is the IAA influx profile along single roots of wild-type, *pgp1*/*pgp19*, and *twd1* plants. Positive fluxes represent a net IAA influx. Data shown were collected continuously over a 10-min period and are the means of eight replicates; *error bars* represent S.E. *Ws*, Wassilewskija.

wild-type plants (Figure 1*A*) and by Western analysis (Figure 1, *B* and *C*). The impact of interfering factors such as vacuolar trapping of IAA and reduced export capacities due to alterations in vacuolar pH (Li *et al.*, 2005) or in protoplast surfaces could be excluded (supplemental Figure 1).

To further investigate the regulatory role of TWD1, we measured IAA efflux in protoplasts generated from *twd1* plants that were fully complemented by a $Pro_{CaMV35S}$-TWD1-hemagglutinin (HA) construct (Geisler *et al.*, 2003). Overexpression of TWD1-HA was verified by Western blotting and did not alter PGP1 or PGP19 expression (Figure 1*B*, *inset*). Interestingly, IAA efflux in TWD1-overexpressor protoplasts was not significantly different from that in wild-type protoplasts (Figure 1*B*), indicating that it is unlikely that TWD1 transports auxin directly. In contrast, constitutive up-regulation of PGP1 or PGP19 greatly enhanced IAA export compared with their corresponding wild-type ecotypes. Interestingly, *Arabidopsis* ecotypes RLD and Columbia seem to have ecotype-specific differences in auxin efflux capacity (Figure 1*C*), consistent with previously documented whole plant ecotype-specific differences in auxin transport (Peer *et al.*, 2004). The reduced increase in IAA efflux stimulated by PGP19 overexpression (122% of the wild-type level (100%)) compared with PGP1 overexpression (130% of the wild-type level) does not reflect the transport capacities of the individual proteins, but is instead the result of differences in expression levels as shown by RT-PCR (relative expression level compared with the wild-type level: PGP1, 8.0 ± 2.2; and PGP19, 3.0 ± 0.6).

To verify these data at the whole plant level, a novel self-referencing IAA-specific microelectrode was used to obtain noninvasive and continuous recordings of auxin fluxes in intact root apices (Mancuso *et al.*, 2005). IAA influxes in *Arabidopsis* are characterized by a distinct peak at 0.2–0.3 mm from the root tip in the so-called root transition or distal elongation zone of the root apex (Santelia *et al.*, 2005), consistent with the current auxin "reflux" model describing auxin transport streams in roots (Blilou *et al.*, 2005). In wild-type roots, the transition zone auxin peak averaged 184.2 ± 16.5 fmol cm^{-2} s^{-1}, whereas in *twd1* roots, the maximal influx in the root transition zone was significantly reduced, averaging 153.6 ± 16 fmol cm^{-2} s^{-1}. (Figure 1*D*). The influx in *pgp1*/*pgp19* roots was more severely reduced (98.5 ± 10.2 fmol cm^{-2} s^{-1}) (Figure 1*D*). Interestingly, the IAA peak was less reduced in *twd1* roots (Figure 1*D*) than in *pgp1* and *pgp19* single mutant roots (supplemental Figure 2). This may be due to the relatively high expression of both PGP1 and PGP19 in root apices and correlates well with the proposed role of these proteins in establishing directional auxin movement away from apical tissues (Blakeslee *et al.*, 2005). However, in addition to reduced peak area, IAA influxes in both *twd1* and *pgp1*/*pgp19* roots were localized more apically (0.05–0.35 mm) compared with the wild-type roots (0.1–0.45 mm) and *pgp1* and *pgp19* single mutant roots (0.1–0.35 mm). Apical shifts have been reported for maize *semaphore* and *lrt1 rum1* mutants, which are also defective in auxin transport (Schlicht *et al.*, 2006). A recent report employing microelectrodes showed that the transition zone presents peaks in the fluxes of O_2, K^+, and H^+ (Mancuso and Marras, 2006), which make this region the most active region of the root. As a consequence, a shift in this active region of 0.5–1 mm could affect many aspects of root physiology and development.

It has been suggested that some mammalian and plant FKBPs possess chaperone activity and play a role in protein secretion (Schiene and Fischer, 2000). To investigate if loss of *TWD1* function does alter the targeting of auxin efflux complexes, PIN1 and PIN2 were immunolocalized in wild-type and *twd1* root tips. PIN1 and PIN2 have been shown to play essential roles as components of the auxin efflux complex, are expressed in the same tissues as PGP1, and are co-purified with PGP1 and PGP19 by NPA affinity chromatography (Blakeslee *et al.*, 2005; Petrášek *et al.*, 2006; Geisler *et al.*, 2005). Neither PIN1 nor PIN2 was mislocalized in *twd1* (Figure 2*A*), suggesting that altered PIN localization is not responsible for the

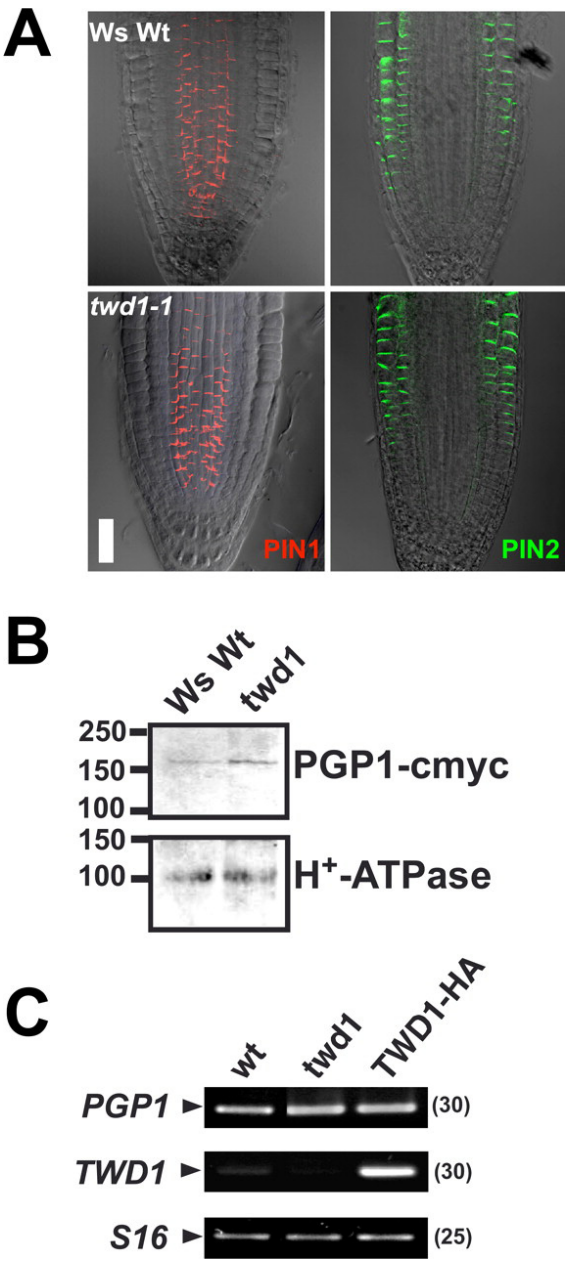

FIGURE 2. **Loss of function of TWD1 does not alter expression and localization of components of the auxin efflux complex such as PIN1, PIN2, and PGP1.**

A, whole mount immunolocalization of auxin facilitator proteins PIN1 (*red*) and PIN2 (*green*), components of the auxin efflux complex, revealed no significant changes in expression. For orientation, colored fluorescence images were superimposed with bright-field pictures. *Scale bar* = 100 µm. *Ws Wt*, wild-type ecotype Wassilewskija. ***B,*** shown are the results from Western analysis of Pro_{PGP1}-PGP1-c-Myc in wild-type and *twd1* plasma membrane-enriched fractions as verified by immunodetection of the plasma membrane marker H^+-ATPase. ***C,*** loss and gain of function of *TWD1* had no significant effect on PGP1 expression as shown by semiquantitative RT-PCR.

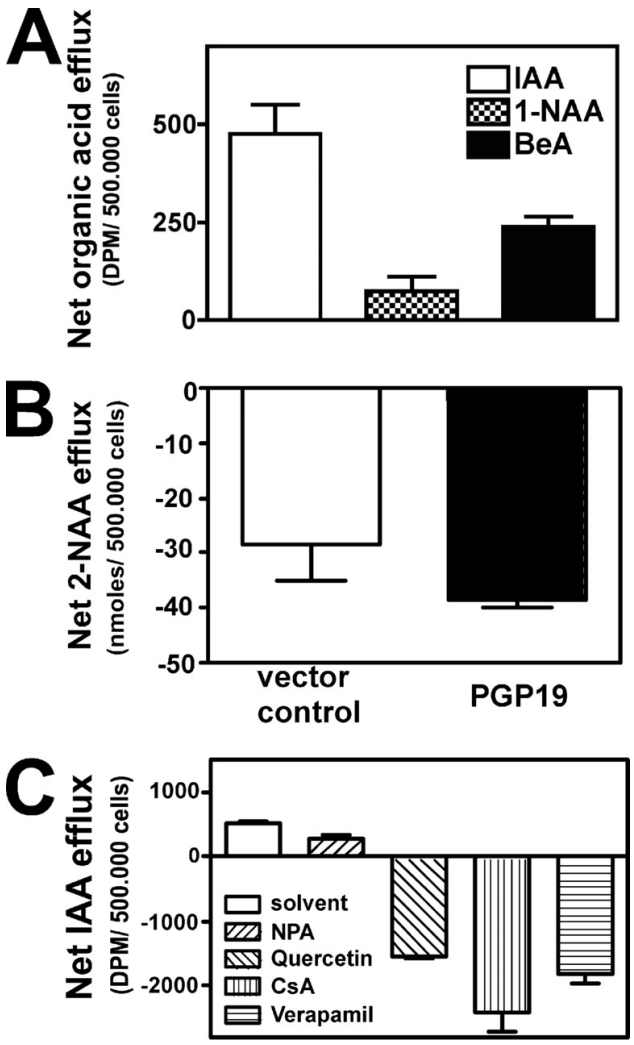

FIGURE 3. **PGP19 mediates auxin export when expressed in HeLa cells.**
A, [^{3}H]IAA efflux was increased in HeLa cells expressing *PGP19*. PGP1 also modulated efflux of 1-[^{3}H]NAA and [^{3}H]benzoic acid (*BeA*). ***B,*** 2-NAA was retained in HeLa cells expressing *PGP19*. Cells were incubated with 62.59 nM unlabeled 2-NAA. 2-NAA levels were measured by liquid chromatography-mass spectrometry. Data are presented as nanomoles of 2-NAA/500,000 cells (means ± S.D.) and represent values obtained from two experiments with three replicates each. ***C,*** [^{3}H]IAA efflux by PGP19 was inhibited by treatment with 10 μM NPA, 200 nM quercetin, and the ABC transport inhibitors cyclosporin A (*CsA*) and verapamil when cells were loaded with 10 nM radiolabeled substrate. Net efflux (the amount of auxin retained by cells transformed with empty vector minus the amount of auxin retained by cells transformed with PGP19) is expressed as disintegrations/min/500,000 cells. Reductions in auxin retention (efflux) in transformed cells are presented as positive values. In all cases, expression and localization of *PGP19* were confirmed by RT-PCR (Blakeslee *at al.*, 2004) and Western blotting (Hrycyna *et al.*, 1998) using standard protocols for the system. Cell viability after treatment was confirmed visually and via cell counting. Data are the means ± S.D. (n = 3).

reduced IAA export in *twd1*. The same was found when PIN1 and PIN2 were immunolocalized in sucrose gradient fractions from wild-type, *pgp1*/*pgp19*, and *twd1* plants (data not shown). Furthermore, PIN1 and PIN2 expression has been shown recently not to be altered in *pgp1* and *pgp19* roots (Geisler *et al.*, 2005).

To investigate *PGP1* expression and location in the *twd1* background, we analyzed the expression of a Pro_{PGP1}-PGP1-c-Myc construct (Geisler *et al.*, 2005) in *twd1* mutants. PGP1 was co-localized with H^+-ATPase using anti-c-Myc antibody in plasma membrane fractions obtained by continuous sucrose gradient fractionation and showed no significant difference in expression compared with the wild type (Figure 2*B*). Similar results were obtained using *twd1* membrane fractions and an antiserum recognizing both PGP1 and PGP19 (supplemental Figure 5). Furthermore, *PGP1* transcript levels were unaltered in both *twd1* and TWD1-overexpressor as measured by RT-PCR (Figure 2*C*). The unaltered expression levels and localization of auxin efflux proteins in *twd1* mutants indicate that TWD1 may function not by altering the localization of PGPs, but instead by regulating the function of PGPs via protein-protein interactions.

PGP19 mediates auxin export when expressed in HeLa cells

Cellular IAA efflux experiments using plant protoplasts suggested that PGP19 might function in auxin export in a manner similar to PGP1 (Geisler *et al.*, 2005). In contrast to PGP1, however, PGP19-mediated auxin transport could not be tested in transgenic yeast, as PGP19 was shown to be improperly localized upon expression in yeast, most likely because of hyperglycosylation (Noh *et al.*, 2001; Geisler *et al.*, 2005). To demonstrate the role of PGP19 in auxin transport, we functionally expressed PGP19 in the vaccinia virus HeLa cell expression system, which has become a standard system for assaying mammalian PGP transport activity (Hrycyna *et al.*, 1998) and which we have used previously to demonstrate PGP1-mediated auxin efflux (Geisler *et al.*, 2005).

Heterologous expression of PGP19 in HeLa cells provided evidence that, similar to PGP1, PGP19 functions as an ATP-activated anion channel capable of mediating auxin efflux. Expression of PGP19 in HeLa cells resulted in net efflux of IAA over a 6-

fold concentration range (10–63 nM) (Figure 3*A* and supplemental Figure 4) and a lower but significant export of 1-naphthylacetic acid (NAA). The antiauxin 2-NAA was not exported (Figure 3*B*). As was shown for PGP1 (Geisler *et al.*, 2005), PGP19 did not exhibit the broad substrate specificity common to mammalian PGP transporters and failed to transport standard MDR substrates, including rhodamine 123, daunomycin, and BODIPY-vinblastine in fluorescence-activated cell sorter assays (supplemental Figure 3) (Geisler *et al.*, 2005). Similar to PGP1, PGP19 mediated efflux of benzoic acid only at higher concentrations (63 nM), but not at lower concentrations (10 nM), at which auxin efflux activities were still active (supplemental Figure 4) (Geisler *et al.*, 2005). Finally, PGP19 expression also increased the efflux of oxidative IAA breakdown products in a manner similar to PGP1 expression (supplemental Figure 4) (Geisler *et al.*, 2005).

Arabidopsis PGPs have been shown to bind the auxin transport inhibitors quercetin (an aglycone flavonoid) and NPA (Geisler *et al.*, 2003; Murphy *et al.*, 2002). PGP19-mediated IAA efflux from HeLa cells was inhibited by both NPA and quercetin as well as by the mammalian PGP inhibitors cyclosporin A and vinblastine (Figure 2*C*).

Roots of twd1 and pgp1/pgp19 reveal greatly elevated free auxin levels and altered gravitropism

Previously, both reduced basipetal auxin transport and reduced IAA levels were reported in 5-day post-germination *pgp1* and *pgp19* mutant roots (Geisler *et al.*, 2005). We analyzed free IAA levels in root and shoot tissues (see Figure 4*C* for the experimental setup) of 9-day post-germination *twd1* and *pgp* mutant seedlings. Absolute values for wild-type tissues were slightly higher but in the same range as reported by others. Surprisingly and in contrast to 5-day roots, we found elevated IAA levels in all mutant roots, whereas the levels in mutant shoots revealed only small differences compared with wild-type levels (Figure 4A). Interestingly, the IAA content in *pgp1*/*pgp19* (308%) and *twd1* (286%) roots was clearly higher than that in *pgp1* (162%) and *pgp19* (154%) roots. This again suggests functional redundancy of PGP1 and PGP19 and a loss of function of PGP1/PGP19-mediated IAA auxin transport in *twd1*.

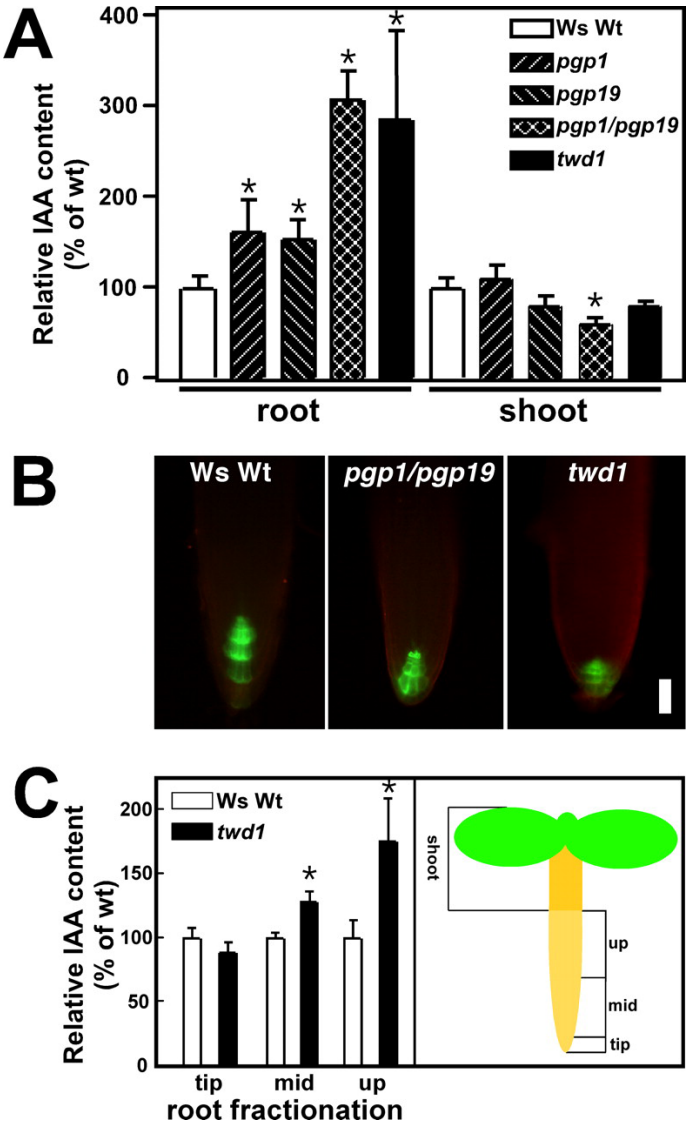

FIGURE 4. **IAA content in *twd1* and *pgp1*/*pgp19* roots is elevated.**
A, relative free IAA content compared with the wild type in 9-day seedlings was determined by GC-MS. Absolute wild-type values were 42.2 ± 5.7 and 49.9 ± 6.1 pg/mg (fresh weight) for roots and shoots, respectively. *Ws Wt*, wild-type ecotype Wassilewskija. *, significantly different from the wild type ($p < 0.05$, analysis of variance). ***B,*** Pro_{DR5}-GFP expression in 9-day seedling root tips showed no significant differences compared with the wild type. ***C,*** fractionation of 9-day seedling roots indicated elevated free IAA levels in the root elongation zone and above. *cot*, cotyledon; *hyp*, hypocotyl. *, significantly different from the wild type ($p < 0.05$, analysis of variance).

To investigate alterations in local auxin concentrations in more detail, we analyzed expression of the auxin reporter construct Pro_{DR5}-GFP (Ottenschläger *et al.*, 2003) in *twd1* and *pgp* mutant root tips. This method was selected as it allows a more noninvasive detection of IAA concentrations compared with the more commonly used Pro_{DR5}-β-glucuronidase construct.

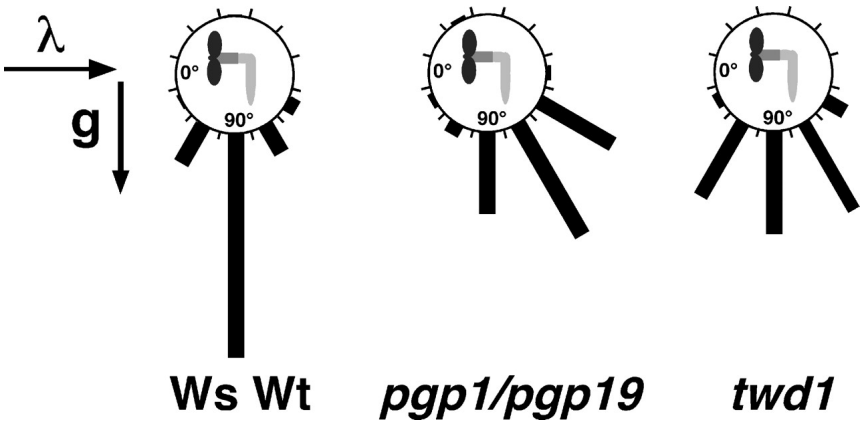

FIGURE 5. ***twd1* and *pgp1*/*pgp19* seedlings are defective in root gravitropism.** For quantification of gravitropism, plants were grown on vertical plates under continuous light conditions (coming from the left as indicated by the *arrow*) (Lariguet and Fankhauser, 2004). Each gravistimulated root was assigned to one of twelve 30° sectors in the circular histograms; the length of each *bar* represents the percentage of seedlings showing the same direction of root growth. The number of seedlings for each genotype was between 72 and 96. *Ws Wt*, wild-type ecotype Wassilewskija.

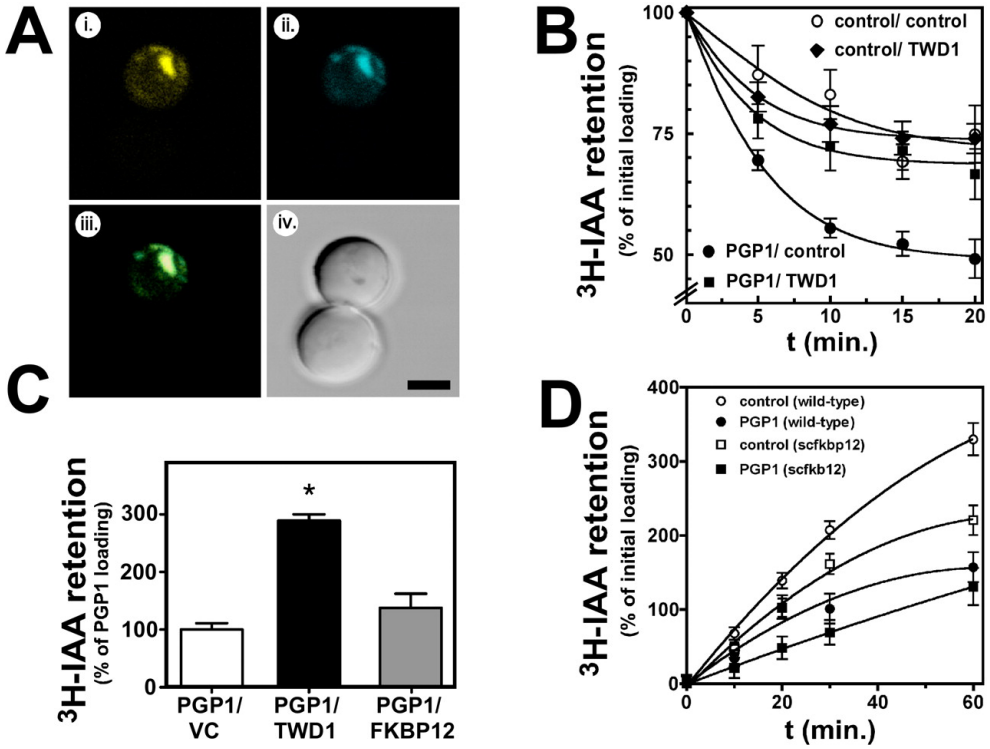

FIGURE 6. **Coexpression of PGP1 and TWD1 specifically inhibits IAA export.** ***A,*** PGP1-YFP (*upper left panel*) was expressed on the plasma membrane and in raft-like structures and co-localized with TWD1-CFP (*lower left panel*) in yeast as shown by superimposition (*upper right panel*). Differential interference contrast images of the same cells are shown (*lower right panel*). *Scale bar* = 2.5 µm. ***B,*** coexpression of TWD1 and PGP1 reduced PGP1-mediated IAA export to vector control levels. Reductions in auxin retention (efflux) are presented as relative export of the initial loading. Data are the means ± S.D. (*n* = 4). ***C,*** coexpressed *Arabidopsis* FKBP12 did not significantly alter PGP1-mediated IAA efflux. Reductions in auxin retention (efflux) after 10 min are presented as relative export of the initial loading. Data are the means ± S.D. (*n* = 3). *, significantly different from the PGP1/vector control (*VC*; $p < 0.05$, analysis of variance test). ***D,*** PGP1-mediated IAA efflux was not dependent on *S. cerevisiae* (*Sc*) FKBP12/FPR as shown by assaying IAA efflux in an *fpr1* strain and the corresponding wild-type strain. Reductions in auxin retention (efflux) are presented as relative loading of the initial loading. Data are the means ± S.D. (*n* = 3).

9-Day *pgp1*/*pgp19* and *twd1* roots showed slightly reduced reporter gene expression in root columella cells compared with wild-type roots (Figure 4*B*). Consistent with previously published Pro_{DR5}-β-glucuronidase data from 5-day post-germination seedlings (Geisler *et al.*, 2005; Lin and Wang, 2005), similar results were observed in *pgp1* and *pgp2* single mutants (data not shown).

Reduction of auxin levels visualized by the reporter gene constructs seemed to contradict at first glance the elevated IAA concentrations measured by GC-MS. Therefore, we dissected *twd1* roots into three parts (Figure 4*C*) and determined the free IAA concentrations of each segment. GC-MS analysis revealed that auxin levels in the "tip" (the region 2 mm from the tip) were indeed slightly reduced (89% of the wild-type levels), whereas the mid-part (128%) and upper part (176%) root fractions contained significantly higher levels (Figure 4*C*). The total IAA levels in this assay were lower than those observed in GC-MS analysis of whole root tissues, possibly because of the unavoidable drastic manipulation during fractionation.

Root gravitropism is known to be dependent on and to be mediated by polar auxin transport (Muday and DeLong, 2001). Therefore, gravitropic growth tests are

an ideal tool to investigate the developmental effects of the alterations in auxin fluxes observed in *twd1* and *pgp* mutants. Previous studies have demonstrated that *pgp19* and *pgp1*/*pgp19* hypocotyls exhibit enhanced gravitropic responses (Noh *et al.*, 2003). Under standard gravitropism assay conditions, the roots of *pgp1* and *pgp19* single mutants exhibited no significant changes in gravitropism (data not shown). However, both *pgp1*/*pgp19* and *twd1* exhibited impaired gravitropic responses compared with the wild type (Figure 5). Consistent with previous results in hypocotyl tissues (Noh *et al.*, 2003), *pgp1*/*pgp19* roots exhibited slight hypergravitropism, whereas *twd1* roots showed impaired gravitropism without any directional preference.

Modulation of pgp1-mediated IAA export by TWD1 is specific and has reverse effects in yeast and mammalian cells

To investigate the regulatory effect of TWD1 on PGP activity in more detail, we coexpressed PGP1 and TWD1 in the yeast *S. cerevisiae*. In yeast, PGP1 and TWD1 co-localized mainly with some unknown punctate structures in the vicinity of the plasma membrane as demonstrated by confocal microscope analysis of PGP1-YFP and TWD1-CFP (Figure 6*A*) and Western detection of plasma membrane-enriched fractions of yeast membranes coexpressing TWD1 and PGP1 (data not shown). Furthermore, coexpression of PGP1-YFP and TWD1 N-terminally fused to *Renilla* luciferase in yeast resulted in a positive bioluminescence resonance energy transfer ratio, verifying the interaction.[1]

Monitoring time-dependent PGP1-mediated IAA efflux (measured as decreased IAA retention) in yeast revealed that coexpression reverted export toward the vector control level (Figure 6*B*), whereas TWD1 alone had only a slight inhibitory effect on background IAA efflux. The same tendency was found when loading kinetics were recorded (see "Experimental procedures") (supplemental Figure 6). Similarly, TWD1 inhibited PGP1-mediated detoxification of the toxic auxin analog 5-fluoroindole (supplemental Figure 6*C*), which has been used to demonstrate PIN2/AGR1 function in yeast (Luschnig *et al.*, 1998).

Inhibition of PGP1-mediated IAA efflux in yeast by TWD1 was specific, as expression of TWD1 alone had

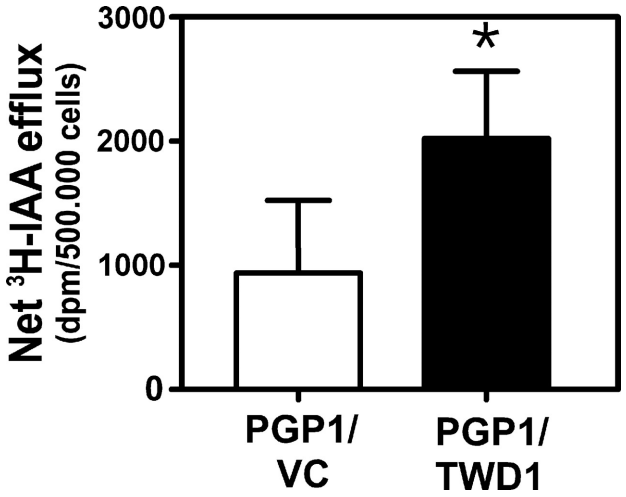

FIGURE 7. **Coexpression of PGP1 and TWD1 enhances PGP1-mediated IAA export in HeLa cells.**
Shown is the efflux of radiolabeled IAA from HeLa cells expressing PGP1 with the indicated ratios of TWD1. Reduction in auxin retention (efflux) is presented as net efflux. Expression and localization of expressed proteins were confirmed by RT-PCR and Western analysis (data not shown). Data are the means ± S.D. (n = 3). *, significantly different from the PGP1/vector control (*VC*; $p < 0.05$, analysis of variance).

no significant effect on background IAA efflux (Figure 6*B*). Furthermore, *Arabidopsis* FKBP12, which represents the most basic FKBP, consisting essentially just of the *cis,trans*-peptidylprolyl isomerase domain, and which functions as a cell cycle regulator (Aghdasi *et al.*, 2001), reduced PGP1-mediated IAA efflux (measured as increased IAA retention) only slightly compared with TWD1 (Figure 6*C*). In the *yap1-1* mutant, only TWD1 (but not the closely related *Arabidopsis* proteins FKBP12 and ROF1/FKBP59) (Vucich and Gasser, 1996), significantly inhibited PGP1-mediated IAA detoxification (supplemental Figure 6*B*). Finally, yeast FKBP12 seemed to somehow activate PGP1-mediated IAA export, resulting in reduced IAA loading in the *S. cerevisiae* FKBP12 mutant (Figure 6*D*), which confirms previous results on murine MDR3 activity (Hemenway and Heitman, 1996). However, the same magnitude of stimulation was found also for the background activity (Figure 6*D*, vector control), suggesting unspecific up-regulation of yeast endogenous export systems.

Inhibition of PGP1 by TWD1 in yeast was surprising, as an opposite effect was expected based on the protoplast efflux assays described above. Therefore, we coexpressed PGP1 and TWD1 in HeLa cells, which represent the standard expression system for analyzing mammalian ABCs (Hrycyna *et al.*, 1998).

1 A.Bailly and M.Geisler, unpublished data.

Interestingly, TWD1 conferred stimulation of PGP1-mediated auxin efflux upon coexpression (Figure 7). The influence of TWD1 on PGP19 could be tested in neither yeast nor HeLa cells, as PGP19 is inactive in yeast (Noh *et al.*, 2001; Geisler *et al.*, 2005), whereas coexpression of PGP19 and TWD1 had destabilizing effects on the HeLa cells (data not shown).

Discussion

To understand the strong developmental phenotype that is caused by loss of function of *Arabidopsis* TWD1/FKBP42, we previously demonstrated interactions between TWD1 and the MDR/PGP transporters PGP1 and PGP19 (Geisler *et al.*, 2003). As both PGP1 and PGP19 have been shown to be capable of catalyzing export of the critical plant hormone auxin (Geisler *et al.*, 2005), a regulatory role of TWD1 in PGP1/PGP19 has been suggested to account for the auxin-related aspects of the *twd1* phenotype. An emerging function of immunophilins is their role in regulating large membrane proteins such as rhodopsin (Stamnes *et al.*, 1991) or integral Ca^{2+} channels such as the ryanodine and 1,4,5-triphosphate receptors (Cameron *et al.*, 1995; Timerman *et al.*, 1995). Regulation of murine MDR3 by yeast FKBP12 has also been demonstrated, although the effects of mammalian PGP-FKBP interactions *in vivo* have not yet been fully investigated (Hemenway and Heitman, 1996).

In this study, we have provided several lines of evidence that TWD1 is an essential regulatory component of the PGP-mediated auxin efflux complex *in planta* by means of protein-protein interactions. PGP1-TWD1 and PGP19-TWD1 interactions have been previously demonstrated by yeast two-hybrid analysis, NPA affinity chromatography, and co-immunoprecipitation pulldown assays (Blakeslee *et al.*, 2005; Geisler *et al.*, 2003; Murphy *et al.*, 2002).

1) Cellular efflux of IAA from mutant cells is reduced compared with that from wild-type cells in the order wild type > *pgp1* > *pgp19* >> *pgp1*/*pgp19* ≥ *twd1*. The magnitude of reduction correlates with both whole plant transport data (Geisler *et al.*, 2003) and with the observable auxin-deficient mutant phenotypes (Geisler *et al.*, 2003; Geisler *et al.*, 2005). Overexpression of TWD1 has no effect on IAA export, whereas up-regulation of the ABC transporters PGP1 and PGP19 strongly enhances efflux.

2) Expression and localization of PIN1 and PIN2 (essential components of the auxin efflux complex) are not altered in *twd1*. Based on RT-PCR and Western analysis, the same seems to be true for PGP1. The observed reduction of auxin export is therefore unlikely due to altered expression or mistargeting of PGPs and PIN proteins. Activation of the transport complex through TWD1 must therefore rely on the physical interaction of TWD1 with the remainder of the transport complex.

3) Modulation by TWD1 is gene-specific, as the related *Arabidopsis* proteins FKBP12 (Harrar *et al.*, 2001; Aghdasi *et al.*, 2001) and ROF1/FKBP59 (Vucich and Gasser, 1996) have only slight effects on PGP1-mediated IAA transport compared with TWD1 when coexpressed with PGP1 in yeast. Surprisingly, coexpression of TWD1 in yeast *versus* protoplast and mammalian cells showed opposite effects on PGP1 activity (inhibition in yeast and stimulation in HeLa cells), suggesting that plant-specific components might be absent in the unicellular eukaryote *S. cerevisiae*. Currently, we are trying to identify the factors that modulate the activity of TWD1 in these systems. Reversible protein phosphorylation by protein kinases might be a possible mechanism, as mammalian PGPs are known to be regulated via phosphorylation (Castro *et al.*, 1999; Ambudkar *et al.*, 2003). Interestingly, PGP1 has been recently shown to be phosphorylated in a so-called regulatory linker domain (Nühse *et al.*, 2004). Another intriguing possibility is that FKBP-interacting proteins (Vespa *et al.*, 2004) might be lacking in yeast. Interestingly, many effects of immunosuppressant drugs are not seen in yeast.

In our current model of a PGP1-TWD1-PGP19 auxin efflux complex, functional interactions take place between the C-terminal nucleotide-binding fold (NBF2) of PGP1 and the N-terminal *cis,trans*-peptidylprolyl isomerase-like domain of TWD1, whereas PGP19 apparently requires the full TWD1 protein (Geisler *et al.*, 2003). The nucleotide-binding folds of the PGPs do not interact with each other[2], which is of interest, as mammalian ABC transporters have been suggested to function as heterodimers (Ramaen *et al.*, 2005). Therefore, we postulate that TWD1 functions as a linker between both PGPs, although the existence of the ternary complex awaits confirmation.

2 R. Bouchard and M.Geisler, unpublished data.

The simplest mechanistic model based on our data would have TWD1-induced conformational changes in the C termini of PGP1 and PGP19 increase ATP access to the second ATP-binding sites of these proteins (NBF2). In the absence of TWD1, the ATP-binding sites would be blocked, leaving PGP1/PGP19 in an inactive state. The activity of heterologously expressed PGP1 argues for activation by host endogenous factors that partially can take over TWD1 function. However, at this time, we cannot exclude that the regulatory domain shift effects alternatively or additionally substrate (IAA) binding. Recognition and binding of the great diversity of drugs by PGPs are still not fully understood (Ambudkar *et al.*, 2003).

Furthermore, the fact that overexpression of PGP1 and PGP19 results in increased IAA efflux argues either that TWD1 is not yet saturated by PGP1/PGP19 or that activation is a transient event. This has been suggested for the missing demonstration of a murine MDR3-FKBP12 complex in yeast (Hemenway and Heitman, 1996). However, overexpression of TWD1 has no significant effect on IAA efflux that might favor a transient interaction.

In addition to this novel role for FKBPs, we have also demonstrated a direct involvement of TWD1 in auxin transport that is at least partially able to explain the drastic overlapping developmental phenotype of both *twd1* and *pgp1*/*pgp19* plants. Loss of function of PGP1/PGP19-mediated auxin export in *twd1* blocks basipetal polar auxin transport (shown for *pgp1* and *pgp19*) (Geisler *et al.*, 2005), resulting in elevated free IAA levels in mature root parts. This correlates with polar (dominantly basal) expression of PGP1 in the mature root regions (Geisler *et al.*, 2005). Alternatively, non-polar expression of PGP1 in meristematic cells of the root apex (Geisler *et al.*, 2005) has been suggested to function as a sink in long-range transport of IAA (Geisler and Murphy, 2006). This further verifies an involvement of PGP1/PGP19 and TWD1 in long-distance transport of IAA, as has been suggested previously (Geisler *et al.*, 2005; Lin and Wang, 2005).

Agravitropic roots and many aspects of the strong developmental phenotype of *twd1* and *pgp1*/*pgp19* plants are in good agreement with altered polar auxin transport and elevated auxin concentrations in the roots. Other growth defects especially in the shoots might be a consequence of altered reflux of auxin into the shoots or of secondary effects. Reduced and apically shifted influx maxima that have been verified for *pgp* and *twd1* roots using an auxin-specific electrode in analogy to other auxin transport mutants (Schlicht *et al.*, 2006) suggest indeed altered reflux capacities.

However, the "twisted syndrome" not seen in *pgp1*/*pgp19* plants suggests that other TWD1-specific functions are missing in *twd1*. In this respect, it is important to keep in mind that the multidomain FKBP TWD1 interacts additionally with HSP90, calmodulin, and MRP-like ABC transporters MRP1 and MRP2 (Geisler *et al.*, 2003; Kamphausen *et al.*, 2002; Geisler *et al.*, 2004), which might account for the more severe pheno-type by loss of additional functions.

The precise expression pattern of TWD1 and PGP19 is still not known, and co-immunolocalization of all components has failed so far because of the extremely low abundance of TWD1 (Geisler *et al.*, 2003). Attempts to localize TWD1 in wild-type cells using antisera or CFP fusions have failed so far.[3] The low expression of TWD1 compared with that of the PGPs as shown by RT-PCR and *in silico* data (www.genevestigator.ethz.ch) (data not shown) further supports a transient but highly functional interaction of TWD1 and PGPs. However, careful gene chip analysis revealed that *TWD1*, despite its low abundance, is coexpressed in virtually all tissues with *PGP1*/*PGP19* and that the expression of all three genes is induced by various common stresses (data not shown).

Finally, our experimental evidence provided here suggests that this mode of PGP regulation by protein-protein interaction might be relevant beyond plants. Transfer of this novel FKBP function could be beneficial for development of novel strategies for cancer therapy via FKBP-mediated down-regulation of drug efflux.

Acknowledgments

We are grateful to Drs. P. Lariguet and C. Fankhauser for help during gravity assays, Drs. A. Düchtig and A. Müller for analyzing free IAA contents, Drs. J. Heitman and G. R. Fink for mutant yeast strains, and Dr. E. Martinoia for continuous support.

3 B.Schulz and M.Geisler, unpublished data.

Supplemental data

The original on-line version of this article (available at http://www.jbc.org) contains the following supplemental figures .

	Ws Wt	twd1
vacuolar pH	6.40	6.52
Rel. protoplast volume	1	0.688 ± 0.067*
(% Ws Wt)	(4)	(4)
Rel. protoplast surface area	1	0.645 ± 0.037*
(% Ws Wt)	(30)	(30)
chloroplast number	37 ± 9	37 ± 7
(per protoplast)	(16)	(17)

▲ SUPPL. FIGURE 1. **Vacuolar pH and morphological features of leaf mesophyll protoplasts.**
The impact of interfering factors such as vacuolar trapping of IAA or reduced export capacities due to alterations in vacuolar pH or in protoplast surfaces during cellular efflux experiments using protoplasts (see Figure 1) could be excluded. Protoplast volumes, surfaces and vacuolar pH were determined as described elsewhere (Geisler *et al.*, 2005). * Significantly different from wild-type ($P < 0.05$, ANOVA test).

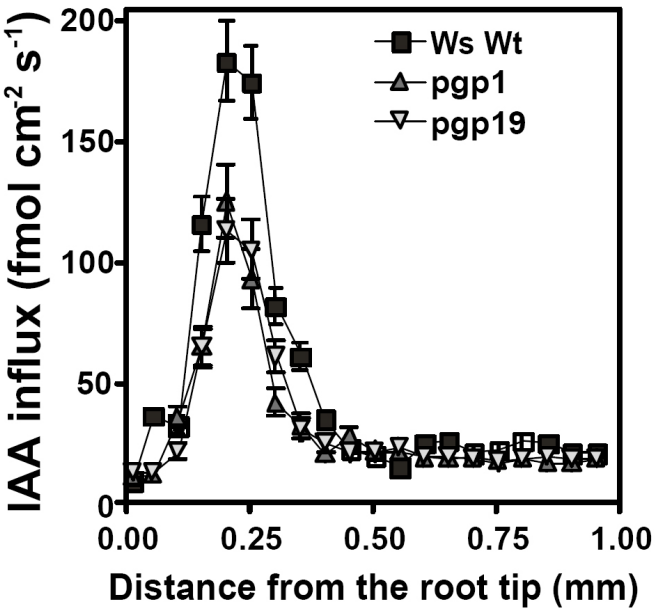

▲ SUPPL. FIGURE 2. **IAA influx is reduced in the transition zone of pgp1 and pgp19 roots.**
IAA influx profile along single roots of wild-type, pgp1 and pgp19 plants determined using an IAA-specific microelectrode as described in (Santelia *et al.*, 2005). Positive fluxes represent a net IAA influx. Data shown were collected continuously over a 10 min. period and are means of 8 replicates; error bars represent standard errors.

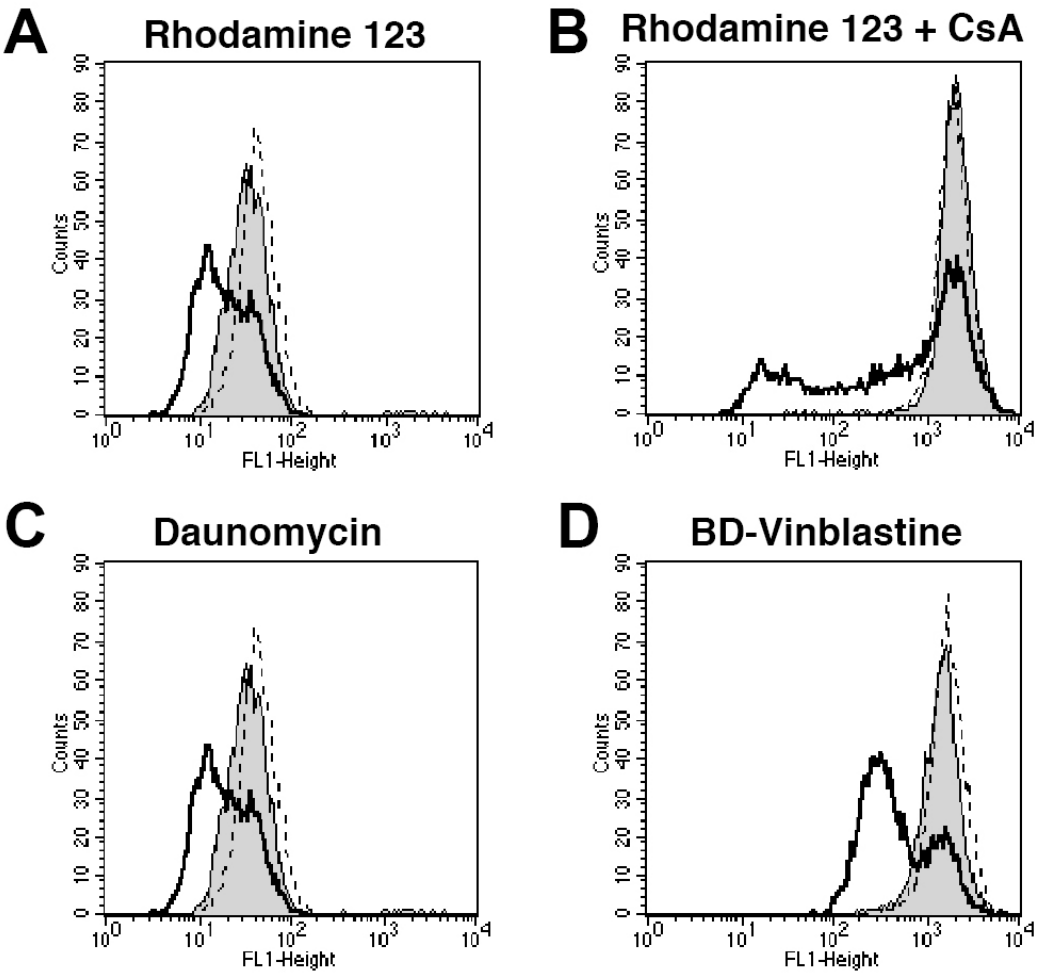

◄ SUPPL. FIGURE 3. **PGP19 expressed in HeLa cells does not transport mammalian MDR substrates.**
Grey peak represents cells transformed with pTM1 control vector (negative control). Solid line: Homo sapiens MDR1 (positive control), small dashes: PGP19. Shifting of observed peaks to the left indicates transport of the fluorescent substrate. Substrates tested included:
(A) Rhodamine 123, ***(B)*** Rhodamine 123 + cyclosporin A,
(C) daunomycin, and ***(D)*** BODIPY-tagged vinblastine.
Assays were performed according previously described protocols (Geisler *et al.*, 2005), and substrate retention was analyzed by FACS.

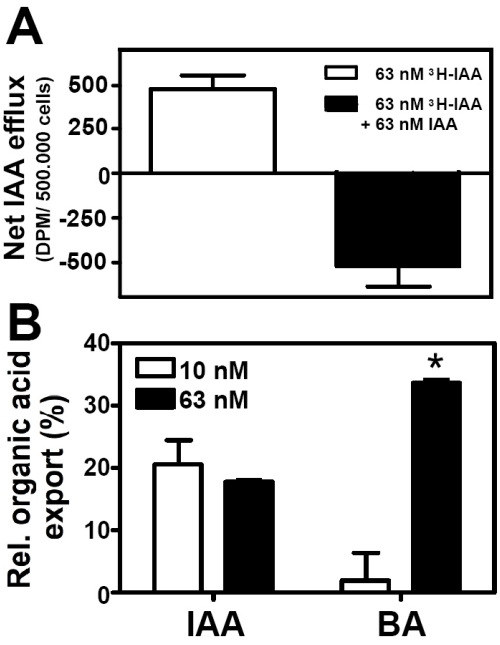

▲ SUPPL. FIGURE 4. **PGP19 expressed in HeLa cells exports benzoic acids at higher concentrations and oxidative IAA breakdown products.**
A, Unlabelled auxin degradation products competitively inhibit PGP19-modulated efflux. HeLa cells expression PGP1 were incubated with a 2:1 mixture of 50.3% 3H-IAA and oxidative IAA breakdown products (20.4% 3H-oxindole-3-acetic acid, 16.8% 3H-oxindole-3-carbinol, 5.7% 3H-indole-3-aldehyde, and 6.8% 3H-methylene oxindole, by LC-MS/MS). ***B,*** HeLa cells expressing PGP19 exhibited increased efflux of IAA, but not benzoic acid, when cells were loaded with 10 nM radiolabeled substrate. *Significantly different from 10 nM organic acid ($P < 0.05$, ANOVA test).

▲ SUPPL. FIGURE 5. **Expression of PGP1 and PGP19 is unchanged in the twd1 background.**
Microsomal fractions of wild-type and twd1 obtained by linear sucrose gradient centrifugation (Geisler *et al.*, 2003) were vacuum-transferred onto nitrocellulose (dot blots) and immunoprobed against anti-PGP1 (Sidler *et al.*, 1998) that cannot differentiate between PGP1 and PGP19 (Geisler *et al.*, 2005). Immunopositive fractions represent plasma membrane fractions as was demonstrated by the usage of marker enzymes as described in Geisler *et al.* (2005).

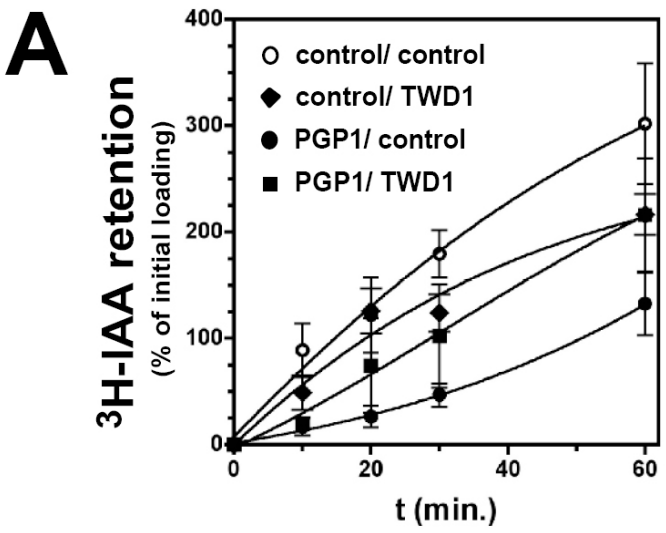

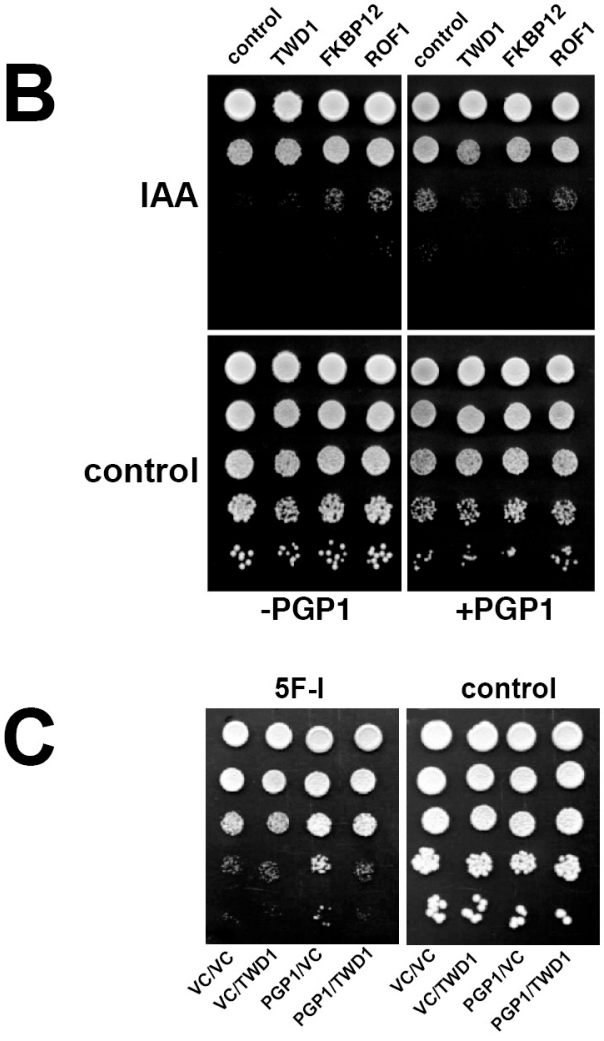

▲ SUPPL. FIGURE 6. **Co-expression of TWD1 with PGP1 reduces PGP1-mediated IAA export.**
A, Reduction in auxin uptake (efflux) is presented as relative loading of initial loading. Shown are means with standard deviations; n = 4. ***B,*** Yeast growth assays on 10 µM IAA show that TWD1 but not Arabidopsis FKBP12 or ROF1/FKBP59 reverts PGP1-mediated complementation of the IAA-hypersensitive *yap1-1* mutant. ***C,*** Yeast growth assays demonstrate inhibition of PGP1-mediated detoxification of the cytotoxic auxin analogue 5-fluoro indole by co-expressing TWD1

Modulation of P-glycoproteins by auxin transport inhibitors is mediated by interaction with immunophilins

Aurélien Bailly[1], Valpuri Sovero[1], Vincent Vincenzetti[1], Diana Santelia[1,5], Dirk Bartnik[2], Bernd W. Koenig[2,3], Stefano Mancuso[4], Enrico Martinoia[1], and Markus Geisler[1,*]

[1] University of Zurich, Institute of Plant Biology and Zurich-Basel Plant Science Center, CH-8008 Zurich, Switzerland
[2] Institute of Neuroscience and Biophysics, Research Centre Jülich, D-52425 Jülich, Germany
[3] Institute of Physical Biology, Heinrich-Heine University Düsseldorf, D-40225 Düsseldorf, Germany
[4] Department of Horticulture, University of Firenze, I-50019 Sesto Fiorentino, Italy
[5] present address: Zurich-Basel Plant Science Center, ETH Zürich Institute of Plant Science, CH-8092 Zurich, Switzerland

* Corresponding author: University of Zurich, Institute of Plant Biology and Zurich-Basel Plant Science Center, CH-8008 Zurich, Switzerland, Tel.: +41-44-634-8277, Fax.: +41-44-634-8204, E-mail: markus.geisler@botinst.uzh.ch

Summary

Immunophilin-like FKBP42, TWISTED DWARF1 (TWD1), has been shown to control plant development by positive modulation of P-glycoprotein (PGP)-mediated transport of the plant hormone auxin. TWD1 functionally interacts with closely related PGP1 and PGP19/MDR1, and both bind the synthetic auxin transport inhibitor, N-1-naphylphtalamic acid (NPA) and are inhibited by NPA and flavonoids. Flavonoids are suspected modulators of auxin transport, however, the mechanisms by which flavonoids and NPA interfere with auxin efflux components are unclear.

Here, we report by using bioluminescence resonance energy transfer (BRET) specific disruption of PGP1-TWD1 interaction by NPA and flavonoids, the latter functioning as established inhibitors of mammalian and plant PGPs. In accordance, TWD1 was shown to mediate modulation of PGP1 efflux activity by auxin transport inhibitors. NPA binds to both PGP1 and TWD1 but was excluded from the PGP1-TWD1 complex. As a consequence, auxin fluxes and gravitropism in twd1 roots are less affected by NPA treatment while TWD1 gain-of-function promotes root bending. Our data support a novel model mode of drug-mediated P-glycoprotein regulation mediated via protein-protein interaction with immunophilin-like TWD1.

Introduction

Bioactive flavonoids derived from plant secondary metabolism serve as important nutraceuticals (Taylor and Grotewold, 2005). They have health-promoting effects, including anti-oxidant, anti-carcinogenic, anti-viral and anti-inflammatory activities, however, the *in vivo* protein cellular targets remain largely unknown (Morris and Zhang, 2006; Taylor and Grotewold, 2005). In plants, among other functions, flavonoids, such as quercetin, kaempferol and other aglycone molecules, have been shown to inhibit polar auxin transport (PAT) (Brown et al., 2001; Jacobs and Rubery, 1988; Murphy et al., 2000; Peer et al., 2004; Taylor and Grotewold, 2005) and consequently to enhance localized auxin accumulation. During PAT, the plant hormone auxin, determining many if not all aspects of plant physiology and development, is moved directionally in a cell-to-cell mode (Blakeslee et al., 2005; Kerr and Bennett, 2007; Vieten et al., 2007).

The regulatory impact of flavonoids on PAT is mainly based on their ability to compete with N-1-naphtylphtalamic acid (NPA), a synthetic auxin transport inhibitor (ATI) (Jacobs and Rubery, 1988; Lomax et al., 1995; Luschnig, 2001; Morris, 2000) and herbicide (naptalam©), for transporter binding sites. This concept is further supported by auxin-related phenotypes of *Arabidopsis* mutants with altered flavonoid levels (Brown et al., 2001; Peer et al., 2001; Taylor and Grotewold, 2005). As fundamental physiological processes occure in the absence of flavonoids, they are better viewed as modulators than as essential transport regulators. However, the mechanisms by which flavonoids interfere with auxin efflux components are not yet clear (Taylor and Grotewold, 2005).

The auxin efflux complex is thought to regulate PAT on the molecular level and consists of at least two proteins: the membrane integral transporter and the NPA-binding protein (NBP) regulatory subunit (Lomax et al., 1995; Luschnig, 2001). Recently, P-glycoproteins/multidrug resistance (MDR) proteins (ABCB; hereafter referred to as PGPs), members of the expanded *Arabidopsis* ABC (ATP-binding cassette) transporter family, have been identified as both auxin transporters (Bouchard et al., 2006; Geisler et al., 2005; Geisler and Murphy, 2006; Santelia et al., 2005; Terasaka et al., 2005) and high-affinity NBPs (Murphy et al., 2002; Noh et al., 2001).

High NPA concentrations cause inhibition of auxin efflux catalyzed by PGP1 and PGP19 (Bouchard et al., 2006; Geisler et al., 2005), most probably by binding to the transporter itself (Noh et al., 2001). This is in analogy to flavonoids, functioning as inhibitors of plant (Bouchard et al., 2006; Geisler et al., 2005; Terasaka et al., 2005) and mammalian PGPs (Morris and Zhang, 2006), probably by mimicking ATP and competing for PGP nucleotide binding domains (Conseil et al., 1998). Over-expression of certain PGPs is associated with increased MDR, whereas loss of function often results in diverse diseases (Dean, 2005) in mammalians.

The immunophilin-like, plasma membrane-anchored (Geisler et al., 2003; Kamphausen et al., 2002) FKBP42, TWISTED DWARF1 (TWD1) (Geisler and Bailly, 2007; Geisler et al., 2003; Romano et al., 2005) belongs to the FK506-binding protein (FKBP)-type family of PPIases (peptidyl-prolyl *cis-trans* isomerases, EC 5.1.2.8) (Fanghanel and Fischer, 2004; Geisler and Bailly, 2007; Romano et al., 2005). Many but not all PPIases catalyze the *cis-trans* isomerization of *cis*-prolyl bonds and have been identified as targets of immunosuppressant drugs, such as FK506 (tacrolimus) (Fanghanel and Fischer, 2004; Geisler and Bailly, 2007; Romano et al., 2005).

TWD1 docks with its N-terminal FKBD (FK506-binding domain), shown to lack PPIase activity and FK506 binding (Geisler et al., 2003; Kamphausen et al., 2002), to C-terminal nucleotide binding folds of PGP1 and PGP19 (see Fig. 1A). In this way, TWD1 acts *in planta* as positive regulator of PGP1- and PGP19-mediated auxin efflux by means of protein-protein interaction (Bouchard et al., 2006; Geisler et al., 2003), modulating long-range auxin transport on the cellular level (Bouchard et al., 2006; Lewis et al., 2007).

Here, we employed a yeast-based BRET (Bioluminescence resonance energy transfer) system in order to investigate PGP1-TWD1 interaction on a molecular level. Auxin transport inhibitors and flavonoids, inhibitors of mammalian and plant PGPs, disrupt PGP1-TWD1 interaction. Auxin transport inhibitors modulate the regulatory effect of TWD1 on PGP1 activity, supporting a novel mode of PGP regulation via immunophilin-like TWD1 (Bouchard et al., 2006). This represents a new concept of drug-

mediated ABC transporter modulation via membrane-anchored immunophilins and may have important agronomic and clinical implications.

Experimental Procedures

Yeast constructs, growth and expression analysis

cDNA covering the N-terminal FKBD of *Arabidopsis* TWD1 (TWD1$^{1-187}$; At3g21640) were cloned into *Bam*HI and *Sal*I sites of the copper-inducible yeast shuttle vector pRS314CUP (Bouchard et al., 2006) resulting in pRS314CUP-FKBD. Point mutations in TWD1 and a stop codon in PGP1 (bp 3.240) were introduced using the QuikChange XL site-directed mutagenesis kit (Stratagene, La Jolla, USA) resulting in pRS314CUP-TWD1$^{C70D, L72E}$ and pNEV-PGP1$^{\Delta NBD2}$-YFP (Bouchard et al., 2006). Empty vector controls pNEV and pRS314CUP as well as pNEV-PGP1, pNEV-PGP1-YFP, pNEV-PGP1$^{\Delta NBD2}$-YFP, pRS314CUP-FKBD, pRS314CUP-FKBD-rLuc, pRS314CUP-TWD1 and pRS314CUP-TWD1-rLuc were transformed into *S. cerevisiae* strains JK93dα (Hemenway and Heitman, 1996) and single colonies were grown in synthetic minimal medium without uracil and tryptophan, supplemented with 2% glucose and 100 µM $CuCl_2$ (SD-UT).

Cells co-expressing PGP1-YFP and TWD1-CFP (Bouchard et al., 2006) grown in the presence of 10 µM drugs or solvent control to an OD_{600} around 0.8 were washed and incubated in mounting media containing DAPI and fluorescence pictures were collected by confocal laser scanning microscopy (Leica, DMIRE2) equipped with argon (488 nm) and UV laser (410 nm). Fluorescence and DIC images were processed using Adobe Photoshop 7.0. Vector controls showed no detectable fluorescence. Plasma membrane fractions were separated via continuous sucrose gradient centrifugation (Geisler et al., 2004), subjected to 4-20% PAGE (Long Life Gels, Life Therapeutics) and Western blots were immunoprobed using anti-GFP (Roche, Switzerland) and anti-rLuc (Chemicon International).

For auxin analogue detoxification assays (Bouchard et al., 2006; Luschnig et al., 1998), transformants grown in SD-U to an OD_{600} around 0.8 were washed and adjusted to an OD_{600} of 1.0 in water. Cells were 5-times 10-fold diluted and each 5 µl were spotted on minimal media plates supplemented with 750 µM 5-fluoro indole (Sigma). Growth at 30°C was assessed after 3-5 days. Assays were performed with 3 independent transformants.

BRET constructs and assays

Renilla luciferase (rLuc, acc. no. AY189980) was amplified by PCR from plasmid pRL-null (Promega) and inserted in-frame into *Asc*I sites generated in the coding regions of pRS314CUP-FKBD and pRS314CUP-TWD1 (bp 64) using the QuikChange XL site-directed mutagenesis kit (Stratagene, La Jolla, USA). In this way, rLuc was inserted into the very N-terminus of TWD1. Single colonies co-expressing PGP1-YFP (Bouchard et al., 2006) and TWD1-rLuc were grown in selective synthetic minimal medium SD-UT in presence of inhibitors or adequate amounts of solvents. 200 ml overnight cultures were harvested at OD_{600}=1 by centrifugation for 10 min. at 1,500xg and washed two times with ice-cold milliQ water. The resulting pellet was suspended in 4 ml ice-cold Lysis Buffer (50 mM Tris, 750 mM NaCl, 10 mM EDTA) supplemented with proteases inhibitors (Complete tablets, Roche Diagnostics GmbH, Germany) and an equivalent volume of acid washed glass beads (Ø=0.5 mm, Biospec Products Inc., USA) was added. Cells were broken by vortexing 10 times for 1 min, with 1 min intervals on ice for cooling. The supernatant was decanted, and the beads were washed four times with 10 ml ice-cold Lysis Buffer. Supernatants were centrifuged at 4,500xg (S1) and 12,000xg (S2) for 10 min at 4°C to remove unbroken cells and other debris. Membranes were collected by centrifugation at 100,000xg (P3) for 1 h at 4°C. The membrane pellet was homogenized using a pestle in 300 µl ice-cold STED10 buffer (10% sucrose, 50 mM Tris, 1 mM EDTA, 1 mM DTT) supplemented with proteases inhibitors to give a suspension of about 3 mg of proteins per ml, as measured using the Bradford assay (BioRad, Germany). All preparations were stored at -80°C for subsequent use. In vitro measurement of BRET signal was performed using 200 µl of yeast membranes suspension (approximately 600 µg of proteins) in white 96-well microplate (OptiPlate-96, PerkinElmer Life Sciences, USA). 5 µM coelenterazine (Biotium Inc., USA) was added and sequential light emission acquisition in the 410 ± 80nm and 515 ± 30nm windows was started after 1 min using the Fusion microplate analyzer (PMT=1100V,

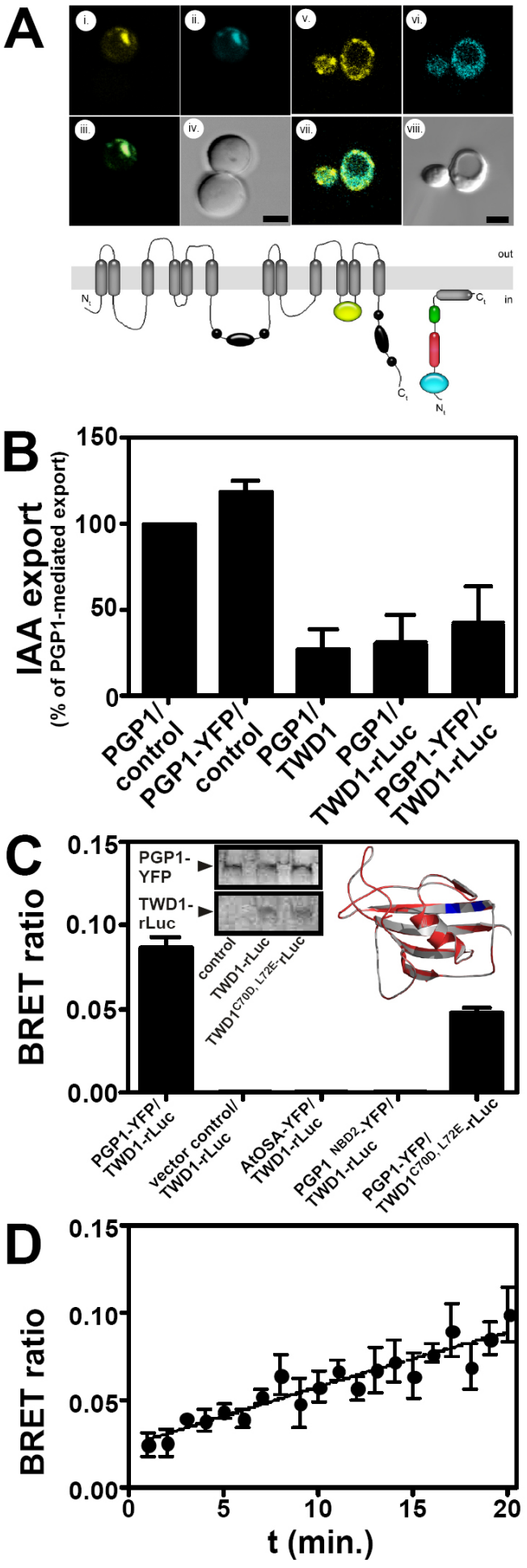

FIGURE 1. **A yeast-based BRET system of TWD1-PGP1 interaction**

A, Co-localization of PGP1-YFP (yellow) and TWD1-CFP (blue) in yeast (upper panel). Illustrating model of PGP1-YFP and TWD1-rLuc interaction resulting in BRET (lower panel). Nucleotide binding folds, black; YFP, yellow; FK506-binding domain (FKBD), red; tetratricopetide repeat (TPR), green; rLuc, blue. The perpendicular orientation of the TWD1 C-terminus forming a so-called amphipatic in-plane membrane anchor (IPM) is based on (Scheidt et al., 2007).

B, PGP1-YFP and TWD1-rLuc are active. PGP1-YFP exports IAA comparable to native PGP1 (set to 100%) and co-expression of TWD1-rLuc reduces PGP1-mediated IAA efflux to a similar extent than wild-type TWD1. Reductions in auxin retention (efflux) were calculated as relative export of initial loading. Data are the means ± S.E. (n=4).

C, PGP1-YFP-TWD1-rLuc interaction quantified by BRET is specific. PGP1-YFP and TWD1-rLuc were co-expressed in yeast, sequential light emission acquisition on microsomes in 410 ± 80 nm and 515 ± 30 nm windows was quantified and BRET ratios were calculated as in (Angers et al., 2000). Inset, Western detection of PGP1/TWD1 on yeast microsomes (left) and structure comparison of native (red) and computed TWD1-rLuc$^{C70D,\ L72E}$ (grey, exchanges in blue) FKBDs (right).

D, PGP1-YFP/TWD1-rLuc interaction determined by BRET is stable over time. Presented are means ± S.E. from 6-10 independent experiments with 4 replicates each.

gain=1, reading time=1s; Packard, USA). BRET ratios were calculated as in Angers et al. (2000) as follows: [(emission at 515 ± 30nm) - (emission at 410 ± 80nm) × Cf] / (emission at 410 ± 80nm), where Cf corresponds to (emission at 515 ± 30nm) / (emission at 410 ± 80nm) for the rLuc fusion protein expressed alone in the same experimental conditions. Results are the average of 10 readings collected every minute; presented are average values from 6-10 independent experiments with 4 replicates each.

Yeast auxin transport assays

IAA transport experiments were performed as in Bouchard et al. (2006). In short, *S. cerevisiae* strains JK93dα (Hemenway and Heitman, 1996) were grown as above, loaded with ^{3}H-IAA (20 Ci/mmol; American Radiolabeled Chemicals Inc., St. Louis) for 20 min on ice, washed 2 times with cold water, and resuspended in 15 ml SD pH 5.5. 0.5 ml aliquots were filtered prior to (t = 0 min.) and after 10 min. incubation at 30°C. PGP1-mediated IAA export is expressed as relative

retention of initial (maximal) loading (t = 0 min.), which is set to 100%. Presented are average values from 6-8 independent experiments with 4 replicates each.

Drug binding assays

Whole yeast NPA binding assays (WYNBA) were essentially performed as in (Noh et al., 2001). 10 ml yeast cultures were grown as described above to an OD_{600} of 1 and cells were resuspended in 10 ml SD pH 4.5. To one ml aliquots (for each experiment 4 replicates were used) 10 nM ^{3}H-NPA (60 Ci/mmol) and 10 nM ^{14}C- benzoic acid (BA, 58 mCi/mmol; all from American Radiolabeled Chemicals Inc., St. Louis) were added in the presence and absence of 10 µM NPA (± 10 µM BA for competition experiments; 1000-fold excess). Cells were incubated for 1h at 4°C under shaking, washed with ice-cold MilliQ water, and tips of centrifuge tubes including pellets were subjected to scintillation counting. Reported values are means of specific binding (^{3}H-NPA bound in the absence of cold NPA (total) minus ^{3}H-NPA bound in the presence of cold NPA (unspecific)) from 4-8 independent experiments with 4 replicates each.

For PPIase affigel pull-down assays (PAPA), 2 mg of the PPIase domain/FKBD of TWD11-180 expressed in *E. coli* and purified as described in (Weiergraber et al., 2006) was coupled to 2 ml Affigel-15 beads (BioRad). 50 µl of Affigel-PPIase or empty Affigel beads (50% slurry) were resuspended in 450 µl of PBS pH 7.4 and 5 µl radiolabeled 7-^{14}C-BA (58 mCi/mmol, 0.1 mCi/ml) and ^{3}H-NPA (60 Ci/mmol, 1 mCi/ml; all from American Radiolabeled Chemicals Inc., St. Louis), diluted 20x in PBS was added to four replications of each. After shaking for one hour at 4°C, the beads were filtered on nitrocellulose, the filters washed three times with cold MilliQ water and finally subjected to scintillation counting. Reported values are means of specific binding (^{3}H-NPA bound to affigel-PPIase minus ^{3}H-NPA bound to empty affigel beads) per 1 µg of coupled protein as measured using the Bradford assay (BioRad, Germany). Presented are average values from 4-8 independent experiments with 4 replicates each.

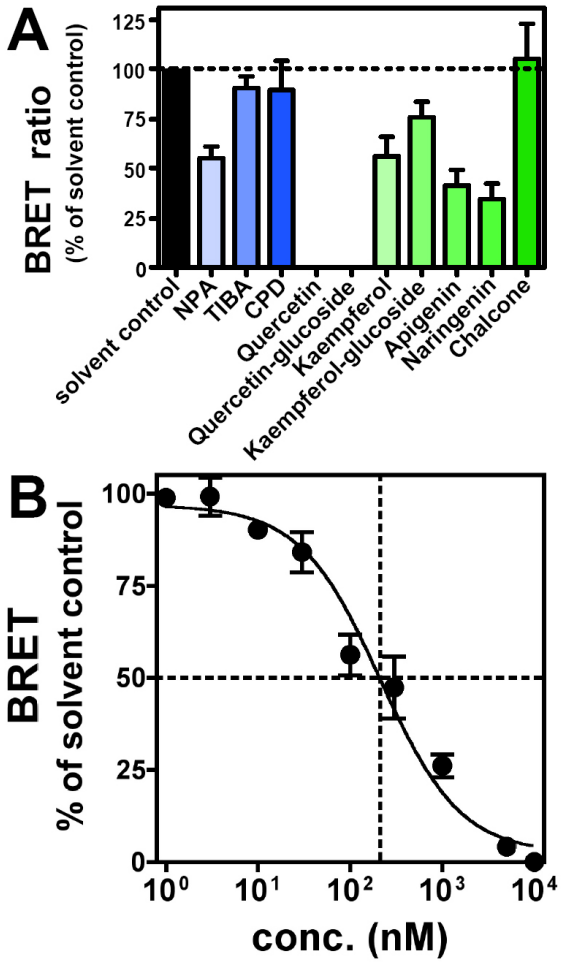

FIGURE 2. **TWD1-PGP1 interaction is disrupted by auxin transport inhibitors.**
A, PGP1-YFP-TWD1-rLuc interaction quantified by BRET is disrupted by ATI NPA and flavonoids (10 µM).
B, Dose-dependency of complex disruption by the flavonol, quercetin (inset).
PGP1-YFP and TWD1-rLuc were co-expressed in yeast, sequential light emission acquisition on microsomes in 410 ± 80 nm and 515 ± 30 nm windows was quantified and BRET ratios were calculated as in (Angers et al., 2000). Presented are means of BRET ratios ± S.E. (n=6-10).

For microsomes of *Arabidopsis* NPA-binding assays (MANBA), *Arabidopsis* seedlings were grown in liquid cultures and microsomes were prepared as described elsewhere (Geisler et al., 2004). Four replicates of each 20 µg of protein in STED10 were incubated with 10 nM ^{3}H-NPA (60 Ci/mmol) and 10 nM ^{14}C-BA (58 mCi/mmol) in the presence and absence of 10 µM NPA (± 10 µM BA for competition experiments; 1000-fold excess). After 1h at 4°C under shaking, membranes were filtered over nitrocellulose filters (MF 0.45 µm, Millipore), washed three times with cold MilliQ water and filters were subjected to scintillation counting. Reported values are means of specific binding (^{3}H-NPA bound in the absence of cold NPA (total) minus ^{3}H-NPA bound in the presence of cold NPA (unspecific)) from 3 independent experiments with 4 replicates each.

Plant growth conditions and quantitative analysis of root gravitropism

Arabidopsis thaliana plants were grown as described previously (Geisler et al., 2003). For quantification of gravitropism, wild type, *pgp1* (At2g36910) and *pgp19* (At3g28860), *pgp1/pgp19* and *twd1* (At3g21640) mutants (all ecotype Wassilewskija (Was)), seeds were surface sterilized and grown on 1/2 Murashige and Skoog (MS) medium, 0.7% phytoagar (Gibco Invitrogen Corporation, Paisley, UK) under continuous light conditions in the presence or absence of 5 µM NPA as described in (Bouchard et al., 2006). In some cases, 5 dag seedlings grown vertically on 1/2 MS medium, 0.7% agar, 1% sucrose were transferred for additional 12 hours onto new plates containing 5 µM NPA or the solvent, DMSO. Plates were rotated 90° from the vertical for 12 hours gravity stimulation in the dark. The angle of root tips from the vertical plane was determined using Photoshop 7.0. (Adobe Systems, Mountain View, CA) and each gravistimulated root was assigned to one of twelve 30°

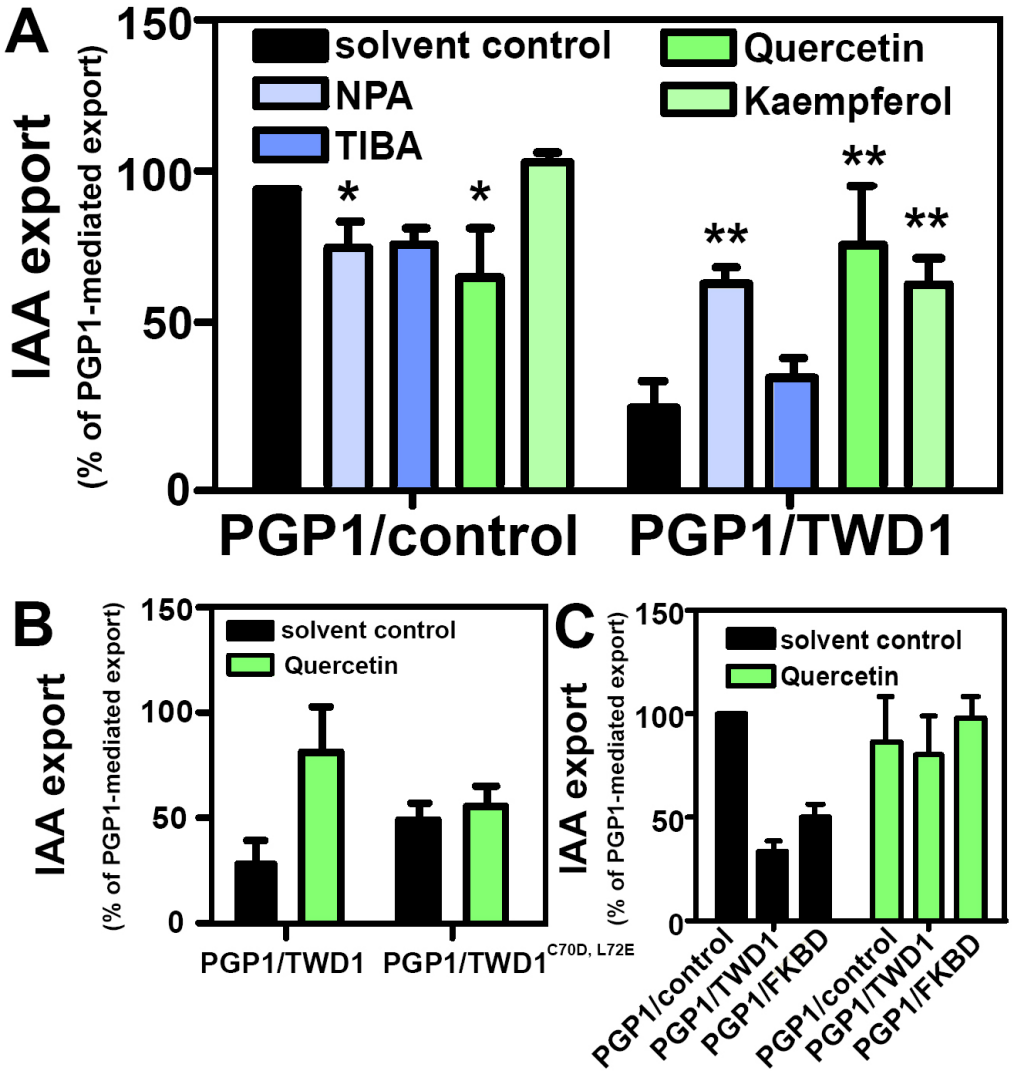

FIGURE 3. **TWD1 confers ATI modulation of PGP1-mediated auxin efflux activity.**
A, Effect of TWD1 on PGP1-mediated IAA export (Bouchard et al., 2006) assayed in the presence of auxin transport inhibitors. Data are means ± S.E. (n=4-6). Reductions in auxin retention (efflux) were determined as relative retention of initial loading; PGP1-mediated IAA export was set to 100%. Data are means ± S.E. (n=4-6). * (**) Significantly different from PGP1 (PGP1/TWD1)-mediated IAA transport ($p<0.05$).
B, Two point mutations in TWD1-rLuc$^{C70D, L72E}$ abolish the modulatory effect of quercetin on PGP1 activity. Data are means ± S.E. (n=4-6). Reductions in auxin retention (efflux) were determined as relative retention of initial loading; PGP1-mediated IAA export was set to 100%. Data are means ± S.E. (n=4-6).
C, The FKBD of TWD1 is responsible for PGP1 regulation. Co-expression of the soluble FKBD of TWD1 reduces PGP1-mediated IAA efflux to a similar extent than membrane-bound, full-length TWD1. Quercetin (10 µM) disrupts the inhibitory effect of TWD1 and FKBD on PGP1 activity.

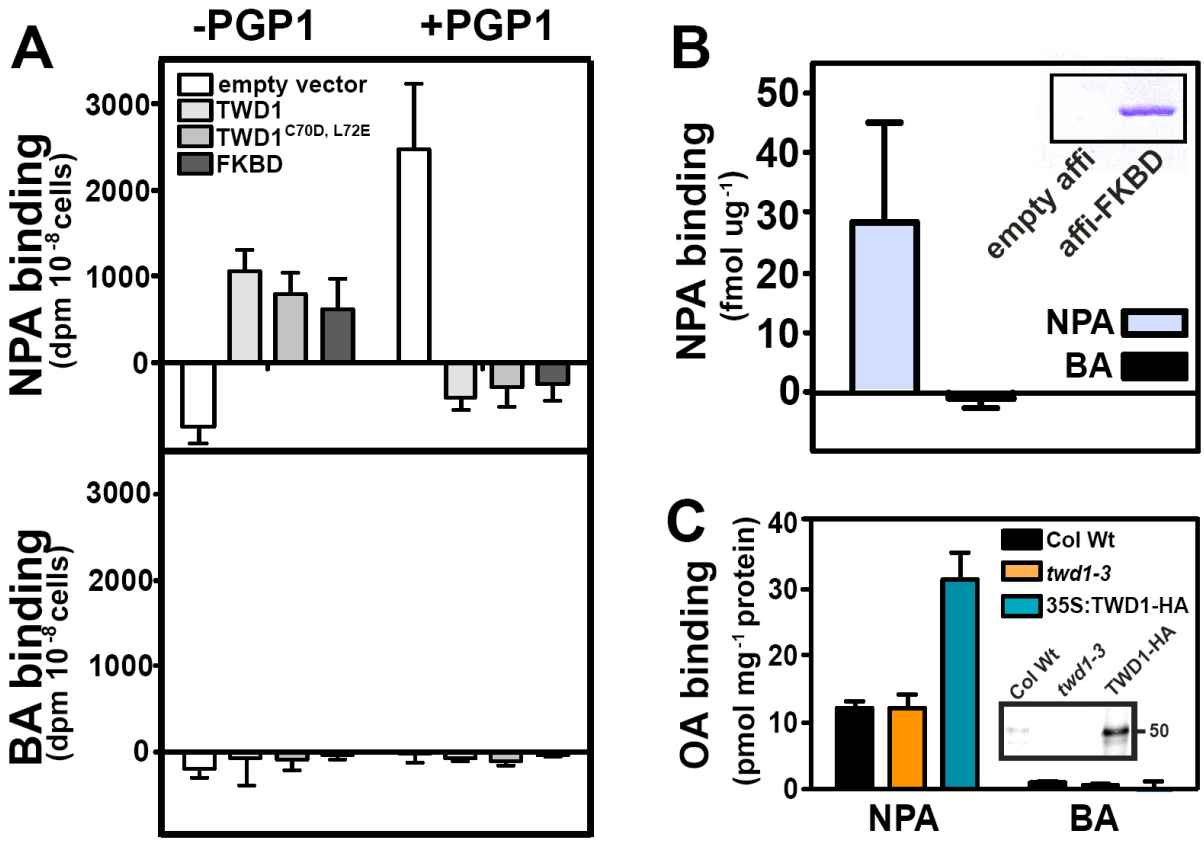

FIGURE 4. **NPA binding to PGP1 and TWD1 is abolished in the PGP1-TWD1 complex.**
A, Binding assays of whole yeast expressing TWD1 and PGP1 (WYNBA) assaying NPA and benzoic acid (BA) in parallel. Reported values are means of specific binding from 4-8 independent experiments with 4 replicates each.
B, NPA binding assay using purified affigel-coupled TWD1 FKBD (PAPA). Reported values are means of specific binding ± S.E (n=4-8). Coomassie stain of coupled FKBD (inset).
C, Binding of organic acids (OA), NPA- and benzoic acid (BA), to microsomal fractions of *twd1* and $Pro_{CaMV35S}$-TWD1-HA. Data are means of specific binding ± S.E. (n=3). Inset, Western detection of TWD1 from microsomes (each 10 μg of protein).

sectors in the circular histograms; the length of each bar represents the percentage of seedlings showing the same direction of root growth. Helical wheels were plotted using the *PolarBar* software (http://botserv1.uzh.ch/home/martinoia/ index.html). The number of seedlings for each genotype was between 72 and 96.

Analysis of IAA responses

Homozygous T4 generations (Bouchard et al., 2006) of *A. thaliana* wild-type (ecotypes Was and Columbia Col)), *pgp1*, *pgp19*, *pgp1/pgp19* and *twd1* mutants (all in Was) expressing the maximal auxin-inducible reporter Pro_{DR5}:GFP (Ottenschlager et al., 2003) were grown vertically for 5 days as described above, and analyzed by confocal laser scanning microscopy (Leica, DMIRE2) equipped with an argon laser (488 nm). In some cases, seedlings were transferred for additional 12 hours onto new plates containing 5 μM NPA or the solvent, DMSO, and gravistimulated for 2 hours by turning plates 90°. For histological signal localization DIC and GFP images were electronically merged using Photoshop 7.0 (Adobe Systems, Mountain View, CA).

Recording of root apex auxin fluxes using an IAA-specific microelectrode

A platinum microelectrode was used to monitor IAA fluxes in Arabidopsis roots as described in (Bouchard et al., 2006; Mancuso et al., 2005). For measurements, plants were grown in hydroponic cultures and used 5 dag. Differential current from an IAA-selective microelectrode placed 2 μm from the root surface was recorded in the absence and presence of 5 μM NPA. Relative NPA inhibition was calculated by dividing peak influx values (at 200 nm from the root tip) in the absence of NPA by those in the presence.

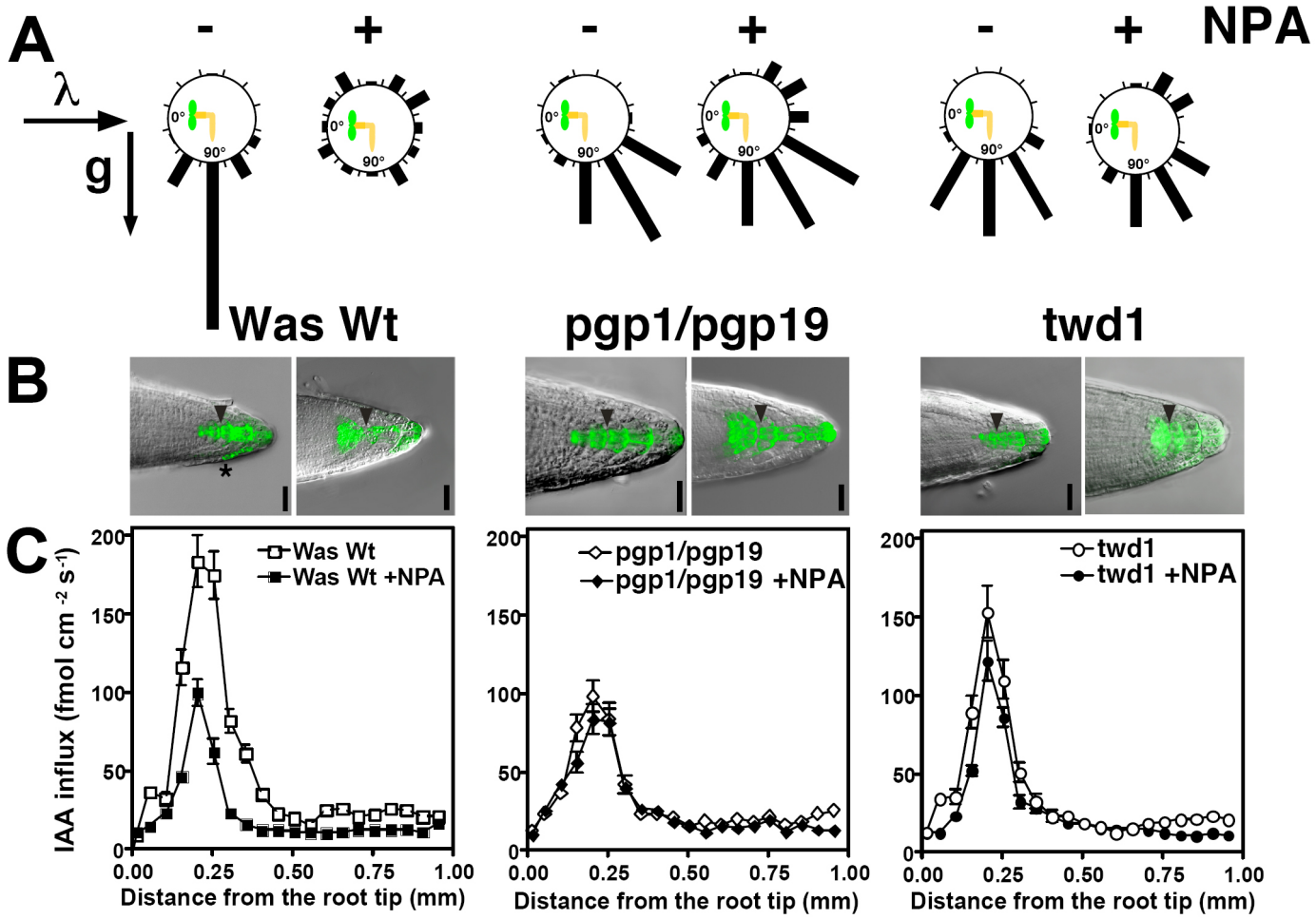

FIGURE 5. ***Twd1* roots are less sensitive to auxin transport inhibitor, NPA.**
A, NPA disrupts gravitropic responses in wild type (Was Wt), and to a lesser extent in *twd1* roots. Arrows indicate direction of light (λ) and gravitropism (g).
B, Expression of the auxin-responsive reporter Pro_{DR5}-GFP (Bouchard et al., 2006) upon gravistimulation (from the top). Note that asymmetric auxin accumulation is more pronounced in the commonly used Columbia than in the Wassilewskija ecotype (Fig. S4). Scale bars, 200 µm.
C, IAA influx profile along wild type, *pgp1*/*pgp19* and *twd1* roots measured using an IAA-specific microelectrode (Bouchard et al., 2006; Mancuso et al., 2005; Santelia et al., 2005); positive fluxes represent a net IAA influx. Data are means ± S.E. (n=6-8).

Data analysis

Data were analyzed using Prism 4.0b (GraphPad Software, San Diego, CA) and statistical analysis was performed using SPSS 11.0 (SPSS Inc., Chicago, IL). FKBD structure alignment was performed using PyMol 0.99 (www.pymol.org).

Results

Establishment of a yeast-based PGP1-TWD1 BRET system

Despite the fact that FKBPs are well-known subunits and modulators of multi-protein complexes (Bouchard et al., 2006; Chelu et al., 2004; Hemenway and Heitman, 1996), ABC transporter regulation by FKBPs has been only reported for murine MDR3 and *Arabidopsis* PGP1 (Bouchard et al., 2006; Geisler et al., 2004; Geisler et al., 2003; Hemenway and Heitman, 1996). Moreover, the mechanisms by which NPA or flavonoids interfere with auxin efflux complex components, and hence with cell-to-cell/polar auxin transport (PAT) (Blakeslee et al., 2005; Kerr and Bennett, 2007; Vieten et al., 2007), are not clear (Brown et al., 2001; Lewis et al., 2007; Peer et al., 2004; Taylor and Grotewold, 2005).
Therefore, and in order to analyze PGP1-TWD1 interaction and its impact on cellular auxin efflux

at the molecular level, we established a yeast-based BRET (Bioluminescence resonance energy transfer) assay by co-expressing TWD1 and PGP1 fused to bioluminescence donor *Renilla* luciferase (rLuc) and acceptor fluorophore YFP, respectively (Figure 1A). PGP1-YFP and TWD1-rLuc fusion proteins are functional as shown by analysis of IAA export upon co-expression and PGP1-YFP mediated detoxification of auxin analogs in yeast (Figure 1B, S1). As shown previously, TWD1 has in yeast, unlike than in mammalian and plant cells, an inhibitory effect on PGP1 (Bailly et al., 2006; Bouchard et al., 2006); the difference might be due to the lack of higher eukaryote components in yeast. However, TWD1-rLuc inhibited PGP1- or PGP1-YFP mediated auxin efflux to wild type level.

PGP1-YFP and TWD1-rLuc co-localize on the plasma membrane and small plasma membrane-attached vesicles (Figure 1A, C, (Bouchard et al., 2006)) and co-expression results in a stable, highly reproducible BRET signal (Figure 1C) that was quantified as a ratio of the light emitted by PGP1-YFP over that emitted by TWD1-rLuc (BRET ratio (Angers et al., 2000)). This BRET signal was specific as, first, no BRET was observed in the absence of PGP1-YFP (Figure 1C), with PGP1 minus YFP (not shown) or with AtOSA-YFP, an unrelated protein kinase that co-localized with TWD1-CFP (Figure 1A). Second, deletion of the interacting C-terminus of PGP1-YFP abolished BRET entirely, while, third, introduction of two point mutations in the ß$_2$ sheet of the TWD1 FKBD (Granzin et al., 2006) (TWD1$^{C70D, L72E}$-rLuc) that does apparently not significantly affect the overall FKBD structure and PGP1-YFP expression (Figure 1C, inset), reduced BRET significantly (46% reduction, Figure 1C).

Moreover, specificity of interaction was further validated by the fact that a soluble FKBD-rLuc was specifically retained by PGP1-, but not by related auxin importer PGP4- (Santelia et al., 2005) or vector control membranes, and restored BRET when added to PGP1-YFP membranes[1] (Supplemental figure 4). Together these results unambiguously demonstrate that PGP1 and TWD1 are compatible partners in yeast and that BRET was specific.

Identification of drugs that alter PGP1-TWD1 interaction using BRET

BRET signal stability and linearity over time (Figure 1D) allowed us to screen a mini-library of putative auxin transport inhibitors (ATIs) for drugs that were able to alter PGP1-TWD1 interaction. The synthetic ATI, NPA, (Jacobs and Rubery, 1988; Lomax et al., 1995; Luschnig, 2001; Morris, 2000) has been shown to bind to Arabidopsis PGPs employing whole yeast assays and NPA-affinity chromatography (Geisler et al., 2003; Murphy et al., 2002; Noh et al., 2001).

NPA reduced BRET by about 50%, thus disrupted PGP1-TWD1 interaction (Figure 2A). This verifies previous *in planta* data where excess of NPA was shown to exclude TWD1 from PGP-positive NPA chromatography fractions (Geisler et al., 2003). Not unexpectedly, the ATIs TIBA (2, 3, 5-triiodobenzoic acid) and CPD (2-carboxylphenyl-3-phenylpropan-1, 3-dione), the former known to employ different loci of action than NPA (Petrasek et al., 2003), did not alter BRET significantly.

Next, we tested representative flavonoids, known inhibitors of PAT on one hand and of plant (Bouchard et al., 2006; Geisler et al., 2005; Terasaka et al., 2005) and mammalian PGPs (Morris and Zhang, 2006) on the other. Interestingly, the flavonol quercetin abolished BRET efficiently with an apparent IC_{50} of about 200 nM (Figure 2B). With the exception of the flavonoid precursor chalcone, all flavonoids tested disrupted PGP1-TWD1 interaction but were less efficient than quercetin. Interestingly, quercetin- and kaempferol-3-O-glucoside, the most common *Arabidopsis* flavonol glycoside derivates (Peer et al., 2004; Peer et al., 2001), were as effective as their aglycones in disrupting PGP1-TWD1 interaction.

In summary, our data indicate that NPA and flavonoids disrupt TWD1-PGP1 interaction with quercetin being the most efficient.

TWD1 confers drug modulation of PGP1 efflux activity

With the intention to investigate the physiological impact of these drug effects, we quantified PGP1-mediated IAA transport in the presence of TWD1 in yeast. As expected, TWD1-mediated inhibition of IAA export catalyzed by PGP1 was reverted by NPA and the flavonols quercetin and kaempferol (Figure 3A)[2], which is in line with decreased interaction and BRET.

1 Direct measurement of PGP1-YFP/FKBD-rLuc BRET was not possible due to the high FKBD-rLuc expression and its strong light emission.

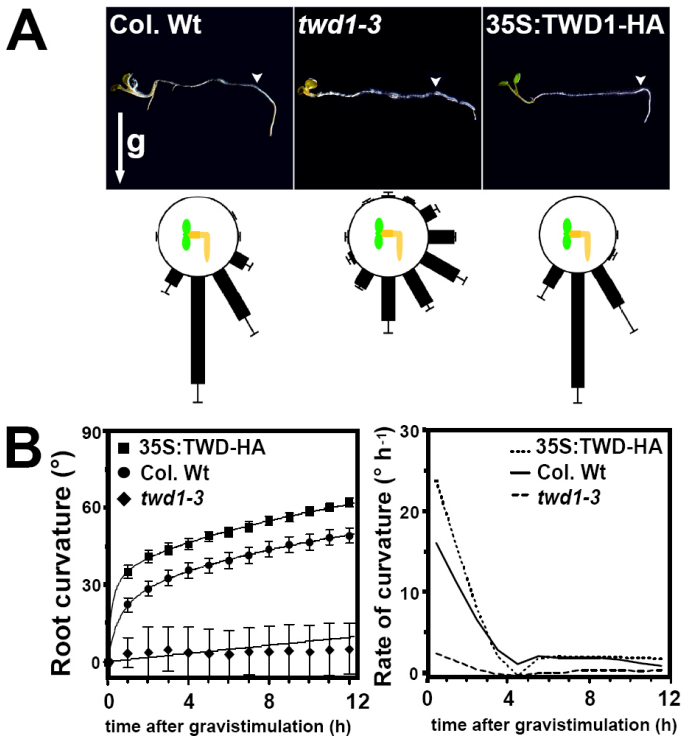

FIGURE 6. **Over-expression of *TWD1* promotes root gravitropism.**
A, Gravitropic root responses of *TWD1* loss- (*twd1-3*) and gain-of-function, $Pro_{CaMV35S}$-TWD1-HA (35S-TWD1-HA) alleles in comparison to wild type (Col. Wt). Arrows indicate direction of gravitropism (g); triangles mark time-point of 90° plate rotation (upper panel). Root curvatures was assigned to one of twelve 30° sectors in the circular histograms; the length of each bar represents the percentage of seedlings showing the same direction of root growth. Data are means ± S.E. (n=3 with each 72 to 96 seedlings).
B, Time series (left panel) of *A* and first derivative of root curvature (right panel).

TIBA, which is not a representative ATI (Petrasek et al., 2003) and which had no significant effect on the TWD1-PGP1 complex (Figure 2A), did not alter IAA transport (Figure 2A).
This modulatory effect was dependent on TWD1 because drug treatments in the absence of TWD1 had no stimulating but only mild inhibitory effects (Figure 3A), as reported recently (Bouchard et al., 2006; Geisler et al., 2005). Indirect effects, like mistargeting or altered PGP1 expression caused by drug treatments, were excluded by co-immunolocalization (Supplemental figure 3) and Western blotting analysis (results not shown) of yeast co-expressing TWD1-CFP and PGP1-YFP.
Point mutations in the FKBD bisecting PGP1-TWD1 interaction (Figure 1C) abolished transduction of regulatory effects of quercetin on PGP1 activity completely (Figure 3B). Moreover, the soluble FKBD of TWD1 alone was sufficient to functionally substitute full-length TWD1 in both PGP1 repression and quercetin-mediated reversal of PGP1 activity (Figure 3C). These results together indicate that the TWD1 functions as a modulator of PGP1-mediated auxin transport that mediates the regulatory impact of ATIs by its FKBD.

NPA binding to PGP1 and TWD1 is abolished in the PGP1-TWD1 complex

NPA was shown to inhibit and bind to PGPs (Bouchard et al., 2006; Geisler et al., 2005), however, excess of NPA was shown to exclude TWD1 from PGP-positive NPA chromatography fractions (Geisler et al., 2003). In order to test the hypothesis that TWD1 competes for NPA-binding on PGP1, we quantified binding of radio-labeled NPA using established whole yeast assays (Noh et al., 2001). NPA binding was specific as it was out-competed by an excess NPA (see *Experimental Procedures*) but not displaced by benzoic acid (not shown).
PGP1-expressing yeast specifically bound NPA (Figure 4A) as was shown previously for close homolog PGP19 (Noh et al., 2001). Surprisingly, less but significant NPA-binding was also observed for yeast expressing TWD1 or its FKBD (Figure 4A). NPA binding was specific as neither PGP1 nor TWD1 bound the organic acid benzoic acid (BA), used as a negative control in auxin research. Indirect effects, like TWD1-induced NPA binding to yeast endogenous proteins, were excluded by demonstrating NPA binding to highly purified, affigel-immobilized FKBD (Figure 4B) that was used for crystallization studies (Granzin et al., 2006). In agreement, NPA-binding was strongly enhanced in microsomal fractions prepared from *TWD1* gain-of-function plants ($Pro_{CaMV35S}$-TWD1-HA; Fig. 4C) compared to wild type. *Twd1* microsomes showed no significant differences in NPA binding compared to wild type, most probably due to the low expression level of *TWD1* (Figure 4C inset) (Bouchard et al., 2006; Geisler et al., 2003).

However, co-expression of PGP1 with TWD1 abolished NPA binding to PGP1 and TWD1 (Figure 4) but did not significantly alter the expression level of the two proteins (Figure 1B), suggesting that the

PGP1-TWD1 (FKBD) complex has a lower affinity for NPA or that binding pockets were simply masked. Again, in analogy to auxin transport assays, co-expression of the FKBD eliminated NPA binding to PGP1 indicating that, the N-terminal FKBD was sufficient to perform TWD1 function.

TWD1 mediates drug-modulation of P-glycoproteins in vivo

To test our conclusions derived from the yeast model and to substantiate the physiological relevance of the proposed TWD1 function *in planta*, we investigated NPA sensitivity of *twd1* roots in comparison with those of *pgp* plants using three different assays.

First, we quantified gravitropic responses, a hallmark of auxin-controlled physiological responses, of *twd1* and *pgp* roots in the presence of NPA, known to disrupt gravitropism in wild type (Rashotte et al., 2000). Similarly, NPA affected *pgp1* and *pgp19* root gravitropism (Supplemental figure 5) but to a lesser extent *twd1* and *pgp1/pgp19* roots (Figure 5A), that showed essentially similar responses as the –NPA controls.

Second, asymmetric auxin accumulation along the lower side of the root tip, the primary cause of root bending, was monitored by expression of the auxin-responsive reporter construct Pro_{DR5}-GFP (Bouchard et al., 2006; Ottenschlager et al., 2003) upon gravistimulation. Compared to wild type, basipetal reflux was reduced in *pgp1* but abolished in *pgp19* (Supplemental figure 5), *pgp1/pgp19 and twd1* roots (Figure 3B) which is inline with reported roles for PGP1 and PGP19 in basipetal and acropetal root auxin fluxes (Bouchard et al., 2006; Lewis et al., 2007), respectively. However, NPA disrupted basipetal reflux and enhanced the DR5-GFP signal in the QC, the columella initials, the S1 cells in wild type (Ottenschlager et al., 2003), *pgp1*, *pgp19* (Supplemental figure 5) and *pgp1*/*pgp19,* but not in *twd1* roots, that showed instead a faint, diffuse columella DR5-GFP signal (Figure 5B).

Third, we employed an IAA-specific microelectrode that is able to non-invasively record IAA influxes into the root transition zone (Bouchard et al., 2006; Mancuso et al., 2005; Santelia et al., 2005). IAA influx in this zone is characterized by a distinct peak at ca. 200 µm from the root tip and is consistent with the current auxin "reflux model" (Blilou et al., 2005). *Pgp1*, *pgp19* (Supplemental figure 5), *pgp1*/*pgp19* and *twd1* show reductions of IAA influx compared to wild type (Figure 3C; Bouchard et al., 2006; Geisler et al., 2005). In agreement with DR5-GFP imaging, relative NPA inhibition of IAA influx was significant in *pgp1* in comparison to wild type but low in *pgp19* and *pgp1/pgp19*. However, NPA had only a negligible inhibitory effect on IAA influx into *twd1* roots (relative inhibition: wild type >> *pgp1* > *pgp19* ≥ *pgp1/pgp19* > *twd1)*.

In order to test the impact of TWD1 on PGP-mediated auxin transport in gain-of-function alleles, we measured gravitropic responses of $Pro_{CaMV35S}$-TWD1-HA roots (Bouchard et al., 2006). Plants over-expressing TWD1-HA (Figure 4C) perform a more efficient and sharper root curvature compared to wild type and agravitope *twd1-3* (Figure 6A). Kinetics of root bending and rates of curvature clearly indicate that $Pro_{CaMV35S}$-TWD1-HA roots bend initially faster (149%) than those of wild type while *twd1* roots respond more slowly (15%) (Figure 6B). Together, these data indicate that *TWD1* loss-of-function results in reduced sensitivities to NPA while *TWD1* gain-of-function promotes root gravitropism and NPA binding.

Discussion

Drug modulation of P-glycoprotein activity is conferred by FKBPs

Previous work has established a role for FKBP42, TWD1, as positive regulator of PGP-mediated auxin efflux by means of protein-protein interaction (Bailly et al., 2006; Bouchard et al., 2006; Geisler and Bailly, 2007; Geisler et al., 2003). Loss of positive regulation of PGP1- and PGP19-mediated auxin efflux activity on the cellular level blocks long-range auxin transport *in planta* (Bouchard et al., 2006; Lewis et al., 2007). As a consequence, *PGP1, 19* single and, more strikingly, double loss-of-function alleles show elevated root auxin levels and defects in root gravitopism (Bouchard et al., 2006).

Here, by employing yeast-based, specific TWD1-rLuc/PGP1-YFP BRET and auxin transport systems, we demonstrate functional disruption of TWD1-PGP1 interaction by synthetic and *bona fide* native auxin transport inhibitors, like NPA and flavonoids (Blakeslee et al., 2005; Peer and Murphy, in press). Disruption by NPA is inline with previous findings

demonstrating NPA binding to and inhibition of plant PGPs involved in auxin transport (Bouchard et al., 2006; Santelia et al., 2005; Terasaka et al., 2005). In contrast to NPA, the ATIs, TIBA and CPD, had no significant effect on the TWD1-PGP1 complex stability and auxin transport. This is not unexpected as TIBA is structurally unrelated, has been shown only partially displace NPA binding and to even own weak auxin activity suggesting different loci and mode of action compared to NPA (Petrasek et al., 2003).

The flavonol quercetin (and its glucose conjugate) was the most capable drug tested in disrupting TWD1-PGP1. This is of interest because quercetin was the most efficient in competing with NPA for auxin transporter binding sites (Jacobs and Rubery, 1988). Further, nanomolar IC_{50} values are in agreement with the effective working concentrations of flavonols in blocking PAT. Disruption of the TWD1-PGP1 complex by NPA and flavonols leads to activation of auxin transport by the TWD1-PGP1 complex (Figures 2 and 3), which is reflected by reversal of TWD1-mediated inhibition of PGP1 auxin transport activity. This reverse, inhibitory effect on PGP1 activity in yeast is, as shown before (Bouchard et al., 2006; Santelia et al., 2005; Terasaka et al., 2005), opposite of what has been found for mammalian and plant cells and seems to reflect a lack of regulatory components in the lower eukaryotic system (Bailly et al., 2006; Geisler and Murphy, 2006). Despite this discrepancy, the disrupting effect of ATIs is in agreement with its proposed inhibitory role in PAT (Peer and Murphy, in press). Interestingly, and in opposite to what is seen *in planta*[2], the inhibitory effect of µM concentration of ATIs on PGP1 expressed alone in yeast is low (around 20-30%), while the reversing effect on the TWD1-PGP1 complex is far higher (Figure 3).

Interaction, transport and NPA binding studies suggest that the TWD1 FKBD provides the surface for PGP1-TWD1 interaction (Geisler et al., 2005), is responsible for PGP1 regulation (Bailly et al., 2006; Bouchard et al., 2006), but confers also drug-mediated regulation of PGP1. The soluble FKBD alone can fully complement the full-length, membrane-bound TWD1 both in respect to PGP1 regulation as well as drug binding and sensing. However, two amino acid exchanges that minimally affect the overall structure and only bisect interaction (Figure 1C) fully destroy the impact of quercetin on TWD1-PGP1 activity (Figure 3B).

Based on specificity patterns a PGP as common protein (or protein complex) mediating hormone efflux as well as hormone action has been proposed (Hossel et al., 2005). Indeed our data support a sensor-like function of TWD1 in PGP regulation by integrating the modulatory impact of flavonoids, intracellular key signaling molecules of auxin transport and action (Blakeslee et al., 2005; Taylor and Grotewold, 2005; Vieten et al., 2007). This concept is sustained by *in planta* data demonstrating reduced NPA sensitivities for TWD1-modulation of root gravitropism and PAT (Figure 5). Moreover, TWD1 gain-of-function alleles show highly improved initial root bending performance. These findings together suggest TWD1 to control PGP-mediated gravisensing by ATIs.

TWD1 and PGP1 are key components of the NPA-binding protein auxin efflux complex

NPA binding to PGP1 and to TWD1 shown by employing yeast assays, immobilized, highly purified FKBD protein and plant microsomes is in-line with past and recent findings on the regulatory roles of NPA (and flavonoids) on auxin export (Blakeslee et al., 2005; Lomax et al., 1995; Peer and Murphy, in press). Until today the identity, number and affinity of putative NPA-binding proteins (NBPs) is still controversial (Sussman 1980, Michalke 1992, Muday 1994, Luschnig 2001). But there is apparently a consensus that Pin-formed (PIN) proteins (Petrasek et al., 2006), recently shown to functionally interact with PGPs in auxin transport (Blakeslee et al., 2007), are not acting as NBPs (Lomax 1995). However, our data are in agreement with the current consensus that the NBP efflux complex consists of at least two proteins, the transporter and the NPA-binding regulatory subunit NBP (Luschnig, 2001; Morris, 2000; Petrasek et al., 2003). Therefore, TWD1 and the regulatory NBP might be identical, especially as the NBP has been suggested to be required for auxin efflux transporter positioning (Gil et al., 2001). Moreover, though this is still controversial, the NBP has been demonstrated to be a peripheral membrane protein (Cox and Muday, 1994), which is inline with the recently proposed perpendicular orientation of the TWD1 C-terminus forming a so-called amphipathic in-plane membrane anchor (IPM) (Scheidt et al., 2007). Our findings obviously also match the original model predicting

2 Note that co-expression of TWD1 in yeast unlike than in mammalian and plant cells has an inhibitory effect on PGP1-mediated auxin transport.

two putative NBPs with the transporter being the low-affinity protein (Michalke et al., 1992).

NPA binding to PGP1 and TWD1 is abolished in the PGP1-TWD1 (FKBD) complex suggesting that the FKBD apparently competes for NPA-binding sites on PGP1. However, individual functional domains on the FKBD are apparently independent as TWD1$^{C70D, L72E}$-rLuc showed reduced affinities to PGP1 (Fig. 1B) but was fully capable of blocking NPA binding to PGP1 (Figure 4A). Two more lines of evidence support the identity of more than one NBP: displacement of NPA from microsomes by flavonoids is biphasic (Murphy et al., 2000) while in *Arabidopsis* the membrane integral NPA-flavonoid interaction site was shown to be associated with PGP1, 2 and 19, whereas a weaker interaction site correlated with periperal membrane proteins TWD1 and aminipeptidase, APM1 (Murphy et al., 2002). Finally, our data provide a mechanistic explanation for the fact that excess of NPA during washing steps led to loss of TWD1 in NPA chromatographies (Geisler et al., 2003).
Although the exact role of two individual NBPs remains open (see below), our data provide good evidence that TWD1 and PGP1 are key components of the long sought for NBP complex.

Flavonoid modulation of P-glycoprotein-mediated auxin transport conferred by TWD1

Our data highlight the functional importance of the PGP1-TWD1 complex but also support a novel mode of action for ATIs, namely the drug-mediated modulation of transport activity conferred by means of protein-protein interaction. In this scenario, plant endogenous or synthetic ATIs (flavonoids or NPA, respectively) would compete with TWD1 for NPA-binding sites on the PGP1 nucleotide binding folds, keeping the TWD1-PGP efflux complex in a dissociated, inactive state, thus allowing flexible fine-modulation of activity.
Disruption and inhibition of the TWD1-PGP complex by flavonoids, as supported by our data, is an intriguing option and supported by several findings: 1.) Lesions in the genes encoding for PGP1 homologs result in reductions in long-distance transport of auxin and consequent dwarfism in mutant plants. These data together with tissue-specific accumulation of flavonols in *Arabidopsis* seedlings that coincide with regions of high auxin levels (Murphy et al., 2000; Peer et al., 2004) suggest that flavonols affect polar auxin transport in apical tissues by modulating auxin loading into the long-distance auxin stream (Peer et al., 2004). 2.) Aglycone flavonols were localized in a developmental- and tissue-specific manner in the plasma membrane (Buer et al., 2007; Peer et al., 2001) of tissues that strongly overlap with *PGP1* and *PGP19* expression (Blakeslee et al., 2007; Geisler et al., 2003). In accordance, flavonol glucoside contents are drastically altered in *twd1* and *pgp1/pgp19* mutants (results not shown).

Agronomic and clinical implications of drug-mediated ABC transporter modulation via immunophilins

Loss-of *PGP1* gene function has been shown to increase stem diameter in the agriculturally important *brachytic2* and *dwarf3* mutants in maize and sorghum (Multani et al., 2003). Our yeast-based BRET system will allow rapid and sensitive chemical genetic screens in order to identify novel growth promoters or inhibitors that influence plant development and thus plant productivity (agrochemicals) in efforts to confer structural stability to crops.
Moreover, two findings imply that this novel mode of ABC transporter regulation via sensor-like immunophilins might be of interest beyond the plant field: Flavonoids have, like in plants, a modulatory impact on mammalian PGP activity and thus on MDR (Conseil et al., 1998; Zhang et al., 2005) but data support both inhibitory and stimulating effects (Zhang et al., 2005). Our findings that inhibitory flavonoid modulation is conferred by interacting FKBPs might explain conflicting results on flavonoid action that might be due to tissue-specific immunophilin-PGP complex formation. Moreover, the mammalian TWD1 homolog, FKBP38, is localized to the outer membrane of mitochondria where it helps to anchor the anti-apoptosis proteins Bcl-2 and Bcl-xL (Shirane and Nakayama, 2003). Taken together, membrane-anchored FKBPs and their interactive partners might be a promising target of genetic or chemical manipulation for new drug development and disease treatments.

Acknowledgements

We thank Aileen Funke for help with protein purification, Sina Henrichs for critical comments on the manuscript, Bo Burla for *PolarBar* software, Michal Jasinski for donation of yeast expression plasmid pNEV-AtOSA-YFP (At5g64940) and Rainer Hertel for sharing timely, historical information and encouraging discussion. This work was supported by funds of the Swiss National Fonds (M.G. and E.M.) and the Novartis Foundation (M.G.).

Supplemental data

The original version of this article contains the following supplemental figures and data.

Supplemental Experimental Procedures

FKBD retention and BRET restoration assays

In vitro measurement of Renilla luciferase activity was performed using soluble S3 or solubilized P3 fractions (see above) of yeast co-expressing FKBD-rLuc and PGP1, PGP4 (Santelia et al., 2005) and AtOSA-YFP. In white 96-well microplate (OptiPlate-96, PerkinElmer Life Sciences, USA) to 200 µl (approximately 500 µg of total protein) of resuspended membranes, 5 µM coelenterazine (Biotium Inc., USA) was added and light emission in the 410 ± 80nm window was recorded after 1min using the Fusion microplate analyzer (PMT=1100V, gain=1, reading time=1s; Packard, USA). Results are the average of 10 readings collected every minute. For FKBD-rLuc enrichment, 200 ml overnight yeast cultures were processed as described above. The soluble S3 fraction containing the 54 kDa chimerical FKBD-rLuc protein was concentrated to 10 mg/ml by Centricon Plus-20 centrifugal filters (Millipore Amicon, 4000 x g for 15 min, 4°C). The partially purified protein was diluted to 5 mg/ml in STED10 buffer, supplemented with proteases inhibitors and stored at -80°C for subsequent use. For restoration, 100 µg of the partially purified FKBD-rLuc protein were incubated in STED10 supplemented with proteases inhibitors for 2h on ice with gentle agitation with 500 µg of P3 fractions from yeast cultures expressing PGP1, PGP1-YFP or AtOSA-YFP proteins. 200 µl of this suspension were used for BRET quantification as described above.

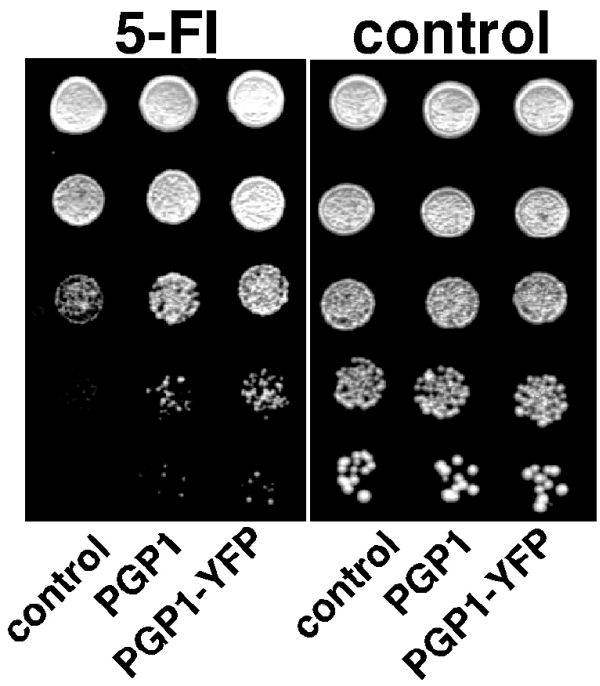

SUPPL. FIGURE 1. **PGP1-YFP is active.**
PGP1-YFP detoxifies the auxin analog 5-fluoro indole (5-FI, (Bouchard *et al.*, 2006; Luschnig *et al.*, 1998)) comparable to native PGP1. Yeast growth assays were performed as in Bouchard *et al.* (2006) with 3 independent transformants showing comparable results.

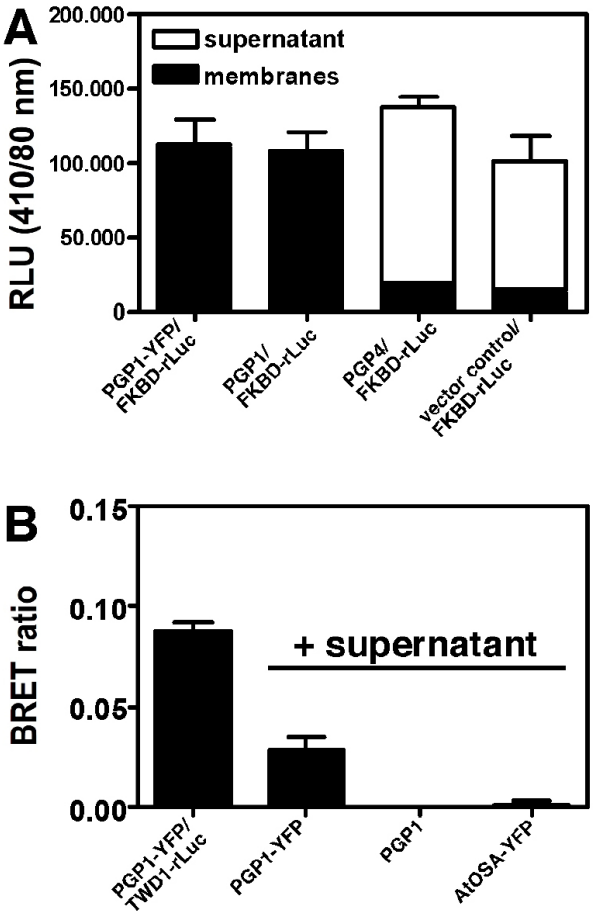

SUPPL. FIGURE 2. **Soluble TWD1 FKBD-rLuc is specifically retained by PGP1 membranes and restores BRET.**
A, *In vitro* measurement of *Renilla* luciferase light emission in the 410±80nm window was performed using soluble S3 (supernatant) or solubilized P3 fractions (membranes, see **Materials and methods**) of yeast co-expressing FKBD-rLuc with PGP1 and PGP4.
B, Soluble FKBD-rLuc enriched by size-exclosure restores partially PGP1-YFP/TWD1-rLuc BRET when added to PGP1-YFP membranes.
Presented are means ± S.E. from minimum 4 independent experiments with 4 replicates each.

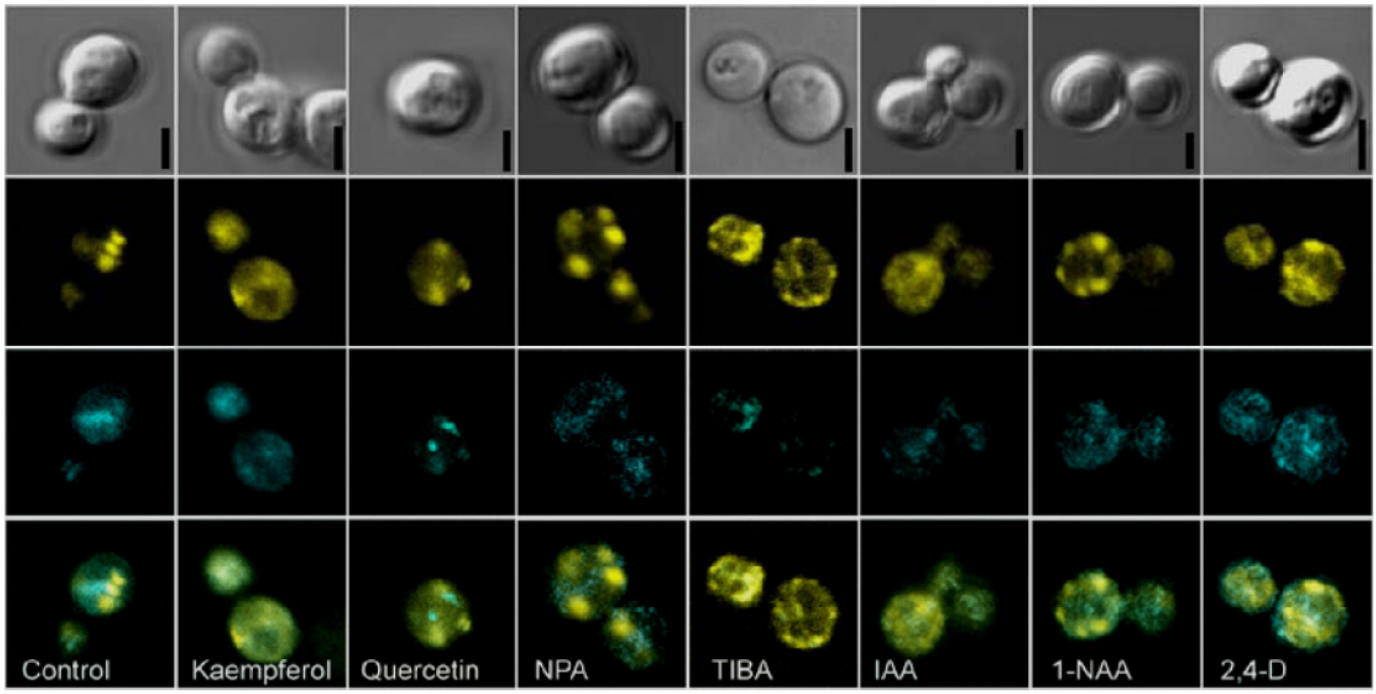

SUPPL. FIGURE 3. **Auxin transport inhibitors and auxins do not alter PGP1 and TWD1 yeast expression and location.**
Cells co-expressing PGP1-YFP and TWD1-CFP were imaged by confocal laser scanning microscopy and DIC- (upper row) and fluorescence images (YFP fluorescence in yellow, CFP fluorescence in blue) were recorded. Co-localization on the plasma membrane and in small, filled vesicles, is shown by superimposition (lower row). Scale bars, 2.5 µm.

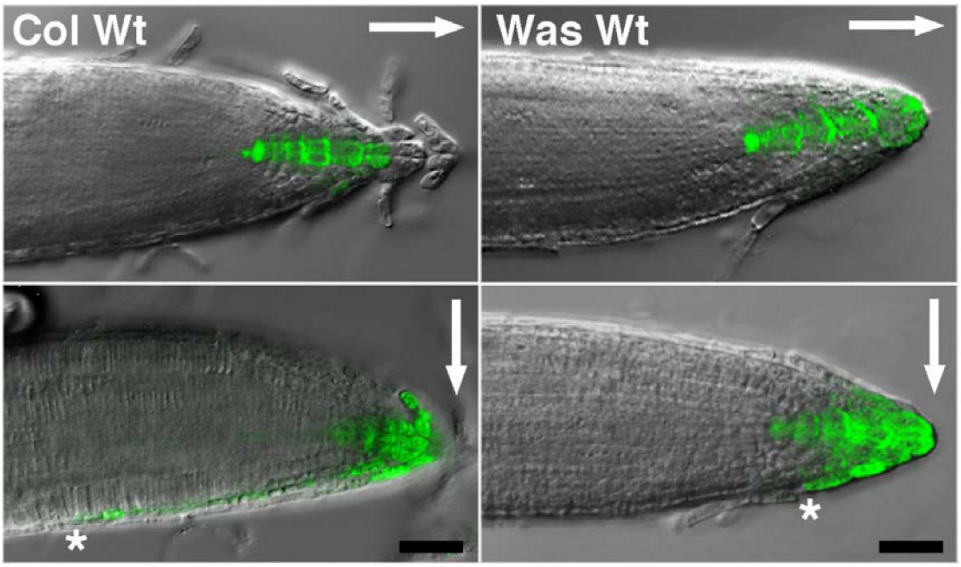

SUPPL. FIGURE 4. **Comparison of directional auxin flow in wild-type root tips of Arabidopsis ecotypes Columbia and Wassilewskija.**
Columbia (Col Wt) and Wassilewskija (Was Wt) wild type grown vertically reveal comparable auxin accumulation in the root apices as monitored by expression of the auxin-responsive reporter Pro_{DR5}-GFP (Ottenschläger *et al.*, 2003) in the quiescent center (QC), the columella initials, and S1-S3 columella cell files. Upon gravistimulation (see arrows), both ecotypes show asymmetric auxin accumumulation along the lower side of the root (mainly in the lateral root cap and the epidermis). Note that asymmetric auxin accumulation reflecting basipetal reflux is more pronounced in the Columbia than in the Wassilewskija ecotype (indicated by asterisks). Scale bars, 200 µm.

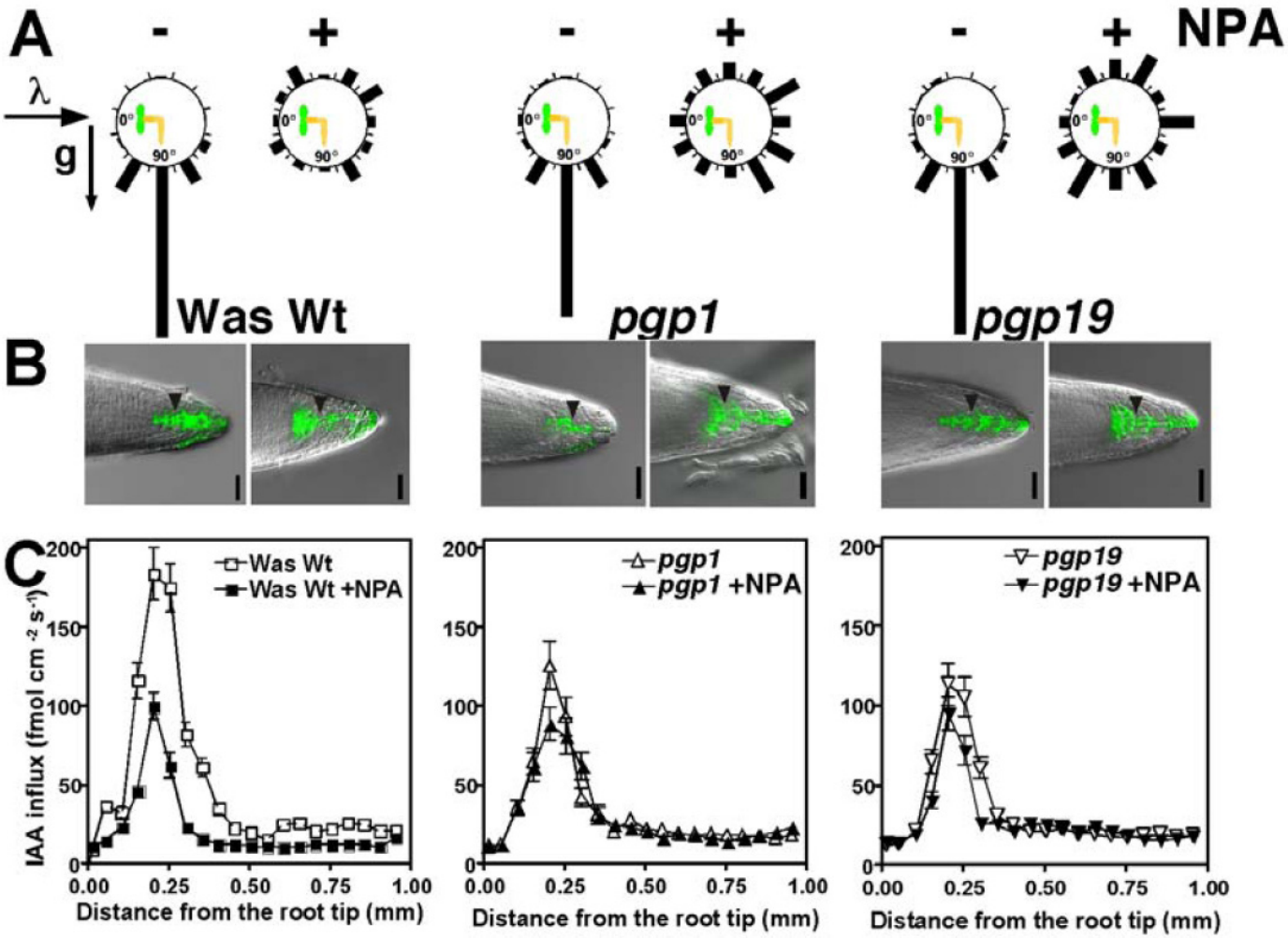

SUPPL. FIGURE 5. ***Pgp1 and pgp19* roots are NPA-sensitive.**

A, External application of the auxin transport inhibitor, NPA (5 µM), disrupts gravitropic responses of *pgp1* and *pgp19* roots to the same extent as in wild-type (Was Wt). For quantification of gravitropism, plants were grown on vertical plates under continuous light. Arrows indicate direction of light (λ) and gravitropism (g).

B, Wild-type and to a reduced extend *pgp1* but not *pgp19* roots show asymmetric auxin accumulation along the lower side of the root tip as monitored by expression of the auxin-responsive reporter Pro_{DR5}-GFP (Ottenschläger *et al.*, 2003) upon gravistimulation (from the top). NPA disrupts the asymmetric signal caused by basipetal auxin reflux and enhances the signal in the QC, the columella initials, the S1 cells (see arrows) with strong extensions into the initials of the epidermis, endodermis and the vasculature in *pgp1* and *pgp19* like as in wild-type roots (Geisler *et al.*, 2005). Scale bars, 200 µm.

C, IAA influx quantified using an IAA-specific microelectrode (Bouchard *et al.*, 2006; Geisler *et al.*, 2005; Mancuso *et al.*, 2005; Santelia *et al.*, 2005) is reduced in the transition zone of *pgp1* and *pgp19* roots (reduction in Wt << *pgp1* ≤ *pgp19*) and therefore only slightly inhibited by NPA compared to the drastic reduction in wild type (Santelia *et al.*, 2005) (inhibition in Wt >> *pgp1* ≥ *pgp19*). Shown is the IAA influx profile along single roots; positive fluxes represent a net IAA influx. Data are means ± S.E. of eight replicates.

Note that taken these data together, the inhibitory effect of NPA on *pgp1* appears to be more pronounced compared to *pgp19* roots.

Plant lessons: Understanding substrate specificity by structure modeling of ABCBs

Aurélien Bailly[1], Angus Murphy[2, 3], Enrico Martinoia[1] and Markus Geisler[1]

[1] Zurich-Basel Plant Science Center and University of Zurich, Institute of Plant Biology, Zurich, Switzerland
[2] Department of Horticulture, Purdue University, West Lafayette, USA
[3] to whom correspondence should be addressed

Summary

Over-expression of human ABCB1 protein, HsABCB1, in cancer cells is mainly responsible for multidrug resistance phenomena. Chemotherapy ineffectiveness is due to the fact that HsABCB1 owns promiscuous substrate specificity and that most of the anti-cancer drugs are themselves moderate HsABCB1 substrates. Moreover, identification of substrate- and inhibitory drug-binding sites in the molecule in the absence of a valid ABCB structure has proven a difficult if not impossible task. On the other, the best-characterized ABCB1 is found in the model plant Arabidopsis thaliana where it catalyzes the specific transport of a few related substrates, the essential phytohormones auxin.

Here we have used robust homology structure models of a variety of plant and mammalian ABCB1 proteins with different substrate specificities based on the only available multidrug ABC exporter structure, Sav1866, a bacterial ABC drug exporter. Human ABCB1 and Arabidopsis ABCB1 transporters share a common architecture. However, our analysis identified candidate substrate regions in the cytosolic parts of the transporter transmembrane domains. This strongly suggests that substrate specificity separated early during evolution but can be monitored and consequently used for the investigation of substrate binding.

Introduction

Multidrug Resistance/ P-glycoproteins are members of the ABCB subgroup of the ATP-binding cassette transporter superfamily found in all existing phyla from prokaryotes to humans (Higgins, 2001; Hrycyna and Gottesman, 1998). Typically they are specific for the transported substrate, which can include metal ions, sugars, vitamins, lipids, amino acids, hormones and peptides (Linton and Higgins, 2007). However, some ABC transporters have apparently lost the ability to recognize only a limited subset of related substrates. In humans, the MDR1/ ABCB1/ P-glycoprotein is the focus of extensive research, as it plays a fundamental role in the resistance of tumours to multiple chemotherapeutic agents resulting in multidrug resistance (MDR; (O'Connor et al., 2007)). According to the fact their *in vivo* function is less clear they are considered as transporters of hydrophobic drugs exporting xenobiotics.

Over the past ten years, a number of ABCB orthologs have been extensively characterised in plants. Most notably, the agriculturally important *brachytic2* and *dwarf3* mutants in maize and sorghum were shown to result from lesions in ABCB1 genes (Fig. 1**A** and **B**; (Multani et al., 2003)). However, the most extensive analysis of ABCB gene function has taken place in the model plant Arabidopsis and has focused on two highly homologous proteins, ABCB1 (PGP1) and ABCB19 (PGP19/ MDR1). Both proteins have been shown to transport the phytohormone auxin (3-indole-acetic acid/IAA) (Bailly et al., 2008; Bouchard et al., 2006; Geisler et al., 2005; Geisler et al., 2003; Noh et al., 2001). Lesions in the genes encoding these proteins result in reductions in long distance transport of the hormone and consequent dwarfism in mutant plants (Figure 1**C**); However, loss of ABCB1/19 gene function can also increase stem diameter and does not result in the dramatic defects in organogenesis observed in some mutations of genes encoding PIN auxin efflux carrier proteins (Galweiler et al., 1998). As such, manipulation of ABCB genes has been proposed to become a powerful tool in efforts to confer structural stability to biofuels crops that have been genetically modified to enhance cell wall digestibility by microbial fermentation (Multani et al., 2003).

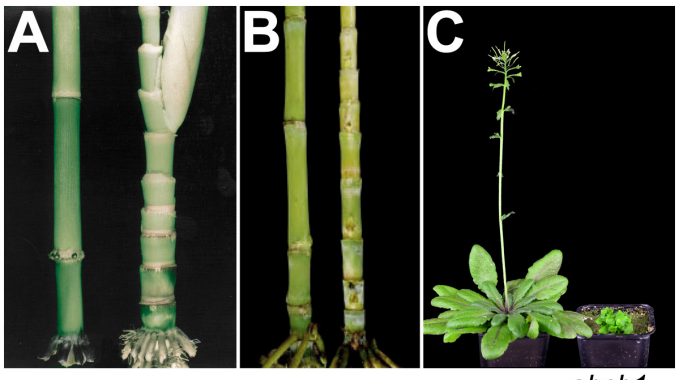

FIGURE 1. **Mutations in ABCB1 orthologs result in reduced basipetal auxin transport and dwarfism. *A*** and ***B***, compressed stalk internodes in maize *br2* (*brachytic2/ zmpgp1*) and sorghum *dw3* (*dwarf3/sbpgp1*) mutants (Multani *et al.*, 2003). ***C,*** drastic dwarfing phenotype in *Arabidopsis abcb1 abcb19* double mutant (Geisler *et al.*, 2005). Wt, wild type.

Two general approaches have been employed to overcome multidrug resistance during chemotherapy. First, modification of anti-cancer drugs, that they are no longer substrate for ABCB1 or related multidrug resistance tansporters. Second, development of novel ABCB1 inhibitors that are co-administered with cytotoxic drug. ABCB1 is highly over-expressed in tumor lines, and the major reason for chemotherapy failure. Both strategies to circumvent MDR have not proven to be satisfactory in clinical trials (Gottesman and Ling, 2006; Modok et al., 2006; Polgar and Bates, 2005), mainly because they have been undertaken "blind" in the absence of structural ABCB1 data.

Despite an emerging dataset of partial ABC-transporter structures, the definition of substrate-binding regions, as well as the development of novel ABCB1 inhibitors, faces a major lack of structural information. The recent publication of the crystal structure of the "half ABC transporter" Sav1866, a bacterial multidrug resistance exporter from *S. aureus* (Dawson and Locher, 2006) has provided a framework for structural comparison of human or plant ABCB proteins. The Sav1866 transporter functions as a dimer and consists of six transmembrane helices followed by an ATP hydrolysis domain and associated conserved Walker A and B motifs (termed nucleotide-binding domain, NBD). ABCB proteins are essentially two tandemly paired half-size transporters and the general architecture observed in the Sav1866 structure is relevant for P-glycoproteins (Figure 2; O'Mara and Tieleman, 2007; Zolnerciks et al., 2007). In the commonly accepted model for an ABC transport mechanism, helices from each TMD form the binding site(s) (Pleban et al.,

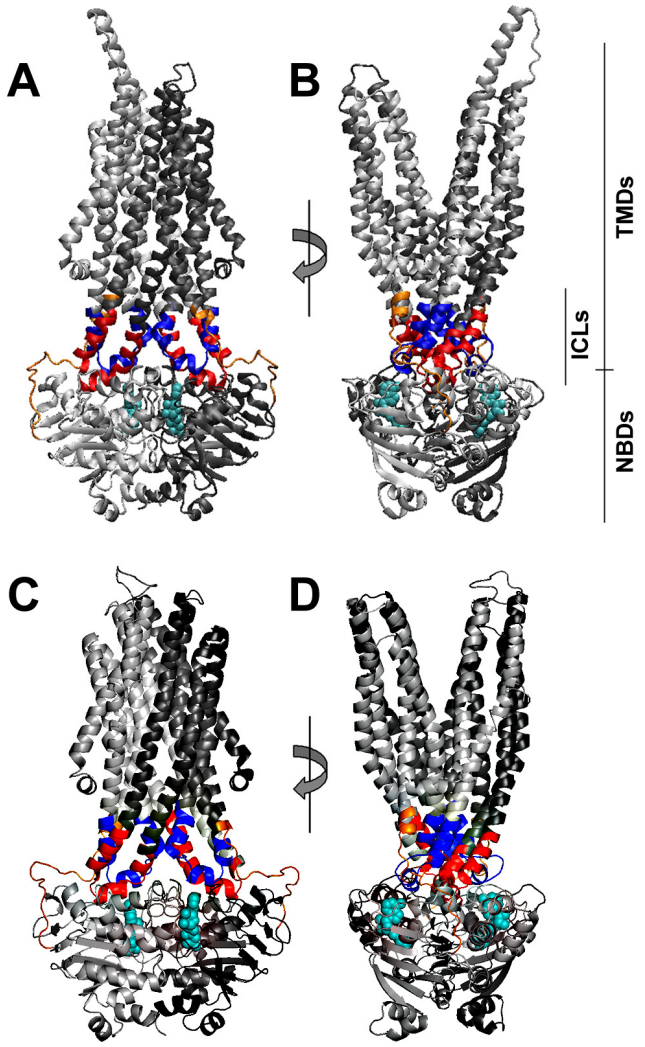

FIGURE 2. **Front and side views of the nucleotide-bound (cyan) closed state HsABCB1 (*A* and *B*) and AtABCB1 (*C* and *D*) homology models.** Side views show a wing-like TMD orientation (***B*** and ***D***). TMD1 and NBD1 are in silver, TMD2 and NBD2 are in dark grey. ICL1 and 4 are in blue, ICL2 and 5 are in red, ICL3 and 6 are in orange.
HsABCB1 and AtABCB1 sequences were aligned with two copies of Sav1866 and essentially modeled as described in O'Mara et al. (2007). Molecular structure diagrams were generated using PyMol 0.99rev8 (http://pymol.sourceforge.net/).

2005) and the translocation pathway for the substrate, while both NBDs provide the necessary energy to perform a complete transport cycle (Hollenstein et al., 2007).

On the other hand, a characteristic of human ABCB1 (HsABCB1) is its substrate promiscuity, as the protein is able to export a wide range of hydrophobic drugs, especially when over-expressed in tumour cells. However, its Arabidopsis ABCB1 orthologs exhibit relatively narrow substrate specificity (Geisler 2005, Bouchard 2006). Arabidopsis ABCB1 and 19 (hereafter referred to as AtABCB1 and AtABCB19) have been shown to transport the principal auxin, indole-3 acetic acid (IAA) and, to a lesser extent, closely related organic acids, but not any of the standard substrates transported by human ABCB1, even when over-expressed in human HeLa cells (Geisler et al., 2005).
Therefore, by using the crystal structure of multidrug exporter Sav1866 as template, we have employed a structure-based comparison of plant and animal ABCB1 proteins for the identification of substrate and drug binding pockets within AtABCB1. The outcome of our work will provide at first hand a molecular understanding of ABCB structure-function in the context of the transport of the plant hormone auxin. Transfer of these findings, however, will help understanding ABC transporter substrate specificity in general and therefore be beneficial for development of novel strategies for linked disease treatment and cancer therapy.

The Sav1866 architecture is relevant for ABCB proteins

Plant and animal ABCB1 homologs share a Sav1866-like architecture.

After the withdrawal of the first reference structure for full size transporters, the *E. coli* MsbA (Chang, 2007), the high resolution crystal of the *S. aureus* "half transporter" Sav1866 (Dawson and Locher, 2006), PDB ID 2HYD) became the only available template for ABC-type exporters. Interestingly, although neither the function nor the substrate of

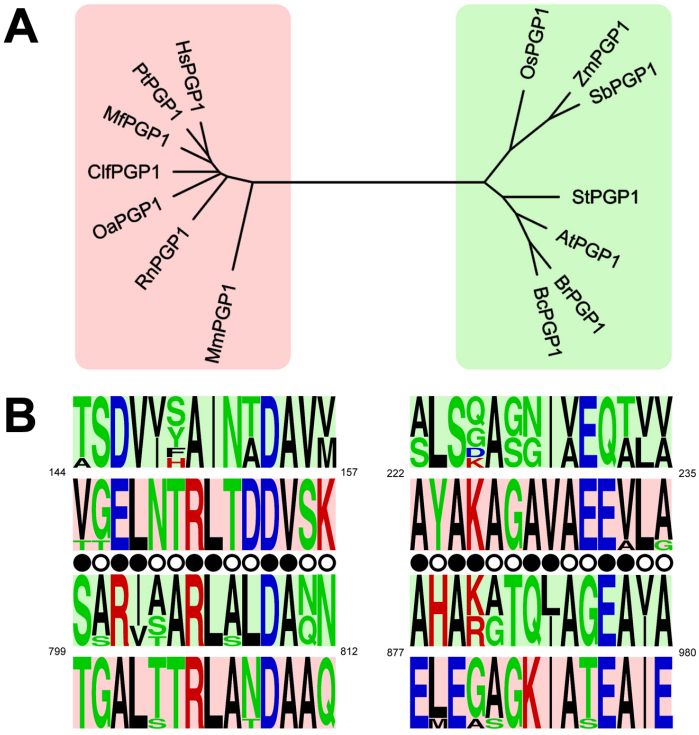

FIGURE 3. **Multiple alignments of 14 ABCB1 orthologs reveal divergent residue conservation between plants (green) and animals (red) within the translocation pathway.**

A, phylogenetic tree of the 14 PSI-blast-isolated ABCB1 orthologs used in this analysis. *Hs, Homo sapiens* (GI:307180)*; Pt, Pan troglodytes* (GI:114614334)*; Mf, Macaca fascicularis* (GI:31442763)*; Clf, Canis lupus familiaris* (GI:67462127)*; Oa, Ovis aries* (GI:57526446)*; Rn, Rattus norvegicus* (GI:149029022)*; Mm, Mus musculus* (GI:387427)*; Os, Oryza sativa* (GI:125604357)*; Zm, Zea mays (GI:37695542); Sb, Sorghum bicolor* (GI:37695542)*; St, Solanum tuberosum* (GI:4204793)*; At, Arabidopsis thaliana* (GI:15228052)*; Br, Brassica rapa* (GI:83032237)*; Bc, Brassica campestris* (GI:157356830). ***B,*** multiple alignments of the regions described in Figure 5 using ClustalX (http://www.clustal.org) and Weblogo (http://weblogo.berkeley.edu/logo.cgi) software. The overall height of the stacked amino acids symbols indicates the sequence conservation relatively to the frequency of each amino acid. Color is given by residue properties. Numbers refer to the AtABCB1 corresponding residues positions. Open circles indicate residues facing the cavity space; filled circles indicate residues buried in the core of the protein.

the bacterial Sav1866 are known, the transporter appears to be phyllogenetically close enough to eukaryotic full-size ABC exporters to explore the potent of comparative homology modelling. Indeed, recent papers from various groups have been using Sav1866 as a backbone to obtain the first coherent computer-generated three-dimensional organizations of HsABCB1 and closely-related ABC-proteins (DeGorter et al., 2008; Federici et al., 2007; Hazai and Bikadi, 2007; Mendoza and Thomas, 2007; O'Mara and Tieleman, 2007; Ravna et al., 2008; Figure. 2). The predicted human ABCB1 model appeared to be consistent with previous biochemical and structural data collected for HsABCB1 (Lee et al., 2002; Lee et al., 2008; O'Mara and Tieleman, 2007), thus becoming a powerful tool to map previous mutational and biochemical work at the atomic scale (Gottesman and Ling, 2006; Lawson et al., 2008; O'Mara and Tieleman, 2007; Zolnerciks et al., 2007).

Following the same logic, we obtained a set of homology-based predictive models for 14 close plant and animal ABCB1 orthologs, using the Sav1866 structure (PDB ID 2HYD) as a template (Figure 3**A**). The published Sav1866 model reflects a bona fide ATP-bound state (Dawson and Locher, 2007) with an asymmetric outward-facing conformation of the transmembrane domains (TMDs), so that the homology models generated would picture the releasing step of the ligand throughout the TMDs (Dawson and Locher, 2006; Ravna et al., 2008; Rosenberg et al., 2005; Rosenberg et al., 2003).

The remarkable homology between the primary protein sequence of Sav1866 and the different employed ABCB1 orthologs allowed us to use Swiss-Model (http://swissmodel.expasy.org; Guex and Peitsch, 1997; Schwede et al., 2003) to compute and refine their three-dimensional structures as described in O'Mara and Tieleman (2007). The overall structure of the predicted Arabidopsis ABCB1 auxin exporter (Geisler et al., 2005), shows the arrangement of two modules that each consist of an amino-terminal TMD (residues 1-374 and 681-1030, ~30% identity with HsABCB1) followed by a carboxy-terminal nucleotide-binding domain (NBD) (residues 375-584 and 1031-1240, ~60% identity with HsABCB1) consistent with the domains arrangement predicted from the polypeptide sequence (Figures1 and 4**A**).[1]

1 Note that the so-called linker-domain (see Fig.4**A**) could not be included in the models using the method described above owing to its lack of counterpart in the Sav1866 homodimeric structure. The influence of this section on the final structure of the protein remains open to

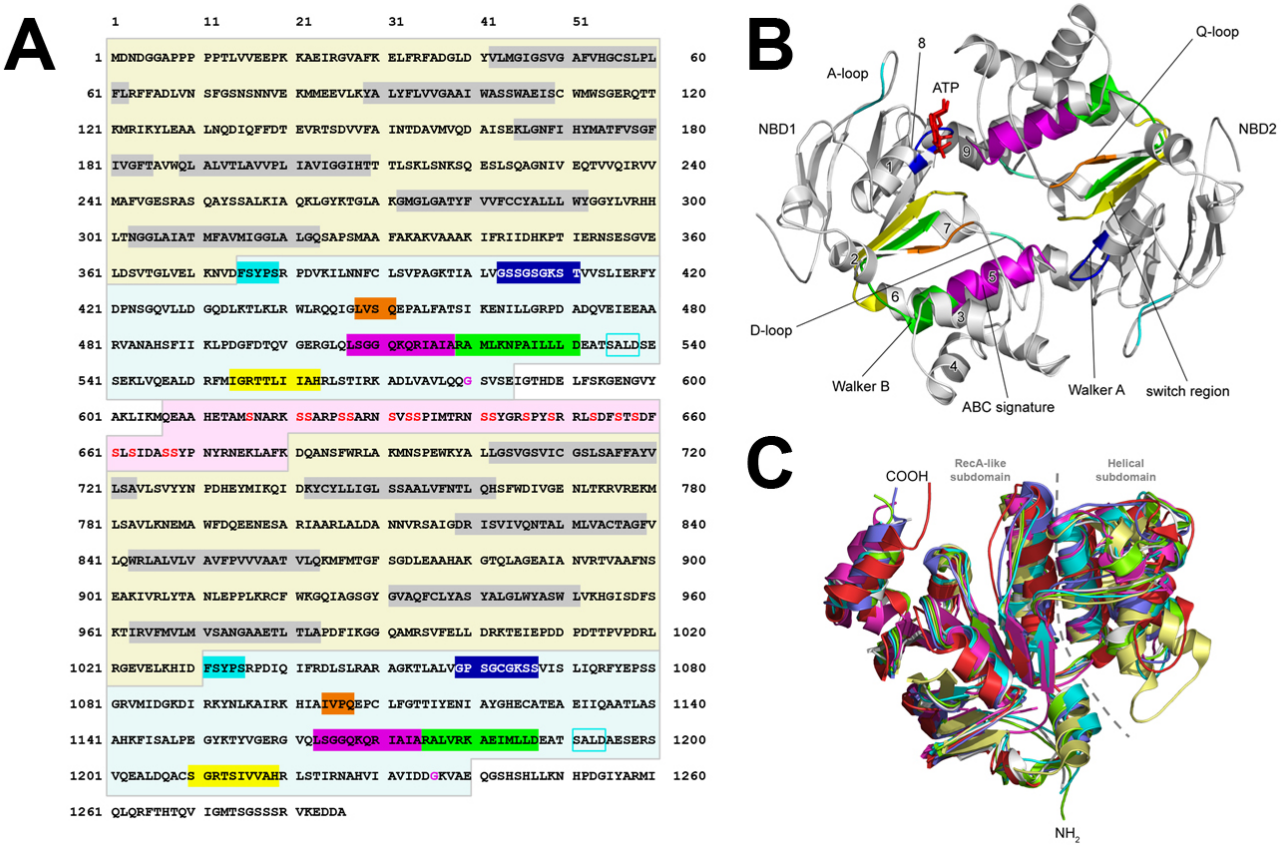

FIGURE 4. **AtABCB1 shares common characteristics with ABC proteins**

***A*, AtABCB1 primary sequence display conserved ABCB features**
Software predictions identified 12 putative transmembrane α-helices (Consensus obtained from http://aramemnon.botanik.uni-koeln.de, At2g36910) and the well characterized ABC domains. Here are presented, according to the colored backgrounds: transmembrane helices in grey; A-loop in cyan; Walker A in blue; Q-loop in orange; ABC signature in purple; Walker B in green; D-loop outlined in cyan; switch region in yellow; conserved Gly-loop glycine in red font; linker domain in pink and serine residues in red font.
***B*, Cartoon representation of the "sandwich dimer" arrangement of the predicted AtABCB1 NBDs**. Numbers refer to the α-helices of one NBD. Color code is given in **A**; ATP molecule shown in the bound state in red sticks.
***C*, Alignment of the ATP-bound state ATPase domains crystal structures** of human TAP1 (cyan, PDB ID 1JJ7), human CFTR (magenta, PDB ID 1R0X), *Escherichia coli* haemolysin B (blue, PDB ID 2FF7), *Methanococcus jannaschii* MJ0796 (yellow, PDB ID 1L2T), *Staphylococcus aureus* Sav1866 (green, PDB ID 2HYD), *Lactococcus lactis* LmrA (red, PDB ID 1MV5) with the predicted NBD2 of AtABCB1 (white). The overall folding of the ATP-binding cassette remains well conserved amongst species; the most variability is observed in the helical subdomain, despite the preserved ABC signature.

These structural features can be extended to all ABCB1 orthologs modeled in this analysis.

As proposed earlier, the transmembrane regions of the protein extend into the cytosol (Dawson and Locher, 2006; Ren et al., 2006; see Figure5**A**) and adopt an asymmetric distribution in the nucleotide-bound state that reveals the conduction chamber to the outer medium (Dawson and Locher, 2007; Rosenberg et al., 2005). Additionally, the consensus ABCB1 overall shape is consistent with that of HsABCB1 studied at low resolution by electron microscopy and its recent structure modelling (Lee et al., 2002; O'Mara and Tieleman, 2007). The prediction models indicate strong similarities between NBD folds of ABCB1 proteins and those of other crystallized ABC transporters, independently of the degree of primary-sequence homology (Figure 4**C**; Kerr, 2002; Linton and Higgins, 2007; Moody and Thomas, 2005; Oswald et al., 2006). Conserved ATP-binding and -hydrolysis motifs display the well-established "head-to-tail" arrangement, involving the P-loops and ABC signatures, that form a so-called nucleotide "sandwich" dimer congruent with the

discussion but, nevertheless, the modelled architecture and arrangement of the ATPase domains seem to be biochemically and physiologically pertinent.

observed catalytic co-operativity in ATP-binding and hydrolysis (Figure 4**B**) (Altenberg, 2004; Chen et al., 2003; Hollenstein et al., 2007a; Linton and Higgins, 2007; Yuan et al., 2001; Zaitseva et al., 2006). The nucleotide binding pockets are therefore composite sites with both NBDs contributing to each site. Both TMDs cross the plasma membrane six times so that the 12 transmembrane helices arrange in a manner consistent with the canonical ABC exporter topology. In the commonly accepted model for ABC transport mechanism, helices from each TMD participate to the binding site(s) (Martin et al., 2001; Pleban et al., 2005) and form the translocation pathway for the substrate, while both NBDs transmit the necessary ATP-dependent "power stroke" to perform a complete transport cycle (Hollenstein et al., 2007a; Hopfner et al., 2000; Linton and Higgins, 2007). The overall Sav1866 architecture and the subsequent structure-based allosteric mechanism proposed by Dawson and Locher (2006) is therefore relevant for all close ABCB-type exporters (Dawson and Locher, 2006; Hollenstein et al., 2007a).

The modeled structure of a plant ABCB importer is not significantly different from those of exporters

This concept can further be applied to bacterial ABC importers (Dawson et al., 2007; Hollenstein et al., 2007a; Hollenstein et al., 2007b), even though the latter do not precisely share the typical Sav1866 "domain swapping" transmission interface (Dawson and Locher, 2006; Dawson and Locher, 2007). Indeed, coupling helices 1 from the intracellular loops (ICLs) of each TMD were described to contact both NBDs in the ATP-bound state Sav1866 architecture (Curier et al., 2005; Dawson and Locher, 2006), whereas coupling helices present in bacterial importers TMD subunits only contact one facing NBD (Daus et al., 2007; Hollenstein et al., 2007a; Locher, 2004; Locher and Borths, 2004; Oldham et al., 2007). These observations would consequently clarify the greater domain rearrangements proposed in prokaryotic transporters during the catalytic cycle when compared to ABCB-like exporters (Daus et al., 2007; Daus et al., 2006; Dawson and Locher, 2006; Hollenstein et al., 2007a).

In summary, the conserved TMD1-NBD1/TMD2-NBD2 domain arrangement along with the use of periplasmic binding proteins (PBPs) to drive the unidirectional substrate transport seems to be the rule in bacterial ABC importers (Dawson et al., 2007; Hollenstein et al., 2007a). However, MDR1 (CjMDR1/CjABCB1, GI:14715462) from the medical plant *Coptis japonica* functions as importer of the alkaloid berberine (Shitan et al., 2003). Recently, the close CjMDR1 homologue, Arabidopsis ABCB4, has been demonstrated by heterologous expression in yeast and HeLa cells to function as auxin importer (Santelia et al., 2005; Terasaka et al., 2005). However, recent data support also an export transport direction of AtABCB4 *in planta* (Cho et al., 2007) when miss-expressed under non-native promoters. In summary, these data raised the possibility that a certain subset of the ABCB subfamily acts depending on its molecular environment as importer (Geisler and Murphy, 2006).

AtABCB4 shares structurally the same ABCB characteristics described above. Our molecular models allowed a coherent mapping of the X-loop motifs [TxVG(E/D)(R/K)G], including the Sav1866 E_{473}, and the notable Sav1866 Y_{391} (Dawson and Locher, 2006) on the ABCB4 protein. These residues greatly participate in the swapped TMD1-NBD2 interface observed in the template structure and appear to be extremely conserved in all ABCB exporters (Figure 6**A**) but not in PBP-dependent prokaryotic importers, implying divergent coupling mechanisms between the different ABCs (Dawson and Locher, 2006). Furthermore, the amino acids forming the described coupling helices (also cited as "EAA loops") and their corresponding contact surfaces in the nucleotide binding domains are functionally and spatially conserved throughout all tested ABCB orthologs, including AtABCB4 (Figure 6**B**). Interestingly, a large number of residues participating in this interface are localized in the direct proximity of the Q-loops (Dawson and Locher, 2006; Locher et al., 2002), regions of the NBDs known to undergo important conformational changes during the catalytic cycle (Dalmas et al., 2005). The importance of these key amino acids is exemplified by the extensively investigated CFTR F_{508}; its deletion causes a large majority of cystic fibrosis cases (Kerem and Kerem, 1996; Tsui, 1992) and it is found to be structurally and functionally conserved in ABCB orthologs.

Altogether, these data suggest a preserved "exporter-like" architecture for auxin importer, AtABCB4, and do not reveal any significant structural differences that might account for the uncommon directionality of transport. An intriguing option is therefore that

the observed basal ATPase activity of ABCBs in the absence of ligand (Ambudkar et al., 1997; Eytan et al., 1996; Shapiro and Ling, 1998) reflects a continuous ABC catalytic cycle which appears to be enhanced in the presence of the substrate accordingly to the "induced-fit" model (Loo et al., 2003b). The observed tissue-specific AtABCB4 function (Cho et al., 2007; Santelia et al., 2005) therefore implies that direction of transport would rather be influenced by the chemical distribution of the substrate and the nature of the TMDs. Alternatively, as discussed above the AtABCB4 transport direction might be controlled by its molecular environment, thus by protein-protein interaction. This is supported by the fact that the import direction of AtABCB4 could be reversed by functional co-expression with auxin/H^+ carrier PIN2 (Blakeslee et al., 2007).

ABCB1 orthologs reveal structural similarities and discrepancies within the TMDs

TMDs are suspected to form the substrate translocation pathway and to hold the drug recognition function in all ABC transporters (Loo et al., 2006a; Loo et al., 2006b; Loo and Clarke, 2000; Loo and Clarke, 2001; Maki and Dey, 2006; Maki et al., 2006; Pleban et al., 2005). The apparent divergent substrate specificity between plant and animal ABCBs should therefore be

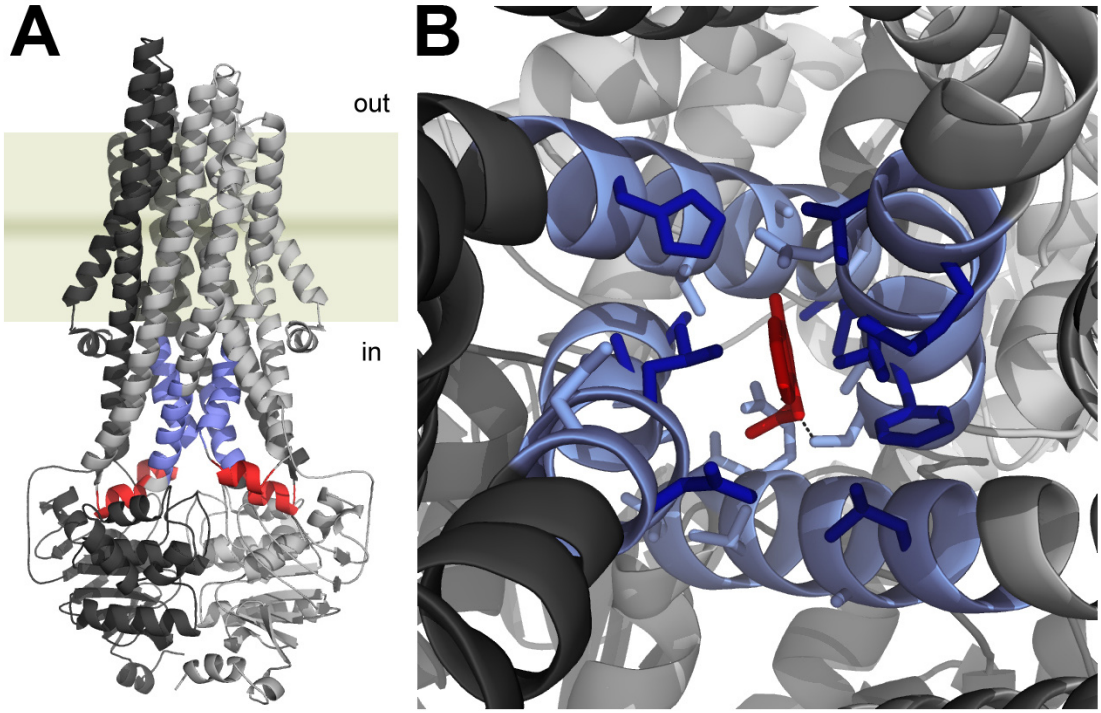

FIGURE 5. **AtABCB1 ICLs residues may participate in drug binding**

***A,* Front view of an AtABCB1 homology model.** ICL residues with low conservation between plant and animal ABCB1 orthologs aligned in Figure 3**B** (light blue) are located in the intracellular space and form the bottom of the translocation chamber. These regions are in the direct vicinity of the four "coupling helices" described by Dawson and Locher (2006).
TMD1 and NBD1 are in silver; TMD2 and NBD2 are in dark grey. Coupling helices are in red. Plasma membrane is shown in brown. The molecular structure diagram was generated using PyMol 0.99rev8 (http://pymol.sourceforge.net/) and Adobe Photoshop 7.0.
***B,* Outward-facing AtABCB1 inner cavity formed by the TMD1-TMD2 interface viewed from the extracellular side.** ICL residues with low conservation between plant and animal ABCB1 orthologs face the translocation chamber. *In silico* binding assays reveal suitable sterical and chemical environment for IAA^- binding/transport (red sticks) in this particular region. TMD1 and NBD1 are in silver; TMD2 and NBD2 are in dark grey. ICL amino acids aligned in **Figure 2B** are in light blue; residues with lowest conservation are in dark blue. Residues facing the translocation chamber are shown as sticks.
The molecular structure diagram was generated using PyMol 0.99rev8 (http://pymol.sourceforge.net/). *In silico* IAA binding against modeled AtABCB1 TMDs was performed using MEDock (Maximum-Entropy based Docking) web server (http://medock.csbb.ntu.edu.tw/).

reflected by the distribution of translocation chamber residues.

To test this hypothesis, we performed multiple alignments of closely related animal and plant ABCB1 orthologs (see Fig.3) that revealed only poor homology in the transmembrane regions. However, subsequent 3D-mapping based on homology models revealed three different levels of residue conservation within TMDs. First, clusters of non-polar and aromatic residues at the external surface of the transmembrane α-helices are functionally conserved. In accordance with experimentally proven ABC topologies and *in silico* consensus predictions, these amino acids describe the membrane-spanning regions. At a second level, structurally relevant residues, distributed over the whole TMDs, are highly conserved and may directly contribute to the core of the protein architecture. Third, kingdom-specific clusters display a preserved divergence between plant and animal ABCB1 proteins (Figure 3**B**). Of most interest, these last regions spatially co-localize with the intracellular loops (ICLs) of the TMDs (Figure 5**A**), where the cytosolic N-terminal ends of transmembrane helices III and IX, together with the cytosolic C-terminal ends of transmembrane helices IV and X form the gate surface of the observed translocation cavity (Altenberg, 2004; Dawson and Locher, 2006; Figure 5**B**). As shown in Figure 3, animal ABCB1s display a higher degree of conservation when compared to plant ones. Strikingly, a more detailed spatial comparison of these helical segments revealed that inter-specific conserved residues are mostly found in the core of the protein whilst divergent amino acids are facing the inner space of the cavity (Figure.5**B**). Inline with these observations, chemical properties and surface electrostatic potentials at the bottom of the cavity were found to be distinct between plant and animal ABCB1s but consistent with their respective transport selectivity (Flanagan and Huber, 2007). Hence, these residues build appealing candidate regions to elucidate the substrate specificity of ABCB1.

ICLs have been neglected in past studies in this respect, mainly because of the well-accepted "membrane vacuum cleaner" model (Shapiro and Ling, 1997a; Siarheyeva et al., 2006). In this model, P-glycoproteins are thought to extrude hydrophobic compounds from the inner leaflet of the plasma membrane. Although this assumption might be valid for hydrophobic substrates of HsABCB1, it can not be easily extended to ABCs with substrate specificities toward charged, hydrophilic compounds, such as the bile salt transporter ABCB11 (Meier and Stieger, 2002; Stieger et al., 2007). Likewise, plant ABCBs are thought to transport auxin in its anionic form (IAA^-) (Geisler et al., 2005; Multani et al., 2003; Noh et al., 2001), due to its cytoplasmic deprotonation (Delker et al., 2008). The substrate IAA^- is therefore more likely to reach its binding site through cytosolic domains of the transporter, further supporting the involvement of ICLs in hydrophilic drugs recognition.

Although different detailed mechanisms have been proposed to explain how ABCs transmit the ATP-binding energy to the translocation of bound substrates (Davidson and Chen, 2004; Higgins et al., 1997; Higgins and Linton, 2004; Hollenstein et al., 2007a; Linton and Higgins, 2007), the consensus concept in which nucleotide- and drug-binding favour major conformational changes in the TMDs spatial organization is today well accepted (Daus et al., 2006; Lee et al., 2008; Loo et al., 2003a; Rosenberg et al., 2003). The observed TMD-NBD interface is therefore the key candidate region to mediate this "power stroke". Indeed, the recently obtained crystal structures place the Sav1866-like coupling helices as fundamental components of the mechanism (Hollenstein et al., 2007a). Interestingly, the ICL kingdom-specific clusters presented here (Figure 3**B**) are residues directly adjacent to coupling helices and, as a result, drug binding in this region might destabilize enough the overall TMD-NBD interface to facilitate allosteric events of the catalytic cycle (Figure 5). However, HsABCB1 substrates are relatively voluminous and complex and therefore, according to the "induced-fit" mechanism, it is easy to understand how they may induce these drastic conformational changes by binding to the pocket. But compared to that, IAA is small and polar and may not cause the expected dramatic sterical shifts by itself. As shown for the auxin receptor TIR1 crystallized in the IAA-bound state (Tan et al., 2007), auxin might engage its carboxyl group to build salt bridges with the ABCB1 cavity residues and consequently present its apolar indole ring to the translocation chamber. Hydrophobic phytosterols might therefore be needed to fill the remaining space as proposed in the HsABCB1 "cholesterol fill-in" model (Kimura et al., 2007).

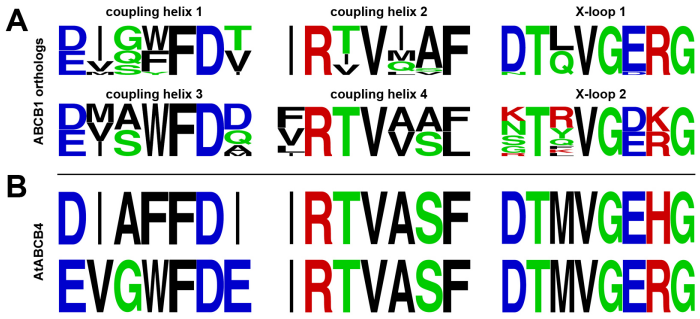

FIGURE 6. **Coupling helices and X-loops regions are functionally conserved in ABCB proteins.**

A, Multiple alignments of the 14 ABCB1 orthologs coupling helices and X-loops reveal the functional conservation of these regions in ABCB exporters.
B, The apparent IAA importer AtABCB4 (GI:15226477) shares the same degree of conservation in these regions than ABCB exporters.

To date there is no biochemical evidence for such AtABCB1 domain movements in response to auxin or phytosterol binding. However, future biochemical investigations based on our kingdom-specific ABCB1 comparisons represent opening step toward our understanding of substrate recognition, binding and translocation.

Conclusion and further direction

The variety of ABCB1 substrates may be explained in two ways: the transporters hold, first, either a unique binding-site of promiscuous specificity, or, second, multiple, narrow-specific binding sites (Shapiro and Ling, 1997b). In the recent decades, tremendous efforts have been conducted on solving this issue (Borowski et al., 2005), but the overall set of structural, mutational, biochemical, physiological and clinical data accumulated waits for correct interpretation. Indeed, the limiting factor to understand the mechanism of multidrug recognition is the lack of a valid and complete ABCB protein structure.
Regarding the incoming body of experimental evidences initiated by the Sav1886 crystal structure an updated understanding of kingdom-specific ABCB1 structural and functional evolution represents a step forward in understanding ABC transporter substrate specificity. Despite diverse substrate specialization, human and Arabidopsis ABCB1 transporters share a close common architecture. However, our analysis identified candidate substrate regions in the cytosolic parts of the transporter transmembrane domains. This strongly suggests that substrate specificity separated early during evolution but can be monitored and consequently used for the investigation of substrate binding.

Plant, animal and bacterial ABCB proteins seem to share a common architecture (Hollenstein et al., 2007a; Locher, 2004), although they transport a broad range of radically different compounds, underlining the essential function of pumping specific drugs in or out cellular compartments. Plant genomes contain an expanded family of ABC-transporter genes - over 120, compared to 50-60 in other organisms of equivalent genome size - (Jasinski et al., 2003; Martinoia et al., 2002; Sanchez-Fernandez et al., 2001a; Sanchez-Fernandez et al., 2001b; Theodoulou, 2000) which seems to reflect the need for narrow-specific transport in these sessile organisms (Geisler and Murphy, 2006). Interestingly, genetic studies from water- to land-plants have demonstrated that the complexity of the ABC-transporter family arose with the emergence of auxin-controlled development (Kelch et al., 2004). Structurally and functionally, ABCB substrate specialization seems to be recent when compared to the ancient origin of ABC proteins. As the drug-specificity lies in the transmembrane domains of the transporter, a large scale comparison of plant and animal ABCB structures and subsequent robust modeling may result in future substrate-prediction. This will allow contributing to the efforts in designing therapeuticals and anti-cancer agents that are not recognized by MDR proteins.

Chapter 2

PLANT IMMUNOPHILINS CONTROL DEVELOPMENT

FK506-binding immunophilins (FKBPs) belong to the widespread superfamily of *cis-trans*-peptidylprolyl-isomerases (PPIase). Thus, many of them exhibit a rotamase activity classifying them as folding proteins. This PPIase activity is classically inhibited by the immunosuppressant FK506. Nevertheless, some plant multidomain immunophilins, such as Arabidopsis TWISTED DWARF1 (TWD1), do not display PPIase activity, nor bind FK506. TWD1 interacts with ABCB-type auxin efflux transporters at the plasma membrane. Thus, TWD1 positively regulates ABCB-mediated auxin efflux, and therefore controls a part of the hormone signaling pathway. Another example is the multidomain FKBP-type PASTICCINO1 (PAS1), suggested to be involved in cytokinin-dependent cell proliferation and cell differentiation. PAS1 binds and translocates a NAC-like transcription factor to the nucleus and repress cytokinin-dependent cellular events. This suggests that multidomain FKBPs are potent interactors of various essential proteins for development and physiology. Therefore, our laboratory focused on TWD1-mediated regulation of the essential polar auxin transport in *Arabidopsis*. The knowledge gathered on plant immunophilin functions may be beneficial to human health: indeed, some mammalian FKBPs are implied in the immune response, regulate calcium release channels or bind to the hormonal glucocorticoid-receptor.

The TWISTED DWARF's ABC: How Immunophilins Regulate Auxin Transport

Aurélien Bailly, Valpuri Sovero and Markus Geisler*

Zurich-Basel Plant Science Center; University of Zurich; Institute of Plant Biology; Zurich, Switzerland
*Correspondence to: Markus Geisler; Zurich-Basel Plant Science Center; University of Zurich; Institute of Plant Biology; Zolliker Strasse 108; Zurich CH-8008 Switzerland; Tel.: +41.1.634.8277; Fax: +41.1.634.8204; Email: markus.geisler@botinst.unizh.ch

Summary

There is increasing evidence that immunophilins function as key regulators of plant development. One of the best investigated members, the multi-domain FKBP TWISTED DWARF1 (TWD1)/FKBP42, has been shown to reside on both the vacuolar and plasma membranes where it interacts in mirror image with two pairs of ABC transporters, MRP1/ MRP2 and PGP1/ PGP19(MDR1), respectively. *Twisted dwarf1* and *pgp1/pgp19* mutants display strongly overlapping phenotypes, including reduction and disorientation of growth, suggesting functional interaction.

In a recent work using plant and heterologous expression systems, TWD1 has been demonstrated to modulate PGP-mediated export of the plant hormone auxin, which controls virtually all plant developmental processes. Here we summarize recent molecular models on TWD1 function in plant development and PGP-mediated auxin tranport and discuss open questions.

FK506-binding Proteins (FKBPs), together with unrelated cyclophilins, belong to the immunophilins, an ancient and ubiquitous protein family (Harrar *et al.*, 2001;Romano *et al.*, 2004; Schreiber, 1991). They were first described as receptors for immunosuppressive drugs in animal and human cells, FK506 and cyclosporine A, respectively (Schreiber, 1991). All FKBP-type immunophilins share a characteristic peptidyl-prolyl cis-trans isomerase domain (PPIase domain or FKBD, Fig. 2A) making protein folding a key feature among immunophilins (Schiene-Fischer and Yu, 2001). The best investigated example, the human cytosolic single-domain FKBP12, modulates Ca^{2+} release channels (Cameron *et al.*, 1995; Jayaraman *et al.*, 1992) and associates with the cell cycle regulator TGF-β (Wang *et al.*, 1996). Furthermore, the human FKBP12/FK506 complex is known to bind and inhibit calcineurin activity, (Dumont, 2000) leading to immune response inhibition. However, not all single- and multiple-domain FKBPs own folding activity and, interestingly, many form distinct protein complexes with diverse functions (Galat, 2003; Harrar *et al.*, 2001; Romano *et al.*, 2004).

Multiple-Domain FKBPs Function as Key players in plant Development

Twenty-three FKBP-type proteins have been identified in the *Arabidopsis thaliana* genome, however, the function of individual FKBPs in plant biology is poorly understood.

Many single-domain FKBPs, like FKBP20-2, seem to be chloroplast targeted and to be involved in redox regulation of photosynthesis (Lima *et al.*, 2006). The multiple-domain FKBP mutant *pasticcino1* (*pas1*), defective in cell elongation and proliferation, shows highly disorganized seedlings. The PAS1 protein (FKBP52) is nuclear, shows little PPIase-activity and controls the targeting and the function of a NAC-like transcription factor (Faure *et al.*, 1998; Smyczynski *et al.*, 2006;Vittorioso *et al.*, 1998). The *Arabidopsis* mutant *twisted dwarf1* (*twd1*, allelic to *ultracurvata2 (ucu2)* (Perez-Perez *et al.*, 2004)) lacks the high-molecular weight FKBP42 and displays a drastic pleiotropic phenotype including reduced development and cell elongation, and disoriented growth of all organs, both on the epidermal and whole plant level (Fig. 1A, E and F) (Geisler *et al.*, 2003; Petrašek *et al.*, 2006).

Based on a yeast two hybrid screen and confirmed by a whole range of methods TWD1 was shown to interact in mirror image with two pairs of ATP-binding cassette (ABC) transporters (Fig. 2B): the multidrug-resistance (MDR) like P-glycoproteins (PGP) PGP1 and PGP19 (MDR1) on the plasma membrane, and the multidrug-resistance associated (MRP) MRP1 and MRP2 on the tonoplast. (Geisler *et al.*, 2003; Geisler *et al.*, 2004) Interestingly, interacting stretches of individual ABC transporters containing C-terminally the nucleotide-binding folds interact with distinct functional domains of TWD1: the FKBD and tripartite tetratricopeptide repeat (TPR) domain, respectively. Strikingly, the double mutant *pgp1/pgp19*, but not the corresponding single mutants, shares with *twd1* highly similar auxin-related phenotypes: dwarfism (Fig. 1A and B) and agravitropic roots (Bouchard *et al.*, 2006). These results suggest a central position for TWD1 in PGP-mediated auxin transport.

TWD1 Functions as Positive Modulator of P-Glycoprotein-Mediated Auxin Transport

Inline with this hypothesis, constitutive upregulation of PGP1 and PGP19 enhanced IAA net efflux, while overexpression of TWD1 did not alter wild type levels, excluding any direct auxin transport activity (Bouchard *et al.*, 2006). Developmental plant phenotypes correlate perfectly with decreased auxin transport rates on the organ (Fig. 1C) and cellular level (Fig. 1D). Moreover, the use of a novel highly selective IAA microelectrode (Mancuso *et al.*, 2005) allowed monitoring decreased auxin influxes in *twd1* and *pgp1/pgp19* mutant root apices compared to the single PGP mutants or the wild type (Bouchard *et al.*, 2006). As a consequence, free IAA levels are greatly elevated in mature *pgp1/pgp19* and *twd1* roots compared to single mutants or wild type, indicating a reduction of PGP-mediated polar auxin transport in *twd1*.

Note
A recent paper by Granzin et al. (2006) describes the crystal structure of TWD1 representing the first three-dimensional structure of a multi-domain immunophilin. While the overall architecture of the two domains matches the known characteristics of the FKBP and TPR folds, respectively, their arrangement is unique and sheds light on the probable binding modes of key interaction partners, including HSP90 and two classes of ABC transporters.

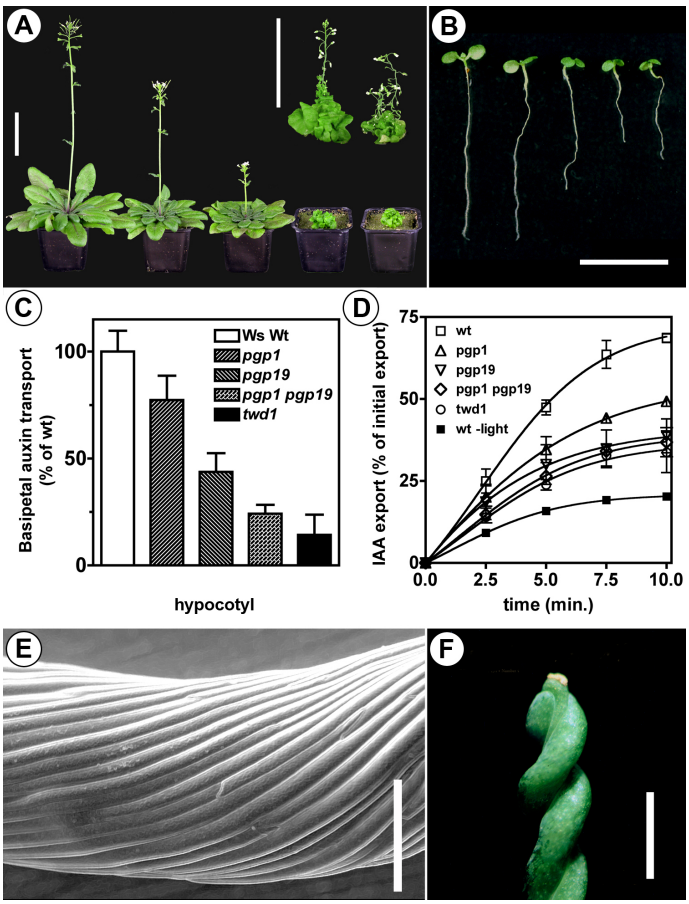

FIGURE 1. **The twisted dwarf1 (*twd1*) mutant displays a pleiotropic developmental phenotype that correlates with reductions in auxin transport.**

A, Growth phenotypes of one-month-old soil-grown plants; from left to right: wild-type (ecotype Wassilewskija), *pgp1*, *pgp19*, *pgp1/pgp19* and *twd1*. Inset: mature *pgp1/pgp19* and *twd1* plants. Bars, 5 cm. ***B,*** Growth phenotypes of light-grown seedlings 5 dag; from left to right: wild-type, *pgp1*, *pgp19*, *pgp1/pgp19* and *twd1*. Bar, 1 cm. (from Geisler *et al.* (2003). ***C,*** Reduced polar IAA transport in hypocotyls of young seedlings reflects growth phenotypes. Means ± S.D. (from Geisler *et al.* (2003), modified). ***D,*** Cellular IAA export in mutant protoplasts is decreased compared to wild-type (open square) in the order wt > *pgp1* (open triangle) > *pgp19* (upside-down open triangle) >> *pgp1/pgp19* (open diamond) ≥ *twd1* (open circle). Dark-treated (de-energized) plant material (filled square) was used as negative control. Means ± S.D. (data taken from Geisler *et al.* (2003, 2005)). ***E,*** Electron micrograph of the twd1 hypocotyl. The "twisted syndrome" of all organs is perceptible at the epidermal level. Bar, 100 µm. (picture taken from Geisler *et al.* (2005), modified). ***F,*** The *twd1* silique displays reduced and disoriented growth. Bar, 500 µm.

The regulatory role of TWD1 on PGP1-mediated auxin transport was confirmed by functional coexpression in *S. cerevisiae* and mammalian HeLa cells. Interestingly, IAA efflux assays in yeast (Bouchard *et al.*, 2006) and functional complementation of the auxin-hypersensitive yeast mutant *yap1* (Prusty *et al.*, 2004) revealed an inhibitory effect of TWD1 on PGP1 function while coexpression in HeLa cells resulted in enhanced auxin export. This difference might result from the lack of higher eukaryotic components in *S. cerevisiae.*

Together, these findings further support the idea of a positive regulatory role for TWD1 on PGP-driven auxin transport *in planta*.

Does the Regulatory Function of TWD1 Involve Chaperone Activity?

It was recently suggested that brassinosteroid-mediated signal transduction in *twd1* may require the activity of the HSP90 chaperone complex (Sangster and Queitsch, 2005). Consistent with these findings, citrate synthase aggregation assays (Buchner *et al.*, 1998) revealed a chaperone-like activity requiring the TWD1 HSP90-binding TPR domain (Fig. 2A) while the FKBD alone did not prevent aggregation (Buchner *et al.*, 1998).

Previous studies suggested yeast single-domain FKBP12 to function as a regulator of murine PGP-like proteins, but independently of its PPIase activity (Hemenway and Heitman, 1996; Mealey *et al.*, 1999). Interestingly, TWD1 function on PGP1-mediated IAA efflux was only slightly mimicked by Arabidopsis FKBP12.18 Moreover, the FKBD of TWD1 displays no PPIase activity (Kamphausen *et al.*, 2002) and TWD1 does not complement yeast FKBP12 (Geisler *et al.*, 2004). Furthermore, TWD1 does not bind FK506 (Kamphausen *et al.*, 2002) which, based on structural data, is due to sterical reasons (Weiergräber *et al.*, 2006).

In agreement it was established that impaired auxin transport in *twd1* was neither caused by changes in PGP1 or PIN1/PIN2 auxin efflux carrier (Petrašek *et al.*, 2006) expression nor by localization, confirming that the regulatory effect is due to physical interaction. Finally, the biochemically and immunologically demonstrated membrane location of TWD1 (Geisler *et al.*, 2003), recently suggested to adopt an orientation perpendicular to the membrane using solid-state NMR (Scheidt *et al.*, 2006), are in disagreement with current models of chaperone function. Although the in vivo lack of TWD1 chaperone function in the auxin-signaling pathway still needs to be demonstrated, it

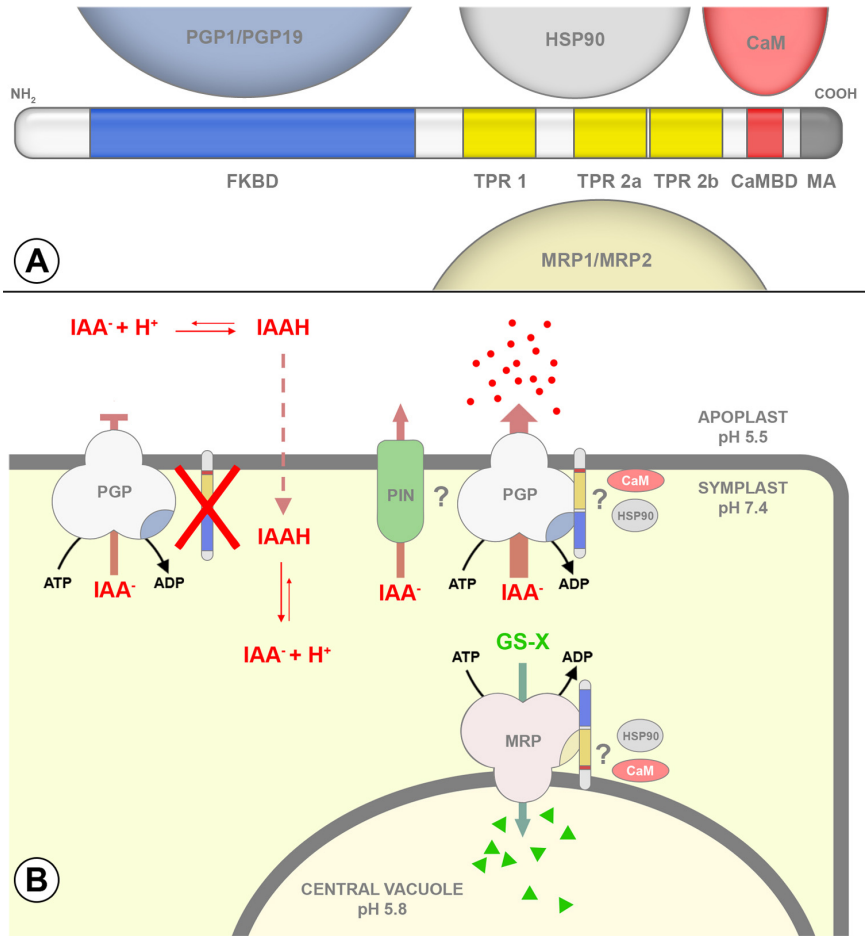

FIGURE 2. **Model of TWISTED DWARF 1 interacting proteins.**

A, Domain structure of TWD1 and putative interacting proteins. FKBD, FK506-binding domain: TPR, tetratricopeptide repeat; CaM(-BD, calmodulin-binding domain; MA, membrane anchor. For details, see text. ***B,*** Functional TWD1-ABC transporter complexes on both the vacuolar and plasma membrane. While for TWD1/PGP pairs, the positive regulatory role on auxin transport was demonstrated (Bouchard *et al.*, 2006), the modulation of MRP-mediated vacuolar import of glutathion conjugates (GS-X) was established using mammalian test substrates (Geisler *et al.*, 2004) because the *in vivo* substrates are unknown. Note that C-terminal nucleotide binding folds of MRP- and PGP-like ABC transporters interact with distinct functional domains of TWD1, the TPR and FKBD, respectively. The native auxin, IAAH, gets trapped by deprotonization upon uptake into the cell. Export is catalyzed by secondary active export via PIN-like efflux carriers (Petrašek *et al.*, 2006) and/or by primary active, ATP-driven P-glycoproteins (PGPs, right panel); loss-of TWD1 function abolishes PGP-mediated auxin export (left panel).

seems likely that the multi-domain immunophilins have gained a distinct function in protein-protein interaction through evolution.

Outlook

The positive regulatory role of TWD1 is well documented but the question remains why nature invented such a complicated mechanism of auxin transport regulation. One plausible explanation might be that regulation via protein-protein interaction is a very economic way of regulation that on the other hand allows very precise fine-modulation. This might be conferred by plant drugs disrupting protein-protein interaction. In this respect it is worth mentioning that excess of NPA removes TWD1 from NPA chromatographies (Geisler *et al.*, 2003).

Although reductions of PGP-mediated auxin transport in twd1 are in agreement with dwarfism and other auxin-related phenotypes, loss of TWD1 action does not directly explain the "twisted syndrome". However, many helical orientations caused by mutations are due to misassembly of microtubuli. Interestingly, mammalian multi-domain FKBPs have been shown to bind dynein via the N-terminal PPIase domain (Galigniana *et al.*, 2001).

Finally, it remains to be solved why *twd1* mutant plant show more pronounced phenotypes at later stages compared to *pgp1/pgp19* (Fig. 1A, inset). One possibility is that other TWD1-interactors contribute to the full twisted phenotype. These might be MRP1/MRP2, but unfortunately their in vivo substrate is hard to guess and quadruplet knock-out lines are difficult to get due to genetical distances. Other obvious candidates include interacting partner HSP90, a well known developmental regulator (Queitsch *et al.*, 2002) and calmodulin (CaM). TWD1 shares some unique structural properties with the human homologue FKBP38 (Maestre-Martinez et al., 2006). Beside their common putative membrane anchoring, TWD1 binds CaM which is essential for HsFKBP38 function. An active FKBP38/CaM/Ca^{2+} complex is required for Bcl-2 interaction, a key protein in apoptosis control. Strong indications are now pointing to the upcoming

role of TWD1-homolog heterocomplexes functioning in regulation of MDR-type transporters and reveal the potential benefits of such investigations for agronomy and human health.

Tête-à-tête: The function of FKBPs in plant development

Markus Geisler and Aurélien Bailly

Zurich-Basel Plant Science Center, University of Zurich, Institute of Plant Biology, Zolliker Strasse 108, CH-8008 Zurich, Switzerland

Corresponding author: Geisler, M. (markus.geisler@botinst.uzh.ch).

Summary

Compared with that of other eukaryotes, the nuclear genome of the model plant Arabidopsis thaliana encodes an expanded family of FK506-binding proteins (FKBPs). Whereas approximately half of the FKBPs are implicated in the regulation of photosynthetic processes, a subcluster appears to be stress responsive. Recent reports indicate that a discrete group of Arabidopsis multidomain FKBPs regulate plant hormone pathways by recruiting or modulating client proteins via direct protein–protein interactions (tête-à-tête). This suggests that multidomain FKBPs function as central elements in plant development by linking hormone responses with other signal transduction pathways. Here, we present a summary of current research demonstrating that, in addition to their role in protein folding, subsets of plant FKBPs exhibit diverse functionality Diversity of plant FKBP functions.

FK506-binding proteins (FKBPs) belong to the superfamily of PPIases (peptidyl-prolyl *cis-trans* isomerases, EC 5.1.2.8), which catalyze the *cis-trans* isomerization of *cis*-prolyl bonds (Barik, 2006; Fanghanel and Fischer, 2004). FKBPs are ubiquitously distributed across most cellular compartments (Barik, 2006; He *et al.*, 2004; Romano *et al.*, 2005). Together with structurally unrelated cyclophilins, mammalian FKBPs have been identified as targets of immunosuppressant drugs and are therefore classified as immunophilins (Fanghanel and Fischer, 2004).

Many FKBPs have PPIase (rotamase) activity, creating the impression that FKBPs function primarily in protein folding (Barik, 2006; Fanghanel and Fischer, 2004). However, extensive research during the past decade has elucidated two independent functions for FKBPs: (i) a PPIase activity classically inhibited by binding of clinically relevant immunosuppressants, such as FK506 (tacrolimus) or rapamycin (sirolimus), and (ii) a chaperone function that is independent of the PPIase activity and unaffected by immunosuppressant drugs (Barik, 2006; Harrar *et al.*, 2001).

Here, we summarize the many recent reports that have added to our understanding of the mechanisms of functionality and the surprising diversity of physiological roles within the plant FKBPs (Harrar *et al.*, 2001; He *et al.*, 2004; Romano *et al.*, 2005). Contemporary structural (Granzin *et al.*, 2006; Weiergraber *et al.*, 2006) and interaction analyses prompted us to focus on the unexpected molecular role of plant multidomain (Bailly *et al.*, 2006; Bouchard *et al.*, 2006; Smyczynski *et al.*, 2006) FKBPs in the control of development, distinct from the classical role in protein folding. The current paradigm suggests that a subset of multidomain FKBPs regulate plant hormone pathways by recruiting or modulating client proteins via direct protein–protein interactions (Bailly *et al.*, 2006; Bouchard *et al.*, 2006; Smyczynski *et al.*, 2006).

As FKBPs emerge as key regulators of plant development, corresponding FKBP complexes might thus represent good targets for tissue-dependent manipulation of growth. Therefore, application of specific inhibitors affecting FKBP activity might be suitable to manipulate hormone transport and/or functional modality, thereby influencing plant development.

Lessons from mammalian FKBPs

In mammals, single-domain (low-molecular weight) FKBPs consist essentially of an FKB domain (FKBD) capable of both PPIase and drug-binding activity (Barik, 2006; Fanghanel and Fischer, 2004; Harrar *et al.*, 2001; He *et al.*, 2004; Romano *et al.*, 2005). In the absence of immunosuppressant drugs, the FKBP minimal representative, FKBP12, binds to and regulates the activity of calcium-release channels, such as the ryanodine receptor (RyR) and the inositol (1,4,5)-triphosphate receptor [Ins(1,4,5)*P*3-R], or associates with transforming growth factor-β (TGF-β) (Barik, 2006; Breiman and Camus, 2002; Romano *et al.*, 2005). Cells from mutant mice lacking FKBP12 isoforms show either significant cardiac defects and altered RyR function or cell-cycle arrest (Breiman and Camus, 2002).

The macrolides FK506 and rapamycin release FKBP12 from its membrane-bound partners, resulting in binding to calcineurin and TOR/FRAP/RAFT. In simplified terms, binding of the FK506/rapamycin-FKBP12 complex blocks the phosphatase activity of calcineurin and/or the kinase activity of TOR homologs leading to inhibition of downstream signal transduction, thereby inhibiting T-cell activation and subsequent graft rejection or cell-cycle arrest, respectively (Breiman and Camus, 2002; Fanghanel and Fischer, 2004; Harrar *et al.*, 2001; He *et al.*, 2004; Romano *et al.*, 2005).

Multidomain (high-molecular weight) FKBPs contain up to three FKBDs, typically followed by tetratricopeptide repeat domains (TPR) and C-terminal calmodulin-binding domains (CaM-BDs), both known to mediate protein–protein interactions (Breiman and Camus, 2002; Fanghanel and Fischer, 2004; Harrar *et al.*, 2001; He *et al.*, 2004; Romano *et al.*, 2005).

The most prominent representative of multidomain FKBPs is the mammalian FKBP52, which is associated with the native glucocorticoid receptor complex. FKBP52 can substitute for FKBP51, resulting in a switching of the cytoplasmic glucocorticoid receptor into a higher affinity hormone binding state (Davies and Sanchez, 2005). Following the substitution, FKBP52 promotes translocation of the receptor to the nucleus by linking the receptor via TPR-bound HSP90 to the dynein motor that binds to the PPIase domain of FKBP52 (Davies and Sanchez, 2005).

Expansion of the *Arabidopsis* FKBP family

As is the case with cyclophilins and several other protein families (Romano *et al.*, 2005), in the model plant *Arabidopsis thaliana,* the number of FKBP family proteins is expanded in comparison to other organisms of similar genome size (He *et al.*, 2004; Romano *et al.*, 2005). *Arabidopsis* has 23 FKBPs[1] (compared with four in *Saccharomyces cerevisiae*, eight in *Caenorhabditis elegans* and 15 in *Homo sapiens* (He *et al.*, 2004; Romano *et al.*, 2005)), of which seven are multidomain FKBPs and 16 are single-domain FKBPs.

Phylogenetic and sequence motif analysis clusters together 11 of the 16 single-domain FKBPs, as *bona fide* thylakoid lumen FKBPs (shown in green in Figure 1a). The remaining five single-domain FKBPs do not contain evident chloroplast-import motifs (Romano *et al.*, 2005). They subcluster with the multidomain FKBPs, are spread over all cellular compartments (excluding the mitochondria) and appear to perform functions unrelated to photosynthesis (Luan *et al.*, 1996) (shown in red in Figure 1a). Stress-related FKBP62/ROF1 and FKBP65/ROF2 (hereafter referred to as ROF1 and ROF2, respectively) (Aviezer-Hagai *et al.*, 2007) branch with FKBP15-1, FKBP15-2 and FKBP20-1, whereas FKBP15-3, FKBP43 and FKBP53 form a putative nuclear subcluster of non-chloroplast FKBPs (He *et al.*, 2004; Romano *et al.*, 2005).

Chloroplast-targeted FKBPs are involved in redox control of photosynthesis

Biochemical and proteomics data support the large number of *Arabidopsis* single-domain FKBPs predicted to reside in the thylakoid lumen based on transit peptide sequences (Romano *et al.*, 2005). Recent reports suggest that the function of at least some single-domain chloroplast FKBPs lies in the redox-dependent control of photosynthetic components (Gopalan *et al.*, 2004; Gopalan *et al.*, 2006; Gupta *et al.*, 2002; Lima *et al.*, 2006; Shapiguzov *et al.*, 2006). FKBP13 interacts with, and provides pH dependent import of the Rieske protein (part of the cytochrome *b6f* complex) into the thylakoid lumen (Gupta *et al.*, 2002). Moreover, 3D-structure analyses support a thioredoxin mediated inhibition of FKBP13 activity via reduction of two unique pairs of disulfide bonds (Gopalan *et al.*, 2004; Gopalan *et al.*, 2006; Shapiguzov *et al.*, 2006). By contrast, in FKBP20-2, reduction of two cysteines at the C-terminus by thioredoxin has no influence on its low PPIase activity (Lima *et al.*, 2006). *FKBP20* loss-of-function mutants (*fkbp20-2*) show reduced growth, PSII activity and PSII assembly, suggesting a direct involvement in PSII regulation. In summary, these findings suggest that a least a subset of chloroplast FKBPs are controlled by thioredoxin-dependent redox regulation.

Box 1. **Outstanding questions**

Do dual family immunophilins (FCBPs) exist in plants?

Members of the newly discovered chimeric dual family immunophilins (or FCBP for FK506- and cyclosporin-binding protein) consist of fusions of cyclophilin domains and FKBDs and, thus, bind both FK506 and cyclosporin (Barik, 2006). It has been speculated that owing to the relative positioning of the FKBD and CYP domains, FCBPs might be able to interact simultaneously with two client proteins in a multiprotein complex (Adams *et al.*, 2005; Barik, 2006). Based on extensive blast searches, FCBPs seem to be absent in *Arabidopsis* and other photosynthetically active organisms. In contrast to cyclophilins and FKBPs, they appear not to be ubiquitous and to be restricted to some protozoa and bacteria.

What is the function of the *Arabidopsis* trigger factor TIG?

The multidomain trigger factor-like FKBP (TIG) is composed of a central FKBD that is flanked by an N-terminal ribosome-binding and a C-terminal chaperone domain. Based on a transit peptide sequence, this protein has been predicted to localize in the chloroplast stroma. Although being distantly related to other FKBPs, a bacterial trigger factor shows highly enhanced folding activity (Adams *et al.*, 2005; Barik, 2006; Harrar *et al.*, 2001). Owing to its unclear function and low homology to other FKBPs, TIG was not included in the phylogenetic tree and was not considered further in this review, but its crucial function in bacteria (ribosomal binding and folding activity) argue for direct participation in chloroplast cotranslational protein folding in plants.

A subset of FKBPs are stress responsive

Little is known of the role of single-domain FKBPs predicted to reside in the ER or nucleus (FKBP15-1, FKBP15-3 and FKBP20-1), despite the fact that ER localized FKBP15 from *Vicia faba* was the first plant FKBP to be characterized (Luan *et al.*, 1996). However, for more than a decade, the function of wheat FKBP73 and FKBP77 (Blecher *et al.*, 1996; Dwivedi *et al.*, 2003; Kurek *et al.*, 1999; Kurek *et al.*, 2002b; Kurek *et al.*, 2002c; Reddy *et al.*, 1998) and the closely related *Arabidopsis* FKBPs, ROF1 and ROF2 (Aviezer-Hagai *et al.*, 2007; Vucich and Gasser,

1 Chimeric dual family immunophilins (FCBPs (Adams *et al.*, 2005; Barik, 2006)) seem to be absent in *Arabidopsis* (Box 1)

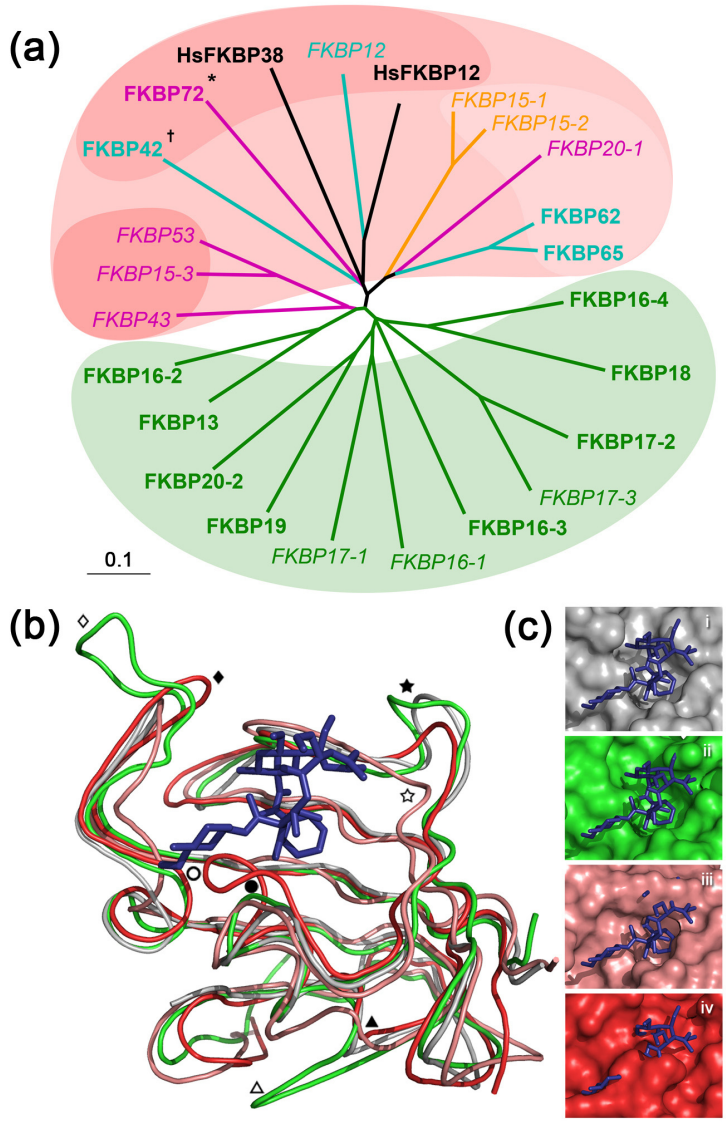

1996), which are thought to have distinct chaperone and PPIase activities, have been studied intensively.

In contrast to their mammalian homologs (such as FKBP51 and FKBP52), the wheat FKBP73, FKBP77 and ROF1, ROF2 contain a third FKBD of unknown function. They are induced by wounding (Vucich and Gasser, 1996), NaCl (Vucich and Gasser, 1996) and malondialdehyde treatment (Weber *et al.*, 2004). FKBP77 and ROF2 are induced by heat-shock, whereas FKBP73 and ROF1 are not (Aviezer-Hagai *et al.*, 2007; Blecher *et al.*, 1996), however, HSP90 binding to the TPR domain has been demonstrated with ROF1, but not with ROF2 (Aviezer-Hagai *et al.*, 2007). Tissue-specific expression has been demonstrated for both ROF1 and ROF2, and transgenic wheat overexpressing FKBP73 and FKBP77 show different morphological abnormalities including altered grain weight and sterility, suggesting different functions of the two isoforms in monocot plant development (Kurek *et al.*, 2002c). In pioneer experiments, it

FIGURE 1. **Phylogenetic and structural comparison of *Arabidopsis* FKBPs.**

(a) In phylogenetic trees, all *bona fide* single-domain FKBPs of the thylakoid lumen cluster together (green shading), whereas the remaining FKBPs subcluster with multidomain FKBPs of different function and location (red shading). Subclades of putative nuclear, stress- or development-related FKBPs are shaded in various shades of red (see main text). Trees of *Arabidopsis* FKBPs were computed by aligning the FKBDs that were closest to FKBP12 using ClustalX 1.83 (Thompson *et al.*, 1997) and default settings. Trees were confirmed by using the Neighbor-joining method and bootstrap analysis (1000 replicates) and drawn using Treeview 1.6.6 (http://taxonomy.zoology.gla.ac.uk/rod/treeview.html). Relevant human (black) FKBP12 and FKBP38 were included; *Arabidopsis* trigger factor TIG (Box 1) was omitted owing to poor homology. Putative subcellular locations are indicated by font colors, whereas experimentally verified locations are depicted in bold: red, nucleus; blue, cytoplasm; yellow, ER or secretory pathway; and green, thylakoid lumen. The nomenclature is based on He *et al.* (2004).

Notes: *PAS1 has been shown to shuttle between the cytoplasm and the nucleus (Bailly *et al.*, 2006). †TWD1 is membrane anchored on the vacuolar and plasma membrane but is considered as cytoplasmic owing to the predicted cytoplasmic orientation of its functional domains (Geisler *et al.*, 2003; Kamphausen *et al.*, 2002).

(b) Structure comparison of human FKBP12 binding FK506 (blue) with FKBPs derived from single and multiple domain FKBPs of human and plant origin suggest overall structural similarity, whereas chloroplast FKBP13 reveals structural insertions. Conserved (closed symbols) and altered FKBD structures (open symbols) in comparison to FKBP12 are marked by stars (FKBP38), triangles (FKBP13), circles (FKBP42) and diamonds (FKBP13), respectively.

(c) Steric exclusion of FK506 (blue) for FKBP38 and FKBP42 correlates with reported loss of PPIase activity (Kamphausen *et al.*, 2002; Shirane *et al.*, 2003). FKBD structure alignment was performed using PyMol 0.99 (http://www.pymol.org) and FK506 (blue) docking was predicted using MEDock (http://medock.csie.ntu.edu.tw/). (i) Human FKBP12 (Protein DataBank ID = 1FKJ; www.rcsb.org) and (iii) FKBP38 (PDBID = 2F2D) are shown in grey and pink, whereas (ii) *Arabidopsis* FKBP13 (PDBID = 1U79) and (iv) FKBP42/TWD1/UCU2 (PDBID = 2F4E) are depicted in green and red, respectively.

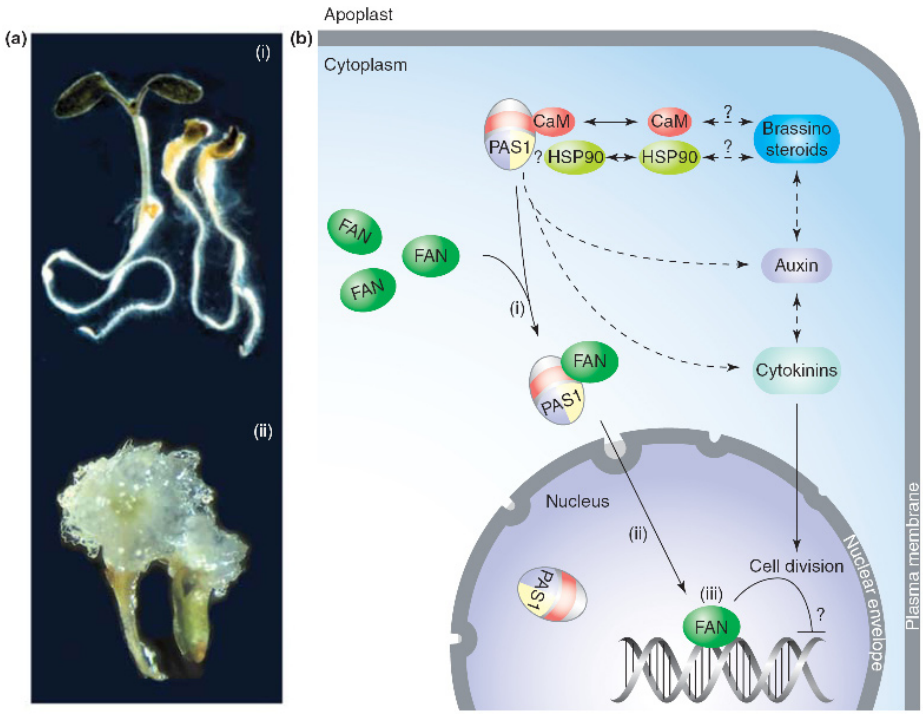

FIGURE 2. **Control of *Arabidopsis* cell proliferation and differentiation through suppression of cytokinin action by PASTICCINO1.**
(a) (i) Light-grown *pasticcino1 (pas1)* seedlings are dwarfed, with short thick hypocotyls, whereas roots are less affected. (i) Wild type seedling shown on the left and two *pas1* mutants on the right. (ii) Growth in the presence of cytokinins leads to exacerbation of growth phenotypes, including uncontrolled cell divisions that cause the *pasticcino* phenotype. Reproduced, with permission, from Harrar *et al.* (2001) and Faure *et al.* (1998).
(b) Model of PAS1 action. In dividing cells, PAS1 binds and translocates the NAC-like transcription factor, FAN (i), to the nucleus (ii), where FAN is thought to repress cytokinin action transcriptionally (iii). The PAS1 C-terminus binds FAN and provides nuclear exclusion, resulting primarily in a cytoplasmic distribution of PAS1 in mature tissues. Direct PAS1-mediated (solid lines) and indirect (dashed lines) signal transduction and hormone crosstalk (brassinosteroid, auxin and cytokinin) are indicated by arrows. Functional domains and interacting proteins are as follows: blue, FKBD; yellow, TPR (tetratricopetide repeat) domain, HSP90; and red, CaM(-BD). Question marks indicate expected or controversial functional connections that await experimental confirmation.

was demonstrated that wheat FKBPs can replace mammalian FKBP52 in forming an active steroid receptor complex, demonstrating that functionality between plant and mammalian orthologs is conserved (Reddy *et al.*, 1998). Interestingly, nuclear import of TaFKBP77 after heat-shock has been demonstrated (Dwivedi *et al.*, 2003), suggesting coordinated involvement of this subset of FKBPs and some HSP90s in stress responses.

Some FKBPs steer hormone-controlled plant development

Unlike *ROF1* and *ROF2* and functionally related isoforms, expression of *Arabidopsis FKBP12*, *FKBP42* and *FKBP72* is, based on microchip data (http://www.geneinvestigator.ethz.ch), ubiquitous throughout development and unaffected by stress treatments. Whereas expression of *FKBP42* (Geisler *et al.*, 2003) and *FKBP72* (Harrar *et al.*, 2003; Vittorioso *et al.*, 1998) is low, *FKBP12* is highly expressed. Interestingly, *Arabidopsis* FKBP12, FKBP42 and FKBP72 subcluster with human FKBP12 and FKBP38, rather than with *Arabidopsis* single- or multidomain FKBPs (Figure 1a).

FKBP12

Despite intensive efforts, the function of *Arabidopsis* FKBP12 *in vivo* is still unclear (Breiman and Camus, 2002; Faure *et al.*, 1998a; Vespa *et al.*, 2004; Xu *et al.*, 1998). It does not functionally complement yeast lacking FKBP12 (Xu *et al.*, 1998), but does interact with FIP37, a homolog of the human FKBP12-interacting protein FAP48 (Faure *et al.*, 1998a; Vespa *et al.*, 2004). FKBP12 docks with FIP37 via its FKBD in an interaction that is disrupted by FK506 (Faure *et al.*, 1998a; Vespa *et al.*, 2004). Loss-of-function mutants of nuclear FIP37 are embryo-lethal (Vespa *et al.*, 2004), as is the case for *Arabidopsis tor* mutants

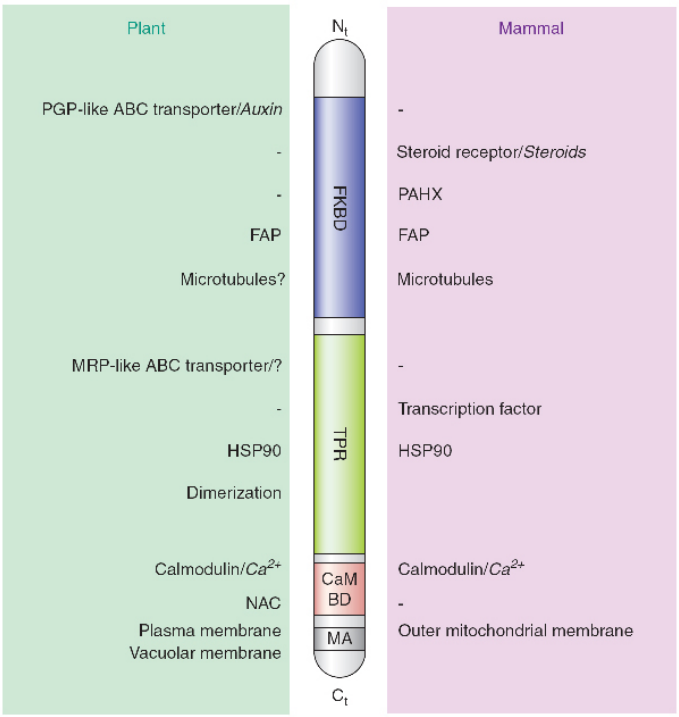

FIGURE 3. **Interactors of mammalian and plant multidomain FKBP and linked signal transduction and hormone networks.**
A comparison between mammalian and plant FKBPs reveals that all functional FKBP domains are involved in the recruitment of interacting proteins (normal fonts) or in affecting signal transduction and hormone (brassinosteroid, auxin and cytokinin) pathways (italic fonts). Although many client proteins are conserved between plant and mammalian FKBPs, some are unique to each system. Functional domains and interacting proteins are as follows: blue, FKBD; yellow, TPR (tetratricopetide repeat) domain; red, CaM(-BD) and grey, MA (membrane anchor). Question marks indicate expected or controversial functional connections that await experimental confirmation. Abbreviations: Ct, C-terminus; FAP, FKBP-associated protein; Nt, N-terminus; PAHX, phytanoyl-CoA 2-hydroxylase.

(Menand *et al.*, 2002).

Interestingly, recent reports indicate that *Arabidopsis* FKBP12 and TOR do not interact (Menand *et al.*, 2002), whereas in the green algae *Chlamydomonas reinhardtii* FKBP12 and TOR do form a complex (Crespo *et al.*, 2005). Moreover, *Arabidopsis* does not appear to be sensitive to rapamycin, whereas *Chlamydomonas fkbp12* gains resistance (Crespo *et al.*, 2005), suggesting a distinct function for the higher plant FKBP12 pathway compared with those found in green algae.

PASTICCINO1

The *Arabidopsis pasticcino1* (*pas1*) mutant was isolated in a forward genetic screen to identify cytokinin hyper-responsive mutants (Faure *et al.*, 1998b; Vittorioso *et al.*, 1998), and is disrupted in a gene encoding FKBP72/PAS1 (hereafter referred to as PAS1). The mutant displays ectopic cell division and defects in cell differentiation in all tissues, except in the roots (Faure *et al.*, 1998b; Harrar *et al.*, 2001; Vittorioso *et al.*, 1998).
Exogenous application of cytokinins leads to the formation of callus-like structures in *pas1* plants (Figure 2), suggesting that PAS1 acts as a negative regulator of cell proliferation and a positive regulator of cell differentiation (Faure *et al.*, 1998b; Harrar *et al.*, 2003; Vittorioso *et al.*, 1998).

Recent work demonstrates that the C-terminus (CaM-BD plus C-terminal extension) of PAS1, previously shown to bind calmodulin (Davies and Sanchez, 2005), also interacts *in vivo* with FAN, a NAC-like transcription factor (Smyczynski *et al.*, 2006). Whereas PAS1 was originally thought to be localized in the nucleus (Carol *et al.*, 2001), recent work confirms that the C-terminus is essential for its exclusion from the nucleus (Smyczynski *et al.*, 2006). However, in dividing cells and upon auxin treatment (inducing cell proliferation), PAS1 and FAN are translocated from the cytoplasm into the nucleus of mature *Arabidopsis* roots. It appears that PAS1 promotes FAN repression of cytokinin dependent cell division and proliferation by targeting FAN to the nucleus (Figure 2b).

This model is supported by the fact that the *pas1* phenotype is partially complemented by FAN overexpression; FAN would be anticipated to diffuse into the nucleus (Smyczynski *et al.*, 2006). FKBP interactions with mammalian transcription factors are commonly observed (Figure 3), and this function appears to be unexpectedly conserved in transcriptional regulation of plant cell division and differentiation (Germain and Shore, 2003; Shirane and Nakayama, 2003; Smyczynski *et al.*, 2006). Whereas, in mammalian FKBPs, the PPIase and TPR domains are essential for interaction with transcription factors the C-terminal extension of PAS1 appears crucial for the same function in plants (Smyczynski *et al.*, 2006).

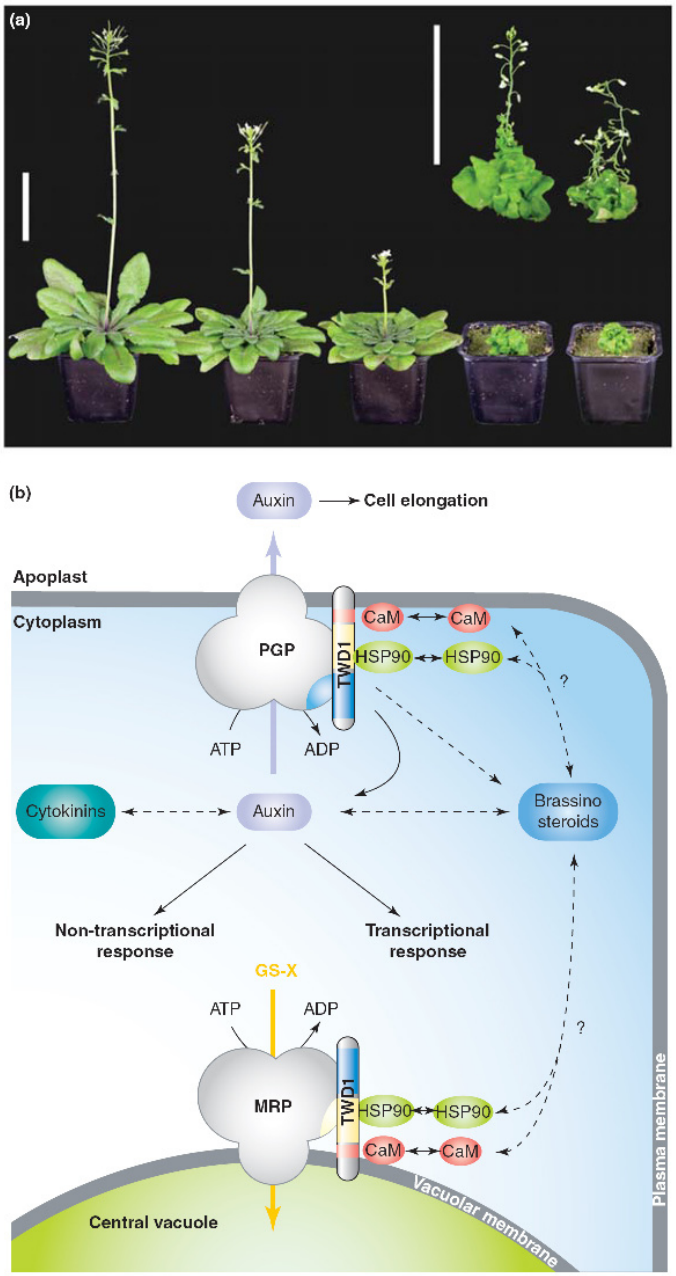

FIGURE 4. **Control of plant development via positive modulation of auxin transport by TWISTED DWARF1.**

(a) The *twisted dwarf1* (*twd1*) mutant displays a pleiotropic developmental phenotype that correlates with reductions in auxin transport catalyzed by the interacting p-glycoproteins (PGPs), PGP1 and PGP19. Growth phenotypes of one-month-old soil-grown plants (from left to right: wild-type, *pgp1*, *pgp19*, *pgp1 pgp19* double mutant and *twd1)*. Mature *twd1* mutant plants show a more pronounced phenotype compared with *pgp1 pgp19* (inset: *pgp1 pgp19* and *twd1* plants) suggesting that other TWD1 interactors contribute to the full *twd1* phenotype. Obvious candidates include interacting MRP1/MRP2, HSP90 and calmodulin. Scale bars = 5 cm. Reproduced, with permission, from Bailly *et al.* (2006).

(b) Model of TWD1 action. TWD1 forms functional ABC transporter complexes on both the vacuolar and plasma membrane. Whereas the positive regulatory role of TWD1 on PGP-mediated auxin transport has been demonstrated (Bouchard *et al.*, 2006), the modulation of MRP-mediated vacuolar import was established using mammalian test substrates [glutathione conjugates (GS-X)] because the *in planta* substrates remain unknown (Geisler *et al.*, 2004). Direct TWD1-mediated (solid lines) and indirect (dashed lines) signal transduction and hormone crosstalk are indicated by arrows. Functional domains and interactor proteins are as follows: blue, FKBD; yellow, TPR domain and HSP90; red: CaM(-BD); and gray, membrane anchor. Question marks indicate expected or controversial functional connections that await experimental confirmation.

TWISTED DWARF1/ULTRACURVATA2

The *Arabidopsis* mutant *twisted dwarf1/ultracurvata2 (twd1/ucu2)* lacks a functional FKBP42/TWD1/UCU2 (hereafter referred to as TWD1) and displays a severe pleiotropic developmental phenotype (Figure 4a), including small plant size, reduced cell elongation, disoriented growth of all organs and misshapen epidermal cells (Bailly *et al.*, 2006; Geisler *et al.*, 2003; Kamphausen *et al.*, 2002; Perez-Perez *et al.*, 2004). It has been isolated independently in large-scale genetic screens for *Arabidopsis* mutants displaying strong developmental defects (Geisler *et al.*, 2003) and abnormally shaped (*ultracurvata*) leaves (Perez-Perez *et al.*, 2004).

Using biochemical methods, TWD1 has been shown to interact with four ATP-binding cassette (ABC) transporters (Figure 4b) (Bailly *et al.*, 2006): the ABCB P-glycoproteins PGP1 and PGP19 in the plasma membrane (Geisler *et al.*, 2003; Lin and Wang, 2005), and the ABCC multidrug-resistance associated proteins MRP1 and MRP2 in the tonoplast (Geisler *et al.*, 2004). Interestingly, interaction with PGPs utilizes the FKBD, whereas MRP interaction occurs via the TPR domain (Bailly *et al.*, 2006; Geisler *et al.*, 2004; Geisler *et al.*, 2003). Noticeably, the double mutant *pgp1 pgp19* (but neither of the corresponding single mutants) share with *twd1* highly similar auxin-related phenotypes, such as dwarfism and roots exhibiting altered gravitropic growth (Bouchard *et al.*, 2006; Lin and Wang, 2005). Reduction of plant growth in *twd1* correlates well with decreased auxin transport rates

observed at both the organ and cellular level (Bailly *et al.*, 2006; Bouchard *et al.*, 2006; Lin and Wang, 2005), in addition to increased localized free IAA accumulation in mature *twd1* (and *pgp1 pgp19)* roots (Bouchard *et al.*, 2006).

Together with results from heterologous coexpression of PGP1 and TWD1, these findings indicate that TWD1 regulates PGP-driven auxin transport *in planta* (Bailly *et al.*, 2006; Bandyopadhyay *et al.*, 2007; Blakeslee *et al.*, 2007; Bouchard *et al.*, 2006; Geisler *et al.*, 2005; Geisler and Murphy, 2006). FKBP activation of transporters by means of direct protein–protein interaction has been suggested for murine MDR3 (Hemenway and Heitman, 1996) and resembles that of mammalian FKBP12 regulating RyR- and Ins(1,4,5)*P*3-R-like calcium channels (Harrar *et al.*, 2001; He *et al.*, 2004; Romano *et al.*, 2005).

FKBPs link signal transduction and hormonal pathways

Plant growth and development is controlled by a complicated web of interacting signal cascades (Friedrichsen and Chory, 2001; Nemhauser *et al.*, 2004; Vieten *et al.*, 2007; Yang and Poovaiah, 2003). Multidomain FKBPs from both mammalian and plant cells appear to act as multifunctional platforms for multiple protein–protein interactions (Harrar *et al.*, 2001; He *et al.*, 2004); similarly, it appears that FKBPs bring different client proteins together to link related signal and hormonal transduction pathways (Lin and Wang, 2005; Perez-Perez *et al.*, 2004; Schapire *et al.*, 2006; Scheidt *et al.*, 2006).

A comparison of interacting networks from mammals and plants (Figure 3) shows that most functional domains of the proteins are involved in the process. As would be expected, many FKBP-dependent interactions, such as those involving transcription factors, HSP90, microtubules and calcium/calmodulin, are conserved between mammals and plants, whereas some (such as PAHX and auxin (Chambraud *et al.*, 1999; Geisler and Murphy, 2006)) are apparently specific to mammals and plants, respectively, and others remain as yet functionally unidentified.

FKBP binding of both HSP90 and CaM is conserved between mammals and plants (Barik, 2006; Carol *et al.*, 2001; Fanghanel and Fischer, 2004; Geisler *et al.*, 2004; Harrar *et al.*, 2001; He *et al.*, 2004; Kamphausen *et al.*, 2002; Romano *et al.*, 2005), but the physiological relevance of those binding activities is still poorly understood (Sangster and Queitsch, 2005; Yang and Poovaiah, 2003). The HSP90 chaperone complex functions as a regulator of development and phenotypic plasticity (Kotak *et al.*, 2007; Queitsch *et al.*, 2002; Sangster and Queitsch, 2005). Treatment of plants with geldanamycin (a target of cancer therapy research) effectively inhibits HSP90 function and results in dwarfism (Queitsch *et al.*, 2002; Sangster and Queitsch, 2005), suggesting that FKBP action might be caused, at least partially, by a disruption of HSP90 action. Interestingly, all five amino acids that are involved in HSP90 binding are ubiquitously conserved in all plant multidomain FKBPs (Aviezer-Hagai *et al.*, 2007), suggesting that HSP90 mediates the binding of FKBPs to other proteins in a manner analogous to FKBP–glucocorticoid receptor binding (Davies and Sanchez, 2005) or ROF dimerization (Kurek *et al.*, 2002a).

Several lines of evidence point to a crucial involvement of CaM in FKBP functionality, because CaM has been shown to bind to most multidomain FKBPs: for example, the human Bcl-2 regulator FKBP38 has been shown to be activated by calcium/CaM (Edlich *et al.*, 2005). Moreover, expression of wheat FKBP73 lacking CaM-BD abolishes calmodulin binding, dimerization and male fertility in transgenic rice (Dwivedi *et al.*, 2003). Interestingly, both HSP90 and CaM action in plants are tightly connected to phytohormone function (Dhaubhadel *et al.*, 1999; Du and Poovaiah, 2005). CaM is crucial for brassinosteroid (BR) biosynthesis and plant growth (Du and Poovaiah, 2005), and BRs have been shown to protect against thermal stress by inducing HSP expression (Dhaubhadel *et al.*, 1999). Interestingly, an increasing number of TPR proteins have been reported to be essential for different plant hormone responses, suggesting that TPR domains reflect a well conserved tool of hormone action (Schapire *et al.*, 2006).

Plant hormone crosstalk, particularly well documented for auxin–BR (Friedrichsen and Chory, 2001; Li *et al.*, 2005; Mouchel *et al.*, 2006; Nemhauser *et al.*, 2004) and auxin–cytokinin (Nordstrom *et al.*, 2004; Swarup *et al.*, 2002) interdependency, occurs at both the transcriptional and post-transcriptional level. In *pasticcino* mutants, downregulation of primary auxin-

responsive genes points to an alteration in the auxin response, whereas upregulation of primary cytokinin-responsive genes argues for auxin–cytokinin crosstalk (Harrar *et al.*, 2003). Furthermore, in auxin induced dividing cells in *Arabidopsis* roots, PAS1 and FAN are translocated into the nucleus (Smyczynski *et al.*, 2006), linking cytokinin function with auxin signaling. Some *twd1* phenotypes might also involve hormone crosstalk. In *twd1* treated with exogenously applied BR, downregulation of BR biosynthesis genes is abolished and root-growth inhibition reduced (Perez-Perez *et al.*, 2004). Compact dark-green rosettes that are rolled downward resemble those found in *ultracurvata1*, an allele of *brassinosteroid insensitive2* (Ishida *et al.*, 2007; Perez-Perez *et al.*, 2004), suggesting that, in addition to auxin, BR signaling might also be affected in *twd1*.

Lessons from 3D-structure analysis

Recently, the crystal structures of FKBDs of *Arabidopsis* FKBP13 (Gopalan *et al.*, 2004; Gopalan *et al.*, 2006) and TWD1 (Granzin *et al.*, 2006; Weiergraber *et al.*, 2006) have been resolved, enabling the comparison of their structures with those of human FKBP12 and FKBP38 (Maestre-Martinez *et al.*, 2006). The structures all include a highly conserved five-stranded antiparallel β-sheet wrapped around a short α-helix (Figure 1b). FKBP12, FKBP38 and TWD1 are structurally closer to each other, whereas chloroplast FKBP13 reveals sequence extensions that correspond partially with two pairs of disulfide bonds ($Cys_{5\text{-}17}$ and $Cys_{106\text{-}111}$) that are reduced by the redox-controlled thioredoxin system (see above).
Elegant comparison of FKBP13 structures crystallized under reducing and oxidizing conditions revealed a small but significant structural change that limits the accessibility of the catalytic residues responsible for PPIase activity. As a result, FKBP13 is inactive under reducing conditions (Gopalan *et al.*, 2006).

The modeling of FK506 docking indicates that both single-domain FKBPs would bind FK506, whereas, consistent with experimental data, FKBP38[2] and TWD1 sterically exclude the immunosuppressant drug (Figure 1c) (Edlich *et al.*, 2005; Geisler *et al.*, 2003; Kamphausen *et al.*, 2002; Shirane and Nakayama, 2003). Even more informative is that FK506 binding correlates with the presence of PPIase activity, which, to date, has only been detected for both crystallized single-domain FKBPs (Gupta *et al.*, 2002; Kamphausen *et al.*, 2002). Therefore, the current picture that emerges is that stress-related FKBPs have apparently conserved PPIase activity to fulfill their proposed chaperone function, whereas others (such as human FKBP38, TWD1 or PAS1) have lost or only retain low PPIase activity (Carol *et al.*, 2001; Edlich *et al.*, 2005; Geisler *et al.*, 2003; Kamphausen *et al.*, 2002; Shirane and Nakayama, 2003).

The X-ray structure at 2.85 Å of the cytoplasmic portion of TWD1 (amino acids 35–292) comprising both the FKBD and the TPR domain has recently been resolved (Granzin *et al.*, 2006); together with human and squirrel monkey FKBP51 (Granzin *et al.*, 2006; Sinars *et al.*, 2003; Weiergraber *et al.*, 2006), this structure represents the only complete structure of a multidomain FKBP. Although the overall architecture of the individual TWD1 FKBD and TPR domains closely resembles other FKBPs, their relative arrangement is both unique and flexible (Granzin *et al.*, 2006; Weiergraber *et al.*, 2006). *In silico*-modeling of the docking with key interacting partners, HSP90 and two classes of ABC transporters has facilitated the prediction of docking sites at the molecular level[3]. Although the docking domains of TWD1 that interact with the nucleotide-binding fold of PGP- and MRP-like ABC transporters are different (FKBD and TPR, respectively (Geisler *et al.*, 2004; Geisler *et al.*, 2003)), both transporters use overlapping surface areas on the transporters, suggesting a new paradigm for the regulation of ABC transporter activity. Co-crystallization of FKBPs with interacting partners will be the method of choice to understand FKBP protein–protein interactions at the molecular level.

Why are some FKBPs membrane-anchored?

TWD1, containing a hydrophobic stretch in the C-terminus (aa 339–357), was the first FKBP thought to be membrane-anchored (Geisler *et al.*, 2003; Kamphausen *et al.*, 2002). Membrane location was verified by electron microscopy and a range of biochemical methods (Geisler *et al.*, 2004; Geisler

2 FK506 binding to FKBP38 has been shown only in the presence of CaM (Edlich *et al.*, 2005).

3 ‡ For *in silico* docking, plant ABC transporter backbones have been modeled on *MsbA* structures from *Salmonella typhimurium* that, owing to software errors, had to be retracted (Miller, 2006). However, as the interacting nucleotide binding folds have been modeled on those from *Escherichia coli* haemolysin B (Granzin *et al.*, 2006), the outcome of the dockings is still relevant.

et al., 2003; Kamphausen *et al.*, 2002), although the exact mode of membrane anchoring remains unclear. A mitochondrial membrane location has been demonstrated for the related human FKBP38, and anchoring also predicted for mouse FKBP38 and *Drosophila* FKBP45 (Geisler *et al.*, 2003; Maestre-Martinez *et al.*, 2006; Shirane and Nakayama, 2003).

Solid-state NMR data on the putative TWD1 membrane-anchor peptide favors a perpendicular orientation of the C-terminus to the membrane (Scheidt *et al.*, 2006), forming a so-called amphipathic in-plane membrane anchor (IPM) (Sapay *et al.*, 2006), instead of the membrane anchoring generally associated with type II membrane proteins. Computer predictions using the AmphipaSeeK algorithm (http://www.npsa-pbil.ibcp.fr) suggest that the C-terminal extension found in PAS1 also contains a putative membrane anchor or an IPM.

Regardless of the mode of membrane anchoring used by multidomain FKBPs, the fundamental question is why the need for membrane anchoring at all? It has been suggested that FKBP38 acts as a mitochondrial docking molecule that concentrates the antiapoptotic membrane protein Bcl-2 at the mitochondria (instead of the ER), thus preventing apoptosis (Germain and Shore, 2003; Shirane and Nakayama, 2003).
A similar mechanism might be involved in TWD1 regulation of ABC transporters both on the tonoplast and plasma membrane: membrane anchoring might increase the probability of contacts by reducing the spatiality of TWD1 diffusion. Furthermore, restraining the mobility of TWD1 by membrane anchoring might serve as a means to decouple the regulation of transporters located on different membranes (Scheidt *et al.*, 2006). An intriguing possibility, therefore, might be that TWD1 contributes to a polar distribution of auxin by vectorial activation of PGP-mediated auxin export, as has been suggested for PGP–PIN-shaped protein auxin export complexes (Bandyopadhyay *et al.*, 2007; Blakeslee *et al.*, 2007; Petrasek *et al.*, 2006).

In summary, it appears that membrane anchoring of FKBPs is more common than was previously thought and reflects a need for the cell to regulate differentially FKBP-connected signal transduction pathways by bundling the essential components to membrane structures.

Conclusion and outlook

Recent interaction and structural analyses have revealed novel interacting partners, mechanisms and roles for plant FKBPs that are distinct from the classical chaperone or foldase function. Although it is now accepted that chaperone functions are likely to be independent of PPIase activity (Barik, 2006), many plant and related mammalian FKBPs appear to have lost or retained low PPIase activity (Carol *et al.*, 2001; Faure *et al.*, 1998b; He *et al.*, 2004; Kamphausen *et al.*, 2002; Romano *et al.*, 2005). Interestingly, PPIase activity coincides with the conservation of five amino acids, which define an active site that seems to predict PPIase activity (DeCenzo *et al.*, 1996). Some plant FKBPs (ROF1 and its homologs) have a chaperone function in stress responses that is dependent on PPIase activity, analogous to the chaperone function of mammalian FKBPs.

By contrast, the functions of a subset of FKBPs, characterized by PAS1 and TWD1, have been elucidated and have been shown to be novel and specific to plants (control of hormone action and transport). These functions are independent of PPIase activity (Bailly *et al.*, 2006; Bouchard *et al.*, 2006; Geisler *et al.*, 2003; Smyczynski *et al.*, 2006). Although PAS1 and TWD1 have different targets, they share interactions (HSP90 and CaM) and are connected by overlapping hormone crosstalk (Figures 2,4). PAS1- and TWD1-mediated pathways might also directly intersect, because PAS1 can bind to the C-terminus of MRP1 (Geisler *et al.*, 2004).

Because it has become increasingly apparent that FKBP action and interaction partnerships are tissue specific (Germain and Shore, 2003), future emphasis should be placed on assessing the precise localization of these interactions using state-of-the-art imaging techniques. This is particularly true in light of the flexible changes of locations and the unexpected locations of some representatives of this family (Germain and Shore, 2003; Shirane and Nakayama, 2003). Interestingly, TWD1 (and partly also PAS1) has many structural (domain structure and membrane anchoring) and biochemical features (e.g. lack of PPIase activity, exclusion of FK506, calmodulin binding, etc.) in common with the mitochondrial inhibitor of apoptosis, human FKBP38. The three proteins also share a common mode of action in recruiting or regulating

their client proteins via protein–protein interaction (*tête-à-tête*). Interaction screens that are also suitable for membrane proteins (such as split-ubiquitin-based systems) as well as proteomic interaction studies ('interactomics' (Popescu *et al.*, 2007; Schoonheim *et al.*, 2007)) applied in concert with reverse genetics of interacting partners are appropriate techniques for the elucidation of FKBP-related signal transduction networks.

Transfer of this knowledge should have an impact on applied sciences, because FKBPs are key regulators of plant development. Therefore, FKBP complexes might represent good targets for tissue-dependent manipulation of growth in foresting and fruiting. Dwarf-like plants [such as those found for *Arabidopsis twd1* (Geisler *et al.*, 2003) and maize and sorghum mutants defective in *PGP1* homologs: *brachytic2 (br2)* and *dwarf3* (*dw3*), respectively (Multani *et al.*, 2003)] are more resistant to natural flattening and show an enhanced fertilizer usage and productivity. Application of specific inhibitors affecting FKBP activity might prove a useful tool to influence hormone transport or action and thereby plant growth.

Acknowledgements

We apologize to colleagues whose results could not be included owing to space restrictions. We thank V. Sovero and S. Peters for critical reading of the article, to J.D. Faure for providing notes on the article and unpublished information, and E. Martinoia for continuous support. Special thanks to the three anonymous reviewers for their valuable comments that are highly appreciated. Work in our laboratory is supported by the Swiss National Fonds and the Novartis foundation (funds to M.G.).

Discussion

Recently, tremendous efforts have been carried out to dissect the molecular mechanisms of polar auxin transport. AUX and PIN proteins have been identified as essential components but seem to require partner proteins to fulfill their function. With this work, we demonstrate the fundamental role for ABCB/MDR/PGP proteins in catalysing active auxin efflux. This primary-energized transport is coupled to PIN auxin-efflux machineries at least in tissues demanding accurate auxin fluxes. This cooperation corresponds well to the long sought for multi-component auxin efflux complex. This complex was previously postulated to comprise a membrane-attached regulatory subunit. Interestingly, the immunophilin-like TWISTED DWARF1 (TWD1) positively regulates ABCB1/PGP1-mediated auxin efflux by means of protein-protein interactions and seems to be the critical hinge for auxin transport inhibitor action. The interaction between TWD1 and ABCB1 may confer substrate-specificity to the transporter, as previously observed for PIN-ABCB interactions, although a tripartite complex is not yet experimentally verified. Understanding of ABCB control and substrate-specificity is the basis step to develop new strategies to improve human health, at both agronomical and medical levels.

What makes the difference between a brilliant hypothesis and a concept? The dazzling history of auxin biology might partially answer this tricky question. Indeed, for over a century, pioneer scientists such as von Sachs (1865), Darwin (1880), Went (1926) and Cholodny (1927) have developed, based on simple but elegant experiments, working ideas that are still in use nowadays. From early observations emerged a simple concept: *an actively transported chemical messenger directs the whole plant life*. However, the fathers of auxin biology were far to imagine how difficult the task would be to validate this concept. Over decades, thousands of experiments and thousands of scientists have dissected step by step the mechanisms of auxin physiology, only to discover the amazing complexity hidden behind this simple abstract idea. In the past ten years, tremendous efforts have been conducted to elucidate the cellular and molecular machinery involved in IAA signaling (Badescu and Napier, 2006; Blakeslee *et al.*, 2005; Geisler and Murphy, 2006; Kerr and Bennett, 2007; Leyser, 2006; Parry and Estelle, 2006; Quint and Gray, 2006; Scheres and Xu, 2006).

Beyond auxin metabolism and homeostasis, it is now well accepted that auxin flows within the plant body virtually control all physiological events. These directed auxin movements create essential hormonal gradients that determine developmental processes that are as apparently diverse as axis formation, organogenesis, tropical responses, apical dominance, fruit development and vascular tissues differentiation (Reviewed in Davies, 2004). The precise understanding of the maintenance and the regulation of these auxin gradients is therefore a key step to comprehend IAA-mediated plant development.

The Chemiosmotic Model

Auxin has been chemically characterized in the beginning of the 20th century and as a result various chemicals developed to mimic or block IAA action became valuable tools to investigate components of the hormone transport and perception pathway. Both mechanisms are so interdependent that they were early proposed to be tightly linked or identical (Hertel *et al.*, 1969). Recently, the major receptor for auxin has been identified as being the F-box protein TIR1 (Dharmasiri *et al.*, 2005; Kepinski and Leyser, 2005) and the overall transduction of the IAA signal has been described in details (Kepinski, 2007; Tan *et al.*, 2007). However, its discovery did not completely solve the processes underneath the broad range of IAA cellular actions. On the contrary, it underlined that beyond hormone signal transduction, auxin local distribution patterns are the key events for plant development and physiology (Vieten *et al.*, 2007). Hence, the proteins driving auxin gradients into cells and tissues are, as presumed by the early concept, the major components of the hormone effects.

The observation that known polar auxin transport inhibitors such as 2,3,5-triiodobenzoic acid (TIBA) increase IAA accumulation in maize coleoptile cells, implied that TIBA blocked IAA efflux, rather than influx (Hertel and Leopold, 1963). This assumption early suggested that auxin fluxes require IAA-specific carrier-mediated cell-to-cell transport and led to the hypothesis of the *chemiosmotic model* for PAT (Raven, 1975; Rubery and Sheldrake, 1974). In short, the acidic apoplastic medium displaces the equilibrium of the weak acid IAA in favour of the readily plasma membrane-diffusible protonated IAAH. Once inside the cytoplasm, the overall neutral pH turns auxin into its anionic form IAA^-. Due to its charge, the latter cannot leave the cell by simple diffusion. As a result, IAA^- accumulates inside the cell and the continuity of the observed auxin flows presumes therefore the existence of specific efflux carriers. The polar auxin transport would require an asymmetric distribution of these proteins. Although auxin can enter cells by passive diffusion, the experimental rates of IAA influx involve as well the presence of dedicated auxin influx carriers (Goldsmith, 1977; Goldsmith *et al.*, 1981).

The chemiosmotic model recently found its candidate proteins as auxin influx and efflux carriers have been predicted. AUX1/LAX(LIKE AUX1) and PIN protein families display asymmetrical plasma membrane localizations congruent with PAT and their corresponding mutants present auxin-defective phenotypes (Bennett *et al.*, 1996; Friml *et al.*, 2002a; Friml *et al.*, 2002b; Galweiler *et al.*, 1998; Luschnig *et al.*, 1998; Muller *et al.*, 1998; Swarup *et al.*, 2001).

AUX1/LAX proteins participate in auxin influx

Cellular auxin uptake is a specific and saturable process that implies the presence of IAA importers at the plasma membrane (Davies and Rubery, 1978; Rubery and Sheldrake, 1974). Specific influx

inhibitors such as 1-NOA (1-naph-thoxyacetic acid) interfere with root growth, gravitropism (Parry *et al.*, 2001) and organ positioning (Stieger *et al.*, 2002), thus underlining the importance of an active auxin uptake beside its sole diffusion across the plasma membrane. The *aux1* mutant has been isolated in a screen for 2,4-D (2,4-dichlorophenoxy acetic acid) resistance (Maher and Martindale, 1980) and its auxin-resistant and agravitropic root growth phenotype suggested an impaired auxin transport. *aux1* root agravitropic response can be rescued much more efficiently by the membrane-permeable auxin NAA than by the less permeable IAA or 2,4-D (Marchant *et al.*, 1999), suggesting that AUX1 is rather involved in auxin uptake than auxin signalling. Additionally, 1-NOA treatments on wild type seedlings mimic the *aux1* phenotype (Parry *et al.*, 2001).

Furthermore, root basipetal auxin transport is defective in *aux1* mutants (Marchant *et al.*, 1999; Yamamoto and Yamamoto, 1998) and auxin uptake assays performed in *aux1* roots revealed less 2,4-D accumulation than in wild type; such a reduced accumulation does not occur with the membrane-permeable 1-NAA (Marchant *et al.*, 1999). Moreover, AUX1 (together with three other LAX homologs; Swarup *et al.*, 2000) displays striking homology with amino acid permeases, data in favour of AUX1 involvement in the tryptophan-like IAA influx (Bennett *et al.*, 1996; Swarup *et al.*, 2004). Recently, heterologous expression in *Xenopus* oocytes clearly demonstrated the role of AUX1 in specific IAA accumulation within cells (Yang *et al.*, 2006). Of most interest, this uptake has been demonstrated to be sensitive to 1-NOA, but not to the auxin-efflux inhibitors (AEIs) NPA and TIBA. Finally, although AUX1 expression is uniformly distributed around the cell plasma membrane in a subset of root tissues, the protein is found to be polarized in the root protophloem. Interestingly, this basal polarity is opposite to the apical auxin-efflux carrier polarity in the same cells (Swarup *et al.*, 2001; Swarup *et al.*, 2004). Altogether, these data match the chemiosmotic model assumptions and describe AUX1 as a specific auxin influx facilitator. However, as revealed by the weak *aux1* phenotypes, active auxin uptake may not be a rate-limiting factor for PAT. Moreover, the inconsistency between the restricted local AUX1 root expression and its suggested role in the long-distance auxin transport suggest a role for AUX1 in unloading auxin from the phloem to the root meristems' PAT system *via* the protophloem (Swarup *et al.*, 2001). Hence, as presupposed by the model, specific auxin exporters are the most critical components of the polar auxin transport machinery.

PIN proteins participate in auxin efflux

During the course of the present work, the central involvement of PIN proteins in PAT and their particular role in the hormone efflux has been described in further detail. The *Arabidopsis pin-formed1* (*pin1*) mutant displays a drastic needle-shaped phenotype that can be mimicked by AEIs applications on wild type seedlings (Okada *et al.*, 1991). In addition, basipetal auxin transport in *pin1* stem segments was significantly reduced, suggesting the function of PIN1 in auxin efflux (Okada *et al.*, 1991). A decade ago, *PIN1* was identified as a plant-specific transmembrane protein with a predicted topology similar to transport facilitators from other kingdoms (Chen *et al.*, 1998; Galweiler *et al.*, 1998; Luschnig *et al.*, 1998; Muller *et al.*, 1998; Utsuno *et al.*, 1998). Several homologous proteins were subsequently identified and characterized: *PIN2/EIR1/AGR1* is required for root gravitropic response (Chen *et al.*, 1998; Luschnig *et al.*, 1998; Muller *et al.*, 1998; Utsuno *et al.*, 1998); *PIN3, PIN4* and *PIN7* have been shown to be respectively important in tropisms, root meristem patterning and early embryogenesis (Friml, 2003; Friml *et al.*, 2002a; Friml *et al.*, 2003; Friml *et al.*, 2002b). Additionally, in some *pin* mutants, the loss of PIN function directly correlates with reduced PAT in the corresponding expression tissues (Okada *et al.*, 1991; Rashotte *et al.*, 2000). Moreover, the analysis of reporter-genes fused to auxin-responsive elements and direct auxin measurements revealed altered IAA distribution patterns in several *pin* backgrounds (Benkova *et al.*, 2003; Friml *et al.*, 2002a; Friml *et al.*, 2003; Luschnig *et al.*, 1998; Ottenschlager *et al.*, 2003). To date, a total of eight PIN genes have been isolated in the *Arabidopsis* genome. Although the physiological characterisation of *PIN5, PIN6* and PIN8 has not been reported before the beginning of this work, the fact that *PIN* orthologs are found in other monocot and dicot plant species implies a conserved function for PIN proteins, probably in auxin-related mechanisms if not PAT (Paponov *et al.*, 2005).

The early chemiosmotic hypothesis proposed a polar localization for the efflux carrier components

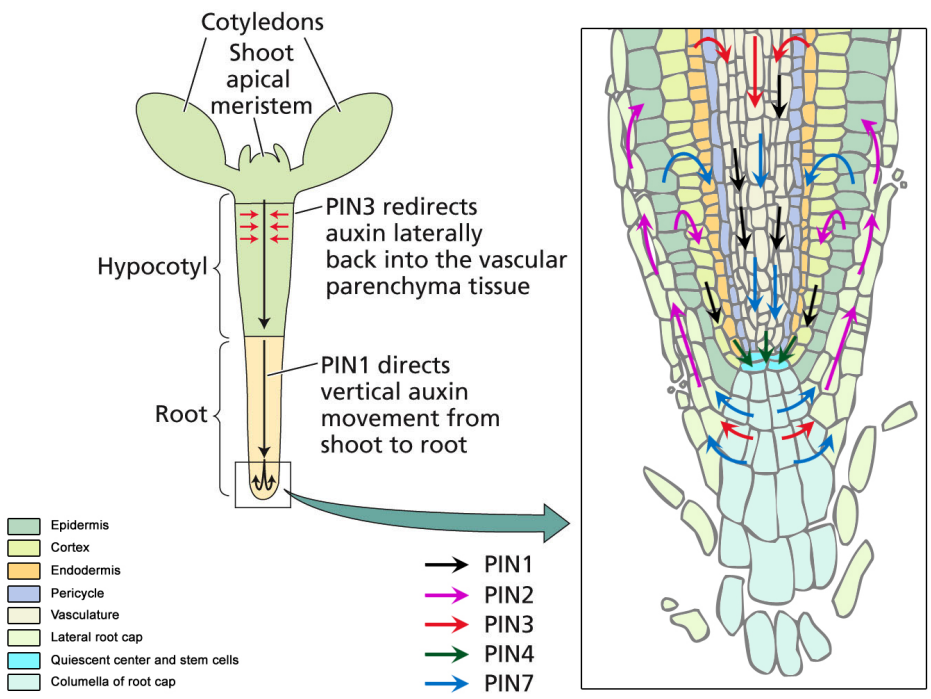

FIGURE 1. **PIN proteins participate in tissue-specific auxin efflux**

Directional auxin fluxes associated with the tissue-specific distribution of PIN IAA efflux facilitator proteins. PIN1 mediates the shoot-to-root transport of auxin. PIN2 further drives auxin into the root-elongation zone. PIN3 might participate in the lateral redirection of IAA into PAT-associated vascular tissues. PIN4 mediates sink-driven auxin flows in the root tip. Inset shows a model for PIN-mediated auxin movement in root apex tissues, supposed to drive auxin accumulation patterns (see text). Arrows indicate the putative PIN-mediated auxin fluxes, bases on protein localizations. (adapted from Taiz and Zeiger, 2006)

(Raven, 1975; Rubery and Sheldrake, 1974). Immunolocalization studies revealed that PIN1 progressively gains polar localization during embryogenesis and organogenesis (Benkova *et al.*, 2003; Friml *et al.*, 2003; Heisler *et al.*, 2005; Reinhardt *et al.*, 2003) and is polarly expressed, in the direction of the root apex, in mature vascular tissues such as shoot xylem parenchyma, and root stele (Friml *et al.*, 2002a; Friml *et al.*, 2003; Galweiler *et al.*, 1998; Scarpella *et al.*, 2006). In contrast to PIN1, PIN2 is only post-embryonically expressed and displays a tissue-dependent differential polarization (Muller *et al.*, 1998). PIN3 expression is mainly found laterally in root pericycle and shoot endodermis cells. Interestingly, PIN3 is also expressed in a symmetrical manner in columella cells of the root apex (Friml *et al.*, 2002b). PIN4 is expressed in the central root meristem, with a polar localization directed towards the quiescent center. PIN4 is also expressed in the quiescent center itself, though without defined polarity (Friml *et al.*, 2002a). Finally, PIN7 was found to be polarly expressed in both basal and apical directions in embryo stages, while it displays a similar localization as PIN3 in root meristematic cells and vasculature (Blilou *et al.*, 2005).

In all cases, plasma membrane-localized PIN proteins display asymmetric localization, in particular cell types, consistently with known directions of auxin fluxes and auxin gradients (Blilou *et al.*, 2005; Friml, 2003; Friml and Palme, 2002; Vieten *et al.*, 2007). The functional role of these polar localizations is illustrated by the dynamic *PIN1* expression in shoot apical meristems, where the apical distribution of the protein is connected to secondary shoot primordia development (Benkova *et al.*, 2003; Heisler *et al.*, 2005; Reinhardt *et al.*, 2003). Another example of the importance of PIN polarity in plant physiology is the mechanistic model proposed for auxin flows in the root tip (Blilou *et al.*, 2005; Vieten *et al.*, 2007). Indeed, all PIN localizations studied so far in this region of the plant seem to fit perfectly in the *auxin fountain* (Figure 1).

Although PIN expression patterns are significant for the overall auxin transport, the direct involvement of PIN proteins in cellular efflux has not yet been fully demonstrated. Few studies reported direct biochemical evidences for PIN influence on IAA export. *pin2* mutant root tips retained slightly more radioactivity than wild type roots when preloaded with radiolabelled IAA (Chen *et al.*, 1998). Therefore, several inducible PIN constructs have been expressed in tobacco or *Arabidopsis* cell lines and indirect measurements of different radiolabelled auxins accumulation revealed enhanced auxins efflux. In addition, the level of efflux stimulation in these assays correlated with the amount of expressed PIN protein, thus proposing PINs as rate limiting factors in auxin efflux (Petrasek *et al.*, 2006). However, PIN5 is genetically distant from other PIN family members and

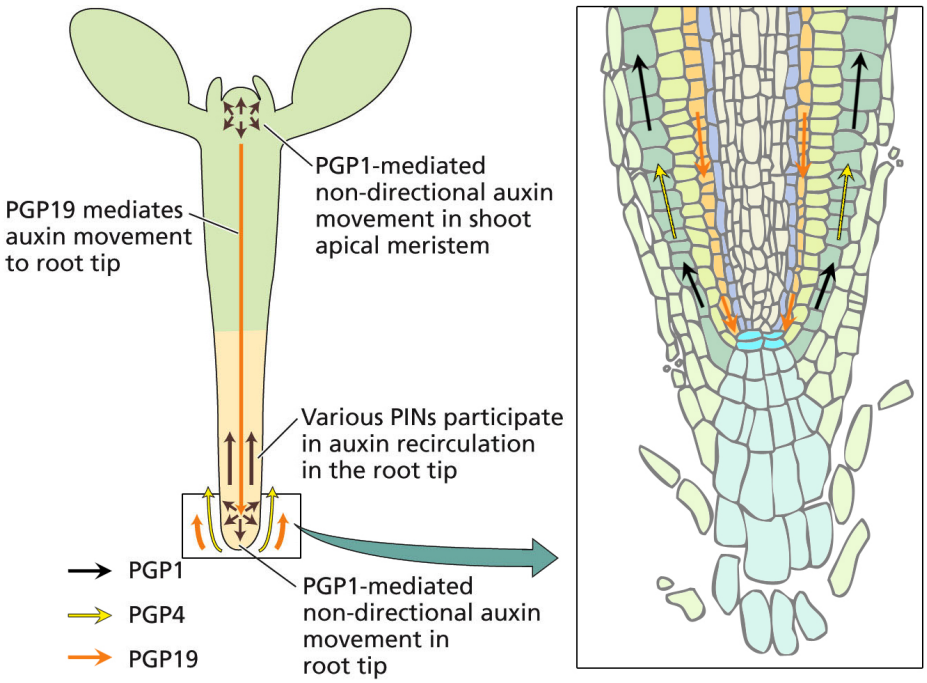

FIGURE 2. **ABCB proteins participate in tissue-specific auxin efflux**

Tissue distribution of the primary-active ABCB-mediated auxin movements. Arrows indicate the direction of transport. Multi-directional arrows indicate ABCB-driven non-directional auxin fluxes. ABCB-mediated directional IAA transport might occur in tissues where ABCBs interact with polarized PIN proteins. Inset shows a model for ABCB-mediated auxin transport in root apex tissues. (adapted from Taiz and Zeiger, 2006)

has been localized at the endoplasmic reticulum (ER) membrane. Additionally, its polypeptidic sequence exhibits structural discrepancies with the canonical PIN topology (Mravec *et al.*, 2008; Zazimalova *et al.*, 2007). Therefore, its involvement in auxin transport has long been uncertain. According to its ER-lumen orientation and functional IAA transport assays, we propose in this manuscript a role for PIN5 in cellular auxin homeostasis (Appendix 3; Mravec *et al.*, 2008). Nevertheless, none of these investigations could clarify whether PINs function as direct auxin transporters or as positive regulators of auxin transport.

Yeast cells overexpressing PIN2 retained less radiolabelled IAA than control cells (Chen *et al.*, 1998) and were shown resistant to the cytotoxic auxin analog 5-FI (5-fluoroindole; Luschnig et al., 1998). Moreover, PIN2 and PIN7 heterologous expression in yeast and mammalian HeLa cells conferred stimulated auxin efflux (Petrasek *et al.*, 2006). All in all, expression and function of PIN proteins in non-plant hosts, free of auxin-related plant-specific components, seem to indicate that PINs may mediate active auxin efflux (Petrasek *et al.*, 2006). Nonetheless, the loss of PIN specificity in these experiments would rather imply that PIN proteins act as components of a larger and more specific auxin efflux carrier complex (Chen *et al.*, 1998; Petrasek *et al.*, 2006).

ABCB proteins are primary-active auxin transporters

Our group and others recently postulated that a third group of proteins is implicated in PAT. Members of the ABCB subfamily of ATP-binding cassette (ABC) transporter superfamily (Martinoia *et al.*, 2002) were shown to actively participate in phytohormone transport (Geisler *et al.*, 2005; Geisler *et al.*, 2003; Multani *et al.*, 2003; Noh *et al.*, 2001). Loss-of-function mutants of *Arabidopsis ABCB19/PGP19/MDR1* and closest homolog *ABCB1* display auxin-defective phenotypes, although not as drastic as the *pin1* mutant (Galweiler *et al.*, 1998; Noh *et al.*, 2001). As a starting point, our laboratory deeper analysed these growth-phenotypes which revealed extreme developmental defects in the *abcb1 abcb19* double mutant, suggesting functional redundancy (Geisler *et al.*, 2003; Noh *et al.*, 2001). Single mutant *abcb1* plants exhibit a more subtle auxin-related phenotype when compared to *abcb19* or double mutants, while no apparent differences with wild type plants is seen in the adult stage under long-day culture conditions. However, a more pronounced dwarfing phenotype is revealed under short-day conditions, congruent with observed reductions in radiolabelled IAA long distance transport (Geisler *et al.*, 2003). In addition, *abcb1 abcb19* mutants exhibit epinastic cotyledons, abnormally wrinkled leaves, reduced apical dominance and partial dwarfism. This indicates altered auxin transport and/or auxin response

(Geisler *et al.*, 2003; Noh *et al.*, 2001). Given the fact that ABCB transporters are known plasma membrane transporters in numerous organisms, plant ABCBs therefore appeared as evident candidates for active auxin transport. Although both ABCB1 and ABCB19 were promising genes for further investigation, the present work focused on a detailed ABCB1 analysis.

The initial step of our study was to verify whether ABCB1 and ABCB19 function is consistent with the observed auxin fluxes *in planta*. Free IAA levels in root tips were measured to be reduced in *abcb1* and *abcb19* mutants and this reduction has been confirmed by a decreased auxin-responsive DR5-GUS signal in single and double mutants root tips (Geisler *et al.*, 2005; Lin and Wang, 2005). These results correlated well with the reduced basipetal radiolabelled auxin transport measured in the mutants' apical root tissues (Geisler *et al.*, 2005), thus implying plant ABCBs as part of the IAA transport machinery. Next, we analysed ABCB1 expression patterns. In contrast to PIN proteins, ABCB1 does not display polar localization in apical meristematic tissues, but surprisingly, an asymmetric distribution of the protein was found in upper mature root tissues, above the distal elongation zone. ABCB1 localisation is predominantly basal in endodermal and cortical cells, although apical distribution has been detected in cortical cells next to the root stele (Geisler *et al.*, 2005). These observations imply a differential role for ABCB1, depending on its cellular environment. We suggest non-directional auxin transport in meristematic cells and auxin reflux during PAT in the mature root tissues. Interestingly, this disparity could imply partner proteins to drive ABCB1 function.

As the lack of direct evidence for IAA transport by PIN proteins has been heavily discussed over years, the second step of our demonstration would require IAA-specific export properties for ABCB1. To assess this issue, we analysed ABCB1-mediated cellular auxin efflux in *Arabidopsis* protoplasts revealing that the protein is an apparent IAA transporter (Geisler *et al.*, 2005). In addition to that, the recent inducible ABCB19 expression in tobacco BY-2 cells resulted in a decreased cellular accumulation of radiolabelled NAA (Petrasek *et al.*, 2006). Moreover, some structure-related synthetic auxins were exported in wild type and *abcb19* protoplasts while the weak acid benzoic acid was not, reflecting a narrow ABCB1 specificity towards auxinic compounds (Geisler *et al.*, 2005). To further investigate the direct function of ABCB1 in auxin efflux, heterologous expression of the transporter in *Saccharomyces* cells and mammalian HeLa cells resulted in an increased cellular efflux of 5-fluoro indole and IAA from cells, although this transport properties were more specific in mammalian cells than in the lower eukaryote yeast (Geisler *et al.*, 2005). ABCB1 did not export the typical hydrophobic mammalian MDR1/HsABCB1 substrates when expressed in mammalian lines (Geisler *et al.*, 2005), further evidence for its substrate specificity. Finally, the similarity between auxin efflux rates from *abcb1 abcb19* mutants and ATP-depleted wild-type protoplasts, together with the fact that specific ABC transporters inhibitors, verapamil and cyclosporinA, blocked ABCB1-mediated IAA efflux from yeast and HeLa cells (Geisler *et al.*, 2005), allowed us to postulate that ABCB1/19 catalyses primary-active auxin extrusion.

Auxin efflux inhibitors such as NPA were early tools in attempts to identify the proteins responsible for the hormone transport. From these studies, membrane protein extracts were shown to specifically bind NPA (Morris, 2000; Rubery, 1990), postulating the existence of a specific NPA-binding protein (NBP). The latter was proposed to be part of a multi-component auxin efflux complex (Morris *et al.*, 1991), but the exact nature of NBP remains to be defined.
Interestingly, ABCB1 and ABCB9, like other p-glycoproteins (ABCB2, 4 and 10) were found to bind NPA *in vitro* (Geisler *et al.*, 2003; Murphy *et al.*, 2002; Noh *et al.*, 2001; Terasaka *et al.*, 2005). The same ABCB NPA-binding activity was shown when expressed in yeast cells (Muday and Murphy, 2002; Noh *et al.*, 2001). Beside this, NPA inhibits ABCB1 auxin extrusion from ^{3}H-IAA loaded protoplasts and yeast cells (Geisler *et al.*, 2005). This strongly suggests that ABCB1 could be one of the long sought and so far molecularly uncharacterized NPA-binding proteins. Moreover, a component of the NBP IAA efflux complex was demonstrated to be phosphorylated (Delbarre *et al.*, 1998). ABCB/p-glycoproteins are known phosphorylation targets and thus could represent this uncharacterized NBP component (Lelong-Rebel and Cardarelli, 2005). This also provides supplementary relationships between ABCBs and auxin transport, since NBPs are known physiological targets of auxin efflux inhibitors.

But NBPs were suggested to be protein-complexes comprising at least an integral membrane protein and a peripheral plasma membrane protein associated with the cytoskeleton (Bernasconi *et al.*, 1996; Cox and Muday, 1994; Muday and Murphy, 2002). Therefore, the functional ABCB NPA-binding properties might involve other proteins participating in the specific transport of auxins.

The strong non-directional ABCB1 expression in meristems correlates with the ABCB1 capacity to transport IAA-breakdown products in these highly metabolic tissues (Geisler *et al.*, 2005). This is of importance since PIN proteins are abundant in these tissues, suggesting that ABCB- and PIN-mediated auxin effluxes could correlate in specific cells. Strikingly, early publications reported that NBPs localized polarly in cells (Jacobs and Gilbert, 1983) and such polar localizations were observed in some tissues for PINs and ABCBs (Friml and Palme, 2002; Geisler *et al.*, 2005). In this respect, although it appears that PINs and ABCBs are two functionally distinct auxin efflux systems (Petrasek *et al.*, 2006), it is easy to imagine that they act in a dependent manner (Figure 1 and 2; Geisler and Murphy, 2006). The recent demonstration of functional interaction between PIN- and PGP-based transport systems has indeed been recently reported (Blakeslee *et al.*, 2007), but the significance of these interactions in plant development has not been fully clarified and is currently under investigation (Bandyopadhyay *et al.*, 2007). Nevertheless, diverse protein-interactions studies (Butler *et al.*, 1998; Geisler *et al.*, 2003; Murphy *et al.*, 2002; Pohl *et al.*, 2005) indicated that other factors could contribute to ABCB-PIN interaction. In this scenario, ABCB-PIN complexes would then be regulated by means of protein-protein interactions.

As a support of this hypothesis, Morris and co-workers (1991) designed a very elegant experiment demonstrating that cycloheximide treatments for a short period affected the inhibitory effect of NPA on IAA efflux, thus without interfering with auxin efflux itself or NPA binding to membrane fractions (Morris *et al.*, 1991). As cycloheximide restrains protein synthesis, it suggests that the NBP complex, besides the integral protein, may comprise an unstable component (Delbarre *et al.*, 1998; Luschnig, 2001; Morris, 2000; Muday and DeLong, 2001). It is impossible to say if this component and the NBP cytoskeleton-associated peripheral plasma membrane protein described by Cox and Muday (1994) are the same or not, but these proteins need to be identified. In our eyes, one candidate protein was the plasma membrane-anchored immunophilin-like TWISTED DWARF1 (TWD1), as it was previously demonstrated to bind ABCB1 and 19 *in vitro* and *in vivo* and consequently proposed as an evident ABC-regulator *in planta* (Geisler *et al.*, 2004; Geisler *et al.*, 2003).

TWISTED DWARF1 regulates ABCB1-mediated auxin export

The extreme dwarf phenotype of *Arabidopsis twd1* mutants (Geisler *et al.*, 2003; Kamphausen *et al.*, 2002) strikingly resembles the traits of *abcb1 abcb19* double mutants, suggesting a link between the immunophilin-like TWD1 and plant ABCBs. A wide range of assays already confirmed the physical interaction of TWD1 with different ABC-type proteins (Blakeslee *et al.*, 2005; Geisler *et al.*, 2004; Geisler *et al.*, 2003; Murphy *et al.*, 2002). These interactions were shown to engage different domains of the plant FKBP: its tetratricopeptide repeat (TPR) domain binds two close ABCC proteins (ABCC1/MRP1 and ABCC2/MRP2) at the tonoplast while its *cis,trans*-peptidylprolyl isomerase (PPIase) domain interacts with ABCB1 and ABCB19 at the plasma membrane (Bailly *et al.*, 2006; Geisler *et al.*, 2004; Geisler *et al.*, 2003). Although several plant multi-domain immunophilins were reported to play important roles in development (reviewed in Geisler and Bailly, 2007), the *in vivo* significance as well as the function of such TWD1-ABCB complexes needed to be clarified.
We employed physiological, cellular and molecular tools developed in our and partner laboratories to verify these assumptions. First, we measured ABCB-mediated cellular IAA efflux in the different mutants and found that *twd1* protoplasts displayed a seriously reduced auxin efflux similar to *abcb1 abcb19* protoplasts (Bouchard *et al.*, 2006). Furthermore, we used a novel IAA-specific electrode to record auxin fluxes in the root tip. Interestingly, the auxin *reflux* observed in the wild-type root apex is decreased in *twd1* and *abcb1 abcb19* mutants, correlating well with the elevated IAA contents observed in their root tip when compared to wild type (Bouchard *et al.*, 2006). As a consequence, *twd1* and *abcb1 abcb19* show altered gravitropic responses, a good indicator of

altered PAT. Together with protoplast transport data, auxin transport assays in heterologous yeast and HeLa cells systems demonstrated that TWD1 is a specific positive regulator of ABCB-mediated IAA transport. Interestingly, the stimulation observed in plant and mammalian HeLa cells was reversed in yeast. One explanation could be that the lack of high eukaryotic elements in yeast cells leads to an unstable ABCB1/TWD1 complex. This would draw a parallel between TWD1 function and the observed ABCB1 affinity for IAA, demonstrated to be reduced in yeast (Geisler *et al.*, 2005). In this scenario, the immunophilin is a specific *in planta* interactor of ABCB auxin exporters that stimulates their transport activity/specificity, consequently modulating the long-range cellular auxin transport (Bouchard *et al.*, 2006; Lewis *et al.*, 2007). FKBP-ABCB functional interactions have been reported before (Hemenway and Heitman, 1996), and these interactions are independent of PPIase activities. TWD1 does not exhibit isomerase activity *in vitro* (Geisler *et al.*, 2003; Kamphausen *et al.*, 2002), suggesting that ABCB1 may be directly regulated by protein-protein interactions between the FK506-binding/PPIase domain of TWD1 and the C-terminal end of the p-glycoprotein (Geisler *et al.*, 2003). Regarding these data, TWD1 would induce conformational changes in the C-termini of ABCB1 and ABCB19 that increase ATP accessibility to these sites. In the absence of TWD1, NBD2 ATP-binding would be reduced, thus decreasing ABCB1/ABCB19 activity.

Drug modulation of ABCB activity is conferred by TWD1

Having in mind that TWD1 is clearly involved in the regulation of auxin transport, that TWD1 may be the membrane-attached NBP factor described earlier (Cox and Muday, 1994) and that TWD1 appears to interact with the NPA-binding ABCB1, it is easy to imagine that both ABCB1 and TWD1 are constitutive components of the auxin efflux complex. As the NBP/auxin efflux complex activity is sensitive to NPA and to other auxin transport inhibitors (Jacobs and Rubery, 1988; Rubery, 1990), the ABCB1-TWD1 interaction would therefore be an interesting ATI target for further examination at the molecular level *in vivo*. The fact that ABCB1 alone mediates the hormone export when expressed in heterologous systems (Geisler *et al.*, 2005), together with the enhanced IAA efflux measured in ABCB1- and ABCB19-overexpressor lines (Bouchard *et al.*, 2006), strongly suggests that TWD1 binding to ABCBs might be transient. This is supported by the unchanged auxin efflux observed in TWD1-overexpressor line compared to wild-type. This short-lived TWD1-ABCB interaction evokes the previous work of Morris and collaborators (1991) describing an unstable NBP component and, for that reason, ATIs applications on the TWD1-ABCB complex may interfere with its stability.

Owing to the low abundance of TWISTED DWARF1 *in planta* (Bouchard *et al.*, 2006; www.genevestigator.ethz.ch), most of the assays we performed to address the drug effect issue on IAA efflux were carried out in heterologous systems. Although this choice is open to further discussion, it had the advantage to easily and rapidly allow us to work at the molecular level. Indeed, we established in our laboratory the emerging technique of bioluminescence resonance energy transfer (BRET, Angers *et al.*, 2000) to precisely monitor the molecular interactions between TWD1 and ABCB1 expressed in yeast. In short, TWD1 was functionally tagged with *Renilla* Luciferase (rLuc), a chemoluminescent enzyme, while a yellow variant of GFP (EYFP, for enhanced yellow fluorescent protein) was inserted into the ABCB1 polypeptide, without disturbing its transport capacity (Bailly *et al.*, 2008b). Upon substrate oxidation, rLuc acts as an energy donor to EYFP that subsequently emits light without fluorescent excitation. This energy transfer is dependent on the distance between donor and acceptor, in a range consistent with protein-protein interactions (Angers *et al.*, 2000). Moreover, BRET is non-invasive, ratiometric and stable over time, thus the technique became the most valuable tool to monitor *in vivo* interactions.

We therefore exploited our yeast-based BRET assay to quantify TWD1-specific interaction with ABCB1 (Bailly *et al.*, 2008b). As measured by the BRET ratio, this interaction is apparently stable over time, allowing further tests. However, this apparent stability does not reflect a constant interaction between the two proteins, but rather multiple transient events (Bouchard *et al.*, 2006). According to previous findings on ABCB1 and TWD1 NPA-sensitivity, it was not surprising to find that TWD1-ABCB1 interaction was disrupted by NPA treatments (Bailly *et al.*, 2008b). These results correlate well with previous data showing that an excess of NPA removed TWD1 from ABCB-positive

NPA-chromatography assays (Geisler *et al.*, 2003). Moreover, a subclass of flavonoids, a family of plant secondary metabolites described to be *in planta* ATIs (Jacobs and Rubery, 1988; Peer and Murphy, 2007), exhibited similar effects on the complex stability. The most potent of them was the flavonol quercetin, a well known PAT and mammalian ABCB modulator (Conseil *et al.*, 1998; Peer and Murphy, 2007; Taylor and Grotewold, 2005; Vieten *et al.*, 2007), which abolished the BRET signal with an apparent IC_{50} as low as 200nM. This specificity may reflect the native role of flavonols in auxin transport regulation (Peer and Murphy, 2007; Vieten *et al.*, 2007). Interestingly, other ATIs structurally unrelated to NPA or flavonoids, such as CPD (2-carboxyphenyl-2-phenylpropan-1,3-dione) and TIBA (2,3,5-triiodobenzoic acid), did not alter TWD1-ABCB1 interaction. Although TIBA is categorized as an auxin efflux inhibitor, it was demonstrated to act on different sites than NPA (Petrasek *et al.*, 2003). In conclusion, NPA/flavonol inhibitory effects on auxin efflux seem to be specific for the TWD1-ABCB1 complex.

To study the physiological relevance of these data, we investigated the effect of NPA and other ATIs on the IAA efflux properties of the TWD1-ABCB1 complex. Co-expression of ABCB1 and TWD1 in *S. cerevisiae* was already proven to decrease ABCB1-mediated auxin efflux from cells, contrasting with the positive function of TWD1 in higher eukaryotes (Bouchard *et al.*, 2006). The disruption of the TWD1-ABCB1 complex by NPA and flavonols would therefore be expected to restore ABCB1 activity to the levels measured in the absence of the immunophilin. In facts, NPA, quercetin and kaempferol restored ABCB1 auxin extrusion whereas TIBA treatments did not exhibit significant changes (Bailly *et al.*, 2008b). Surprisingly, the inhibitory effects of ATIs observed *in planta* on ABCB1 activity were only mild when the protein was expressed alone in yeast. Together with the fact that the NPA-binding properties of ABCB1 are abolished in the TWD1-ABCB1 complex (Bailly *et al.*, 2008b; Murphy *et al.*, 2002), these data strongly suggest that the TWD1 PPIase domain, previously shown to interact and regulate ABCB1 (Bouchard *et al.*, 2006; Geisler *et al.*, 2005; Geisler *et al.*, 2003), also mediates drug-modulation of the complex activity. The proposed function is greatly supported by the use of a mutated version of TWD1 that conserved the ability to bind ABCB1, but failed to mediate ATI effects in yeast IAA export experiments (Bailly *et al.*, 2008b).

This novel role for a plant immunophilin is in line with the drastic *twd1* mutant phenotype and its impaired polar auxin transport reported before (Bouchard *et al.*, 2006; Geisler *et al.*, 2005; Geisler *et al.*, 2003). Nevertheless, in order to functionally define the meaning of ATI influence on the TWD1-ABCB1 complex, we performed auxin-related physiological tests at the plant organ level. As roots are the classical model to study auxin flows, we analyzed their gravitropic answers and corresponding specific IAA fluxes in the different mutant backgrounds (Bailly *et al.*, 2008b). In summary, wild-type roots are extremely sensitive to NPA whereas *twd1* and *abcb1 abcb19* mutants are, in similar extent, only slightly sensitive to ATI treatments. This represents the first demonstration that TWD1-mediated drug modulation of the auxin exporter ABCB1 is of significant relevance *in planta*. Although future work should focus on testing this influence for diverse endogenous and synthetic ATIs at the plant level, our current model places the NPA-responsive TWD1-ABCB1 complex at the crossroads of auxin transport and regulation *in vivo*. In this concept, high concentrations of specific flavonols would compete with the TWD1 FKBD/PPIase domain for apparent NPA-binding sites at the ABCB1 C-terminal domain, resulting in a decreased ABCB1-mediated auxin efflux. Interestingly, flavonoids, especially aglycone flavonols, were described to accumulate at the plasma membrane periphery in high auxin-content tissues expressing ABCB1 and ABCB19 (Buer *et al.*, 2007; Murphy *et al.*, 2000; Peer *et al.*, 2004; Peer *et al.*, 2001). These observations further support our hypothesis, but do not provide molecular explanations to the mechanisms involved.

AtABCB1 structure reveals its substrate-specificity towards auxin

To deeper investigate the molecular bond between TWD1 and ABCB1, the three-dimensional structure of TWD1/FKBP42 has been solved (Granzin *et al.*, 2006; PDBID 2IF4). *In silico* predictions confirmed that the TWD1 PPIase domain is likely to interact with the C-terminal nucleotide-binding domain (NBD) of ABCB1 in cells (Figure 3; Granzin *et al.*, 2006; Weiergraber *et al.*, 2006). This is of major interest since ABC-transporter NBDs are responsible for

the catalytic cycle of the protein, hence its transport activity (Linton, 2007). Furthermore, flavonoids were described as competitors for nucleotide-binding at NBD sites in mammalian ABCB1 (Conseil *et al.*, 1998; Di Pietro *et al.*, 2002). The importance of such a NBD-FKBD interaction in the regulation of auxin transport is also supported by the apparent relationship between nucleotide-binding and substrate-recognition in ABC-transporters (Loo *et al.*, 2003; Maki *et al.*, 2006; Martin *et al.*, 2001). The TWD1 positive effect observed on ABCB1-mediated auxin export could, from this point of view, be explained by the influence of protein contacts on ABCB1 molecular dynamics and/or substrate specificity.

For more than thirty years, tremendous efforts have been made to understand the factors that determine ABC-transporter substrate specificity (Higgins, 2001; Linton, 2007; Loo *et al.*, 2003; Modok *et al.*, 2006; Siarheyeva *et al.*, 2006). The most intensive research arose with the discovered implication of the human ABCB1/PGP1 gene in multi-drug resistance (MDR) phenomena (Gottesman and Ling, 2006). Indeed, HsABCB1/MDR1 up-regulation confers to tumors the ability to extrude diverse compounds out of the diseased cells, including chemotherapeutics (Gottesman and Ling, 2006; Modok *et al.*, 2006). This HsABCB1 substrate promiscuity contrasts with the apparent AtABCB1 specificity towards auxins, although both proteins are relatively close in primary amino acid sequence and architecture (Bailly *et al.*, 2008a; O'Mara and Tieleman, 2007). The overall mechanism of ABCB-protein-mediated drug transport is currently being understood, and the consensus model for the molecular mechanisms involved is well accepted (Linton and Higgins, 2007). In this model, which seems to be pertinent for all ABC-transporters, both transmembrane- and nucleotide-binding domains (TMDs and NBDs, respectively) form the basic functional units of the proteins (Higgins, 2001; Higgins and Linton, 2004; Hollenstein *et al.*, 2007; Linton and Higgins, 2007). While two NBDs are necessary to bind and catalyze ATP, TMDs associate in biological membranes to form the substrate binding- and translocation-chamber (Hollenstein *et al.*, 2007; Linton and Higgins, 2007). The entire machinery of ABC proteins is therefore based on the communication between NBDs and TMDs to couple ATP-binding and hydrolysis to substrate translocation.

The high homology between human and *Arabidopsis* ABCB1 genes allowed us to investigate whether the divergent substrate specificities of both proteins were reflected in their residues distribution (Bailly *et al.*, 2008a). Multiple alignments of close plant and animal ABCB1 orthologs revealed kingdom-specific amino acid clusters in the intra-cellular loops (ICLs) of the TMDs. This is of major interest since TMDs are supposed to provide the substrate-binding pockets to the proteins (Loo *et al.*, 2006a; Loo *et al.*, 2006b; Pleban *et al.*, 2005). Moreover, ICLs are cytoplasmic and may therefore represent binding regions for hydrophilic drugs such as auxin (Ren *et al.*, 2006). This is in contrast with hydrophobic regions of the TMDs suggested to interact with apolar HsABCB1 substrates according to the "membrane vacuum-cleaner" model (Shapiro and Ling, 1997; Siarheyeva *et al.*, 2006).

To further explore this issue, we used the recent crystal structure of the ABCB-like bacterial transporter Sav1866 (Dawson and Locher, 2006) to generate three-dimensional homology models for ABCB1 orthologs (Bailly *et al.*, 2008a). Our structure-based comparison of the models obtained suggests that kingdom-specific ICL residues are exposed to the cavity of the substrate translocation chamber. These particular regions may therefore represent the molecular basis for the divergent substrate-specificity

FIGURE 3. **ABCB1 NBD2 provides the molecular surface for TWD1 interaction**

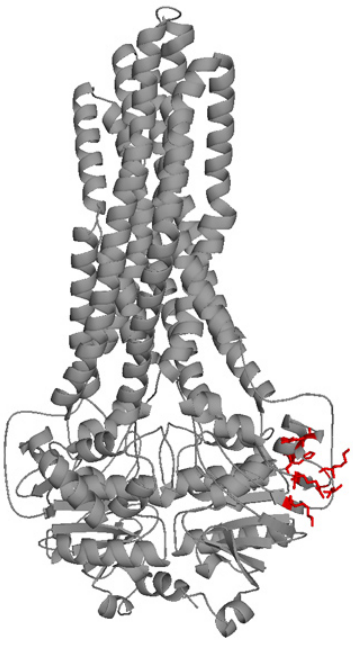

ABCB1 homology model. Putative TWD1-interacting residues reported in Granzin *et al.* (2006) are represented in red sticks. Similar results were obtained in our hands from *in silico* simulations using the TWD1 FKBD crystal structure against ABCB1 homology models (results not shown). The NBD2 Q-loop and helical sub-domain are likely to participate in ABCB1 TWD1-mediated regulation. For clarity, some ABCB1 transmembrane helices are not represented. The molecular structure diagram was generated using PyMol 0.99rev8 (http://pymol.sourceforge.net/).

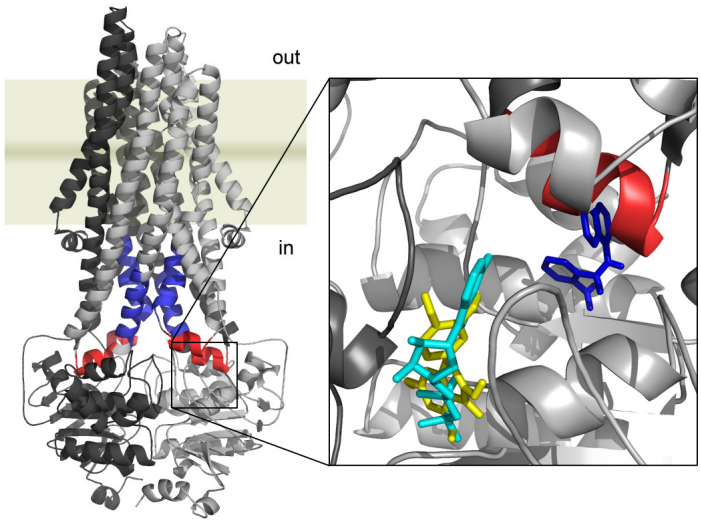

FIGURE 4. ***In silico* drug-binding assay on AtABCB1 homology model reveals putative binding sites for ATIs.**

Front view of an AtABCB1 homology model. ICL residues with low conservation between plant and animal ABCB1 orthologs (in blue) are located in the intracellular space and form the bottom of the translocation chamber. These regions are in the direct vicinity of the four "coupling helices" (in red) described by Dawson and Locher (2006). Inset: Quercetin (yellow sticks) competes for ATP-(cyan sticks) binding site at the NBD1/NBD2 interface, while NPA (blue sticks) clusters at the ICL5-NBD1 interface. TMD1 and NBD1 are in silver; TMD2 and NBD2 are in dark grey.
The molecular structure diagrams were generated using PyMol 0.99rev8 (http://pymol.sourceforge.net/). *In silico* NPA and quercetin binding against modeled AtABCB1 halves was performed using MEDock (Maximum-Entropy based Docking) web server (http://medock.csbb.ntu.edu.tw/).

in plant and animal ABCB1 proteins. Although the interest of these observations expands to the general concept of drug recognition in ABC-transporters, it specifically focuses our attention on a putative mechanism for the auxin transport specific TWD1-ABCB1 complex. Indeed, the TMD/NBD interface is known to drive the energy stroke conferred by ATP-binding from the NBDs to the transmembrane domain rearrangements necessary for substrate extrusion (Hollenstein *et al.*, 2007). These allosteric movements are suspected to be favored by both ATP- and substrate-binding according to the "induced-fit" hypothesis of the ATP-switch model (Ghosh *et al.*, 2006; Higgins and Linton, 2004; Maki and Dey, 2006). As a consequence, the particular ICL coupling helices described for the Sav1866 architecture are key structures of the NBD/TMD interface (Dawson and Locher, 2006; Hollenstein *et al.*, 2007). Therefore, less surprisingly, our three-dimensional mapping of the discrepancies observed between plant and animal ABCB1 ICLs revealed atome-scaled proximity with the coupling helices (Figure 4; Bailly *et al.*, 2008a).

Furthermore, the NBD-TMD coupling mechanism is likely to involve the Q-loop, a conserved region of the nucleotide-binding folds known to undergo large conformational changes during the ABC catalytic cycle (Dalmas *et al.*, 2005). Q-loops indeed contact ICLs *via* coupling helices and, according to the "induced-fit" model, substrate-binding in these regions might destabilize enough these contacts to facilitate the described allosteric events. The importance of these inter-domain contacts has been illustrated by several Q-loop-defective mutants in the human CFTR ABC-transporter, leading to cystic fibrosis syndromes (Kerem and Kerem, 1996; Mendoza and Thomas, 2007). Structural data from our ABCB1 homology models and the Sav1866 architecture indicate that these NBD regions partially participate to the cytosolic-accessible surface of the protein.

Interestingly, yeast two-hybrid and BRET assays described the C-terminal NBD of AtABCB1 as the molecular interactor of the TWD1 FKBD domain (Bailly *et al.*, 2008a; Bailly *et al.*, 2006; Bouchard *et al.*, 2006; Geisler *et al.*, 2005; Geisler *et al.*, 2003). Adding to this, the intriguing parallel between Q-loop rotational movements and the lost TWD1 *cis,trans*-peptidylproly isomerase activity (Dalmas *et al.*, 2005; Geisler *et al.*, 2003; Kamphausen *et al.*, 2002), may emphasize the mutual functional conservation between the immunophilin and its interacting ABCB1 partner, as proposed earlier (Dolinski *et al.*, 1997; Hemenway and Heitman, 1996). We therefore propose that TWD1 interacts directly with the second ABCB1 NBD *via* its PPIase domain and that this interaction might facilitate Q-loop movements. This is further supported by the transient nature of this interaction (Bouchard *et al.*, 2006), as constant protein-protein contacts would not favor such domain motion. As a consequence, the TWD1-ABCB1 interaction could influence ABCB1-mediated auxin efflux in two ways: either it would ease the molecular dynamics of the transporter catalytic cycle by means of Q-loop-related allosteric events; either it would grant better ATP- or substrate-binding properties to the protein. Both explanations are currently difficult to confirm or

infirm, and may even be one unique process. Indeed, unpublished transport and interaction studies results strongly suggest that auxin itself promotes TWD1-ABCB1 interaction and subsequent IAA export (Bailly and Geisler, unpublished results). Similar self-promoting auxin signals have already been observed for PIN-mediated auxin efflux, although it uses different processes (Paciorek *et al.*, 2005). A precise study on auxins effects at the TWD1-ABCB1 molecular level added of a pertinent Q-loop mutagenesis analysis would therefore give further indications in this respect. At the end of this work, TWD1 can be viewed as a positive regulator that enhances ABCB1 auxin transport and most-probably substrate-specificity properties by means of protein-protein interactions. In the same extent, interaction studies between PIN and ABCB auxin efflux systems suggested an increased auxin transport, substrate specificity and ATI sensitivity in high eukaryotic cells (Bandyopadhyay *et al.*, 2007; Blakeslee *et al.*, 2007). In conclusion, our and other physiological, cellular and molecular studies have established that both auxin efflux systems are essential for PAT and auxin-dependent developmental processes (Bailly *et al.*, 2008b; Blakeslee *et al.*, 2007; Morris, 2000). Additionally, they offer insights into the composition of the long-sought auxin efflux carrier complex depicting it as a highly dynamic and finely regulated multi-component complex that is targeted by auxin efflux inhibitors such as NPA or flavonols (see Figure 5).

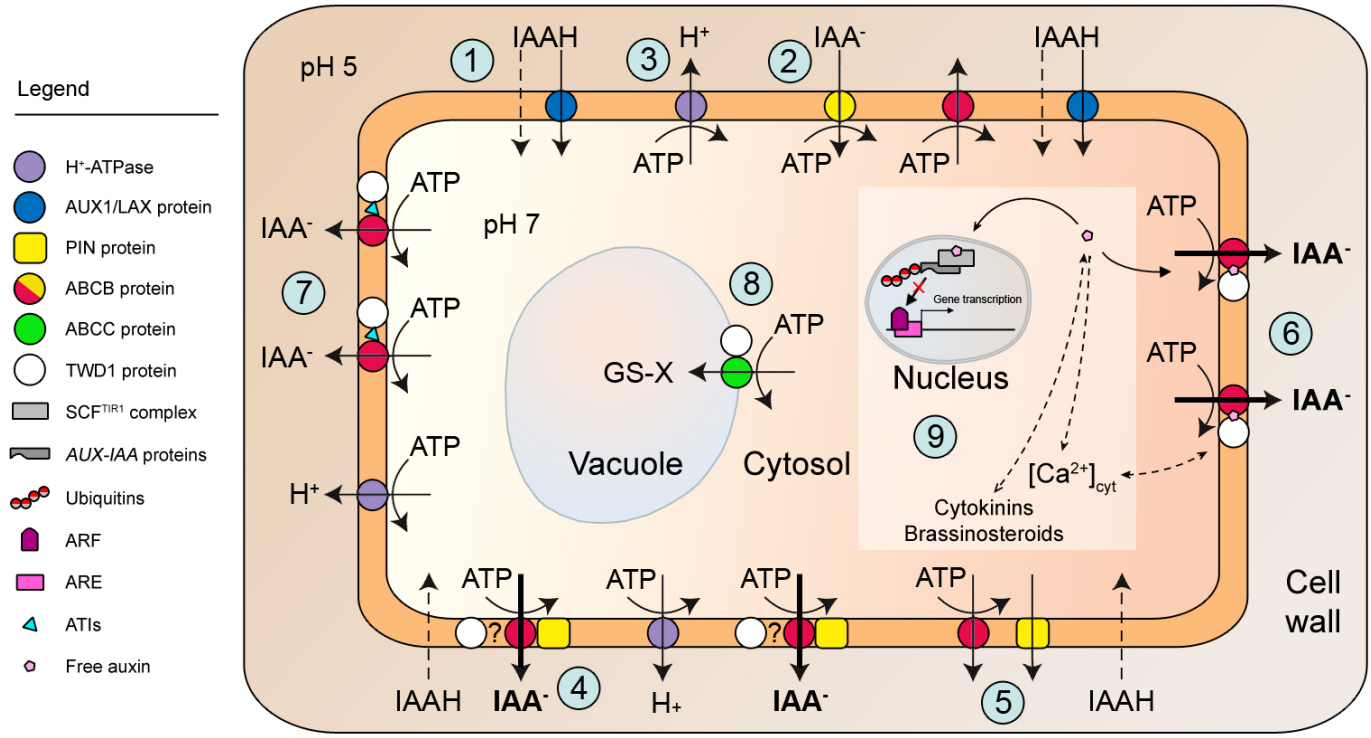

FIGURE 5. **A revised model for cellular auxin transport and regulation**

(1) IAA enters the cell either passively in the undissociated form (IAAH) or by secondary active co-transport in the anionic form (IAA^-). ***(2)*** ABCB proteins such as ABCB4 might participate in active auxin influx. ***(3)*** The plasma membrane H^+-ATPase contributes to IAA diffusion by maintaining the acidic apoplastic pH. ***(4)*** ABCB and PIN proteins might work synergistically to drive the auxin efflux based on their positive interaction. It is still unknown if TWD1 could or not regulate this complex, as is the case for ABCB1-mediated IAA efflux system ***(5)*** ABCBs and PINs might as well act additively, but independently in the same cells. ***(6)*** The ABCB1-TWD1 complex has been demonstrated to drive auxin efflux independently of PIN proteins in different tissues. This interaction could be stabilized by auxin, thus promoting its own efflux. (7) in contrast, ATIs destabilize the ABCB1-TWD1 complex, decreasing its auxin-efflux capacity. ***(8)*** Some mechanisms involving TWD1-ABCC interactions need to be further investigated. ***(9)*** The amount of free auxin in the cell triggers subsequent cellular responses, such as gene transcription, hormone cross-talk and secondary messengers like calcium, involved in many developmental and physiological aspects. GS-X, Glutathion-conjugates; ARF, auxin response factors; ARE; auxin response elements; ATIs, auxin transport inhibitors. (adapted from Taiz and Zeiger, 2006)

Immunophilin-regulated ABCB function: implications and perspectives

Despite this satisfying progress in the last decades, many issues concerning cellular auxin transport are not yet solved. To date, the exact nature of ATI inhibition remains unclear, although diverse explanations have been proposed (Peer and Murphy, 2007). In our model, NPA and flavonols may directly interact with the TWD1-ABCB1 complex and consequently decrease its auxin-pumping activity (Bailly *et al.*, 2008b; Bouchard *et al.*, 2006; Geisler *et al.*, 2005; Geisler *et al.*, 2003). *In silico* binding assays carried out on ABCB1 modelled structure suggest distinct processes for flavonols and NPA actions. Flavonols like quercetin were simulated to compete for ATP-binding sites at the NBD/NBD catalytic interface, as previously indicated in mammalian studies (Badhan and Penny, 2006; Conseil *et al.*, 1998). Again, in our model, this competition might interfere with post-ATP-binding processes and subsequently uncouple the Q-loop-related TWD1-ABCB1 interaction (Figure 4). This scenario would greatly clarify the observed flavonoid effects on TWD1-ABCB complex-mediated auxin efflux. On the other hand, *in silico* predictions target NPA to different, but equally pertinent binding-pockets. NPA would act at the NBD/TMD interface, predominantly at the exact coupling helices/Q-loop interface, therefore suggesting a disruption of the overall ABCB1 molecular architecture and dynamics, in concert with the loss of TWD1 interaction (Figure 4). As a supportive clue, long-term treatments with low NPA concentrations and short-term treatments with high NPA concentrations lead to similar effects on auxin distribution (Ottenschlager *et al.*, 2003). According to our model, flavonol and NPA interferences may then alter ATP-binding/hydrolysis or substrate recognition.

Despite these appealing postulations, further molecular work is required to enlighten our understanding in the general process of auxin-transport regulation. The first path to explore is the overall ABCB specialization towards transported substrates. Although *Arabidopsis* ABCBs display conserved architectures and mechanisms compared to the extensively studied HsABCB1 (Bailly *et al.*, 2008a); Bailly and Geisler, unpublished data), it is yet impossible to predict their function. If ABCB1 and 19 were demonstrated to be auxin exporters, another family member, ABCB4 (and its close homolog ABCB21) seems to be involved in auxin import (Santelia *et al.*, 2005; Terasaka *et al.*, 2005), without sharing the canonical ABC-importer features (Bailly *et al.*, 2008a). The actual number of plant ABCBs involved in auxin transport is not yet defined, and only the systematic characterization of individual family members could provide this information. Finally, compared to mammalian ABCB1 substrates, IAA is a very small molecule that probably cannot undertake the expected "induced fit" mechanism described above by itself. The group of Kazumitsu Ueda proposed a "cholesterol fill-in" model for small ABCB1 substrates (Kimura *et al.*, 2007), that could complete IAA-binding events (Figure 6). The translocation of phytosterols together with IAA could be relevant for auxin transport in that biological membranes composition is an important factor for transmembrane transporters (Garrigues *et al.*, 2002; Orlowski *et al.*, 2006). Nevertheless, a large-scale comparison of ABCB orthologs from different organisms based on protein sequences, structure and function could offer new elements to broader our understanding of substrate-specificity.

Another issue to address is the trafficking of the proteins involved in PAT. Indeed, the use of intracellular protein trafficking inhibitors such as BFA (brefeldin

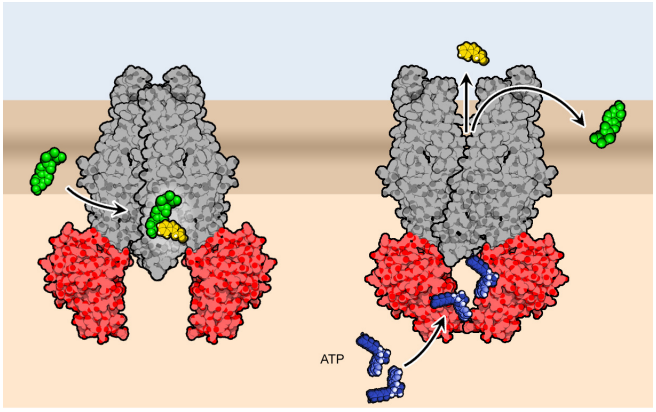

FIGURE 6. **The "cholesterol fill-in" model proposes alternative strategies for ABCB1 substrate-binding**

Adapted to the plant model, this hypothesis suggests that phytosterols (in green) could interact from the lipid bilayer with the ABCB1 IAA-specific recognition site at the TMD/TMD interface (in grey). This interaction could therefore increase IAA (in yellow) binding affinity and ease its co-translocation. Additionally, translocated phytosterols might influence the lipid membrane in a way consistent with auxin efflux mechanisms. NBDs are in red. (adapted from Kimura *et al.*, 2007)

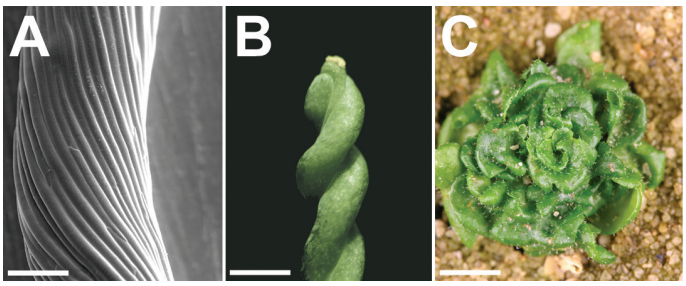

FIGURE 7. ***twd1*** **mutants display an helical-disoriented growth suggesting the involvement of an actin-dependant mechanism.**

A, Electron micrograph of *twd1-1* hypocotyl. The "twisted syndrome" of all organs is perceptible at the epidermal level Bar, 100 µm.
B, The *twd1-1* silique displays reduced and disoriented growth. Bar, 1 mm
C, Leaf phyllotaxy is also affected in *twd1* mutants . Bar, 1 cm

A) revealed the amazing complexity of the auxin efflux complex machinery. BFA treatments inhibit cellular auxin efflux (Delbarre *et al.*, 1998; Morris, 2000; Muday *et al.*, 2003) by blocking constitutive PINOID-driven PIN cycling (Benjamins *et al.*, 2001; Friml *et al.*, 2004). Interestingly BFA does not affect NPA binding to membrane preparations, suggesting that the NPA-binding protein and auxin efflux carriers are separate proteins (Robinson *et al.*, 1999).

Although the degree of ABCB1/19 trafficking has not been clarified, their interaction with TWD1 implies cytoskeleton involvement (Geisler *et al.*, 2003; Murphy *et al.*, 2005). Indeed, whereas auxin and actin are described to be connected in developmental processes (Bainbridge *et al.*, 2008; Dhonukshe *et al.*, 2008; Maisch and Nick, 2007), *twd1*mutants display the actin-related "twisted syndrome" that do not appear in *abcb1 abcb19* double mutants (Geisler *et al.*, 2005; Geisler *et al.*, 2003; Ishida *et al.*, 2007; Kamphausen *et al.*, 2002; Figure 7). TWD1 possesses a *bona fide* amphipathic in-plane membrane-anchor (IPM) (Geisler *et al.*, 2003; Kamphausen *et al.*, 2002; Scheidt *et al.*, 2007) that could link the immunophilin to the cytoskeleton-associated plasma membrane peripheral NBP-component described in Cox and Muday (1994). We currently develop tools, such as an IPM-truncated version of TWD1, to further investigate this possibility. Nonetheless, other uncharacterized components could participate in the "twisted syndrome" since TWD1 was shown to interact with vacuolar ABCC transporters (Geisler *et al.*, 2004) and possesses domains to interact with heat shock proteins (HSPs) and calmodulin (CaM) (Geisler and Bailly, 2007; Kamphausen *et al.*, 2002). Interestingly, both HSPs and CaM seem to play critical roles in plant hormones functions (Dhaubhadel *et al.*, 1999; Du and Poovaiah, 2005) while calcium ions are essential second messengers of auxin signal transduction (Scherer, 2002). Furthermore, the substrates transported by the TWD1-interacting ABCC-type proteins MRP1 and MRP2 are still unidentified (Geisler *et al.*, 2004). One could easily imagine that these proteins may participate in the vacuolar export of auxinic compounds, such as IAA-conjugates or -breakdown products, similarly to the unspecific auxin transport we observed in the pleiotropic drug resistance-type transporter ABCG37 (Ruzicka *et al.*, 2008, see Appendix 2). As an intriguing option, TWD1 might as well confer substrate-specificity to its ABCC partners, but such ABCB-like regulation has not been functionally demonstrated until now.

Regardless of these limitations, the present thesis has, in my eyes, clarified cellular and molecular aspects of the complex but fascinating auxin efflux transport system. The knowledge gathered here will therefore help to understand the subtle mechanisms of IAA-related plant physiology and to develop new agronomical strategies. Indeed, through a long process of natural selection, human kind has favored crops presenting dwarfing characteristics for their resistance to wind- and rain-flattening, their high yield-to-biomass ratio and their decreased need in resources (Khush, 2001). The use of optimized natural and synthetic auxin inhibitors to finely control the auxin flows would therefore represent promising alternative strategies to gene modifications for our sustainable-development oriented future agriculture.
Moreover, transfer of this knowledge might be extremely helpful for human-health research. Partner proteins such as FKBPs should be investigated for their ability to control ABCB transporters, and are therefore interesting candidate proteins to indirectly target MDR. Indeed, substrate ABCB-specificity seems to be recent when compared to the ancient origin of ABC proteins. A large scale analysis of plant and animal ABCB structures or more robust homology models might finally contribute to substrate-prediction and subsequent efforts in designing therapeuticals that are not recognized by MDR/ABCB proteins.

Appendices

Flavonoids Redirect PIN-mediated Polar Auxin Fluxes during Root Gravitropic Responses

Diana Santelia[1, 5], Sina Henrichs[1], Vincent Vincenzetti[1], Michael Sauer[2], Laurent Bigler[3], Markus Klein[1], Aurélien Bailly[1], Youngsook Lee[4], Jirí Friml[2], Markus Geisler[1,*] and Enrico Martinoia[1,*]

[1]Laboratory of Molecular Plant Physiology, Institute of Plant Biology, University of Zürich, Zollikerstrasse 107, 8008 Zürich, Switzerland
[2]Department of Plant Cell Biology, University of Göttingen, Untere Karspüle 2, 30073 Göttingen, Germany
[3]Institute of Organic Chemistry, University of Zürich, Winterthurerstrasse 190, 8057 Zürich, Switzerland
[4]Postech-UZH Global Research Laboratory, Pohang University of Science and Technology, Pohang, 790-784, Korea
[5]Present address: Institute of Plant Science, ETH Zürich, Universitätstrasse 2, 8092 Zürich, Switzerland

*Correspondence: markus.geisler@botinst.uzh.ch, phone +41 44 6348277, fax +41 44 6348204; enrico.martinoia@botinst.uzh.ch
Correspondence and request for material should be addressed to J.F. (e-mail: jiri.friml@psb.ugent.be)

Summary

The rate, polarity and symmetry of the flow of the plant hormone auxin are determined by the polar cellular localization of PIN-FORMED (PIN) auxin efflux carriers. Flavonoids, a class of secondary plant metabolites, have been suspected to modulate auxin transport and tropic responses. Nevertheless the identity of specific flavonoid compounds involved and their molecular function and targets in vivo are essentially unknown.

Here we show that the root elongation zone of agravitropic *pin2/eir1/wav6/agr1* has an altered pattern and amount of flavonol glycosides. Application of non-inhibitory concentrations of flavonols to pin2 roots is sufficient to restore root gravitropism. By employing a quantitative cell-biological approach, we demonstrate that flavonoids restore the formation of lateral auxin gradients in the absence of PIN2. Chemical complementation by flavonoids strictly correlates with an asymmetric distribution of the PIN1 protein. *Pin2* complementation does not result from inhibition of auxin efflux, as supply of the auxin transport inhibitor N-1-naphtylphtalamic acid failed per se to restore *pin2* gravitropism.

We propose that flavonoids promote asymmetric PIN shifts upon gravity stimulation, thus redirecting basipetal auxin streams necessary for root bending.

Introduction

The plant hormone auxin (3-indolyl acetic acid, IAA) controls virtually all plant developmental and physiological processes. In roots, the differential growth response associated with gravity stimulation (gravitropism) occurs in the elongation zone (Muday, 2001; Chen *et al.,* 1998) and is a result of the asymmetric distribution of auxin to the lower side of epidermal cells (Moore, 2002). In these tissues accumulating auxin, cell elongation is inhibited and the root tip bends downwards. This cell-to-cell or polar auxin transport (PAT) is determined by the asymmetric cellular localization of auxin in- and efflux components of the PGP/MDR/ABCB, AUX1/LAX and PIN-FORMED (PIN) family (Vieten *et al.,* 2007; Wisniewska *et al.,* 2006; Geisler and Murphy, 2006; Kerr and Bennett, 2007). While PGPs are apparently more involved in long-range auxin transport (Blakeslee *et al.,* 2007; Lewis *et al.,* 2007; Wu *et al.,* 2007), AUX1 and PIN2/*EIR1/WAV6AGR1* channel auxin from the lateral root cap basipetally to the expanding epidermal cells (Swarup *et al.,* 2001; Marchant *et al.,* 1999; Abas *et al.,* 2006).

The regulation of auxin transport during root gravitropic responses is still largely unclear. Among various possible mechanisms, the localized synthesis and directed transport of flavonoids, plant-specific phenylpropanoid compounds, have been shown to modulate the rate of the gravity response (Buer and Muday, 2004; Buer *et al.,* 2007). A number of lines of experimentation have suggested that flavonoids may act as non-essential auxin transport inhibitors (Brown *et al.,* 2001; Geisler *et al.,* 2005; Murphy *et al.,* 2000; Peer *et al.,* 2004; Peer and Murphy, 2006). This is mainly based on the finding that flavonoids displace binding of synthetic auxin transport inhibitors, like 1-*N*-naphtylphtalamic acid (NPA), *in vitro* (Jacobs and Rubery, 1988; Lomax *et al.*, 1995; Luschnig, 2001; Morris, 2000). Moreover, roots of *transparent testa* (*tt*) Arabidopsis mutant with manipulated flavonoid levels, exhibit altered gravitropic curvature and auxin transport, which are restored to wild-type level by exogenous application of flavonoids (Brown *et al.,* 2001; Taylor and Grotewold, 2005). Nonetheless, the identity of the specific flavonoid compounds involved, their molecular targets as well as their mode of action *in vivo* are essentially unknown. While several lines of evidence suggest that PGPs are modulated by aglycone flavonols (Blakeslee *et al.,* 2007; Lewis *et al.,* 2007; Wu *et al.,* 2007; Geisler *et al.,* 2005; Bouchard *et al.,* 2006), the expression and sub-cellular location of PIN auxin efflux carriers is thought to be a consequence of flavonoid-mediated alteration of auxin concentrations (Peer *et al.,* 2004; Peer and Murphy, 2006).

Here, we report that a gravitropic loss-of-function mutant *pin2/eir1/wav6/agr1* has impaired patterns of flavonol glycosides. We found that nM concentrations of exogenous flavonols, which have no inhibitory effect on root elongation and gravitropic response in wild-type plants, can rescue the agravitropic phenotype of *pin2* roots by promoting asymmetric PIN1 shifts, re-establishing polar auxin fluxes. This is the first report that mechanistically links flavonoid action to polar auxin transport, suggesting that the role of flavonoids is not restricted to inhibition of efflux transporters (Geisler *et al.,* 2005; Bouchard *et al.,* 2006; Terasaka *et al.,* 2005; Morris and Zhang, 2006), but that they are able to function as versatile modulators of polar auxin flows establishing the basis for physiological flexibility.

Experimental procedures

Chemicals

MeCN (HPLC Supra grade, Scharlau, E-Barcelona), HCOOH (Fluka, puriss, Switzerland), Methanol (MEOH, Fisher Scientific, UK), HPLC-grade acetonitrile (Fisher Scientific, UK), H_3PO_4 (Applichem, Germany). Water was purified with a MilliQ Gradient apparatus (<5ppb, Millipore, Milford, MA, USA). Diphenilyboric acid 2-aminoethyl ester (DPBA, Sigma, Germany). NPA, (Fluka, Germany), kaempferol (CalbioChem, La Jolla, CA) and quercetin (Fluka, Germany) were dissolved in 100% dimethyl sulfoxide (DMSO).

Growth conditions and plant material

Seeds were surface sterilized for 5h in a chamber containing vaporous HCl and Na-Hypochlorite and stratified in a 0.1% agar solution for 2d at 4°C. Subsequently, the seeds were plated on sterile half-strength MS medium at pH 5.7 containing 2% sucrose solidified with 0.6% phytagel (Sigma, Buchs, Switzerland), and vertically grown at 22°C with 16h/8h light/dark cycle. The mutant alleles used in this study are the following: *pin2-1* (Muller *et al.,* 1998) and *eir1-4* (Luschnig *et al.,* 1998).

Flavonoid fluorescence staining

Flavonoid compound locations were visualized *in vivo* by the fluorescence of flavonoid-conjugated DPBA to the compounds after excitation with blue light. Plants were grown for 5d before staining. Fluorescent staining of whole seedlings was performed according to Buer and Muday (2004). Fluorescence was achieved by excitation with FITC filters (450 to 490nm, suppression long pass 515nm) on a Leica DMR fluorescence microscope and a 10X or 20X objective. Digital images were captured with a Leica DC300 F charge coupled device (CCD) camera.

Extraction of phenolic compounds and HPLC analysis

Excised roots were incubated over night in the dark at 4°C in 0.5ml of 80% (v/v) methanol (MeOH), extracted and centrifuged at 18'000g for 10min. The supernatant was concentrated to dryness and resuspended in 0.1ml 80% MeOH. Aliquots (50 ml) were analyzed by a reverse-phase HPLC (Gynkotek, Germany). Absorbance spectra were recorded with a UVD340S diode array detector (Dionex, Switzerland). Data integration analysis was conducted using the Chromeoleon software (v6.4, Dionex, Switzerland). The peak height was quantified at 330 nm. A calibration curve for kaempferol was used as reference for single peak quantification. All analyses were performed with at least three independent replicates, each representing 100 roots. Chromatographic conditions: Nucleosil 100-5 C_{18} column (5µm, 2 x 250 mm, Macherey-Nagel, Düren, Germany); flow rate 1.00ml min^{-1}, gradient (step, time, %B over A) 1, 25min, 10-25%; 2, 10min, 25-70%). Solvent A: H_2O/0.1% (v/v) H_3PO_4; solvent B: MeCN.

Structural elucidation: HPLC-ESI-MS/MS analysis

HPLC-MS analyses were performed on an Agilent 1100 HPLC system (Agilent Technologies, Palo Alto, CA, U.S.A.) fitted with a HTS PAL autosampler (CTC Analytics, Zwingen, Switzerland), an Agilent 1100 binary pump, and an Agilent 1100 photodiode-array detector. Chromatographic conditions: Nucleosil 100-3 C_{18} column (3µm, 2 x 250mm, Macherey-Nagel, Hoerdt, France); flow rate 0.170ml min^{-1}, gradient (step, time, %B over A) 1, 25min, 10-25%; 2, 10min, 25-70%). Solvent A: H_2O/0.1% (v/v) HCOOH; solvent B: MeCN/0.1% (v/v) HCOOH. The HPLC was connected to a Bruker ESQUIRE-LC quadrupole ion trap instrument (Bruker Daltonik GmbH, Bremen, Germany), equipped with a combined Hewlett-Packard Atmospheric Pressure Ion (API) source (Hewlett-Packard Co., Palo Alto, CA, USA). The HPLC output was directly interfaced to the ESI ion source. The MS-conditions were: Nebulizer gas (N_2) 40psi, dry gas (N_2) 9 l/min, dry temperature 300°C, HV capillary 4000V, HV EndPlate offset –500 V, capillary exit –100V, skimmer1 –28.9 V, and trap drive 53.4. The MS acquisitions were performed in the negative electro spray ionization mode, at normal resolution (0.6u at half peak height), under ion charge control (ICC) conditions (10'000) in the mass range from *m/z* 100 to 1000.

The MS^2 acquisitions were obtained in the auto-MS/MS mode. The isolation width was 4u, the fragmentation cut-off set by "fast calc", and the fragmentation amplitude set at 0.9V in the "SmartFrag" mode. The total amounts of flavonoid compounds were calculated as the sum of the areas ($x10^6$ AU, arbitrary unit) of the mass signals identified during HPLC-ESI-MS/MS analysis. Each extraction consists of a pull of 100 different roots. Quantification of RT-EZ flavonoid compounds is the result of two independent extractions in which each time 150 5-mm long root apices from 12 different agar plates were pulled together.

Gravitropic assays

4d light-grown seedlings were transferred from control plates to plates containing nutrient media optionally supplemented with quercetin or kaempferol (100nM or 200nM). After 24h of adaptation and growth in the new media, plates were turned 90°. In one type of gravitropic assay, after additional 24h of growth under gravistimulation, seedlings were scanned using Epson Perfection 2450 photo and angles of gravitropic curvature were measured from digital pictures using the tool "Image Manager" of the Leica IM1000 software (Leica, Heerbrug, CH). Each gravity stimulated root was assigned to one of twelve 30° sectors; the length of each bar represents the percentage of seedlings showing the same direction of root tip growth. Short pulses of gravity stimulation were achieved by turning the plates of 90° for 2h, which corresponds to the peak of gravity-induced flavonoid accumulation (Buer and Muday, 2004). After 2h of gravity stimulation, roots were excised and flavonoids extracted as described, or expression of $DR5_{rev}$-GFP reporter protein analysed on a Leica TCS SP2 CLSM. All gravitropic assays were performed in the dark to prevent phototropic

responses. In some cases, angles of gravitropic curvature were measured in a blind assay, to reduce possible unbiased calculations.

Immunocytochemistry

PIN1 immunolocalization was performed as previously described (Friml *et al.,* 2003) with PIN1 specific antibody (Paciorek *et al.,* 2005) at 1:1000 dilution and anti-rabbit CY3 conjugated secondary antibodies. Confocal imaging of CY3 and *DR5rev::GFP* was carried out on a Leica SP2 AOBS microscope.

Data analyses

Statistical analysis was performed using SPSS 11.0 (SPSS Inc., Chicago, Illinois).

Results

Pin2 roots have an altered flavonoid pattern

Pin2/eir1/wav6/agr1 Arabidopsis mutant (referred to as *pin2* hereafter), one of the best-characterized auxin transport mutants, exhibits reduced basipetal auxin transport and agravitropic root growth (Chen *et al.,* 1998; Muller *et al.,* 1998; Luschnig *et al.,* 1998; Utsuno *et al.,* 1998). As a starting point of this work, we investigated whether defects in basipetal auxin transport in *pin2*, which result in agravitropic responses (Rashotte *et al.,* 2000), are linked to an altered accumulation of specific endogenous flavonoids and whether flavonoids could be directly implicated in the control of the gravitropic responses. Diphenylboric acid 2-amino-ethylester (DPBA), a fluorescent dye that specifically interacts

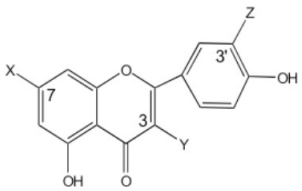

compound	Rt (min)	MW	trivial name	entire root (Area x 10^6 AU)		root tip (Area x 10^6 AU)	
				Col	*pin2*	Col	*pin2*
2	13.6	756	**Q-R-G-3-R-7**	5.9 ± 0.47	3.7 ± 0.4	1.25 ± 0.2	0.2 ± 0.1
3	14.2	610	**K-G-3-G-7**	1.7 ± 0.32	1.2 ± 0.3	0.2 ± 0.1	0.1 ± 0.0
4	15.5	740	**K-R-G-3-R-7**	10.1 ± 0.51	9.0 ± 0.7	1.3 ± 0.2	0.4 ± 0.1
5	15.8	772	**Q-G-G-3-R-7**	1.2 ± 0.05	1.5 ± 0.1	0.2 ± 0.1	0.1 ± 0.0
7	16.8	594	**K-R-3-G-7**	0.7 ± 0.15	0.2 ± 0.03	0.1 ± 0.03	< 0.1
8	17.8	756	**Q-G-R-R**	2.3 ± 0.25	0.9 ± 0.2	0.3 ± 0.1	< 0.1
9	18.1	610	**Q-G-3-R-7**	52 ± 4.1	43.5 ± 1.0	15.6 ± 3.5	5.3 ± 0.7
10	18.3	756	**K-G-G-3-R-7**	n.d.	1.1 ± 0.2	n.d.	< 0.1
12	20.8	594	**K-G-3-R-7**	49.8 ± 7.7[1)]	41.5 ± 3.7	12.03 ± 2.5	6.15 ± 0.2
13	21.1	594	**Q-R-3-R-7**				
14	21.3	624	**I-G-3-R-7**	16.7 ± 4.3	20 ± 2.3	2.5 ± 0.4	1.5 ± 0.1
15	22.5	610	**Q-R-G-3**	0.7 ± 0.3	0.6 ± 0.13	0.1 ± 0.0	n.d.
16	23.9	464	**Q-G-3**	1.5 ± 0.1	2.0 ± 0.4	0.3 ± 0.1	0.1 ± 0.0
17	24	578	**K-R-3-R-7**	3.8 ± 0.3	1.1 ± 0.1	0.6 ± 0.1	0.3 ± 0.1
18	27.4	448	**K-G-3**	1.7 ± 0.1	12.1 ± 1.6	0.2 ± 0.1	0.4 ± 0.1
19	28	478	**I-G-3**	1.3 ± 0.1	2.6 ± 0.6	0.1 ± 0.0	< 0.1
20	32.8	432	**K-R-3**	1.0 ± 0.2	1.3 ± 0.2	0.1 ± 0.0	< 0.1
non flavonoids							
1	11.5	448	Glucobrassicin	5.6 ± 0.8	6.9 ± 0.8	4.7 ± 1.2	6.0 ± 1
6	15.8	478	4-Methoxyglucobrassicin	5.3 ± 1.3	5.4 ± 1.1	2 ± 0.1	2.2 ± 0.9
11	20.3	478	Neoglucobrassicin	42.3 ± 6.4	26 ± 5.0	8.8 ± 1.2	4.0 ± 2

TABLE 1. **Flavonoid derivatives detected in the MeOH extracts of entire root and RT-EZ of wild type and *pin2*.**

The identification of the flavonoid derivatives was achieved by HPLC-UV(-)-MS/MS, comparison to reference compounds and/or according to (43-46). Each compound was quantified by integration of the corresponding signal area (x10^6 AU) presents in the extract ion chromatogram (EIC, [M-H]-) after HPLC-MS experiment. Values of entire roots represent means ± SE of at least three independent experiments (Student's *t*-test, $P<0.05$, n=2-4). Each extraction consists of a pool of 100 different roots. Quantification of RT-EZ flavonoid compounds is the result of at least two independent extractions in which each time 150 5mm-long root apices from 12 different agar plates were pooled. The natural flavonoid derivates described in this table have abbreviations as follows: G, glucose; K, kaempferol; I, isorhamnetin; Q, quercetin; R, rhamnose. Numbers indicate the position of glycosylation relative to the flavonol core. All flavonols identified are *O*-glycosylated.

[1)] Compound 12 and 13 are co-eluting in the HPLC-(-)-ESI-MS chromatogram and show the same quasi-molecular ions (*m/z* 593); therefore, they were integrated together.

with flavonoids, allows *in situ* flavonoid staining and localization in *Arabidopsis* seedlings (Peer *et al.,* 2004; Peer *et al.,* 2001; Peer and Murphy, in press). In wild-type seedlings, flavonoid DPBA staining is restricted to the shoot apex and cotyledons, the root-shoot junction, along the primary root, and most intensely to the root elongation zone (Figure 1A and Figures S1A-C) (Peer *et al.,* 2001). In contrast, flavonoid-DPBA fluorescence in *pin2* mutant was clearly lower at the root tip-elongation zone (RT-EZ) (Figure 1B and Figures S1E-G). Manipulation of endogenous auxin levels by addition of 100nM IAA increased DPBA fluorescence in the wild type (Peer *et al.,* 2004) and, although to a lesser extend, also in the *pin2* RT-EZ (Figures S1D and S1H), suggesting that auxin and flavonoid levels *in planta* are interconnected (Peer *et al.,* 2004; Peer and Murphy, in press).

To determine how flavonoid distribution was affected by PAT alterations, we qualitatively and quantitatively investigated endogenous flavonoid derivatives present in wild-type and *pin2* RT-EZ and entire roots using HPLC-UV-(-)-ESI-MS/MS and HPLC-ESI-MS, respectively (Table I). Consistent with DPBA staining profiles (Figures 1A-B and S1), we found that the total amount of flavonoids was significantly reduced in the RT-EZ of *pin2* mutant (Figures 1C and 1D) whereas no significant difference was observed over the entire root (Figures 1C and S2). *Pin2* roots showed altered accumulation of specific flavonol glycosides both in the RT-EZ and in the entire root (Table 1 and arrows in the extraction ion chromatograms (EIC) of the masses of interest in Figures 1D and S2). In *pin2* entire roots and RT-EZ, a shift from di- and triglycosylated flavonols to monoglycosylated flavonols, like for K-G-3 (compound **18**), was observed (Table 1). Intriguingly, accumulation of compounds glycosylated in the 7-*O*-position was strongly reduced in *pin2* (Table 1), which

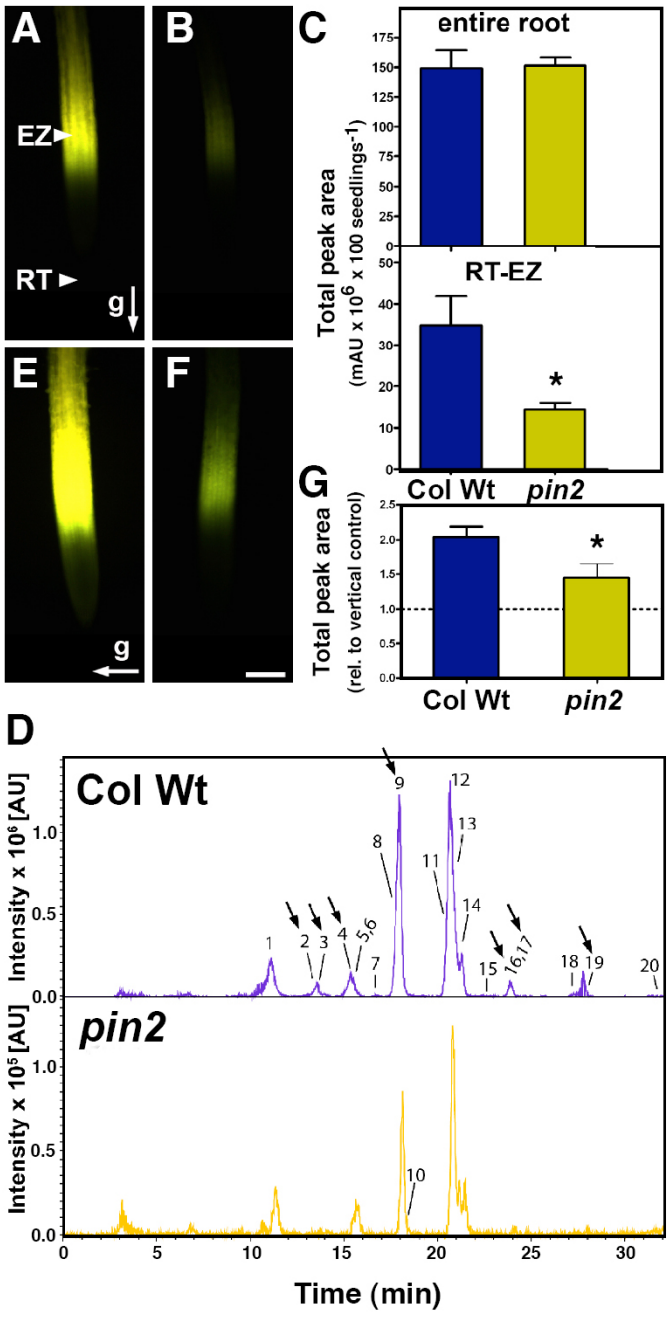

FIGURE 1. **Defects in basipetal auxin transport are associated with altered root flavonoid accumulation.**

A-D, Flavonoid accumulation in the entire root and root elongation zone of wild type (Col Wt) and *pin2* (***A,*** wild type; ***B,*** *pin2*). EZ, elongation zone; RT, root tip. Bar, 100µm. ***C,*** Total amount of flavonoid derivatives detected in the entire root and RT-EZ of wild type and *pin2*. Values represent means ± SE (*n*=2-5 replicates); * significantly different from the wild type (Student's *t*-test, *P*<0.05).

D, Representative sum of extracted ion chromatograms $[M-H]^-$ of flavonoid derivatives found in wild type and *pin2* RT-EZ analyzed by HPLC-ESI-MS. Significantly altered compounds are indicated by arrows. Peak numbers correspond to flavonoid derivates listed in Table I. Note 10-times lower intensitiy scale for *pin2* root elongation zone in comparison to wild type.

E-G, Accumulation of flavonoids in 2h gravity stimulated roots (***E,*** wild type; ***F,*** *pin2*). The arrows indicate the direction of the gravity vector relative to the root. Bar, 100µm. *In situ* flavonoid visualization (***A, B, E, F***) using DPBA (yellow fluorescence) was performed as described in Materials and methods.

G, Gravity-induced root phenolic compound accumulation normalized to phenolic compound accumulation in vertical control. Values represent means ± SE (*n*=2-5 replicates); * significantly different from the wild type (Student's *t*-test, *P*<0.05).

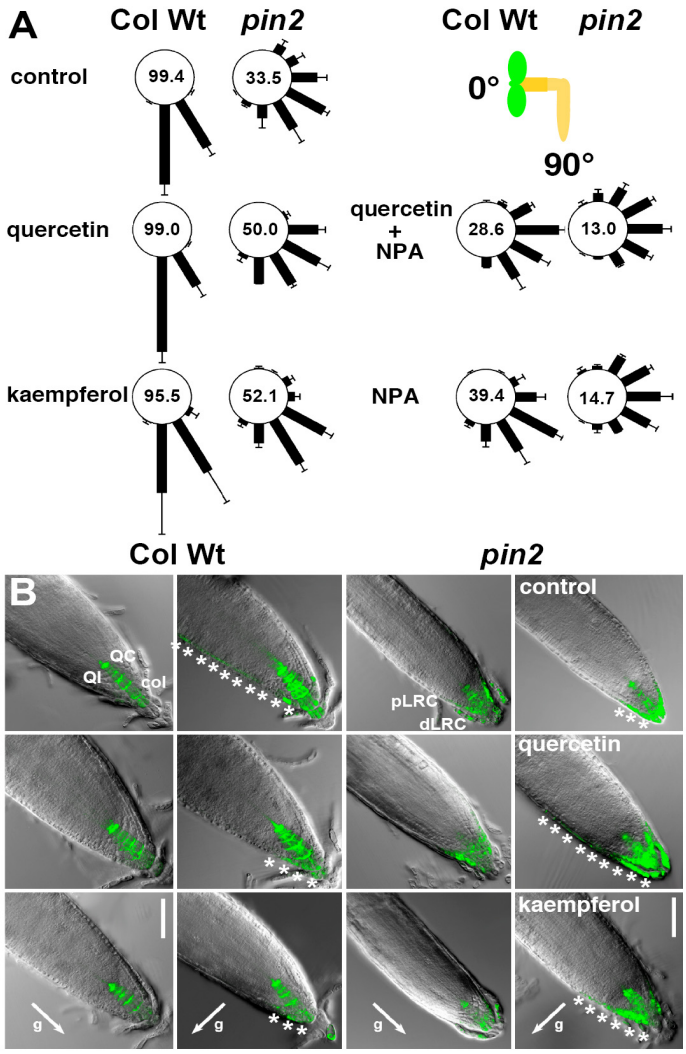

FIGURE 2. **Exogenous flavonols but not NPA partially rescue the agravitropic response of *pin2* by restoring asymmetric auxin gradients.**
A, Gravity responses of wild type (Col Wt) and *pin2* (*eir1-4)* roots after reorientation of 90° to horizontal (see sketch). The length of each bar represents the mean percentages ± SE of seedlings showing the same direction of root growth of at least three independent experiments; numbers correspond to the sum of 90° and 120° sectors.
B, Expression of the auxin-reporter construct $DR5_{rev}$-GFP in wild type (Col Wt) and *pin2* (*eir1-4)* root tips was assessed prior to, and after 2h gravity stimulation on control (top row), quercetin (mid row) and kaempferol treated roots (bottom row). White asterisks indicate more pronounced *DR5-GFP* expression at the lower side of gravistimulated roots indicating enhanced basipetal auxin reflux. The gravity vector relative to the root tip is indicated by an arrow. QC, quiescent center; QI, columella initials; col, mature columella cells; dLRC, distal lateral root cap; pLRC, proximal lateral root cap. Bar, 75 µm.

suggests that auxin levels may have an effect on the corresponding glycosyltransferases. Conversely, those peaks, whose accumulation is affected in *pin2* roots, may be functionally important for the regulation of auxin transport during root gravitropism.

As previously reported (Buer and Muday, 2004; Buer *et al.,* 2006), gravity stimulation increased the DBPA fluorescence in wild type RT-EZ by nearly two-fold, with a maximum at 1.5 to 2.5h after stimulation. A smaller but significant increase in DPBA fluorescence was observed also in *pin2* mutant (Figures 1E-F). Flavonoid quantification by HPLC-UV (Figure 1G) was consistent with the DPBA staining (Figures 1E-F).

Collectively, our results demonstrate that the synthesis and the transient accumulation of specific flavonoid glycosides in the root tip-elongation zone - but not over the entire root or in the shoot - are impaired quantitatively and qualitatively in *pin2* (Figures 1, S1, S2).

Flavonoids rescue the agravitropic response of *pin2* roots

To test whether flavonoid concentrations play a critical role in the response to gravity stimuli, we searched for conditions in which flavonoids could be supplied without affecting root growth and gravitropism by acting as auxin transport inhibitors (Brown *et al.,* 2001; Peer *et al.,* 2004). Concentrations up to 100 nM kaempferol or quercetin did not significantly influence wild-type gravitropic responses (95.5% and 99.0% instead of 99.4% (sum of 90° and 120° sectors), Figure 2A). Roots of the *eir1-4* mutant, a severe agravitropic allele of *pin2* (Luschnig *et al.,* 1998), were gravity-stimulated in the presence of 100 nM flavonoids. Intriguingly, *pin2* gravitropic root bending was partially restored by quercetin (50.0%) and kaempferol (52.1%, Figure 2A). The same gravitropic assay was performed in the presence of 5µM 1-*N*-naphtylphtalamic acid (NPA), a synthetic polar auxin efflux inhibitor and herbicide (naptalam©), blocking basipetal IAA movement from the root tip (Casimiro *et al.,* 2001). In wild type plants, NPA treatment resulted in an agravitropic phenotype (39.4%) (16,30). However, NPA failed to restore but rather impaired *pin2* root gravitropism (14.7%). We repeated the quercetin treatment in the presence of NPA, and found that in wild type NPA and quercetin had additive effect (28.6%), while in *pin2* the quercetin action was prevented by NPA (13.0%), indicating that

the rescue of *pin2* agravitropic response by quercetin is NPA sensitive.

The cause of *pin2* agravitropic root growth is a failure in the accumulation of auxin at the lower side of the root elongation zone (Luschnig *et al.,* 1998). We therefore tested whether flavonoid treatment restored the asymmetric auxin distribution necessary for differential growth of the epidermal cells during gravitropic responses by monitoring the *DR5:GFP* expression, which reflects relative auxin levels. As previously reported (Ottenschlager *et al.,* 2003), in wild type seedlings with vertically grown roots, the GFP fluorescence appeared in specific stele cell files and was localized in the quiescent center (QC), in the columella initials (QI) and in the mature columella cells (col) (Figure 2B). Vertically oriented *pin2* roots exhibited a strong signal in the distal lateral root cap (dLRC) with only weak extension towards the proximal lateral root cap (pLRC), reflecting defect in basipetal auxin distribution. In vertically oriented roots treatments with 100nM quercetin or kaempferol resulted in fluorescence essentially similar to the control condition in both the wild type and *pin2* mutant (Figure 2B). Upon gravity stimulation, fluorescent signals in wild-type roots appeared in the lower sides, in the distal lateral root cap and EZ, both in solvent controls (control) and, although slightly reduced, in the presence of flavonoids (Figure 2B, asterisks). In contrast, flavonoid treatment of gravity stimulated *pin2* roots resulted in a gain of a strong asymmetric signal in the entire lateral root cap with significantly increased fluorescence on the lower half of the root and decreased fluorescence on the upper half of the root (Figure 2B, asterisks).

In order to statistically quantify auxin accumulation after gravity stimulation, we determined auxin gradient intensities (in arbitrary units from 0 to 3) in root tips differently oriented relative to the gravity stimulation vector (for experimental details see legends of Table 2 and S1). Compared to wild type (11.7%, Table 2), the majority of *pin2* seedlings tested exhibited a symmetrical auxin distribution (53.8% of auxin gradient intensity 0). Only occasionally clear auxin gradients (defined as sum of 2 + 3) could be observed in *pin2* upon gravity stimulation (27.7% (2+3), Table 2), which is in line with the results of the gravitropic assays (Figure 2A). Interestingly, a similar frequency of clear auxin gradients in *pin2* was also observed in vertically grown roots (31.7%) but not found in the wild type (1.7%, Table S1). The gain of signal asymmetry between lower and upper side in flavonoid-treated, gravity stimulated *pin2* roots continued in the elongation zone and was observed in the majority of the flavonoid treated roots tested

	0	1	2	3		
root tip orientation	g				total (0+1+2+3)	% (2+3) of total (0+1+2+3)
Solvent control						
A	3 17	10 3	17 1	2 0	32 21	59.4 4.8
B	4 14	15 7	9 5	0 8	28 34	32.1 38.2
C	0 4	0 2	0 4	0 0	0 10	0 40
Total	7 35	25 12	26 10	2 8	60 65	**46.7 27.7**
% of total	**11.7 53.8**	**41.7 18.5**	**43.3 15.4**	**3.3 12.3**		
Quercetin						
A	12 11	27 9	32 12	6 4	77 36	49.6 44.4
B	2 5	9 5	11 13	5 20	27 43	59.3 76.7
C	1 5	0 3	0 7	0 6	1 21	0 61.9
total	15 21	36 17	43 32	11 30	105 100	**51.4 62**
% of total	**14.3 21**	**34.3 17**	**41 32**	**10.5 12.3**		

TABLE 2. **The majority of quercetin-treated *pin2* roots form IAA gradients upon gravity stimulation.**
Absolute and relative numbers of wild type (black) and *pin2* (red) seedling showing IAA gradients. Definition of IAA gradients is based on the strength of IAA movement from the LRC to the EZ, as assessed by confocal imaging of DR5-GFP fluorescent signals upon 2h gravity stimulation. Gradient intensity is quantified in arbitrary units (0= symmetric signal; 1= weak signal asymmetry, up to distal lateral root cap; 2= intermediate signal asymmetry, up to proximal lateral root cap; 3= strong signal asymmetry, up to elongation zone). Classification of root tip orientation is relative to the gravity stimulation vector, as depicted (A= neutral; B= towards the gravity stimulation vector; C= opposite to the gravity stimulation vector). Number of analysed wild type (*pin2*) seedlings was 60 (65) on solvent control and 105 (100) on 100 nM quercetin plates, respectively. Gravity vector (g) relative to the root is indicated by an arrow.

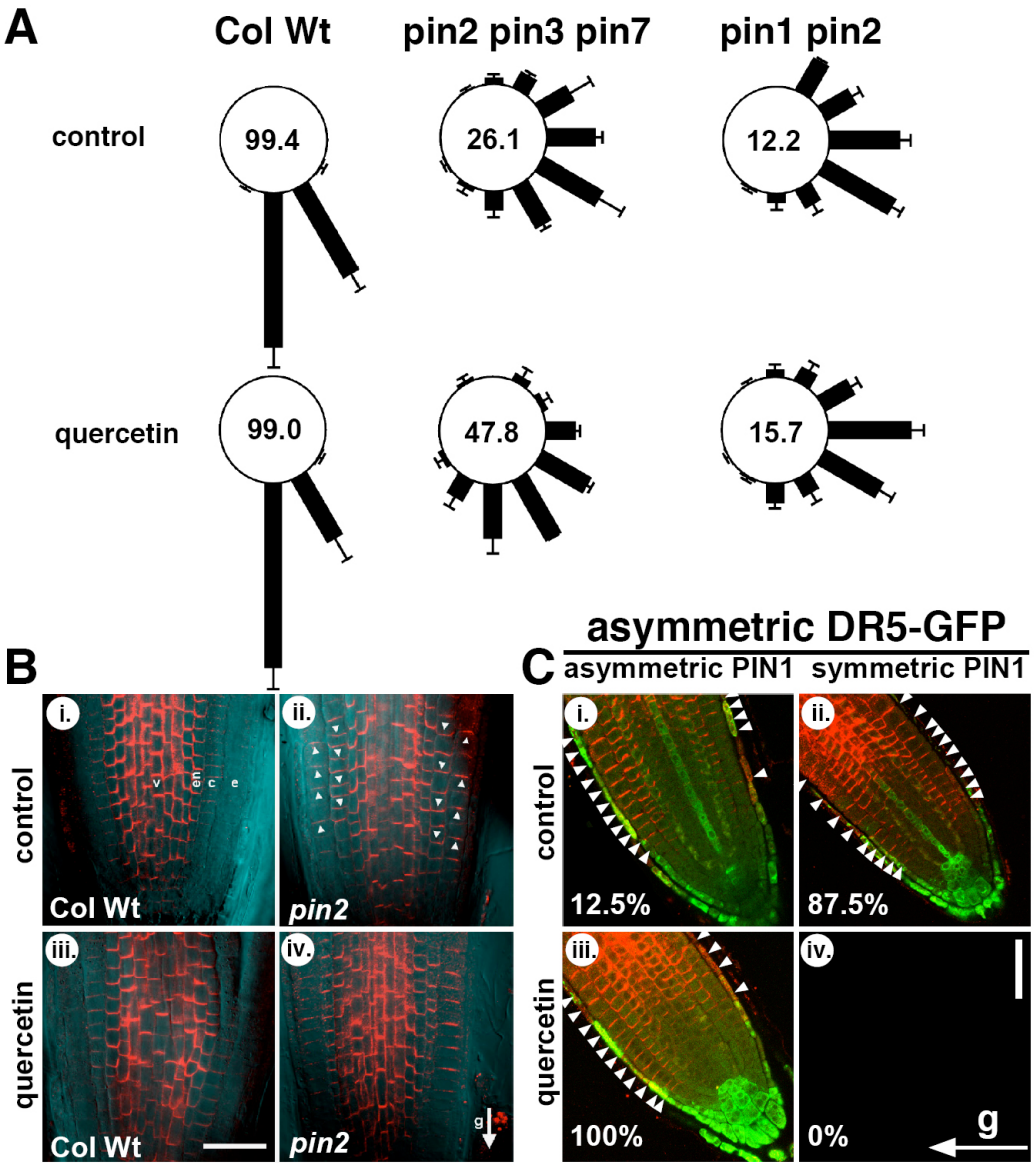

FIGURE 3. **Flavonoid-dependent rescue of *pin2* agravitropic phenotype requires PIN1 and is correlated with asymmetric PIN1 distribution across gravity-stimulated tissues.**

***A*,** Gravity responses of *pin2 pin3 pin7* and *pin1 pin2* (*pin1 eir1*) roots. The length of each bar represents the mean percentages ± SE of seedlings showing the same direction of root growth of at least three independent experiments; numbers correspond to the sum of 90° and 120° sectors.

***B*,** Whole-mount *in situ* immunolocalization of PIN1 protein (red) in 5d *pin2* (*eir1-4*; ii. and iv.) and wild type (Col Wt; i. and iii.) vertically seedlings transferred on media supplemented with 100nM quercetin. Gravity vector is indicated by an arrow. White arrows indicate PIN1 protein apical localization in the epidermis and basal localization in the cortex cells of *pin2* root tip. Note that the appearance of slightly different PIN1 signals in the *pin2* epidermis and cortex (ii.-iv.) do not reflect unequal expression but are the result of unequal background intensities due to scattered light. v, vascular bundle; en, endodermis; c, cortex; e, epidermis. Bar, 30 µm.

***C*,** Whole-mount *in situ* immunolocalization of PIN1 protein in *pin2* after 2h of gravity stimulation; gravity vector is indicated by an arrow. 4d *pin2* seedlings were transferred on media supplemented with 100nM quercetin or the solvent (control). Red, PIN1; green, $DR5_{rev}$-GFP expression. White arrows indicate more pronounced PIN1 proteins levels at the lower or upper side of gravity stimulated root tip. Bar, 30µm. Percentages indicate relative occurrence of asymmetric or symmetric PIN1 distributions with asymmetric DR5-GFP signals; the total number of analysed roots that showed simultaneous clear DR5-GFP and PIN1 signals was 47.

(62.0% compared to 27.7% without treatment, Table 2). In contrary, quercetin treatment had only low effect on wild type (51.4% compared to 46.7% without treatment). These data show that exogenous flavonoids are able to re-establish the asymmetric *DR5-GFP* activity in the *pin2* mutant roots and restore their gravitropic responses.

Flavonoids promote asymmetric PIN1 shifts

Since some levels of functional redundancy between PIN proteins have been already demonstrated (Vieten *et al.,* 2005; Blilou *et al.,* 2005), we tested the root gravitropic responses of the triple *pin2 pin3 pin7* mutant in the presence of 100nM quercetin. A strong agravitropic root phenotype was evident for *pin2 pin3 pin7* in control conditions (Figure 3A) (Blilou *et al.,* 2005), which could be partially rescued by the application of 100 nM of quercetin (47.8% compared to 26.1% without treatment, Figure 3A) or kaempferol (data not shown). From this result, we conclude that neither PIN3 nor PIN7 are required for flavonoid-dependent rescue of the agravitropic response of *pin2*, being in-line with their proposed role and expression in gravity perception tissues (Blilou *et al.,* 2005). Importantly, when we performed the same gravitropic assay with roots of the double mutant *pin1 pin2*, quercetin could not complement its agravitropic phenotype (15.7% compared to 12.2% without treatment, Figure 3A). These data demonstrate that PIN1 is essential for flavonoid-dependent complementation of *pin2* gravitropism, which is in agreement with its expression in gravity transduction or response tissues.

To trace the behaviour of PIN1 protein during *pin2* gravitropic responses and to uncover a possible link between the action of flavonoids and PIN1 activity *in vivo*, we analysed PIN1 localization in *pin2* roots exposed to 100nM quercetin prior to, and during gravity stimulation. Consistent with previous reports (Blilou *et al.,* 2005; Vieten *et al.,* 2005), in vertically oriented wild type roots PIN1 was mainly found at the basal (lower) end of vascular and endodermis cells with occasional weak expression in the epidermis and in the cortex (Figure 3B, i.). In vertical *pin2* roots, PIN1 was ectopically expressed in the endogenous PIN2 domain, showing symmetric apical (up) localization in the epidermis and basal (down) localization in cortex cells (arrows in Figure 3B, ii.) (Vieten *et al.,* 2005). This symmetric PIN1 location was only rarely altered by a gravity stimulus on solvent control (12.5% of roots showing this pattern, Figure 3C, i.). Treatments with 100nM quercetin did not affect PIN1 expression or its symmetry neither in wild type nor in *pin2* vertically grown roots (Figures 3B, iii.- iv.). In contrast, gravity stimulation of *pin2* roots in the presence of 100nM quercetin resulted in asymmetric expression of PIN1 protein, with stronger PIN1-specific signals at the lower side of the root tip (Figure 3C, iii.). The establishment of flavonoid-mediated PIN1 gradients strictly correlated with the development of asymmetric DR5-GFP signals (100%, Fig. 3C, iii), while in the absence of quercetin asymmetric PIN1 patterns correlating with asymmetric DR5-GFP signals were only rarely found (12.5%, Fig. 3C,i). We never found asymmetric DR5-GFP gradients that correlated with symmetric PIN1 patterns (0%, Figure 3C, iv.) or symmetric DR5-GFP gradients correlating with asymmetric PIN1 expression (0%, Figure S3, i.). But for few roots we found a weak correlation between asymmetric PIN1 patterns and symmetric DR5-GFP (22.2%, Figure S3, iii.).

Discussion

Current paradigm in auxin research is that flavonoids act as non-essential, endogenous modulators of PAT by transiently accumulating in the epidermal cells of the root elongation zone (Buer and Muday, 2004; Brown *et al.,* 2001; , Murphy *et al.,* 2000; Peer *et al.,* 2004; Peer and Murphy, 2006; Peer *et al.,* 2001). Our data demonstrate that defects in basipetal auxin transport are associated with altered root flavonoid accumulation. In conditions in which PIN2-dependent auxin transport is genetically blocked, synthesis and transient accumulation of specific flavonoid glycosides in the root tip-elongation zone - but not over the entire root or in the shoot - are impaired quantitatively and qualitatively (Figures 1, S1-S2). However, *pin2* roots retain the ability to accumulate flavonoids in response to a gravity stimulus, but not as efficiently as the wild type.

Application of low concentrations of exogenous flavonoids restores gravitropic root tip bending in a genetic background defective in basipetal auxin transport and this mode of flavonoid action is distinct from that of NPA. Moreover, our results showing that gravity stimulation of *pin2* roots in the presence of

inhibitory concentrations of NPA did not complement *pin2* gravitropism, suggest that in our experimental conditions flavonoids do not act as PAT inhibitors. Quantitative cell biology analysis of DR5-GFP signals show that chemical complementation of gravitropism by exogenous flavonoids is accompanied by re-establishment of asymmetric distribution of *DR5-GFP* in the *pin2* mutant roots. This suggests that restoration of gravitropic responses is achieved via bypassing the requirement of an active PIN2 protein, thus implying the activation of a PIN2-independent mechanism for basipetal auxin transport.

Quantification of root gravitropic response of different *pin* mutant combinations suggests that PIN1 is essential for flavonoid-dependent complementation of *pin2* gravitropism, which is in agreement with its expression in gravity transduction or response tissues. Using a quantitative cell biological approach, we also provide evidence that flavonoid-dependent rescue of *pin2* agravitropism by PIN1 is correlated with asymmetric PIN1 distribution across gravity-stimulated tissues. In summary, our findings suggest that PIN1 is the auxin efflux complex component that facilitates basipetal auxin fluxes for gravitropic responses in flavonoid-treated *pin2* roots. The observed basal-apical PIN1 shifts in *pin2* roots (Figure 3B, ii) are in line with the finding that PIN1 and PIN2 have redundant roles in the root meristem size control (Blilou *et al.,* 2005) and that PIN1 can functionally replace PIN2 when ectopically expressed and localized at the upper side of epidermal cells (Wisniewska *et al.,* 2006). Moreover, PIN1 showed a "PIN2-like" apical localization in epidermis and basal localization in cortex cells in roots of *pin2* mutants (Vieten *et al.,* 2005). However, our data indicate that flavonoids are the native key effectors that promote asymmetric PIN1 shifts with stronger PIN1-specific signals at the lower side of the root tip in response to a gravity stimulus, thus redirecting basipetal auxin streams necessary for the root tip bending.

The fact that flavonols can inhibit PAT and displace NPA from their membrane binding sites has led to the idea that flavonoids and NPA act on similar targets using identical mechanisms. While several lines of evidence suggest that plant PGPs, like PGP1, PGP4 and PGP19, are direct targets of flavonoid regulation (Blakeslee *et al.,* 2007; Geisler *et al.,* 2005; Bouchard *et al.,* 2006) either via protein phosphorylation, inhibition of ATPase activity or allosteric binding in analogy to mammalian PGPs (Conseil *et al.,* 1998), the effect of flavonoids on the members of the PIN family has received less attention and seems to be indirect (Peer *et al.,* 2004; Peer and Murphy, in press). With this work we provide two lines of evidence demonstrating that flavonoids, at least under our experimental conditions, do not solely inhibit efflux transporters (in analogy to NPA) (Geisler *et al.,* 2005; Bouchard *et al.,* 2006; Terasaka *et al.,* 2005), but are able to function as versatile modulators of polar auxin flows. Firstly, flavonoid concentrations applied to the roots did not significantly alter wild type gravitropism and therefore most likely also not PAT. Secondly, NPA failed to restore *pin2* root gravitropism while rescue of *pin2* agravitropic response by quercetin was NPA sensitive. Our data showing that flavonoids can promote PIN1 shifts in response to a gravity stimulus underline an involvement of flavonoids in cellular trafficking of auxin transport complex components as recently suggested (Peer *et al.,* 2004; Peer and Murphy, in press). The modulation of root gravitropism by flavonoids may result from a combination of PGP regulation and PIN trafficking that might be concentration-dependent and interconnected.

While the cellular targets of flavonoid action are now known, the underlying mechanism remains elusive. Transport assays with PIN proteins suggest that flavonoids probably do not interact with PINs directly. However, flavonoids affect specific PIN expression, location and cellular trafficking probably through interaction with regulatory proteins (Peer *et al.,* 2004; Peer and Murphy, in press). Recently, plasma membrane PIN shifts have been demonstrated to be caused by antagonistic PIN phosphorylation via protein kinase PINOID (PID) and protein phosphatase 2A (PP2A) (Friml *et al.,* 2004; Michniewicz *et al.,* 2007). Our data together with the fact that flavonols are routinely used as both protein phosphatase and kinase inhibitors make PID or PID-related WAG kinases (Santner and Watson, 2006) and/or PP2A-like phosphatases the most likely candidate targets for flavonol-mediated PIN-shifts.

Acknowledgements

We would like to thank Dr. Heller (GSF, Munich) and Dr. Veit (Kaufering) for providing us with flavonol standards that were invaluable for the flavonol structure analysis and V. Sovero and S. Peters for comments on the manuscript. This work was supported by funds of the Swiss National Foundation to M.G. (3100AO-111912) and to E.M. (within the NCCR Plant Survival)), the Novartis foundation (to M.G.) and by the Ministry of Science and Technology of South Korea (to Y.L. and E.M.).

Supplemental data

The original on-line version of this article (available at http://www.jbc.org) contains the following supplemental figures .

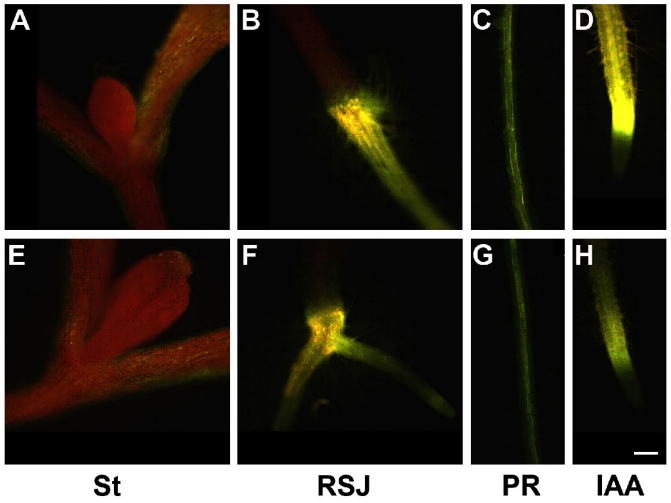

SUPPL. FIGURE 1. **Flavonoid distribution in cotyledons, root-shoot junction and primary root of *pin2* mutant is not affected, but exogenous supply of IAA resulted in increased flavonoid accumulation in the EZ.**
In situ flavonoid visualization of *Arabidopsis* seedlings using diphenylboric acid 2-aminoethyl ester (DPBA, a fluorescent dye that interacts with flavonoids) by epifluorescence microscopy (yellow fluorescence). These patterns were observed in all stained seedlings. ***A-D***, wild type (Col Wt); ***E-H***, *pin2*. St, stem; RSJ, root-shoot junction; PR, primary root; IAA, application of 100 nM IAA. Bar, 100 µm.

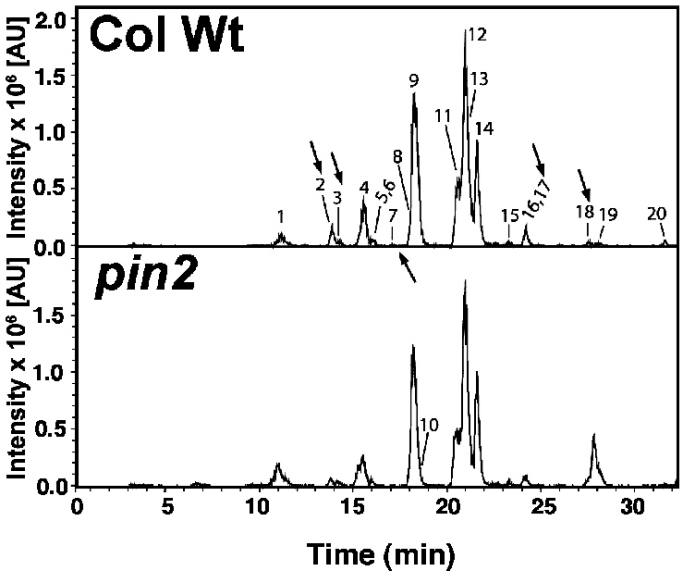

SUPPL. FIGURE 2. **Accumulation of specific flavonoid glycosides in the entire *pin2* root is altered qualitatively but not quantitatively.**
Representative sum of EIC of flavonoid derivatives found in wild type (Col) and *pin2* entire roots analysed by LC-ESI-MS. Selected ions are *m/z* 431, 447, 463, 477, 577, 593, 609, 623, 739, and 755, 771. Altered compounds are indicated by arrows. Peak numbers correspond to flavonoid derivates listed in Table 1. Note 10-fold higher intensities at the whole root level for *pin2* compared to the root tip-elongation zone (Figure 1D).

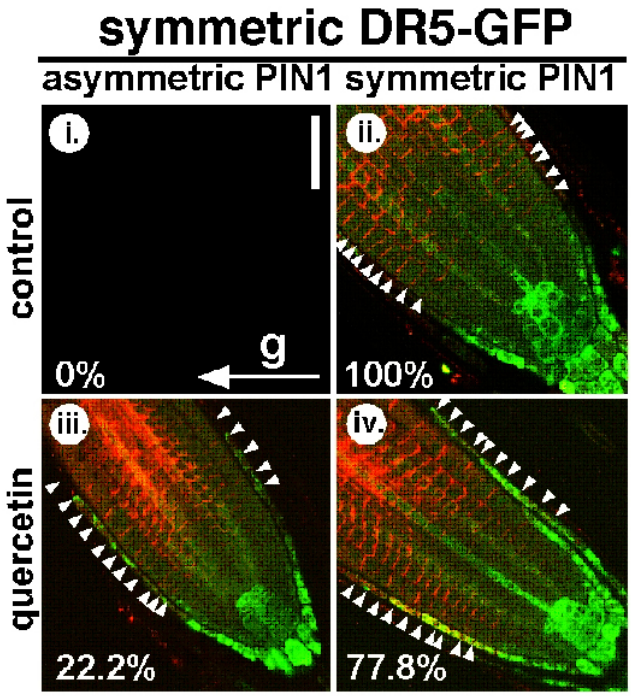

SUPPL. FIGURE 3. **Flavonoid-dependent rescue of basipetal auxin reflux *pin2* is correlated with PIN1 asymmetric distribution across gravity-stimulated tissues.**
Whole-mount *in situ* immunolocalization of PIN1 protein in *pin2* after 2h of gravity stimulation. 4 dag *pin2* seedlings were transferred on media supplemented with 100nM quercetin or the solvent (control) for 24h. Red, PIN1; green, $DR5_{rev}$-GFP expression. White arrows indicate more pronounced PIN1 proteins levels at the lower or upper side of gravity stimulated root tip. Bar, 30 mm. Gravity vectors relative to the root are indicated by an arrow. Percentages indicate relative occurrence of asymmetric or symmetric PIN1 distributions with symmetric DR5-GFP signals; the total number of analysed roots showing both clear DR5-GFP and PIN1 signals was 47.

root tip orientation	0	1	2	3	total	% (2+3) of total
	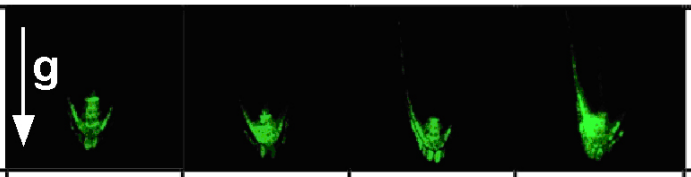					
A 	51/ 12	5/ 3	0/ 4	0/ 0	56/ 19	0/ 21.1
B 	2/ 11	0/ 3	0/ 6	0/ 9	2/ 29	0/ 51.7
C 	1/ 10	0/ 4	1/ 0	0/ 1	2/ 15	50/ 6.7
total	**54/ 33**	**5/ 10**	**1/ 10**	**0/ 10**	**60/ 63**	**1.7/ 31.7**
% of total	**90/ 52.4**	**8.3/ 15.9**	**1.7/ 15.9**	**0/ 15.9**		

SUPPL. TABLE 1. **Weak asymmetric IAA gradients were occasionally observed in vertically oriented *pin2* roots.**
Absolute and relative numbers of wild type (black) and *pin2* (red) seedling showing IAA gradients. Definition of IAA gradients is based on the strength of IAA movement from the LRC to the EZ, as assessed by confocal imaging of DR5-GFP fluorescent signals upon gravity stimulation. Gradient intensity is quantified in arbitrary units (0= symmetric signal; 1= weak signal asymmetry, up to distal lateral root cap; 2= intermediate signal asymmetry, up to proximal lateral root cap; 3= strong signal asymmetry, up to EZ). Classification of root tip orientation is relative to the gravity stimulation vector, as depicted (A = neutral; B = to the left (lower than 90°); C = to the right (higher than 90°). Number of analysed wild type (*pin2*) seedlings was 60 (63). Gravity vector (g) relative to the root is indicated by an arrow.

PIS1 Exporter for Auxinic Compounds Defines Outer Polar Domain in Plants

Kamil Růžička[1,2], Eliška Nejedlá[3], Angus Murphy[4], Jürgen Kleine-Vehn[1,2], Aurélien Bailly[5], Vassilena Gaykova[2], Hironori Fujita[6], Hironori Ito[7], Kunihiko Syōno[8], Jan Hejátko[3], William M. Gray[7], Enrico Martinoia[5], Markus Geisler[5], and Jiří Friml[1,3]

[1]VIB Department of Plant Systems Biology, Ghent University, Technologiepark 927, 9052 Gent, Belgium
[2]Zentrum für Molekularbiologie der Pflanzen (ZMBP), University of Tübingen, Auf der Morgenstelle 3, D-72076 Tübingen, Germany
[3]Department of Functional Genomics and Proteomics, Kamenice 25, Masaryk University, CZ-62500 Brno, Czech Republic
[4]Department of Horticulture, Purdue University, West Lafayette, Indiana 47907-2010, U.S.A.
[5]University of Zurich, Institute of Plant Biology and Zurich-Basel Plant Science Center, CH-8008 Zurich, Switzerland
[6]National Institute for Basic Biology, 38 Nishigounaka, Okazaki 444 - 8585, Japan
[7]Department of Plant Biology, University of Minnesota-Twin Cities, St. Paul, MN 55108, U.S.A.
[8]Faculty of Science, Japan Women's University, Bunkyo-ku, Tokyo 112-8681, Japan

Correspondence and request for material should be addressed to J.F. (e-mail: jiri.friml@psb.ugent.be)

Summary

Cell polarity is manifested by the polar delivery of cargos to different plasma membrane domains and is a fundamental feature of multicellular organisms. In plants, cell polarity and tissue patterning are linked by the directional intercellular flow of the signalling molecule auxin. Auxin efflux and influx carriers from PIN and AUX1 families, respectively, define opposite polar domains in plant cells and their polar localization mediates auxin flow and hence multiple developmental processes. Here we identified a transporter for auxinic compounds that defines a novel outer polar domain in plant cells. We mapped the polar auxin transport inhibitor sensitive (pis1) mutation, which confers enhanced auxin sensitivity in Arabidopsis, to a gene encoding the pleiotropic drug resistance-type transporter ABCG37. PIS1 acts in plants and heterologous systems as an efflux transporter for natural/synthetic auxins and auxin transport inhibitors. PIS1 functions in root surface extrusion of auxin-like compounds, not in directing auxin flow along the apical-basal axis, and localizes asymmetrically to the outer lateral plasma membrane domain of root epidermis. PIS1 outer lateral delivery does not require established components of apical or basal targeting. Simultaneous localization of PIN1, PIN2 and PIS1 transporters to distinct polar domains of the same cell demonstrates that plant cells posses at least three polar targeting pathways operating in parallel. This demonstrates that, unlike other eukaryotes, plants can independently regulate material and information flow across cell boundaries in both apical-basal and outer-inner directions.

Introduction

Cell polarity is an elementary attribute of multicellularity. Individual cell polarities are translated into tissue and organ polarity and, ultimately, shape. At the level of the individual cell, polarity is typically reflected by the asymmetric distribution of intracellular components that can form functionally and/or morphologically distinct domains. Both in animal and plant models, a maximum of two polar domains along with corresponding targeting pathways have been demonstrated in a single cell. In animal epithelial cells, a number of cargos targeted to the apical and basolateral domains have been identified that functionally define the two opposing surfaces of the epithelium (Drubin, 2000; Knoblich, 2000). In plants, apical and basal domains are designated by polar localization of the PIN1 and AUX1 auxin carriers, which mediate the directional flow of the plant signalling molecule auxin (Swarup *et al.*, 2001; Yang *et al.*, 2006; Petrasek *et al.*, 2006; Luschnig *et al.*, 1998) and thus provide a connection between cell polarity and auxin gradient-dependent tissue patterning (Sauer *et al.*, 2006; Scarpella *et al.*, 2006; Wisniewska *et al.*, 2006).

Results and Discussion

To gain further insight into mechanisms of auxin transport, we analyzed the *polar auxin transport inhibitor sensitive1* (*pis1*) mutant of *Arabidopsis thaliana*, which is the only reported

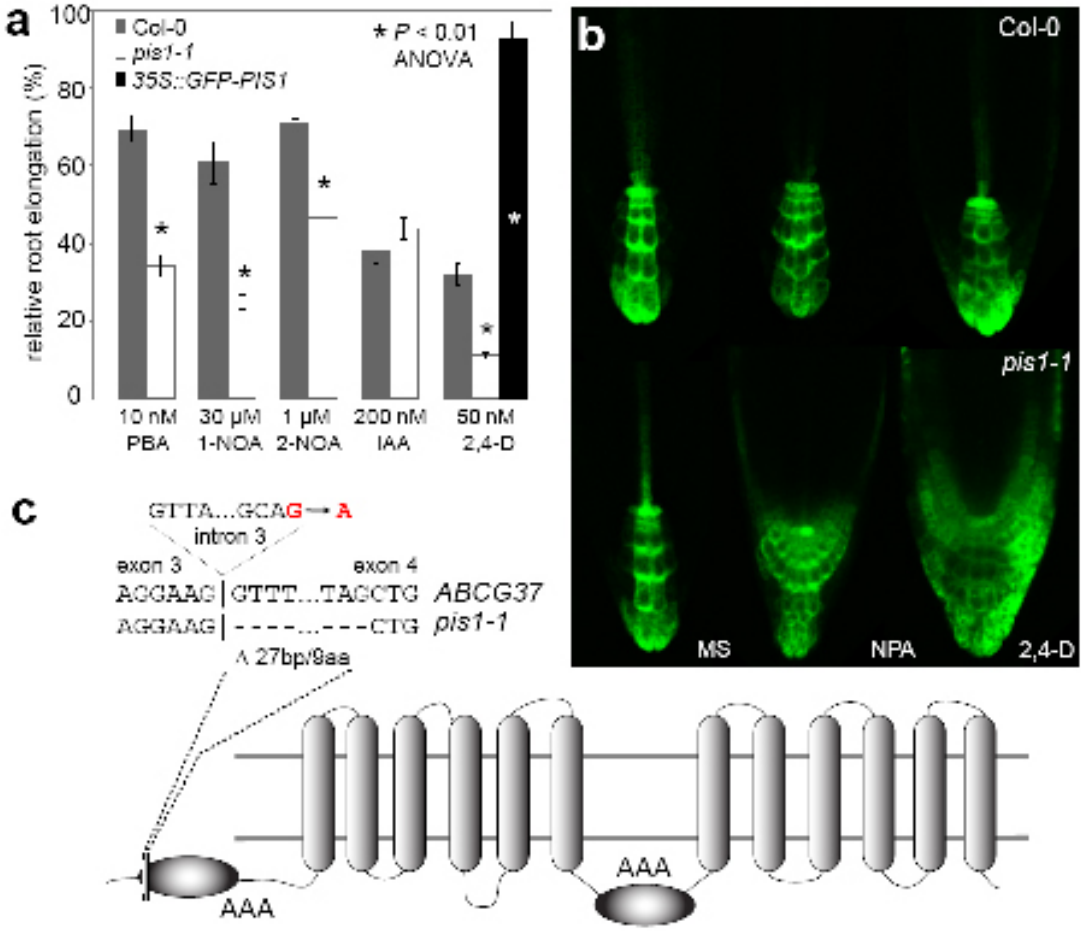

FIGURE 1. ***pis1* mutation leads to hypersensitivity to auxinic compounds and is caused by a defective PDR-type ABCG37 transporter.**

(a) *pis1-1* root growth is hypersensitive to different auxinic compounds (PBA, 1-NOA, 2-NOA, 2,4-D) but not to natural auxin IAA. In contrast, overexpression of *PIS1/ABCG37* in *35S::GFP-PIS1* seedlings results in resistance to these compounds (shown for 2,4-D).

(b) *pis1-1* mutation confers increased auxin signalling (as monitored by the activity of synthetic auxin reporter *DR5rev::GFP*) in response to exogenously applied synthetic auxins or auxin transport inhibitors.

(c) The *pis1-1* mutation leads to a G-to-A transition in the splice acceptor site of the third intron and causes incorrect splicing. The predominant transcription product contains a 27 nucleotide deletion resulting in deletion of 9 amino acids in the conserved AAA-ATP-binding domain.

mutant hypersensitive to auxins and inhibitors of auxin transport (Fujita and Syono, 1997). *pis1* mutant roots show normal sensitivity to other common plant hormones (cytokinins, gibberellins, abscisic acid, salicylic acid or ethylene, Fujita and Syono (1997) and data not shown) but strongly enhanced susceptibility to a wide selection of auxinic compounds including synthetic auxins (2,4-D, 2-NOA) and inhibitors of auxin transport (NPA, PBA, TIBA) (Fig. 1a, not shown). Root growth (Fig. 1a) as well as other aspects or auxin-related development such as lateral root organogenesis (not shown) showed increased sensitivity to these auxinic compounds. To test whether the increased *pis1* sensitivity is also reflected at the level of auxin signalling, we introduced *DR5rev::GFP* auxin reporter (Benkova *et al.*, 2003) into *pis1* plants. On control medium, we did not observe any difference in the spatial pattern or strength of *DR5* expression between *pis1* and the wild type. However, exogenously applied 2,4-D or NPA activated *DR5*-monitored auxin response in *pis1* at concentration levels markedly lower than in wild type seedlings (Fig. 1b). Thus auxin signalling in *pis1* shows increased sensitivity to auxinic compounds similarly to other phenotypic aspects.

We mapped the *pis1* mutation using 2800 chromosomes to an 80 kb region on the lower arm of chromosome 3. Candidate genes were sequenced and the *pis1-1* mutation was found to cause altered splicing and subsequent deletion of 9 amino acids in the gene coding for pleiotropic drug resistance(PDR)-type protein ABCG37 (previously known as PDR9), a member of the ATP-binding cassette transporter superfamily (Ito and Gray, 2006; Verrier *et al.*, 2008; Geisler and Murphy, 2006) (Fig. 1c). Phenotype similarity and the allelic test between *pis1-1* and insertional *abcg37-2* (Ito and Gray, 2006) mutant further confirmed that hypersensitivity of the *pis1* mutant to auxinic compounds is due to loss of ABCG37 function. In line with this, PIS1/ABCG37 overexpression in *35S::GFP-PIS1* lines complemented the *pis1-1* mutation and even conferred resistance of roots to auxinic compounds (Fig. 1a). The phenotype features of both loss- and gain-of-function *PIS1* mutants (Ito and Gray, 2006) suggest that PIS1 acts as an exporter for auxinic compounds.

To study the requirement of PIS1 for auxin export, we assessed export of different radioactively labelled auxinic compounds from protoplasts derived from *pis1-1* knock-out mutant leaves. *pis1-1* protoplasts exported markedly less the synthetic auxin 2,4-D and the auxin transport inhibitor NPA, as well as (to small extent) the endogenous auxin IAA (Fig. 2a-c). This demonstrates a smaller export capacity of auxinic compounds from *pis1* loss-of-function cells. To test the ability of PIS1 to export auxin directly, we examined transport activity of PIS1 in a heterologous system. When expressed in mammalian HeLa cells, which do not endogenously contain PDR-type proteins, PIS1 confers significantly higher export of 2,4-D, NPA and with lower affinity also of IAA (Fig. 2d). Similarly, PIS1 overexpression in *35S::GFP-PIS1 Arabidopsis* seedlings leads to markedly lower accumulation of exogenously applied IAA in the root tips (Fig. 2e). These transport assays indicate that PIS1 acts as exporter for auxinic compounds including (albeit with lower affinity) endogenous auxin IAA. This functional data on PIS1 fully explain the changed sensitivities to auxinic compounds and other physiological phenotypes of PIS1 gain- and loss-of-function mutants (Fujita and Syono, 1997; Ito and Gray, 2006).

The functional data for PIS1 auxin exporter show similar molecular function as previously characterised auxin exporters from the PIN and PGP families (Petrasek *et al.*, 2006; Geisler and Murphy, 2006). Consistent with a role of PDR-type transporters as detoxifiers in yeast and plants (Geisler and Murphy, 2006), PIS1 seems to have broader substrate specificity than PIN or PGP1/ABCB1 and PGP19/ ABCB19 proteins as it can transport also structurally related components such as auxin efflux (NPA) and influx (NOA) inhibitors in addition to auxins. In addition, PIS1 activity in auxin export is not sensitive to the auxin efflux inhibitor NPA (Supplementary Fig. S1), unlike the activity of PINs *in planta* (Luschnig *et al.*, 1998) or PGPs in HeLa cells (Geisler and Murphy, 2006; Geisler *et al.*, 2005). Next we tested whether PIS1 is involved in long-distance auxin transport as has been shown for PIN and PGP proteins (Luschnig *et al.*, 1998; Geisler *et al.*, 2005). Basipetal auxin transport in both shoots and roots of *Arabidopsis* seedlings was measured and found unchanged in *pis1* mutant as compared to the wild type (Fig. 2f, g). These data collectively show that PIS1 has a function in auxin efflux that is distinct from PIN and PGP protein families. PIS1 appears not to act

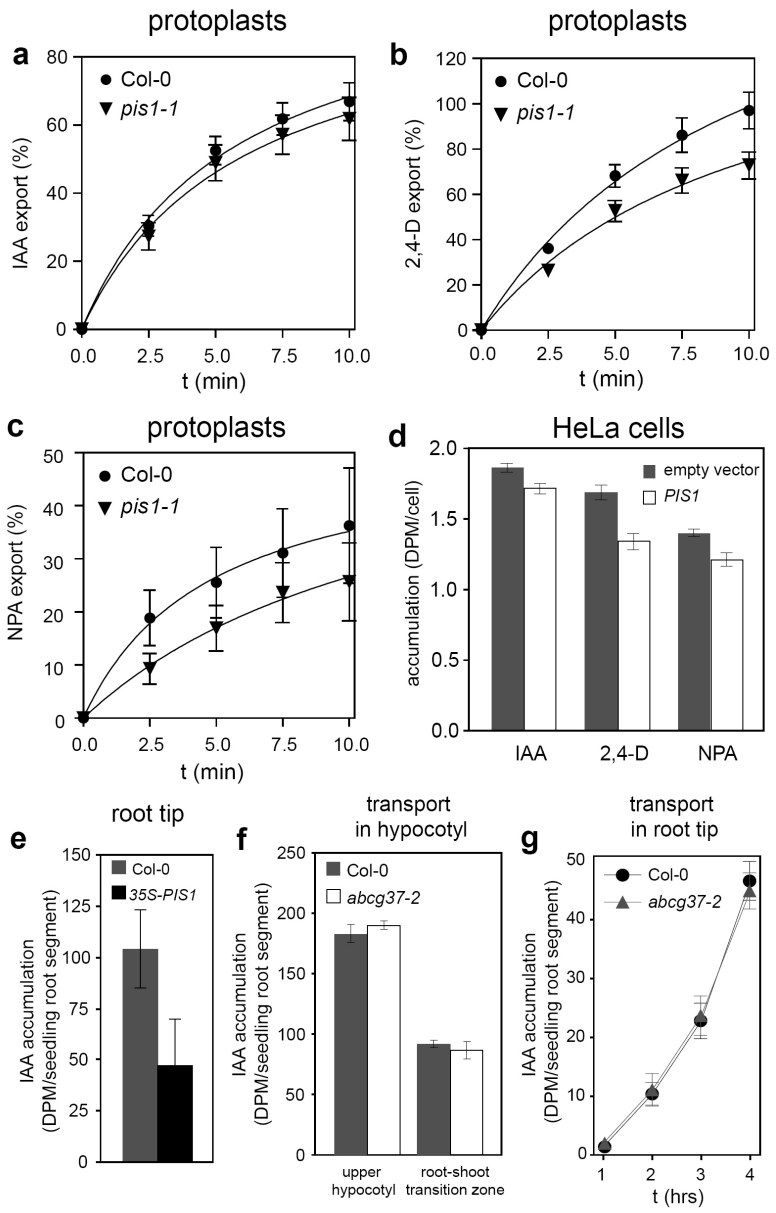

FIGURE 2. **PIS1 is exporter for auxinic compounds.**

(a-c) Protoplasts from *pis1-1* mutant plants show decreased ability to export radioactively labeled IAA ***(a)***, 2,4-D ***(b)*** and NPA ***(c)***. The difference is significant for 2,4-D and NPA at $P < 0.05$ (analysis of variance).

(d) Mammalian HeLa cells expressing PIS1 show significantly less accumulation of IAA, 2,4-D and NPA comparing to empty vector controls ($P < 0.05$, analysis of variance).

(e) Overexpression of *PIS1* leads to decreased IAA accumulation in the root tip 2 hrs after application of auxin droplet on the root cap ($P < 0.05$, analysis of variance).

(f, g) Loss of function in *PIS1* (*abcg37-2* allele) does not interfere with basipetal polar auxin transport in the hypocotyl (f, 5 hrs after application) and in the root (g).

on long-distance auxin transport but rather to export different auxinic compounds out of the seedling.

To further characterise the action of PIS1 *in planta*, we generated polyclonal anti-PIS1 antibodies (Ito and Gray, 2006) and performed immunocytochemistry experiments. The PIS1 signal was detected exclusively in the outermost lateral root cap and epidermal cells of wild-type but not *pis1-1* (Fig. 3a) or *abcg37-2* (not shown) mutant root tips. PIS1 was localized asymmetrically to the outer lateral sides of cells with occasional limited spreading to the apical and basal domains (Fig. 3a-c). Previous reports show that *Arabidopsis* epidermal cells possess two polar domains, the apical at the upper side of cells defined by the localization of PIN2, and the basal marked by the PIN1 auxin carrier protein (Wisniewska *et al.*, 2006). Co-localization experiments with PIN1 and PIN2 (Fig. 3b, c) explicitly demonstrated that PIS1 defines a third, additional polar domain in root epidermal cells, which we designated the outer polar domain.

To confirm the antibody-based experiments and examine the outer polar domain in different cell types, we generated *35S::GFP-PIS1 Arabidopsis* transgenic lines expressing functional *GFP-PIS1* in different cell types. As found for the endogenous protein, GFP-PIS1 was detected at the outer sides of epidermal cells (Fig. 3d, e). Ectopically expressed GFP-PIS1 localized to outer lower sides of columella cells (Fig. 3g) as well as to outer lateral sides of cortex and endodermal cells (Fig. 3e) but in other, more interior root cell types, showed symmetric localization (Fig. 3f). This shows that the outer polar domain is specified in the three most peripheral cell layers. Such localization would

have a clear functional importance for transporting compounds between the root and surrounding environment and is in line with the function of PIS1 as exporter for auxinic compounds. PIS1 localization to the outer polar domain in root tips together with the functional data strongly suggest that PIS1 participates in polar export of auxin and related compounds from the root tip to the surrounding rhizosphere. In the natural situation of the rhizosphere, root systems can mutually influence each other's growth and are under additional influence of complex soil micro-organisms, some of which can produce auxin and related active compounds (Lambrecht *et al.*, 2000). These interactions are common and to large extent determine the composition and prosperity of such community. Therefore, having a possibility to control exclusion of exogenous auxinic compounds from the root tip might provide an important regulatory mechanism in these complex interactions.

Next, we addressed the cellular and molecular mechanism underlying the localization of PIS1 at the novel outer polar domain. PIS1 represents a transmembrane protein, which implies a regulated vesicle-based mechanism for its delivery to or its retention at the outer polar domain of the plasma membrane. In plants, the targeting of polar cargos including PIN and AUX1 auxin transporters depends predominantly on actin cytoskeleton but not directly on microtubules (Geldner *et al.*, 2001; Kleine-Vehn *et al.*, 2006). Actin depolymerization led to limited intracellular aggregations of PIS1 (Fig. 4a), similar as observed for PIN and AUX1 polar cargos (Geldner *et al.*, 2001; Kleine-Vehn *et al.*, 2006). On the other hand, disruption of microtubules resulted in a specific change of PIS1 polar localization – the outer domain became gradually depleted and PIS1 remained to a larger extent at the apical and basal border of the outer polar domain. In extreme cases, PIS1 or GFP-PIS1 disappeared from the outer lateral domain and

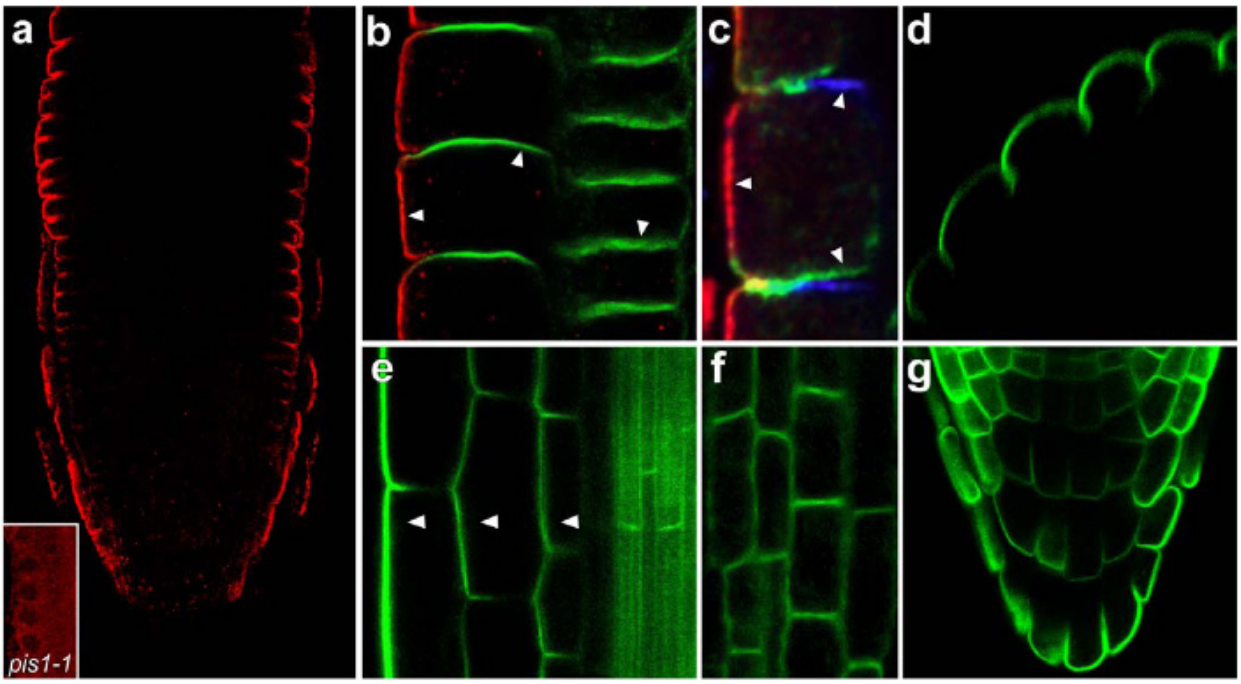

FIGURE 3. **PIS1 localizes to outer polar domain.**

(a-c) Immunostaining using anti-PIS1 antibodies: PIS1 localizes asymmetrically to outer sides of lateral root cap and epidermal cells. Inset shows absence of staining in *pis1-1* root ***(a)***. PIS1 (in red) defines the outer polar domain in epidermal cells, additional to the PIN2-marked apical (***(b)*** in green, ***(c)*** in blue) and the PIN1-marked basal (green in ***(c)***) domains ***(b, c)***.

(d-g) *35S::GFP-PIS1* signal in *Arabidopsis* root: Transversal optical section confirms localization of GFP-PIS1 to the outer polar domain ***(d)***. GFP-PIS1 localizes to the outer polar domain (arrowheads) of epidermal, cortex and endodermis cells ***(e)*** but is symmetrically localized in the stele ***(f)***. Outer-polar-domain of GFP-PIS1 is directed out from the plant body in the root cap ***(g)***.

Arrowheads indicate polar localization PIS1, PIN2 and PIN1 proteins.

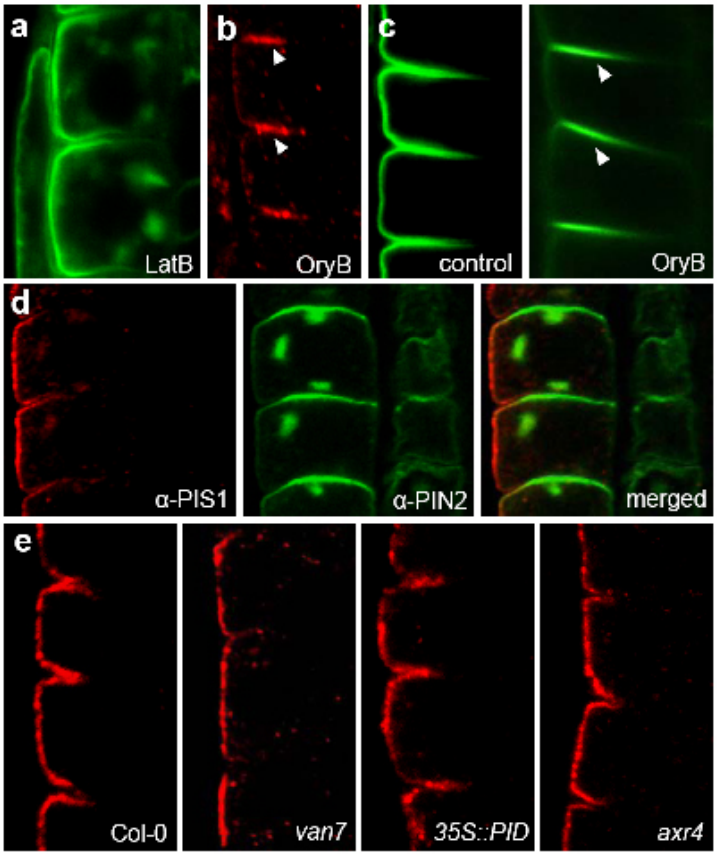

FIGURE 4. **Outer polar targeting pathway for PIS1 is distinct from apical/basal pathways.**
(a-c) Requirements of PIS1 outer polar localization: Partial intracellular aggregation of GFP-PIS1 after actin depolymerization by latrunculin B (20 μM, 3 hrs) ***(a)***. Microtubule depolymerization by oryzalin B (20 μM, 4 hrs) results in depletion of PIS1 ***(b)*** and GFP-PIS1 ***(c)*** from the outer domain and its persistence (arrowheads) in apical and basal domains.
(d) Limited intracellular accumulation of PIS1 and its colocalization with PIN2 after BFA treatment (50 μM, 1 hr 30 min).
(e) No changes in outer lateral PIS1 localization in mutants defective in basal PIN targeting (*van7*, *35S::PID*), and apical AUX1 targeting (*axr4*).

localized to the apical and basal sides of cells (Fig. 4b, c). These results show that PIS1 localization to the outer polar domain, unlike the basal or apical localizations of PIN1 and AUX1, requires an undisrupted microtubule cytoskeleton.

The polar localization of PIN1 and AUX1 cargos to the basal and apical domains depends on distinct pathways, which are sensitive to Brefeldin A (BFA), an inhibitor of ARF GEF action in vesicle budding. BFA treatment leads to internalization of PIN1 from the basal plasma membrane and its accumulation in so called "BFA compartments", whereas AUX1 accumulates in BFA compartments but also remains to large extent at the apical plasma membrane (Geldner *et al.*, 2001; Kleine-Vehn *et al.*, 2006; Grebe *et al.*, 2002). GFP-PIS1 localized to "BFA compartments" only to a very limited extent and its localization at the outer polar remained unaffected (Fig. 4d). Furthermore, in partial loss-of-function mutants in the BFA-sensitive GNOM ARF GEF (*van7*) (Koizumi *et al.*, 2000), the outer PIS1 targeting was undisrupted (Fig. 4e) in contrast to the severe defects in polar localization of PIN1 and PIN4 basal cargos (not shown). This data shows that PIS1 targeting is distinct from GNOM-dependent PIN targeting.

The other characterized components of apical/basal targeting are the Ser/Thr kinase PINOID and the phosphatase PP2A (Friml *et al.*, 2004; Michniewicz *et al.*, 2007). Loss of PP2A function or overexpression of PID leads to a pronounced basal-to-apical polarity shift of PIN localization (Friml *et al.*, 2004; Michniewicz *et al.*, 2007); PIS1 localization, however, remained entirely unaffected in *35S::PID* roots (Fig. 4e) further confirming that PIS1 and PIN polar targeting mechanisms are distinct.

Unlike the BFA-sensitive, GNOM-dependent basal targeting of PIN proteins, the apical targeting of the AUX1 auxin transport protein depends on the Endoplasmic Reticulum (ER)-localized AXR4 protein. In the *axr4* mutant, otherwise apically localized AUX1 is retained in the ER (Dharmasiri *et al.*, 2006). In contrast, PIS1 localization to the outer lateral domain remained entirely unaffected in *axr4* roots (Fig. 4e) highlighting a difference between PIS1 outer lateral and AUX1 apical targeting. In summary, these data show that outer polar targeting of PIS1 utilizes a novel, GNOM-, PID- and AXR4-independent pathway. In addition, in contrast to the apical and basal targeting of PIN and AUX1 proteins, the PIS1 outer polar localization largely depends on microtubule cytoskeleton.

Our identification of PIS1 at the outer lateral plasma membrane domain of epidermal cells reveals that cells of multicellular organisms can be characterized by more than two polar domains with corresponding distinct targeting pathways. It is likely that also the inner polar domain is characterized by cargos yet to be identified. Potential candidates might be silicon transporters localizing to uncharacterised lateral domains in rice (Ma *et al.*, 2006; Ma *et al.*, 2007) or boron transporting proteins in *Arabidopsis* (Miwa *et al.*, 2007; Takano *et al.*, 2005). Based on these observations, we assume that, in addition to apical-basal polarity, root cells of outer layers also possess outer-inner polarity and can regulate material and signal exchange in these principle directions. The ability of plant cells to subcellularly distribute cargos in both apical-basal and inner-outer directions would have a profound functional importance. In a specific example, independent targeting of PIN, AUX1 and PIS1 provides a possibility of directional signalling not only within but also between cell files. The relationship between apical/basal and inner/outer polarity is still unexplored. Our data strongly suggest that outer polar targeting utilizes a mechanism distinct from the targeting of apical or basal cargos and can be thus regulated independently. There are no indications that a similar diversity of targeting pathways is operational in animals. It may be that plants evolved more versatile polar targeting mechanisms distinct from other eukaryotes as an additional evolutionary adaptation reflecting their strictly modular body organization and fixed cell positions. The more diversified polar targeting in plants would underlie, among others, plant-specific mechanisms for the flexible regulation of development via intercellular auxin fluxes.

Experimental procedures

Material and growth conditions

Arabidopsis seedlings were grown under a 16 hours photoperiod, 22/18°C, on 0.5 x MS medium with sucrose as described in Benkova *et al.* (2003). The following mutants, transgenic plants and constructs have been described previously: *pis1-1* (Fujita and Syono, 1997), *abcg37-2* (SALK insertional line previously known as *pdr9-2*; Ito and Gray, 2006), *van7* (Koizumi *et al.*, 2000), *35::PID* (Friml *et al.*, 2004), *axr4-1* (Dharmasiri *et al.*, 2006). For *35S::GFP-PIS1*, the PIS1 genomic fragment was cloned into an appropriate pEPA vector (Dhonukshe *et al.*, 2007). Fusion construct was then subcloned into binary vector pML-BART (Gleave *et al.*, 1992) and transformed into *pis1-1* mutants. Following chemicals were used: 2-(1-pyrenoyl)benzoic acid (PBA), 1- and 2- naphtoxyacetic acid (1- and 2-NOA), indole-3-acetic acid (IAA), 2,4-dichlorophenoxyacetic acid (2,4-D) (all Sigma), latrunculin B (Calbiochem), oryzalin B (ChemService), brefeldin A (Molecular Probes).

Transport measurements

Leaf protoplast transport assays were performed as described in Geisler *et al.* (2005). Transport activities in HeLa cells were determined as published (Geisler *et al.*, 2005; Petrasek *et al.*, 2006). Root basipetal auxin transport was measured as described (Geisler *et al.*, 2005; Peer and Murphy, 2007), with following modifications: A 6 nl droplet with radioactively labelled auxin (1µM 20 $Ci.mmol^{-1}$ [^{3}H]IAA, American Radiochemicals) was applied on the third tier of columella cells, after 2 hours, the root cap was removed and radioactivity of excised 2 mm root tip segment was measured. Auxin transport measurement in hypocotyls was described (Geisler *et al.*, 2005), the 6 nl droplet was applied on the shoot apical meristem and after 5 hours the activity in upper parts of hypocotyls (2 mm segment below the cotyledonal node) and in the root-shot transitional zones was measured.

Localization analysis

Immunolocalizations in *Arabidopsis* were performed as described in Sauer *et al.* (2006). The following antibodies and dilutions were used: anti-PIS1 (Ito and Gray, 2006) (1:500) and anti-PIN2 (raised in mice, a kind gift from C. Luschnig) (1:800) primary antibodies; and CY3-conjugated anti-rabbit (1:600), and FITC or CY-5-conjugated anti-mouse (1:600) secondary antibodies (Dianova). For triple labelling, the *PIN2::PIN1-GFP2* transgenic line (Wisniewska *et al.*, 2006) was used.

Phenotype analysis, statistics and microscopy

Arabidopsis root lengths were measured by ImageJ. At least 20 seedlings were processed and at least three

independent experiments were done, giving the same statistically significant results.
Equal variance of values was verified by Levene test, Kruskal-Wallis non-parametric test was performed simultaneously with ANOVA. Data were statistically evaluated with NCSS 2007. Data are presented as means +/- s.e.m.

For confocal laser scanning microscopy, a Leica TCS SP2 was used. Images were processed in Adobe Photoshop.

Acknowledgements

We thank C. Luschnig for anti-PIN2 antibodies, J. Mravec for pEPA vectors and Y. Cheng, A. Diggs and B. Titapiwatanakun for technical assistance. Supported by the Volkswagen Stiftung to J.F. (K.R., V.G., J. K-V.), the EMBO Young Investigator Programme (J.F.), the Grant Agency of the Academy of Sciences of the Czech Republic (E.N., J.H.), the Novartis Foundation (M.G.), the Swiss National Fonds (M.G. and E.M.), the Japanese Society for the Promotion of Science (H.I.), and National Institutes of Health (W.M.G.).

Supplemental data

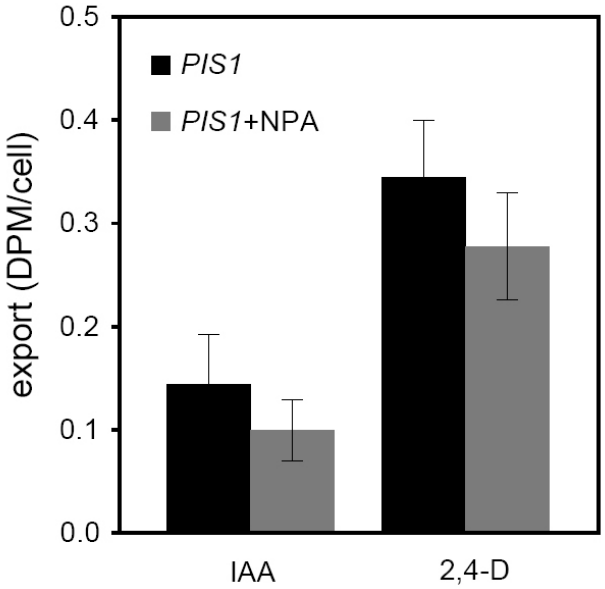

SUPPL. FIGURE 1. **NPA insensitivity of auxin transport mediated by PIS1 in mammalian HeLa cells.**

PIS1-mediated net export of IAA and 2,4-D is not sensitive to the auxin efflux inhibitor NPA. The minor decrease in export following treatment with NPA is due to competitive inhibition (not shown) because NPA is

ER localized PIN5 auxin transporter mediates cellular auxin homeostasis

Jozef Mravec,[1,2] Aurélien Bailly,[3] Klára Hoyerová,[4] Agnieszka Bielach,[1] Petr Skůpa,[4] Jan Petrášek,[4] Vassilena Gaykova,[2] York Dieter Stierhof,[2] Christian Luschnig,[5] Eva Benková,[1] Eva Zažímalová,[4] Markus Geisler[3], Jiří Friml[1,2]*

[1]Department of Plant Systems Biology, VIB, and Department of Molecular Genetics, Ghent University, 9052 Gent, Belgium.
[2]Center for Plant Molecular Biology (ZMBP), University Tübingen, D 72076 Tübingen, Germany.
[3]Zürich Basel Plant Science Center, University of Zurich, Institute of Plant Biology, Molecular Plant Physiology, CH 8008 Zurich, Switzerland.
[4]Institute of Experimental Botany, ASCR, 165 02 Praha 6, Czech Republic.
[5]Center for Applied Genetics and Cell Biology, University of Natural Resources and Applied Life Sciences BOKU, A 1190 Wien, Austria

* To whom correspondence should be addressed. E mail: jiri.friml@psb.ugent.be

Summary

Transport mediated distribution of the phytohormone auxin provides positional cues for multiple plant developmental processes. PIN auxin exporters on behalf of their polar, plasma membrane localization determine direction and rate of intercellular auxin flow. Here we show that PIN5 an atypical member of the PIN family encodes a functional auxin transporter that regulates growth and patterning in *Arabidopsis*. Loss and gain of function phenotypes, changes in free auxin levels and the PIN5 localization at the endoplasmic reticulum (ER) suggest a role of PIN5 in transport from the cytosol into the lumen of the ER. Our data identify unexpected mechanism of regulating cellular auxin homeostasis that involves transport based subcellular compartmentalization.

Introduction

The plant signaling molecule auxin plays a central role in a wide variety of developmental processes that provides positional and directional information via its differential distribution in neighboring cells (Tanaka *et al*., 2006). Thus, cellular auxin levels often play a decisive role in the developmental output of auxin signaling. Conceptually, transmembrane transport and metabolic processes, such as biosynthesis, degradation and conjugation, regulate the steady-state levels of auxin in any given cell. Interference with either of these processes leads to pronounced developmental defects (Tanaka *et al*., 2006; Woodward and Bartel, 2005; Cheng *et al*., 2006). In particular, carrier-mediated, directional auxin transport between cells has been shown to be central in most aspects of auxin-dependent development. Genetic approaches in *Arabidopsis* have identified a plant-specific gene family coding for transporters involved in auxin export from the cells - the PIN proteins (Gälweiler *et al*., 1998; Petrášek *et al*., 2006). PIN proteins are integral membrane proteins whose asymmetric localization on the plasma membrane determines the directionality of the auxin flow (Wiśniewska *et al*., 2006) and are required for many aspects of auxin-related plant development, including embryogenesis (Friml *et al*., 2003), organogenesis (Okada *et al*., 1991; Benková *et al*., 2003; Reinhardt *et al*., 2003), root meristem patterning and activity (Friml *et al*., 2002; Blilou *et al*., 2005), tissue differentiation and regeneration (Scarpella *et al*., 2006; Xu *et al*., 2006; Sauer *et al*., 2006), and tropisms (Luschnig *et al*., 1998; Friml *et al*., 2002). The *Arabidopsis* genome encodes eight PIN-related sequences, most of which have already been characterized at the cellular and developmental levels (Zažímalová *et al*., 2007; Vieten *et al*., 2007). PIN5 (At5g16530), however, is functionally still uncharacterized, and represent the most distant member of the *Arabidopsis* PIN family. PIN5 is characterized by the lack of a hydrophilic loop that is found in the central portion of all, so far, characterized PINs. Moreover, hydrophobicity plot predictions of PIN5 imply only 9 instead of 10 transmembrane domains (Figure 1A). Consistently, phylogenetic analysis positions PIN5, together with PIN5-like proteins from other plant species, into a distinct subclade within the PIN family (Figure 1B), evoking questions about its role in auxin transport (Zažímalová *et al*., 2007).

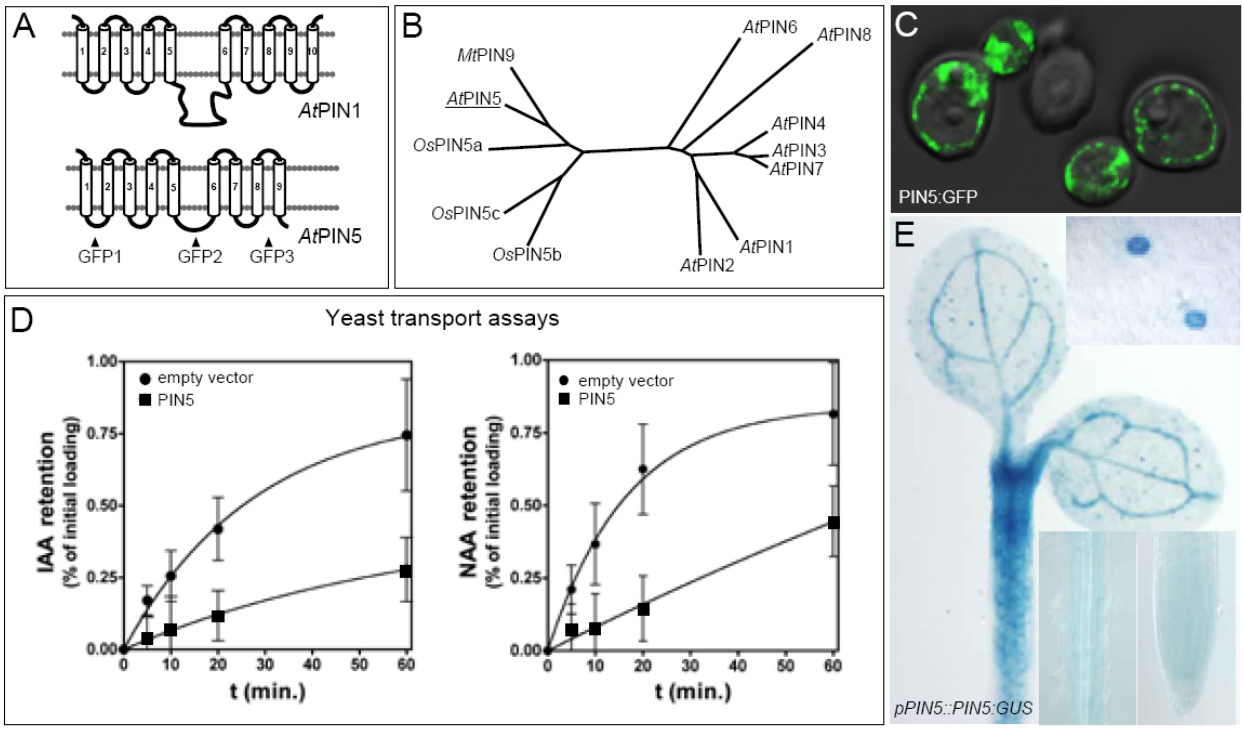

FIGURE 1. **Broadly expressed functional auxin transporter encoded by the distant family member *PIN5*.** ***(A)*** Predicted organization of transmembrane domains reveals the reduced middle hydrophilic loop in PIN5 that is the hallmark of other PINs including PIN1. ***(B)*** Phylogenetic tree of the PIN protein family. PIN5 and its homologues represent the distant subclade. ***(C)*** PIN5:GFP targeted to the plasma membrane in yeast. ***(D)*** Decreased retention of IAA and NAA in the PIN5-expressing yeast, suggesting an auxin export function for PIN5. Error bars show SEM (n=5). ***(E)*** Expression of PIN5 visualized by *pPIN5::PIN5:GUS* construct. PIN5 shows moderate, but broad, expression.

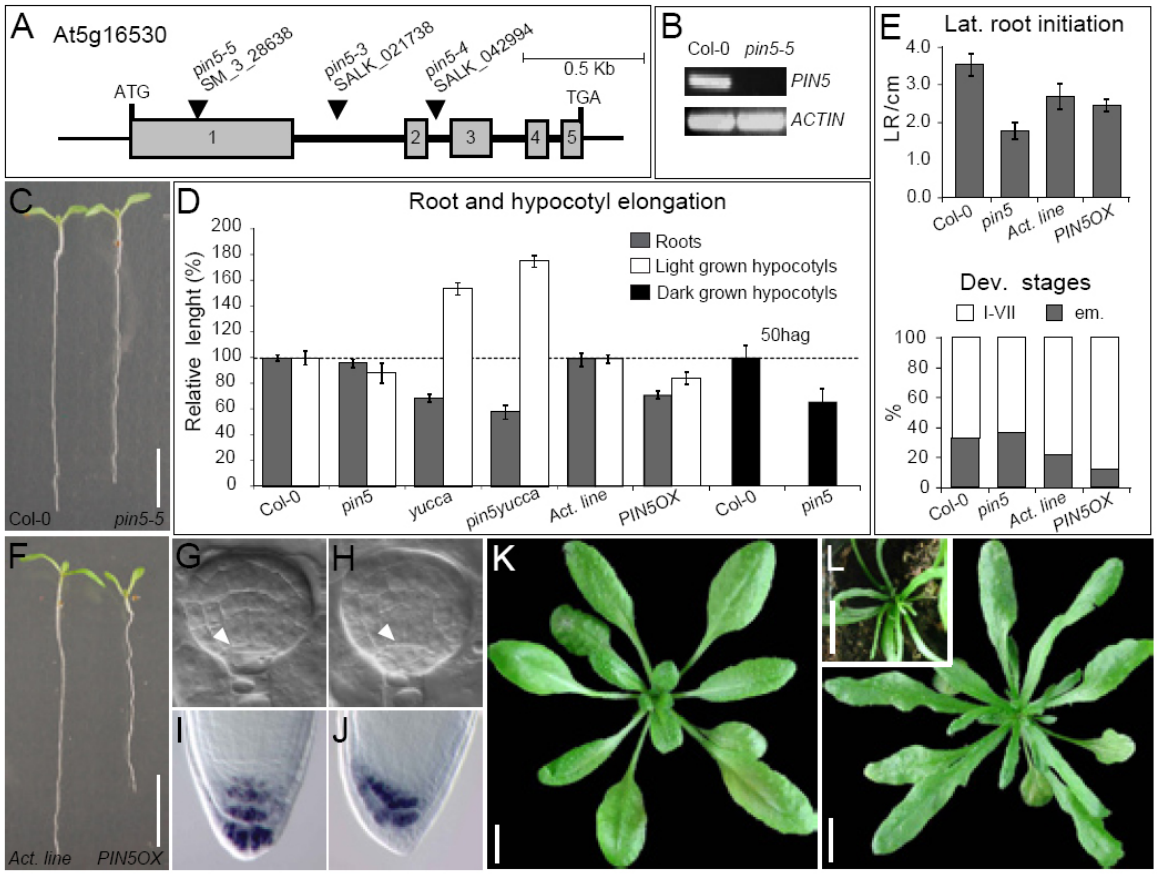

FIGURE 2. **Developmental defects for the *pin5* knock-out and gain-of-function mutants.**
(A) Structure of the *PIN5* gene with depiction of three T-DNA insertions characterizing *pin5* loss-of-function mutations. ***(B)*** *PIN5* mRNA is not detected in *pin5-5* mutant. ***(C)*** *pin5-5* seedling compared to wild type. ***(D)*** *pin5-5* and *RPS5A>>PIN5*:*myc* (*PIN5OX*) lines show defects in hypocotyl and root elongation; *pin5* mutation enhances *yucca* phenotype. ***(E)*** *pin5-5* initiate less lateral roots whereas *RPS5A>>PIN5*:*myc* overexpression line show defects in primordia development. ***(F)*** *RPS5A>>PIN5*:*myc* (*PIN5OX*) seedling compared to control (*RPS5A>>GAL4* activator line). ***(G, H)*** *RPS5A>>PIN5*:*myc* embryos ***(H)*** show aberrations in hypophysis division as compared to the wild type (indicated by arrows) ***(G)***. ***(I, J)*** Organization of root meristem as visualized by lugol staining: wild type (**I**) and *RPS5A>>PIN5*:*myc* showing defects in columella specification ***(J)***. ***(K, L)*** *RPS5A>>PIN5*:*myc* plants ***(L)*** show wrinkled and narrow rosette leaves (inset shows a more affected line) compared to control ***(K)***. Error bars show SEM (n=30). Scale bars, 1 cm.

Results and Discussion

To test whether PIN5 functions, similarly to the conventional PIN proteins, in auxin efflux, we utilized a yeast heterologous system. PIN5 tagged with a hemagglutinin epitope (PIN5:HA) was targeted predominantly to the plasma membrane in yeast, as was confirmed both by sucrose gradient fractionation (Supplemental Figure 1) and localization of PIN5:GFP (Fig. 1C). As shown previously for representative members of the PIN family (Petrášek *et al*., 2006), PIN5 expression in yeast led to increased auxin efflux as indicated by decreased retention of the radioactively labeled auxins, indole-3-acetic acid (IAA) and α-naphthaleneacetic acid (NAA) (Figure 1D). These results show that, despite the differences in the overall protein structure and the compromised hydrophilic loop, PIN5 can also function as auxin exporter. This observation is also in line with previous reports that the hydrophilic loop in secondary transporters is not important for catalytic function but rather for targeting or regulation (Matsuoka *et al*., 1993).

Next, to test the PIN5 expression *in planta*, we fused a *PIN5* genomic fragment, including 1.7 kb of the promoter region, with the β-glucuronidase (*GUS*) reporter gene. GUS staining observed in independently transformed seedlings revealed *PIN5* transcriptional activity in hypocotyls, cotyledon vasculature, and guard cells. Weaker staining was detected in root endodermal and pericycle tissues as well as in the root tip (Figure 1E). At later developmental stages, moderate *GUS* expression was observed in leaves, stems, and flowers (Supplemental Figure 2C). Such wide-ranging, but moderate, expression of the *PIN5* reporter construct was confirmed by semi-quantitative

reverse-transcription polymerase chain reaction (RT-PCR) (Supplemental Figure 2A) and was consistent with publicly available microarray data (Supplemental Figure 2B, Zimmermann *et al*. (2004), https://www.genevestigator.ethz.ch/at/). Thus, PIN5 appears to function as a broadly expressed auxin transport protein in contrast to other PIN proteins that show typically well-defined expression in different parts of the plant.

To analyze the role of PIN5 in plant development, we characterized three T-DNA insertional mutants disrupting the *PIN5* locus (Figure 2A). The full-length *PIN5* transcript was not detectable in any of these *pin5* mutant alleles (Figure 2B; data not shown). The *pin5* mutant seedlings initiated fewer lateral roots and had defects in root and hypocotyl growth (Figure 2C, D, E). In particular, the rapid expansive growth of etiolated hypocotyls was delayed in the *pin5* mutant (Figure 2D). To get further insights into the role of PIN5, we generated gain-of-function lines. To this end, we fused the strong CAMV 35S-promoter to the *PIN5* cDNA (*35S::PIN5*) and used a two-component UAS/GAL4-based system, driving the PIN5-*myc* expression by a strong meristematic promoter in *RPS5A>>PIN5*:*myc* (Weijers *et al*., 2003). Both *35S::PIN5* and *RPS5A>>PIN5*:*myc* seedlings had defects in root and hypocotyl growth; cotyledons did not fully expand and were epinastic (data not shown; Figure 2F, D). The *RPS5A>>PIN5-myc* embryos that expressed PIN5 from early embryogenesis on, were also defective in axis formation during establishment of the hypophysis (n=8/62; Figure 2G, H) and postembryonically in columella differentiation and organization, as visualized by lugol staining (n=7/25; Figure 2I, J). The initiation of lateral root occurred normally, but the development of primordia progressed more slowly toward the later stages (Figure 2E). The less affected *RPS5A>>PIN5*:*myc* grown-up plants formed narrow wrinkled leaves and bushy inflorescences (Figure 2K, L, not shown), while the most affected had small filamentous leaves and failed to flower (Figure 2L, inset). In summary, the *pin5* loss- and gain-of-function mutant phenotypes suggest a role for PIN5 in different aspects of plant development, presumably in auxin-regulated processes.

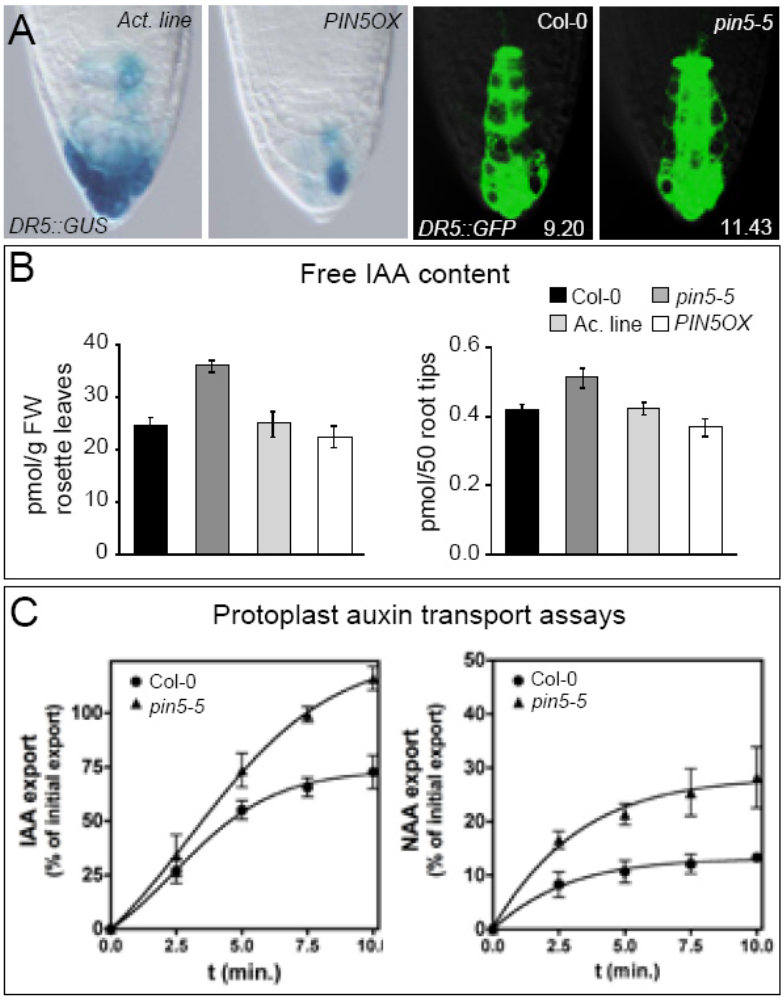

FIGURE 3. **PIN5 requirement for cellular auxin homeostasis.** ***(A)*** Expression of *DR5* auxin response reporters is decreased in *RPS5A>>PIN5*:*myc* and slightly increased in *pin5* root tips (respective mean signal intensities are indicated). ***(B)*** *pin5-5* mutant has elevated and *RPS5A>>PIN5-myc* decreased levels of free IAA in both rosette leaves and root tips. Error bars show SEM (n=3). ***(C)*** Protoplasts of *pin5-5* mutant exhibit higher export of auxins (IAA and NAA). Error bars show SEM (n=5).

To further test the involvement of PIN5 in auxin-mediated regulation of plant growth and development, we examined the activity of the synthetic auxin-responsive reporters *DR5::GUS* (Ulmasov *et al*., 1999) and *DR5rev::GFP* (Friml *et al*., 2003) in *pin5* mutants. In contrast to other *pin* mutants (*pin1*, *9*; *pin2*, *6, 16*; *pin4*, *11*; *pin7*, *7*), the overall spatial pattern of the auxin response did not change in *pin5* loss- or gain-of-function mutants when compared to that of the wild type (Figure 3A). Nevertheless, the DR5 signals in the root meristems were slightly increased in *pin5* mutant roots, but decreased in *RPS5A>>PIN5*:*myc* (Figure 3A), indicating defects in auxin signaling or homeostasis. To explore this issue, we tested sensitivity of *pin5* mutants to different auxin and auxin transport inhibitors. The sensitivity of the root elongation

of loss- and gain-of-function alleles to different auxins was unchanged (Supplemental Figure 3), arguing against defects in auxin signaling. On the other hand, both types of alleles showed increased sensitivity to the auxin efflux inhibitor, 1-naphthylphthalamic acid (NPA) (Supplemental Figure 3). As these results suggest defects in auxin homeostasis, we introduced *pin5* into the *yucca* mutant that has increased auxin levels (Y. Zhao *et al*., 2001). In the *pin5 yucca* double mutant, we observed a considerable enhancement of the *yucca* phenotype characterized by the inhibition of root growth and increased hypocotyl elongation (Figure 2D), supporting the notion that PIN5 is involved in the regulation of cellular auxin homeostasis. We also directly tested the auxin levels in the *pin5* mutants. Extraction and Gas Chromatography/Mass Spectroscopy (GC/MS) detection of IAA showed that loss-of-function *pin5* mutants had higher levels of free auxin than the controls (Figure 3B). On the other hand, the *RPS5A>>PIN5*:*myc* plants had decreased IAA levels (Figure 3B), consistent with the observed changes in the DR5 activity. Both rosette leaves and root tips showed comparable changes in auxin levels, further indicating widespread alterations in auxin homeostasis but not in the auxin distribution. To address how the *pin5* mutation might affect cellular auxin levels, we measured the auxin efflux from mesophyll protoplasts (Geisler *et al*., 2005) isolated from rosette leaves expressing reasonable amounts of PIN5 (Supplemental Figure 2). Protoplasts prepared from *pin5* mutants exhibited an increased efflux of both natural (IAA) and synthetic (NAA) auxins (Figure 3C). This observation was surprising since, as has been demonstrated (Geisler *et al*., 2005), loss-of-function of a plasma membrane localized auxin exporter would be expected to result in reduced export. These results suggest that PIN5, although functional as auxin exporter in yeast (Figure 1D), does not mediate cellular auxin efflux *in planta* as shown for other PIN proteins. The data rather imply that PIN5 is involved in regulating auxin (free IAA) homeostasis by another mechanism.

To try to clarify the discrepancy between the transport function of PIN5 and its role *in planta*, we examined the subcellular localization of PIN5 in *Arabidopsis*. A characteristic feature of other PIN proteins is their asymmetric (polar) plasma membrane localization that correlates and determines the direction of auxin flow between cells (Wiśniewska *et al*., 2006; Friml *et al*., 2004; Michniewicz *et al*., 2007). To determine the subcellular localization of PIN5 in plant cells, we fused the *PIN5* genomic fragment with a green fluorescent protein (GFP) and constitutively expressed it under control of the 35S promoter. To minimize a possible interference with targeting and protein folding, we placed GFP at three different positions within the PIN5-coding region (Figure 1A). In contrast to the localization of other PIN or PIN:GFP proteins, all PIN5:GFP variants as well as the PIN5:*myc* in the *RPS5A>>PIN5*:*myc* (Supplemental Figure 4B) did not localize to the plasma membrane but showed strong intracellular localization (Figure 4A and Supplemental Figure 4A). This PIN5 localization is, unlike that of other PIN proteins (Geldner *et al*., 1997), insensitive to treatment with the secretion inhibitor Brefeldin A (Figure 4A, inset). The PIN5:GFP signal appeared to be mainly restricted to the endoplasmatic reticulum (ER), as confirmed by co-localization with the ER markers, the ER-tracker dye in living cells (Supplemental Figure 4A) and the ER-specific marker antibody (α-Sec12, Bar-Peled and Raikhel, 1997) in co-immunological staining (Figure 4B). In addition, immunogold labeling on ultrathin cryo-sections confirmed a predominant ER localization of PIN5 (Figure 4C, D). Taken together, these data strongly suggest that the ER is the site of the PIN5 action and not the plasma membrane, as shown for other members of the PIN family. This also suggests that the export function of PIN5 in yeast cells (Figure 1D, E) is due to its ectopic localization at the plasma membrane in the heterologous system. However, the inward transport orientation of the protein at ER membranes *in planta* would imply a role for PIN5 in transporting auxin from the cytoplasmatic auxin pool into the lumen of the ER. As a likely consequence, free auxin would be sequestered, limiting the availability of cytosolic auxin for auxin exporters at the plasma membrane, which is fully consistent with higher levels of free IAA and increased auxin efflux in *pin5* mutants.

Little is known about the subcellular compartmentalization of signaling molecules in eukaryotic cells. Signaling components have been shown to act from different compartments, for example the TGF-β receptor in animals (Panopoulou *et al*., 2002) or the brassinosteroid receptor in plants (Geldner *et al*., 2007) that are active in endosomes. Nevertheless, the compartmentalization of signaling molecules themselves and mechanisms underlying this process are largely unexplored. Our analysis of

PIN5, a member of the PIN auxin efflux protein family suggests an unexpected regulation mechanism of the cellular homeostasis of the plant signaling molecule auxin by subcellular compartmentalization. PIN5, unlike other PIN proteins is not localized to the plasma membrane, but to the ER. When targeted to the plasma membrane of yeast, PIN5 facilitates the auxin efflux similarly as other PIN proteins. However, its function *in planta* would be, based on its ER localization and changes in cellular auxin levels in the *pin5* mutant, rather regulation of cellular auxin homeostasis than in mediating intercellular auxin transport. The localization, genetic, and physiological data on PIN5 support a view in which PIN5 transports auxin into the lumen of the ER, thus reducing the auxin availability for plasma membrane-based auxin efflux and possibly also for nucleus-located TIR1-based auxin perception (Kepinski and Leyser, 2005; Dharmasiri *et al*., 2005). The importance of the ER in auxin biology has been highlighted by the presence of several components of auxin metabolism as well as signaling (Woodward and Bartel, 2005; Bartel and Fink, 1995). Importantly, the auxin-binding protein ABP1 that is essential for plant growth resides predominantly in the ER; yet its role in the regulation of auxin responses is still poorly understood (Chen *et al*., 2001). Thus, PIN5-mediated auxin uptake might play a relevant role in the control of ER-resident auxin metabolism, as well as in signaling events that require ABP1-mediated auxin perception in this compartment.

Our studies revealed previously unknown mechanism for controlling auxin homeostasis by means of transport-mediated intracellular auxin compartmentalization. Tight control of the cellular auxin concentration at several levels would be important in particular for auxin signaling because most of the auxin-based development is triggered by differential auxin distribution in different cells (Tanaka *et al*., 2006). ER and plasma membrane are the destinations of the same secretory targeting pathway and, generally, only a small sequence modification is sufficient to change the protein targeting between these two destinations. Thus, similar events have probably occurred repeatedly during evolution for different plasma membrane proteins, including transporters. In this view, it would be interesting to explore whether other signaling molecules can be compartmentalized by means of intracellular traffic and what functions such compartmentalization might have.

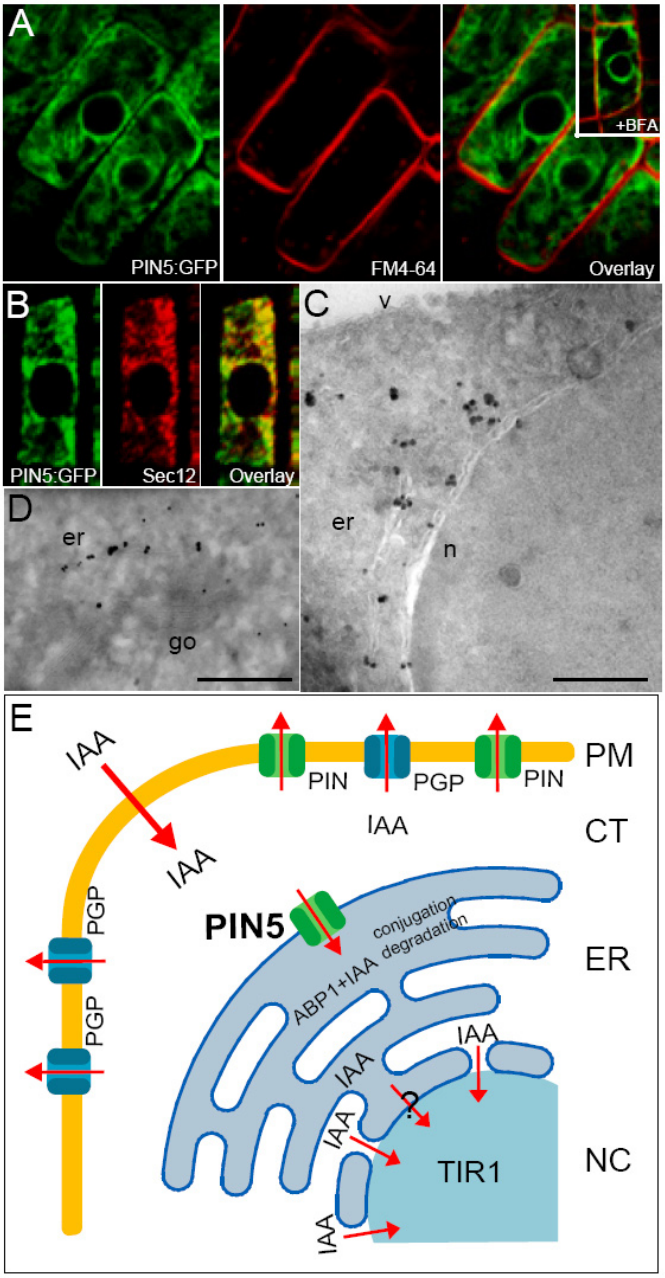

FIGURE 4. **Localization of PIN5 to the ER.** ***(A)*** Intracellular localization of PIN5:GFP (green) as compared to FM4-64 plasma membrane staining (red). No co-localization of PIN5:GFP and FM4-64 was observed; the PIN5:GFP localization is insensitive to Brefeldin A (inset). ***(B)*** Immunological staining of PIN5:GFP (green) together with the ER marker Sec12 (red). Overlay of both stainings show reliable co-localizations (Mander's overlap coefficient: R=0,78). ***(C, D)*** GFP-immunogold labeling on ultrathin cryo-sections, confirming the presence of PIN5:GFP at the ER. Abbreviations, er, endoplasmic reticulum; n, nucleus; v, vacuole; go, Golgi network. Scale bars, 2 µm. ***(E)*** Model for the PIN5 function in plant cells.

Experimental procedures

Plant material and growth conditions

For all experiments, we used *Arabidopsis thaliana* (L.) Heynh. plants of ecotype Columbia 0 (Col-0). Insertional mutant lines were *pin5-5* (SM_3_28638), *pin5-3* (SALK_021738), and *pin5-4* (SALK_042994). Insertion sites were verified, homozygous lines were selected and the absence of the PIN5 transcript was shown by RT-PCR. Transgenic lines were *DR5::GUS* (Sabatini *et al*., 1999), *DR5rev::GFP* (Friml *et al*., 2003), *RPS5A>>GAL4* (Weijers, *et al*., 2003), and *yucca* (Zhao *et al*., 2001). All SALK lines were obtained from the Nottingham Arabidopsis Stock Center. The EXOTIC line SM_3_28638 was a kind gift from Jonathan Clarke (John Innes Centre, Norwich, UK). Seeds were sterilized with chlorine gas and stratified at 4°C for 2 days in the dark. Seedlings were grown vertically on half Murashige and Skoog (MS) medium supplemented with 1% sucrose and respective drugs. Drugs were purchased from Sigma-Aldrich. Plants were grown under the stable long day (16 h light/8 h dark) conditions at 20-22°C in growth chambers.

Phenotype analyses and GUS staining

Plates were scanned on a flat-bed scanner and root and hypocotyl lengths were measured with the ImageJ (http://rsb.info.nih.gov/ij/) software. Lateral root initiation, developmental stage progression analyses, and GUS staining were as described (Benková *et al*., 2003). Chloralhydrate clearing was used for embryonal analyses as described (Friml *et al*., 2003). For all experiments, n≥30.

DNA constructs and yeast and plant transformation

The *pPIN5:PIN5:GUS* was constructed by amplification of the *PIN5* genomic fragment including the 1.7 kb promoter region and cloning to the *BamH*I and *Nco*I sites of pCAMBIA1391Z (http://www.cambia.org/daisy/cambia/-materials/vectors/585.html#dsy585_table). The obtained construct was transformed to Col-0 plants. For the *PIN5-GFP* constructs, the enhanced GFP sequence was introduced into three different positions in the *PIN5* genomic sequence by three fragment ligations to pGREENII-35S-tNos (Roger *et al*., 2000, www.pgreen.ac.uk/) between the 35S promoter and the tNOS terminator. The interrupted amino acid positions were: GFP1-37 (RD/QC), GFP2-164 (NI/SD), GFP3-319 (YG/LH). The resulting constructs were transformed to Col-0 plants. For the *PIN5* overexpression, the *PIN5* genomic fragment was amplified by primer extension PCR by introduction of the *myc* tag sequence and cloning to the pTA7002 (Aoyama and Chua, 1997) between the *Xho*I and *Spe*I sites to create the pUASPIN5-*myc*. This plasmid was used to transform the *RPS5A>>GAL4* activator line (Weijers, *et al*., 2003) to create the *RPS5A>>PIN5:myc* line. For the yeast heterologous system, the *PIN5* cDNA was fused with hemagglutinin by primer extension PCR and cloned to the pNEV yeast expression vector (Geisler *et al*., 2005). The *PIN5:GFP* cDNA sequence was amplified from *35S:PIN5:GFP3* plants and cloned to the *Not*I site of the pNEV plasmid to create pNEV-PIN5:GFP. Lithium acetate/polyethylene glycol transformation was used to transform the yeast strains JK93da (transport assays) or EGY48 (PIN5:GFP localization analyses). A standard floral dip method was used for plant transformation.

RT-PCR

The whole RNA of 10-day-old seedlings was extracted with the Qiagen RNA extraction kit according to the manufacturer's instructions. The following whole cDNA was synthesized with the reverse transcriptase kit SuperscriptII (Stratagene) and the polyT primer. The whole coding region of the *PIN5* gene was amplified by standard PCR. Primers specific for tubulin or actin were used as a control.

Free IAA determination, protoplast, and yeast auxin transport assays

To determine internal levels of endogenous auxin in *Arabidopsis* leaves, free IAA was extracted by methanol/formic acid/water (15/1/4, v/v/v) from leaf rosettes (of 23-day-old) *Arabidopsis* homogenized in liquid nitrogen. The extract was purified with the dual-mode solid phase extraction method as described (Dobrev and Kamínek, 2002). Free IAA was purified on two different HPLC columns and determined on Finigan Polaris Q GC-MS/MS. Internal levels of endogenous auxin in *Arabidopsis* root tips were determined by collecting root tips (3-5 mm) of 8-day-old *Arabidopsis* seedlings in a 1.5% sucrose solution. For extraction of free IAA from the tips, 2 volumes of methanol were

added to 1 volume of the solution. After disintegration by sonication for 5 min, root tips were separated by centrifugation. Free IAA released to the solution was determined on the Finigan Polaris Q GC-MS/MS. The protoplast and yeast transport assays were as described (Geisler *et al*., 2005).

Immunological staining and electron and fluorescent microscopy

Immunological staining was as described (Sauer *et al*., 2006). The antibodies used at the final dilutions were polyclonal rabbit α-Sec12 at 1:200 (Bar-Peled and Raikhel, 1997), monoclonal mouse α-GFP at 1:600 (Roche), and polyclonal rabbit α-*myc* at 1:600 (Sigma-Aldrich). Immunogold labeling on ultrathin cryo-sections was performed and analyzed as described (Geldner *et al*., 2001). The confocal imaging was done on a Leica SP2 confocal microscope. The GFP samples were scanned without fixation. For the FM4-64 double labeling, PIN5:GFP seedlings were incubated for 3 minutes in the medium with a 1:1000 dilution of FM4-64 (Invitrogen). For BFA treatment, we incubated seedlings in liquid MS medium supplemented with 50 μM Brefeldin A (Molecular Probes) for 1 h.

Acknowledgements

We thank David G. Robinson and Jonathan Clarke for providing material and M. De Cock for help with the preparation of the manuscript. This work was supported by the European Molecular Biology Organization Young Investigator programme (J.F.), the Volkswagenstiftung (J.F., J.M., A.B., V.G.), the Grant Agency of the Academy of Sciences of the Czech Republic, project A6038303 (E.Z., P.S., J.P., and K.H.), the Novartis Foundation (M.G.), the Swiss National Funds (M.G. and A.B.), and Austrian Science Fund (FWF) grant 16311 (C.L).

Supplemental data

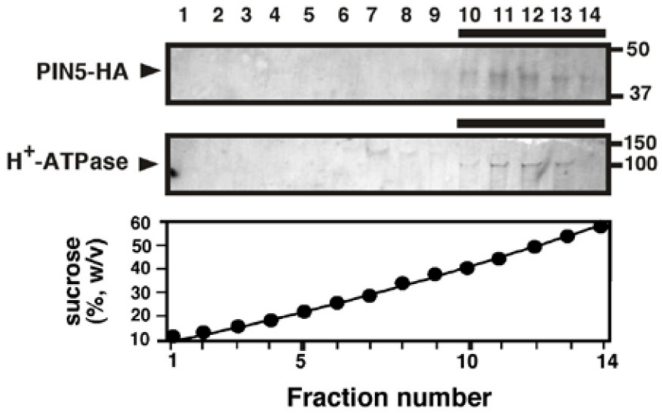

SUPPL. FIGURE 1. **Confirmation of plasma membrane localization of the PIN5:HA fusion protein by sucrose fractionation**. α-H+-ATPase antibodies were used as a plasma membrane control marker.

A

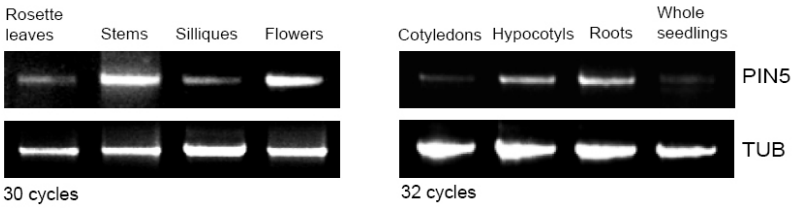

B

Anatomy	# of Chips	Mean	Std_Error
0 callus	6	267	45
1 cell suspension	87	149	7
2 seedling	493	178	4
21 cotyledons	9	241	33
22 hypocotyl	6	267	32
23 radicle	9	235	29
3 inflorescence	232	173	7
31 flower	85	168	9
311 carpel	15	157	16
3111 ovary	4	236	24
3112 stigma	3	105	21
312 petal	6	86	19
313 sepal	6	71	4
314 stamen	15	209	35
3141 pollen	2	445	78
315 pedicel	3	142	13
32 silique	19	219	24
33 seed	53	118	8
34 stem	28	274	19
35 node	3	201	6
36 shoot apex	25	104	9
37 cauline leaf	3	443	26
4 rosette	710	216	4
41 juvenile leaf	87	187	7
42 adult leaf	243	194	5
43 petiole	12	258	25
44 senescent leaf	3	260	33
45 hypocotyl	12	516	105
451 xylem	3	185	28
452 cork	3	1074	69
5 roots	236	214	7
52 lateral root	4	238	41
53 root tip	4	139	32
54 elongation zone	7	173	16
55 root hair zone	4	173	32
56 endodermis	3	150	45
57 endodermis+cortex	3	232	49
58 epid.	3	185	5

C

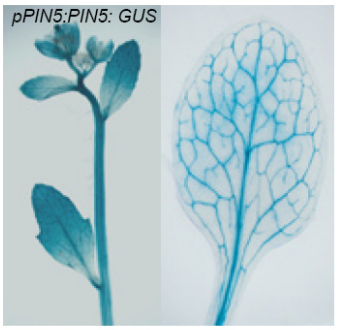

SUPPL. FIGURE 2. Broad expression pattern of PIN5 confirmed by semi-quatitative RT-PCR ***(A)*** and consistent with publicly available microarray data (https://www.genevestigator.ethz.ch/at/) ***(B)***. Expression of the *pPIN5::PIN5:GUS* reporter construct in inflorescences and rosette leaves ***(C)***.

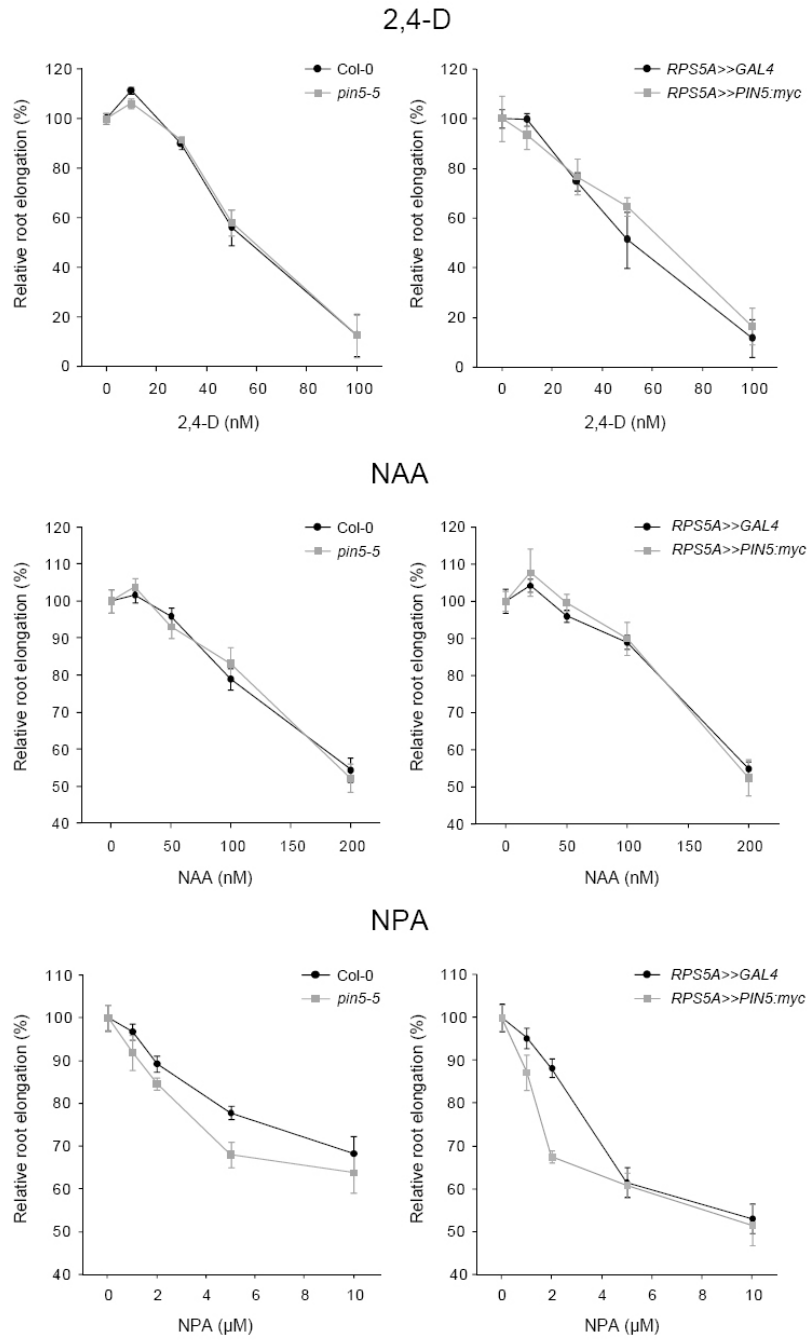

SUPPL. FIGURE 3. **Sensitivity of the pin5-5 mutant and the RPS5A>>PIN5:myc line** to auxin analogs (2,4-dichlorophenoxyacetic acid [2,4-D] and α-naphthaleneacetic [NAA] acid) and an auxin transport inhibitor (1-naphthylphthalamic acid [NPA]). Root length inhibition of a 10-day-old seedling grown on plates supplemented with the respective drugs. Only a slight increase in sensitivity to NPA was observed in the *pin5-5* mutant and the *RPS5A>>PIN5:myc* seedlings. Col-0 was used as a control for the *pin5-5* mutant and the *RPS5A* activator line for the *RPS5A>>PIN5:myc* line.

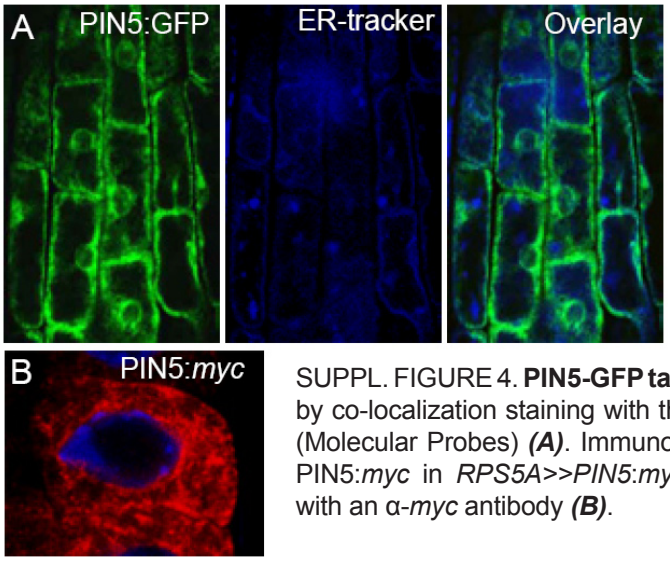

SUPPL. FIGURE 4. **PIN5-GFP targeting** confirmed by co-localization staining with the ER-tracker dye (Molecular Probes) ***(A)***. Immunological staining of PIN5:*myc* in *RPS5A>>PIN5:myc* epidermal cells with an α-*myc* antibody ***(B)***.

References

A

Abas, L., Benjamins, R., Malenica, N., Paciorek, T., Wisniewska, J., Moulinier-Anzola, J.C., Sieberer, T., Friml, J. and Luschnig, C. (2006) Intracellular trafficking and proteolysis of the Arabidopsis auxin-efflux facilitator PIN2 are involved in root gravitropism. *Nat Cell Biol*, **8**, 249-256.

Adams, B., Musiyenko, A., Kumar, R. and Barik, S. (2005) A novel class of dual-family immunophilins. *J Biol Chem*, **280**, 24308-24314.

Aghdasi, B., Ye, K., Resnick, A., Huang, A., Ha, H.C., Guo, X., Dawson, T.M., Dawson, V.L. and Snyder, S.H. (2001) FKBP12, the 12-kDa FK506-binding protein, is a physiologic regulator of the cell cycle. *Proc Natl Acad Sci U S A*, **98**, 2425-2430.

Altenberg, G.A. (2004) Structure of multidrug-resistance proteins of the ATP-binding cassette (ABC) superfamily. *Curr Med Chem Anticancer Agents*, **4**, 53-62.

Ambudkar, S.V., Cardarelli, C.O., Pashinsky, I. and Stein, W.D. (1997) Relation between the turnover number for vinblastine transport and for vinblastine-stimulated ATP hydrolysis by human P-glycoprotein. *J Biol Chem*, **272**, 21160-21166.

Ambudkar, S.V., Kimchi-Sarfaty, C., Sauna, Z.E. and Gottesman, M.M. (2003) P-glycoprotein: from genomics to mechanism. *Oncogene*, **22**, 7468-7485.

Angers, S., Salahpour, A., Joly, E., Hilairet, S., Chelsky, D., Dennis, M. and Bouvier, M. (2000) Detection of beta 2-adrenergic receptor dimerization in living cells using bioluminescence resonance energy transfer (BRET). *Proc Natl Acad Sci U S A*, **97**, 3684-3689.

Arndt, C., Cruz, M.C., Cardenas, M.E. and Heitman, J. (1999) Secretion of FK506/FK520 and rapamycin by Streptomyces inhibits the growth of competing Saccharomyces cerevisiae and Cryptococcus neoformans. *Microbiology*, **145 (Pt 8)**, 1989-2000.

Aviezer-Hagai, K., Skovorodnikova, J., Galigniana, M., Farchi-Pisanty, O., Maayan, E., Bocovza, S., Efrat, Y., von Koskull-Doring, P., Ohad, N. and Breiman, A. (2007) Arabidopsis immunophilins ROF1 (AtFKBP62) and ROF2 (AtFKBP65) exhibit tissue specificity, are heat-stress induced, and bind HSP90. *Plant Mol Biol*, **63**, 237-255.

B

Badescu, G.O. and Napier, R.M. (2006) Receptors for auxin: will it all end in TIRs? *Trends Plant Sci*, **11**, 217-223.

Badhan, R. and Penny, J. (2006) In silico modelling of the interaction of flavonoids with human P-glycoprotein nucleotide-binding domain. *Eur J Med Chem*, **41**, 285-295.

Bailly, A., Murphy, A., Martinoia, E. and Geisler, M. (2008a) Plant lessons: Understanding substrate specificity by structure modeling of ABCBs. *Nat Rev Mol Cell Biol,* in preparation.

Bailly, A., Sovero, V. and Geisler, M. (2006) The TWISTED DWARF's ABC: How Immunophilins Regulate Auxin Transport. *Plant Signaling and Behavior*, **1**, 277-280.

Bailly, A., Sovero, V., Vincenzetti, V., Santelia, D., Bartnik, D., Koenig, B.W., Mancuso, S., Martinoia, E. and Geisler, M. (2008b) Modulation of P-glycoproteins by auxin transport inhibitors is mediated by interaction with immunophilins. *J Biol Chem*, ms: M7.100122, resubmission.

Bainbridge, K., Guyomarc'h, S., Bayer, E., Swarup, R., Bennett, M., Mandel, T. and Kuhlemeier, C. (2008) Auxin influx carriers stabilize phyllotactic patterning. *Genes Dev*, **22**, 810-823.

Baluska, F., Samaj, J. and Menzel, D. (2003) Polar transport of auxin: carrier-mediated flux across the plasma membrane or neurotransmitter-like secretion? *Trends Cell Biol*, **13**, 282-285.

Bandyopadhyay, A., Blakeslee, J.J., Lee, O.R., Mravec, J., Sauer, M., Titapiwatanakun, B., Makam, S.N., Bouchard, R., Geisler, M., Martinoia, E., Friml, J., Peer, W.A. and Murphy, A.S. (2007) Interactions of PIN and PGP auxin transport mechanisms. *Biochem Soc Trans*, **35**, 137-141.

Bar-Peled, M. and Raikhel, N.V. (1997) Characterization of AtSEC12 and AtSAR1. Proteins likely involved in endoplasmic reticulum and Golgi transport. *Plant Physiol*, **114**, 315-324.

Barik, S. (2006) Immunophilins: for the love of proteins. *Cell Mol Life Sci*, **63**, 2889-2900.

Bartel, B. (1997) Auxin Biosynthesis. *Annu Rev Plant Physiol Plant Mol Biol*, **48**, 51-66.

Bartel, B. and Fink, G.R. (1995) ILR1, an amidohydrolase that releases active indole-3-acetic acid from conjugates. *Science*, **268**, 1745-1748.

Bartel, B., LeClere, S., Magidin, M. and Zolman, B.K. (2001) Inputs to the active indole-3-acetic acid pool: de novo synthesis, conjugate hydrolysis, and indole-3-butyric acid β-oxidation. *J. Plant Growth Regul.*, **20**, 198–216.

Benjamins, R., Quint, A., Weijers, D., Hooykaas, P. and Offringa, R. (2001) The PINOID protein kinase regulates organ development in Arabidopsis by enhancing polar auxin transport. *Development*, **128**, 4057-4067.

Benkova, E., Michniewicz, M., Sauer, M., Teichmann, T., Seifertova, D., Jurgens, G. and Friml, J. (2003) Local, efflux-dependent auxin gradients as a common module for plant organ formation. *Cell*, **115**, 591-602.

Bennett, M.J., Marchant, A., Green, H.G., May, S.T., Ward, S.P., Millner, P.A., Walker, A.R., Schulz, B. and Feldmann, K.A. (1996) Arabidopsis AUX1 gene: a permease-like regulator of root gravitropism. *Science*, **273**, 948-950.

Bernasconi, P., Patel, B.C., Reagan, J.D. and Subramanian, M.V. (1996) The N-1-Naphthylphthalamic Acid-Binding Protein Is an Integral Membrane Protein. *Plant Physiol*, **111**, 427-432.

Blakeslee, J.J., Bandyopadhyay, A., Lee, O.R., Mravec, J., Titapiwatanakun, B., Sauer, M., Makam, S.N., Cheng, Y., Bouchard, R., Adamec, J., Geisler, M., Nagashima, A., Sakai, T., Martinoia, E., Friml, J., Peer, W.A. and Murphy, A.S. (2007) Interactions among PIN-FORMED and P-glycoprotein auxin transporters in Arabidopsis. *Plant Cell*, **19**, 131-147.

Blakeslee, J.J., Bandyopadhyay, A., Peer, W.A., Makam, S.N.

and Murphy, A.S. (2004) Relocalization of the PIN1 auxin efflux facilitator plays a role in phototropic responses. *Plant Physiol*, **134**, 28-31.

Blakeslee, J.J., Peer, W.A. and Murphy, A.S. (2005) Auxin transport. *Curr Opin Plant Biol*, **8**, 494-500.

Blecher, O., Erel, N., Callebaut, I., Aviezer, K. and Breiman, A. (1996) A novel plant peptidyl-prolyl-cis-trans-isomerase (PPIase): cDNA cloning, structural analysis, enzymatic activity and expression. *Plant Mol Biol*, **32**, 493-504.

Blilou, I., Xu, J., Wildwater, M., Willemsen, V., Paponov, I., Friml, J., Heidstra, R., Aida, M., Palme, K. and Scheres, B. (2005) The PIN auxin efflux facilitator network controls growth and patterning in Arabidopsis roots. *Nature*, **433**, 39-44.

Borowski, E., Bontemps-Gracz, M.M. and Piwkowska, A. (2005) Strategies for overcoming ABC-transporters-mediated multidrug resistance (MDR) of tumor cells. *Acta Biochim Pol*, **52**, 609-627.

Bouchard, R., Bailly, A., Blakeslee, J.J., Oehring, S.C., Vincenzetti, V., Lee, O.R., Paponov, I., Palme, K., Mancuso, S., Murphy, A.S., Schulz, B. and Geisler, M. (2006) Immunophilin-like TWISTED DWARF1 modulates auxin efflux activities of Arabidopsis P-glycoproteins. *J Biol Chem*, **281**, 30603-30612.

Boumendjel, A., Di Pietro, A., Dumontet, C. and Barron, D. (2002) Recent advances in the discovery of flavonoids and analogs with high-affinity binding to P-glycoprotein responsible for cancer cell multidrug resistance. *Med Res Rev*, **22**, 512-529.

Breiman, A. and Camus, I. (2002) The involvement of mammalian and plant FK506-binding proteins (FKBPs) in development. *Transgenic Res*, **11**, 321-335.

Brown, D.E., Rashotte, A.M., Murphy, A.S., Normanly, J., Tague, B.W., Peer, W.A., Taiz, L. and Muday, G.K. (2001) Flavonoids act as negative regulators of auxin transport in vivo in arabidopsis. *Plant Physiol*, **126**, 524-535.

Brunn, S.A., Muday, G.K. and Haworth, P. (1992) Auxin Transport and the Interaction of Phytotropins: Probing the Properties of a Phytotropin Binding Protein. *Plant Physiol*, **98**, 101-107.

Buer, C.S. and Muday, G.K. (2004) The transparent testa4 mutation prevents flavonoid synthesis and alters auxin transport and the response of Arabidopsis roots to gravity and light. *Plant Cell*, **16**, 1191-1205.

Buer, C.S., Muday, G.K. and Djordjevic, M.A. (2007) Flavonoids are differentially taken up and transported long distances in Arabidopsis. *Plant Physiol*, **145**, 478-490.

Buer, C.S., Sukumar, P. and Muday, G.K. (2006) Ethylene modulates flavonoid accumulation and gravitropic responses in roots of Arabidopsis. *Plant Physiol*, **140**, 1384-1396.

Butler, J.H., Hu, S., Brady, S.R., Dixon, M.W. and Muday, G.K. (1998) In vitro and in vivo evidence for actin association of the naphthylphthalamic acid-binding protein from zucchini hypocotyls. *Plant J*, **13**, 291-301.

C

Cameron, A.M., Steiner, J.P., Roskams, A.J., Ali, S.M., Ronnett, G.V. and Snyder, S.H. (1995a) Calcineurin associated with the inositol 1,4,5-trisphosphate receptor-FKBP12 complex modulates Ca2+ flux. *Cell*, **83**, 463-472.

Cameron, A.M., Steiner, J.P., Sabatini, D.M., Kaplin, A.I., Walensky, L.D. and Snyder, S.H. (1995b) Immunophilin FK506 binding protein associated with inositol 1,4,5-trisphosphate receptor modulates calcium flux. *Proc Natl Acad Sci U S A*, **92**, 1784-1788.

Campanella, J.J., Ludwig-Mueller, J. and Town, C.D. (1996) Isolation and characterization of mutants of Arabidopsis thaliana with increased resistance to growth inhibition by indoleacetic acid-amino acid conjugates. *Plant Physiol*, **112**, 735-745.

Carol, R., Breiman, A., Erel, N., Vittorioso, P. and Bellini, C. (2001) Pasticcino 1 (AtFKBP70) is a nuclear-localised immunophilin required during Arabidopsis thaliana embryogenesis. *Plant Sci.*, **161**, 527-535.

Casimiro, I., Marchant, A., Bhalerao, R.P., Beeckman, T., Dhooge, S., Swarup, R., Graham, N., Inze, D., Sandberg, G., Casero, P.J. and Bennett, M. (2001) Auxin transport promotes Arabidopsis lateral root initiation. *Plant Cell*, **13**, 843-852.

Castro, A.F., Horton, J.K., Vanoye, C.G. and Altenberg, G.A. (1999) Mechanism of inhibition of P-glycoprotein-mediated drug transport by protein kinase C blockers. *Biochem Pharmacol*, **58**, 1723-1733.

Chambraud, B., Radanyi, C., Camonis, J.H., Rajkowski, K., Schumacher, M. and Baulieu, E.E. (1999) Immunophilins, Refsum disease, and lupus nephritis: the peroxisomal enzyme phytanoyl-COA alpha-hydroxylase is a new FKBP-associated protein. *Proc Natl Acad Sci U S A*, **96**, 2104-2109.

Chan, K.F., Zhao, Y., Burkett, B.A., Wong, I.L., Chow, L.M. and Chan, T.H. (2006) Flavonoid dimers as bivalent modulators for P-glycoprotein-based multidrug resistance: synthetic apigenin homodimers linked with defined-length poly(ethylene glycol) spacers increase drug retention and enhance chemosensitivity in resistant cancer cells. *J Med Chem*, **49**, 6742-6759.

Chang, G. (2003) Multidrug resistance ABC transporters. *FEBS Lett*, **555**, 102-105.

Chang, G. (2007) Retraction of "Structure of MsbA from Vibrio cholera: a multidrug resistance ABC transporter homolog in a closed conformation" [J. Mol. Biol. (2003) 330 419-430]. *J Mol Biol*, **369**, 596.

Chelu, M.G., Danila, C.I., Gilman, C.P. and Hamilton, S.L. (2004) Regulation of ryanodine receptors by FK506 binding proteins. *Trends Cardiovasc Med*, **14**, 227-234.

Chen, J., Lu, G., Lin, J., Davidson, A.L. and Quiocho, F.A. (2003) A tweezers-like motion of the ATP-binding cassette dimer in an ABC transport cycle. *Mol Cell*, **12**, 651-661.

Chen, J.G., Ullah, H., Young, J.C., Sussman, M.R. and Jones, A.M. (2001) ABP1 is required for organized cell elongation and division in Arabidopsis embryogenesis. *Genes Dev*, **15**, 902-911.

Chen, L. and Bush, D.R. (1997) LHT1, a lysine- and histidine-specific amino acid transporter in arabidopsis. *Plant Physiol*, **115**, 1127-1134.

Chen, R., Hilson, P., Sedbrook, J., Rosen, E., Caspar, T. and Masson, P.H. (1998) The arabidopsis thaliana AGRAVITROPIC 1 gene encodes a component of the polar-auxin-transport efflux carrier. *Proc Natl Acad Sci U S A*, **95**, 15112-15117.

Cheng, Y., Dai, X. and Zhao, Y. (2006) Auxin biosynthesis by the YUCCA flavin monooxygenases controls the formation of floral organs and vascular tissues in Arabidopsis. *Genes Dev*, **20**, 1790-1799.

Cho, M., Lee, S.H. and Cho, H.T. (2007) P-glycoprotein4 displays auxin efflux transporter-like action in Arabidopsis root hair cells and tobacco cells. *Plant Cell*, **19**, 3930-3943.

Cholodny, N. (1927) Wuchshormone und Tropismen bei den Pflanzen. *Biol Zentbl*, **47**, 604–626.

Cleland, R. (1967) Inhibition of cell elongation in Avena coleoptile by hydroxyproline. *Plant Physiol*, **42**, 271-274.

Cohen, J.D. and Bandurski, R.S. (1982) Chemistry and Pysiology of the Bound Auxins. *Annual Review of Plant Physiology*, **33**, 403-430.

Conseil, G., Baubichon-Cortay, H., Dayan, G., Jault, J.M., Barron, D. and Di Pietro, A. (1998) Flavonoids: a class of modulators with bifunctional interactions at vicinal ATP- and steroid-binding sites on mouse P-glycoprotein. *Proc Natl Acad Sci U S A*, **95**, 9831-9836.

Cox, D.N. and Muday, G.K. (1994) NPA binding activity is peripheral to the plasma membrane and is associated with the cytoskeleton. *Plant Cell*, **6**, 1941-1953.

Crespo, J.L., Diaz-Troya, S. and Florencio, F.J. (2005) Inhibition of target of rapamycin signaling by rapamycin in the unicellular green alga Chlamydomonas reinhardtii. *Plant Physiol*, **139**, 1736-1749.

Cruz, M.C., Cavallo, L.M., Gorlach, J.M., Cox, G., Perfect, J.R., Cardenas, M.E. and Heitman, J. (1999) Rapamycin antifungal action is mediated via conserved complexes with FKBP12 and TOR kinase homologs in Cryptococcus neoformans. *Mol Cell Biol*, **19**, 4101-4112.

D

Dalmas, O., Orelle, C., Foucher, A.E., Geourjon, C., Crouzy, S., Di Pietro, A. and Jault, J.M. (2005) The Q-loop disengages from the first intracellular loop during the catalytic cycle of the multidrug ABC transporter BmrA. *J Biol Chem*, **280**, 36857-36864.

Darwin, C. and Darwin, F. (1880) *The Power of Movement in Plants*. Murray, London.

Daus, M.L., Grote, M., Muller, P., Doebber, M., Herrmann, A., Steinhoff, H.J., Dassa, E. and Schneider, E. (2007) ATP-driven MalK dimer closure and reopening and conformational changes of the "EAA" motifs are crucial for function of the maltose ATP-binding cassette transporter (MalFGK2). *J Biol Chem*, **282**, 22387-22396.

Daus, M.L., Landmesser, H., Schlosser, A., Muller, P., Herrmann, A. and Schneider, E. (2006) ATP induces conformational changes of periplasmic loop regions of the maltose ATP-binding cassette transporter. *J Biol Chem*, **281**, 3856-3865.

Davidson, A.L. and Chen, J. (2004) ATP-binding cassette transporters in bacteria. *Annu Rev Biochem*, **73**, 241-268.

Davies, P.J. (2004) The plant hormones: their nature, occurence, and function. In Davies, P.J. (ed.), *Biosynthesis, Signal Transduction, Action!* Kluwer Academic Publishers, Dordrecht, The Netherlands, pp. 1-15.

Davies, P.J. and Rubery, P.H. (1978) Components of auxin transport in stem segments of Pisum sativum. *Planta*, **142**, 211-219.

Davies, T.H. and Sanchez, E.R. (2005) Fkbp52. *Int J Biochem Cell Biol*, **37**, 42-47.

Dawson, R.J., Hollenstein, K. and Locher, K.P. (2007) Uptake or extrusion: crystal structures of full ABC transporters suggest a common mechanism. *Mol Microbiol*, **65**, 250-257.

Dawson, R.J. and Locher, K.P. (2006) Structure of a bacterial multidrug ABC transporter. *Nature*, **443**, 180-185.

Dawson, R.J. and Locher, K.P. (2007) Structure of the multidrug ABC transporter Sav1866 from Staphylococcus aureus in complex with AMP-PNP. *FEBS Lett*, **581**, 935-938.

Dean, M. (2005) The genetics of ATP-binding cassette transporters. *Methods Enzymol*, **400**, 409-429.

DeCenzo, M.T., Park, S.T., Jarrett, B.P., Aldape, R.A., Futer, O., Murcko, M.A. and Livingston, D.J. (1996) FK506-binding protein mutational analysis: defining the active-site residue contributions to catalysis and the stability of ligand complexes. *Protein Eng*, **9**, 173-180.

DeGorter, M.K., Conseil, G., Deeley, R.G., Campbell, R.L. and Cole, S.P. (2008) Molecular modeling of the human multidrug resistance protein 1 (MRP1/ABCC1). *Biochem Biophys Res Commun*, **365**, 29-34.

Delbarre, A., Muller, P. and Guern, J. (1998) Short-Lived and Phosphorylated Proteins Contribute to Carrier-Mediated Efflux, but Not to Influx, of Auxin in Suspension-Cultured Tobacco Cells. *Plant Physiol*, **116**, 833-844.

Delker, C., Raschke, A. and Quint, M. (2008) Auxin dynamics: the dazzling complexity of a small molecule's message. *Planta*.

Deruere, J., Jackson, K., Garbers, C., Soll, D. and Delong, A. (1999) The RCN1-encoded A subunit of protein phosphatase 2A increases phosphatase activity in vivo. *Plant J*, **20**, 389-399.

Dharmasiri, N., Dharmasiri, S. and Estelle, M. (2005) The F-box protein TIR1 is an auxin receptor. *Nature*, **435**, 441-445.

Dharmasiri, S., Swarup, R., Mockaitis, K., Dharmasiri, N., Singh, S.K., Kowalchyk, M., Marchant, A., Mills, S., Sandberg, G., Bennett, M.J. and Estelle, M. (2006) AXR4 is required for localization of the auxin influx facilitator AUX1. *Science*, **312**, 1218-1220.

Dhaubhadel, S., Chaudhary, S., Dobinson, K.F. and Krishna, P. (1999) Treatment with 24-epibrassinolide, a brassinosteroid, increases the basic thermotolerance of Brassica napus and tomato seedlings. *Plant Mol Biol*, **40**, 333-342.

Dhonukshe, P., Aniento, F., Hwang, I., Robinson, D.G., Mravec, J., Stierhof, Y.D. and Friml, J. (2007) Clathrin-mediated constitutive endocytosis of PIN auxin efflux carriers in Arabidopsis. *Curr Biol*, **17**, 520-527.

Dhonukshe, P., Grigoriev, I., Fischer, R., Tominaga, M.,

Robinson, D.G., Hasek, J., Paciorek, T., Petrasek, J., Seifertova, D., Tejos, R., Meisel, L.A., Zazimalova, E., Gadella, T.W., Jr., Stierhof, Y.D., Ueda, T., Oiwa, K., Akhmanova, A., Brock, R., Spang, A. and Friml, J. (2008) Auxin transport inhibitors impair vesicle motility and actin cytoskeleton dynamics in diverse eukaryotes. *Proc Natl Acad Sci U S A*, **105**, 4489-4494.

Di Pietro, A., Conseil, G., Perez-Victoria, J.M., Dayan, G., Baubichon-Cortay, H., Trompier, D., Steinfels, E., Jault, J.M., de Wet, H., Maitrejean, M., Comte, G., Boumendjel, A., Mariotte, A.M., Dumontet, C., McIntosh, D.B., Goffeau, A., Castanys, S., Gamarro, F. and Barron, D. (2002) Modulation by flavonoids of cell multidrug resistance mediated by P-glycoprotein and related ABC transporters. *Cell Mol Life Sci*, **59**, 307-322.

Dolinski, K., Muir, S., Cardenas, M. and Heitman, J. (1997) All cyclophilins and FK506 binding proteins are, individually and collectively, dispensable for viability in Saccharomyces cerevisiae. *Proc Natl Acad Sci U S A*, **94**, 13093-13098.

Drubin, D.G. (2000) *Cell polarity*. Oxford University Press, Oxford.

Du, L. and Poovaiah, B.W. (2005) Ca2+/calmodulin is critical for brassinosteroid biosynthesis and plant growth. *Nature*, **437**, 741-745.

Dunnwald, M., Varshavsky, A. and Johnsson, N. (1999) Detection of transient in vivo interactions between substrate and transporter during protein translocation into the endoplasmic reticulum. *Mol Biol Cell*, **10**, 329-344.

Dwivedi, R.S., Breiman, A. and Herman, E.M. (2003) Differential distribution of the cognate and heat-stress-induced isoforms of high Mr cis-trans prolyl peptidyl isomerase (FKBP) in the cytoplasm and nucleoplasm. *J Exp Bot*, **54**, 2679-2689.

E

Edlich, F., Weiwad, M., Erdmann, F., Fanghanel, J., Jarczowski, F., Rahfeld, J.U. and Fischer, G. (2005) Bcl-2 regulator FKBP38 is activated by Ca2+/calmodulin. *Embo J*, **24**, 2688-2699.

Epand, R.F. and Epand, R.M. (1991) The new potent immunosuppressant FK-506 reverses multidrug resistance in Chinese hamster ovary cells. *Anticancer Drug Des*, **6**, 189-193.

Evans, M.L. (1991) Gravitropism: interaction of sensitivity modulation and effector redistribution. *Plant Physiol*, **95**, 1-5.

Eytan, G.D., Regev, R. and Assaraf, Y.G. (1996) Functional reconstitution of P-glycoprotein reveals an apparent near stoichiometric drug transport to ATP hydrolysis. *J Biol Chem*, **271**, 3172-3178.

F

Fanghanel, J. and Fischer, G. (2004) Insights into the catalytic mechanism of peptidyl prolyl cis/trans isomerases. *Front Biosci*, **9**, 3453-3478.

Faure, J.D., Gingerich, D. and Howell, S.H. (1998a) An Arabidopsis immunophilin, AtFKBP12, binds to AtFIP37 (FKBP interacting protein) in an interaction that is disrupted by FK506. *Plant J*, **15**, 783-789.

Faure, J.D., Vittorioso, P., Santoni, V., Fraisier, V., Prinsen, E., Barlier, I., Van Onckelen, H., Caboche, M. and Bellini, C. (1998b) The PASTICCINO genes of Arabidopsis thaliana are involved in the control of cell division and differentiation. *Development*, **125**, 909-918.

Federici, L., Woebking, B., Velamakanni, S., Shilling, R.A., Luisi, B. and van Veen, H.W. (2007) New structure model for the ATP-binding cassette multidrug transporter LmrA. *Biochem Pharmacol*, **74**, 672-678.

Flanagan, J.U. and Huber, T. (2007) Structural Evolution of the ABC Transporter Subfamily B. *Evolutionary Bioinformatics*, **3**, 309-316.

Folkes, L.K. and Wardman, P. (2003) Enhancing the efficacy of photodynamic cancer therapy by radicals from plant auxin (indole-3-acetic acid). *Cancer Res*, **63**, 776-779.

Friedrichsen, D. and Chory, J. (2001) Steroid signaling in plants: from the cell surface to the nucleus. *Bioessays*, **23**, 1028-1036.

Friml, J. (2003) Auxin transport - shaping the plant. *Curr Opin Plant Biol*, **6**, 7-12.

Friml, J., Benkova, E., Blilou, I., Wisniewska, J., Hamann, T., Ljung, K., Woody, S., Sandberg, G., Scheres, B., Jurgens, G. and Palme, K. (2002a) AtPIN4 mediates sink-driven auxin gradients and root patterning in Arabidopsis. *Cell*, **108**, 661-673.

Friml, J. and Palme, K. (2002) Polar auxin transport--old questions and new concepts? *Plant Mol Biol*, **49**, 273-284.

Friml, J., Vieten, A., Sauer, M., Weijers, D., Schwarz, H., Hamann, T., Offringa, R. and Jurgens, G. (2003) Efflux-dependent auxin gradients establish the apical-basal axis of Arabidopsis. *Nature*, **426**, 147-153.

Friml, J. and Wisniewska, J. (2005) Intercellular communication in Plants. In Fleming, A. (ed.). Blackwell Publishing, Oxford, pp. 1-26.

Friml, J., Wisniewska, J., Benkova, E., Mendgen, K. and Palme, K. (2002b) Lateral relocation of auxin efflux regulator PIN3 mediates tropism in Arabidopsis. *Nature*, **415**, 806-809.

Friml, J., Yang, X., Michniewicz, M., Weijers, D., Quint, A., Tietz, O., Benjamins, R., Ouwerkerk, P.B., Ljung, K., Sandberg, G., Hooykaas, P.J., Palme, K. and Offringa, R. (2004) A PINOID-dependent binary switch in apical-basal PIN polar targeting directs auxin efflux. *Science*, **306**, 862-865.

Fujita, H. and Syono, K. (1997) PIS1, a negative regulator of the action of auxin transport inhibitors in Arabidopsis thaliana. *Plant J*, **12**, 583-595.

G

Galweiler, L., Guan, C., Muller, A., Wisman, E., Mendgen, K., Yephremov, A. and Palme, K. (1998) Regulation of polar auxin transport by AtPIN1 in Arabidopsis vascular tissue. *Science*, **282**, 2226-2230.

Garbers, C., DeLong, A., Deruere, J., Bernasconi, P. and Soll, D. (1996) A mutation in protein phosphatase 2A regulatory subunit A affects auxin transport in Arabidopsis. *Embo J*, **15**, 2115-2124.

Garrigues, A., Escargueil, A.E. and Orlowski, S. (2002) The multidrug transporter, P-glycoprotein, actively mediates cholesterol redistribution in the cell membrane. *Proc Natl Acad Sci U S A*, **99**, 10347-10352.

Geisler, M. and Bailly, A. (2007) Tete-a-tete: the function of FKBPs in plant development. *Trends Plant Sci*, **12**, 465-473.

Geisler, M., Blakeslee, J.J., Bouchard, R., Lee, O.R., Vincenzetti, V., Bandyopadhyay, A., Titapiwatanakun, B., Peer, W.A., Bailly, A., Richards, E.L., Ejendal, K.F., Smith, A.P., Baroux, C., Grossniklaus, U., Muller, A., Hrycyna, C.A., Dudler, R., Murphy, A.S. and Martinoia, E. (2005) Cellular efflux of auxin catalyzed by the Arabidopsis MDR/PGP transporter AtPGP1. *Plant J*, **44**, 179-194.

Geisler, M., Frangne, N., Gomes, E., Martinoia, E. and Palmgren, M.G. (2000) The ACA4 gene of Arabidopsis encodes a vacuolar membrane calcium pump that improves salt tolerance in yeast. *Plant Physiol*, **124**, 1814-1827.

Geisler, M., Girin, M., Brandt, S., Vincenzetti, V., Plaza, S., Paris, N., Kobae, Y., Maeshima, M., Billion, K., Kolukisaoglu, U.H., Schulz, B. and Martinoia, E. (2004) Arabidopsis immunophilin-like TWD1 functionally interacts with vacuolar ABC transporters. *Mol Biol Cell*, **15**, 3393-3405.

Geisler, M., Kolukisaoglu, H.U., Bouchard, R., Billion, K., Berger, J., Saal, B., Frangne, N., Koncz-Kalman, Z., Koncz, C., Dudler, R., Blakeslee, J.J., Murphy, A.S., Martinoia, E. and Schulz, B. (2003) TWISTED DWARF1, a unique plasma membrane-anchored immunophilin-like protein, interacts with Arabidopsis multidrug resistance-like transporters AtPGP1 and AtPGP19. *Mol Biol Cell*, **14**, 4238-4249.

Geisler, M. and Murphy, A.S. (2006) The ABC of auxin transport: the role of p-glycoproteins in plant development. *FEBS Lett*, **580**, 1094-1102.

Geldner, N., Anders, N., Wolters, H., Keicher, J., Kornberger, W., Muller, P., Delbarre, A., Ueda, T., Nakano, A. and Jurgens, G. (2003) The Arabidopsis GNOM ARF-GEF mediates endosomal recycling, auxin transport, and auxin-dependent plant growth. *Cell*, **112**, 219-230.

Geldner, N., Friml, J., Stierhof, Y.D., Jurgens, G. and Palme, K. (2001) Auxin transport inhibitors block PIN1 cycling and vesicle trafficking. *Nature*, **413**, 425-428.

Geldner, N., Hyman, D.L., Wang, X., Schumacher, K. and Chory, J. (2007) Endosomal signaling of plant steroid receptor kinase BRI1. *Genes Dev*, **21**, 1598-1602.

Germain, M. and Shore, G.C. (2003) Cellular distribution of Bcl-2 family proteins. *Sci STKE*, **2003**, pe10.

Ghosh, P., Moitra, K., Maki, N. and Dey, S. (2006) Allosteric modulation of the human P-glycoprotein involves conformational changes mimicking catalytic transition intermediates. *Arch Biochem Biophys*, **450**, 100-112.

Gil, P., Dewey, E., Friml, J., Zhao, Y., Snowden, K.C., Putterill, J., Palme, K., Estelle, M. and Chory, J. (2001) BIG: a calossin-like protein required for polar auxin transport in Arabidopsis. *Genes Dev*, **15**, 1985-1997.

Gleave, A.P. (1992) A versatile binary vector system with a T-DNA organisational structure conducive to efficient integration of cloned DNA into the plant genome. *Plant Mol Biol*, **20**, 1203-1207.

Globisch, C., Pajeva, I.K. and Wiese, M. (2008) Identification of Putative Binding Sites of P-glycoprotein Based on its Homology Model. *ChemMedChem*, **3**, 280-295.

Goldsmith, M.H. (1977) The polar transport of auxin. *Annu. Rev. Plant Physiol.*, **28**, 439-478.

Goldsmith, M.H., Goldsmith, T.H. and Martin, M.H. (1981) Mathematical analysis of the chemosmotic polar diffusion of auxin through plant tissues. *Proc Natl Acad Sci U S A*, **78**, 976-980.

Gopalan, G., He, Z., Balmer, Y., Romano, P., Gupta, R., Heroux, A., Buchanan, B.B., Swaminathan, K. and Luan, S. (2004) Structural analysis uncovers a role for redox in regulating FKBP13, an immunophilin of the chloroplast thylakoid lumen. *Proc Natl Acad Sci U S A*, **101**, 13945-13950.

Gopalan, G., He, Z., Battaile, K.P., Luan, S. and Swaminathan, K. (2006) Structural comparison of oxidized and reduced FKBP13 from Arabidopsis thaliana. *Proteins*, **65**, 789-795.

Gottesman, M.M. and Ling, V. (2006) The molecular basis of multidrug resistance in cancer: the early years of P-glycoprotein research. *FEBS Lett*, **580**, 998-1009.

Granzin, J., Eckhoff, A. and Weiergraber, O.H. (2006) Crystal structure of a multi-domain immunophilin from Arabidopsis thaliana: a paradigm for regulation of plant ABC transporters. *J Mol Biol*, **364**, 799-809.

Grebe, M., Friml, J., Swarup, R., Ljung, K., Sandberg, G., Terlou, M., Palme, K., Bennett, M.J. and Scheres, B. (2002) Cell polarity signaling in Arabidopsis involves a BFA-sensitive auxin influx pathway. *Curr Biol*, **12**, 329-334.

Guex, N. and Peitsch, M.C. (1997) SWISS-MODEL and the Swiss-PdbViewer: an environment for comparative protein modeling. *Electrophoresis*, **18**, 2714-2723.

Gupta, R., Mould, R.M., He, Z. and Luan, S. (2002) A chloroplast FKBP interacts with and affects the accumulation of Rieske subunit of cytochrome bf complex. *Proc Natl Acad Sci U S A*, **99**, 15806-15811.

H

Hadfi, K., Speth, V. and Neuhaus, G. (1998) Auxin-induced developmental patterns in Brassica juncea embryos. *Development*, **125**, 879-887.

Hadjeri, M., Barbier, M., Ronot, X., Mariotte, A.M., Boumendjel, A. and Boutonnat, J. (2003) Modulation of P-glycoprotein-mediated multidrug resistance by flavonoid derivatives and analogues. *J Med Chem*, **46**, 2125-2131.

Harrar, Y., Bellec, Y., Bellini, C. and Faure, J.D. (2003) Hormonal control of cell proliferation requires PASTICCINO genes. *Plant Physiol*, **132**, 1217-1227.

Harrar, Y., Bellini, C. and Faure, J.D. (2001) FKBPs: at the crossroads of folding and transduction. *Trends Plant Sci*, **6**, 426-431.

Hazai, E. and Bikadi, Z. (2007) Homology modeling of breast cancer resistance protein (ABCG2). *J Struct Biol*.

He, Z., Li, L. and Luan, S. (2004) Immunophilins and parvulins. Superfamily of peptidyl prolyl isomerases in Arabidopsis. *Plant Physiol*, **134**, 1248-1267.

Heisler, M.G., Ohno, C., Das, P., Sieber, P., Reddy, G.V., Long,

J.A. and Meyerowitz, E.M. (2005) Patterns of auxin transport and gene expression during primordium development revealed by live imaging of the Arabidopsis inflorescence meristem. *Curr Biol*, **15**, 1899-1911.

Heitman, J., Movva, N.R. and Hall, M.N. (1992) Proline isomerases at the crossroads of protein folding, signal transduction, and immunosuppression. *New Biol*, **4**, 448-460.

Hemenway, C.S. and Heitman, J. (1996) Immunosuppressant target protein FKBP12 is required for P-glycoprotein function in yeast. *J Biol Chem*, **271**, 18527-18534.

Hertel, R., Evans, M.R., Leopold, A.C. and Sell, H.M. (1969) The specificity of the auxin transport system. *Planta*, **85**, 238-249.

Hertel, R. and Leopold, A.C. (1963) Versuche zur Analyse des Auxintransports in der Koleoptile von Zea mays. *Planta*, **59**, 535-562.

Higgins, C.F. (2001) ABC transporters: physiology, structure and mechanism--an overview. *Res Microbiol*, **152**, 205-210.

Higgins, C.F., Callaghan, R., Linton, K.J., Rosenberg, M.F. and Ford, R.C. (1997) Structure of the multidrug resistance P-glycoprotein. *Semin Cancer Biol*, **8**, 135-142.

Higgins, C.F. and Linton, K.J. (2004) The ATP switch model for ABC transporters. *Nat Struct Mol Biol*, **11**, 918-926.

Hollenstein, K., Dawson, R.J. and Locher, K.P. (2007a) Structure and mechanism of ABC transporter proteins. *Curr Opin Struct Biol*, **17**, 412-418.

Hollenstein, K., Frei, D.C. and Locher, K.P. (2007b) Structure of an ABC transporter in complex with its binding protein. *Nature*, **446**, 213-216.

Hopfner, K.P., Karcher, A., Shin, D.S., Craig, L., Arthur, L.M., Carney, J.P. and Tainer, J.A. (2000) Structural biology of Rad50 ATPase: ATP-driven conformational control in DNA double-strand break repair and the ABC-ATPase superfamily. *Cell*, **101**, 789-800.

Hossel, D., Schmeiser, C. and Hertel, R. (2005) Specificity patterns indicate that auxin exporters and receptors are the same proteins. *Plant Biol (Stuttg)*, **7**, 41-48.

Hrycyna, C.A. and Gottesman, M.M. (1998) Multidrug ABC transporters from bacteria to man: an emerging hypothesis for the universality of molecular mechanism and function. *Drug Resist Updat*, **1**, 81-83.

I

Ishida, T., Thitamadee, S. and Hashimoto, T. (2007) Twisted growth and organization of cortical microtubules. *J Plant Res*, **120**, 61-70.

Ito, H. and Gray, W.M. (2006) A gain-of-function mutation in the Arabidopsis pleiotropic drug resistance transporter PDR9 confers resistance to auxinic herbicides. *Plant Physiol*, **142**, 63-74.

J

Jacobs, M. and Gilbert, S.F. (1983a) Basal localization of the presumptive auxin carrier in pea stem cells. *Science*, **220**, 1297-1300.

Jacobs, M. and Gilbert, S.F. (1983b) Basal Localization of the Presumptive Auxin Transport Carrier in Pea Stem Cells. *Science*, **220**, 1297-1300.

Jacobs, M. and Rubery, P.H. (1988a) Naturally Occurring Auxin Transport Regulators. *Science*, **241**, 346-349.

Jacobs, M. and Rubery, P.H. (1988b) Naturally occurring transport regulators. *Science*, **241**, 346-349.

Jasinski, M., Ducos, E., Martinoia, E. and Boutry, M. (2003) The ATP-binding cassette transporters: structure, function, and gene family comparison between rice and Arabidopsis. *Plant Physiol*, **131**, 1169-1177.

Jones, A.M. (1998) Auxin transport: down and out and up again. *Science*, **282**, 2201-2203.

K

Kamphausen, T., Fanghanel, J., Neumann, D., Schulz, B. and Rahfeld, J.U. (2002) Characterization of Arabidopsis thaliana AtFKBP42 that is membrane-bound and interacts with Hsp90. *Plant J*, **32**, 263-276.

Kelch, D.G., Driskell, A. and Mishler, B. (2004) In B. Goffinet, V.H., R. Magill (ed.), *Molecular Systematics of Bryophytes*. Missouri Botanical Garden Press, St. Louis, MO., pp. 3-12.

Kepinski, S. (2007) The anatomy of auxin perception. *Bioessays*, **29**, 953-956.

Kepinski, S. and Leyser, O. (2005a) The Arabidopsis F-box protein TIR1 is an auxin receptor. *Nature*, **435**, 446-451.

Kepinski, S. and Leyser, O. (2005b) Plant development: auxin in loops. *Curr Biol*, **15**, R208-210.

Kerem, B. and Kerem, E. (1996) The molecular basis for disease variability in cystic fibrosis. *Eur J Hum Genet*, **4**, 65-73.

Kerhoas, L., Aouak, D., Cingoz, A., Routaboul, J.M., Lepiniec, L., Einhorn, J. and Birlirakis, N. (2006) Structural characterization of the major flavonoid glycosides from Arabidopsis thaliana seeds. *J Agric Food Chem*, **54**, 6603-6612.

Kerr, I.D. (2002) Structure and association of ATP-binding cassette transporter nucleotide-binding domains. *Biochim Biophys Acta*, **1561**, 47-64.

Kerr, I.D. and Bennett, M.J. (2007) New insight into the biochemical mechanisms regulating auxin transport in plants. *Biochem J*, **401**, 613-622.

Khush, G.S. (2001) Green revolution: the way forward. *Nat Rev Genet*, **2**, 815-822.

Kimura, Y., Kodan, A., Matsuo, M. and Ueda, K. (2007) Cholesterol fill-in model: mechanism for substrate recognition by ABC proteins. *J Bioenerg Biomembr*, **39**, 447-452.

Kleine-Vehn, J., Dhonukshe, P., Swarup, R., Bennett, M. and Friml, J. (2006) Subcellular trafficking of the Arabidopsis auxin influx carrier AUX1 uses a novel pathway distinct from PIN1. *Plant Cell*, **18**, 3171-3181.

Knoblich, J.A. (2000) Epithelial polarity: the ins and outs of the fly epidermis. *Curr Biol*, **10**, R791-794.

Koizumi, K., Sugiyama, M. and Fukuda, H. (2000) A series of novel mutants of Arabidopsis thaliana that are defective in the formation of continuous vascular network: calling the auxin signal flow canalization hypothesis into question. *Development*, **127**, 3197-3204.

Kolukisaoglu, H.U., Bovet, L., Klein, M., Eggmann, T., Geisler, M., Wanke, D., Martinoia, E. and Schulz, B. (2002) Family business: the multidrug-resistance related protein (MRP) ABC transporter genes in Arabidopsis thaliana. *Planta*, **216**, 107-119.

Kotak, S., Vierling, E., Baumlein, H. and von Koskull-Doring, P. (2007) A novel transcriptional cascade regulating expression of heat stress proteins during seed development of Arabidopsis. *Plant Cell*, **19**, 182-195.

Kramer, E.M. and Bennett, M.J. (2006) Auxin transport: a field in flux. *Trends Plant Sci*, **11**, 382-386.

Krishna, R. and Mayer, L.D. (2001) Modulation of P-glycoprotein (PGP) mediated multidrug resistance (MDR) using chemosensitizers: recent advances in the design of selective MDR modulators. *Curr Med Chem Anticancer Agents*, **1**, 163-174.

Kunzelmann, K. and Schreiber, R. (1999) CFTR, a regulator of channels. *J Membr Biol*, **168**, 1-8.

Kurek, I., Aviezer, K., Erel, N., Herman, E. and Breiman, A. (1999) The wheat peptidyl prolyl cis-trans-isomerase FKBP77 is heat induced and developmentally regulated. *Plant Physiol*, **119**, 693-704.

Kurek, I., Dulberger, R., Azem, A., Tzvi, B.B., Sudhakar, D., Christou, P. and Breiman, A. (2002a) Deletion of the C-terminal 138 amino acids of the wheat FKBP73 abrogates calmodulin binding, dimerization and male fertility in transgenic rice. *Plant Mol Biol*, **48**, 369-381.

Kurek, I., Kawagoe, Y., Jacob-Wilk, D., Doblin, M. and Delmer, D. (2002b) Dimerization of cotton fiber cellulose synthase catalytic subunits occurs via oxidation of the zinc-binding domains. *Proc Natl Acad Sci U S A*, **99**, 11109-11114.

Kurek, I., Pirkl, F., Fischer, E., Buchner, J. and Breiman, A. (2002c) Wheat FKBP73 functions in vitro as a molecular chaperone independently of its peptidyl prolyl cis-trans isomerase activity. *Planta*, **215**, 119-126.

Kurek, I., Stoger, E., Dulberger, R., Christou, P. and Breiman, A. (2002d) Overexpression of the wheat FK506-binding protein 73 (FKBP73) and the heat-induced wheat FKBP77 in transgenic wheat reveals different functions of the two isoforms. *Transgenic Res*, **11**, 373-379.

L

Lambrecht, M., Okon, Y., Vande Broek, A. and Vanderleyden, J. (2000) Indole-3-acetic acid: a reciprocal signalling molecule in bacteria-plant interactions. *Trends Microbiol*, **8**, 298-300.

Lania-Pietrzak, B., Michalak, K., Hendrich, A.B., Mosiadz, D., Grynkiewicz, G., Motohashi, N. and Shirataki, Y. (2005) Modulation of MRP1 protein transport by plant, and synthetically modified flavonoids. *Life Sci*, **77**, 1879-1891.

Lariguet, P. and Fankhauser, C. (2004) Hypocotyl growth orientation in blue light is determined by phytochrome A inhibition of gravitropism and phototropin promotion of phototropism. *Plant J*, **40**, 826-834.

Lawson, J., O'Mara, M.L. and Kerr, I.D. (2008) Structure-based interpretation of the mutagenesis database for the nucleotide binding domains of P-glycoprotein. *Biochim Biophys Acta*, **1778**, 376-391.

Lee, J.Y., Urbatsch, I.L., Senior, A.E. and Wilkens, S. (2002) Projection structure of P-glycoprotein by electron microscopy. Evidence for a closed conformation of the nucleotide binding domains. *J Biol Chem*, **277**, 40125-40131.

Lee, J.Y., Urbatsch, I.L., Senior, A.E. and Wilkens, S. (2008) Nucleotide-induced Structural Changes in P-glycoprotein Observed by Electron Microscopy. *J Biol Chem*, **283**, 5769-5779.

Lelong-Rebel, I.H. and Cardarelli, C.O. (2005) Differential phosphorylation patterns of P-glycoprotein reconstituted into a proteoliposome system: insight into additional unconventional phosphorylation sites. *Anticancer Res*, **25**, 3925-3935.

Lewis, D.R., Miller, N.D., Splitt, B.L., Wu, G. and Spalding, E.P. (2007) Separating the roles of acropetal and basipetal auxin transport on gravitropism with mutations in two Arabidopsis multidrug resistance-like ABC transporter genes. *Plant Cell*, **19**, 1838-1850.

Leyser, O. (2006) Dynamic integration of auxin transport and signalling. *Curr Biol*, **16**, R424-433.

Li, J., Yang, H., Peer, W.A., Richter, G., Blakeslee, J., Bandyopadhyay, A., Titapiwantakun, B., Undurraga, S., Khodakovskaya, M., Richards, E.L., Krizek, B., Murphy, A.S., Gilroy, S. and Gaxiola, R. (2005a) Arabidopsis H+-PPase AVP1 regulates auxin-mediated organ development. *Science*, **310**, 121-125.

Li, L., Xu, J., Xu, Z.H. and Xue, H.W. (2005b) Brassinosteroids stimulate plant tropisms through modulation of polar auxin transport in Brassica and Arabidopsis. *Plant Cell*, **17**, 2738-2753.

Lima, A., Lima, S., Wong, J.H., Phillips, R.S., Buchanan, B.B. and Luan, S. (2006) A redox-active FKBP-type immunophilin functions in accumulation of the photosystem II supercomplex in Arabidopsis thaliana. *Proc Natl Acad Sci U S A*, **103**, 12631-12636.

Limtrakul, P., Khantamat, O. and Pintha, K. (2005) Inhibition of P-glycoprotein function and expression by kaempferol and quercetin. *J Chemother*, **17**, 86-95.

Lin, R. and Wang, H. (2005) Two homologous ATP-binding cassette transporter proteins, AtMDR1 and AtPGP1, regulate Arabidopsis photomorphogenesis and root development by mediating polar auxin transport. *Plant Physiol*, **138**, 949-964.

Linton, K.J. (2007) Structure and function of ABC transporters. *Physiology (Bethesda)*, **22**, 122-130.

Linton, K.J. and Higgins, C.F. (2007) Structure and function of ABC transporters: the ATP switch provides flexible control. *Pflugers Arch*, **453**, 555-567.

Ljung, K., Bhalerao, R.P. and Sandberg, G. (2001) Sites and homeostatic control of auxin biosynthesis in Arabidopsis during vegetative growth. *Plant J*, **28**, 465-474.

Ljung, K., Hull, A.K., Kowalczyk, M., Marchant, A., Celenza, J., Cohen, J.D. and Sandberg, G. (2002) Biosynthesis, conjugation, catabolism and homeostasis of indole-3-acetic acid in Arabidopsis thaliana. *Plant Mol Biol*, **49**, 249-272.

Locher, K.P. (2004) Structure and mechanism of ABC transporters. *Curr Opin Struct Biol*, **14**, 426-431.

Locher, K.P. and Borths, E. (2004) ABC transporter architecture and mechanism: implications from the crystal structures of BtuCD and BtuF. *FEBS Lett*, **564**, 264-268.

Locher, K.P., Lee, A.T. and Rees, D.C. (2002) The E. coli BtuCD structure: a framework for ABC transporter architecture and mechanism. *Science*, **296**, 1091-1098.

Lomax, T.L., Mehlhorn, R.J. and Briggs, W.R. (1985) Active auxin uptake by zucchini membrane vesicles: quantitation using ESR volume and delta pH determinations. *Proc Natl Acad Sci U S A*, **82**, 6541-6545.

Lomax, T.L., Muday, G.K. and Rubery, P.H. (1995) Auxin transport. In Davies, P.J. (ed.), *Physiology, Biochemistry and Molecular Biology*. Kluwer Academic Publishers, Norwell, MA, pp. 509-530.

Loo, T.W., Bartlett, M.C. and Clarke, D.M. (2003a) Drug binding in human P-glycoprotein causes conformational changes in both nucleotide-binding domains. *J Biol Chem*, **278**, 1575-1578.

Loo, T.W., Bartlett, M.C. and Clarke, D.M. (2003b) Substrate-induced conformational changes in the transmembrane segments of human P-glycoprotein. Direct evidence for the substrate-induced fit mechanism for drug binding. *J Biol Chem*, **278**, 13603-13606.

Loo, T.W., Bartlett, M.C. and Clarke, D.M. (2006a) Transmembrane segment 1 of human P-glycoprotein contributes to the drug-binding pocket. *Biochem J*, **396**, 537-545.

Loo, T.W., Bartlett, M.C. and Clarke, D.M. (2006b) Transmembrane segment 7 of human P-glycoprotein forms part of the drug-binding pocket. *Biochem J*, **399**, 351-359.

Loo, T.W. and Clarke, D.M. (2000) Identification of residues within the drug-binding domain of the human multidrug resistance P-glycoprotein by cysteine-scanning mutagenesis and reaction with dibromobimane. *J Biol Chem*, **275**, 39272-39278.

Loo, T.W. and Clarke, D.M. (2001) Defining the drug-binding site in the human multidrug resistance P-glycoprotein using a methanethiosulfonate analog of verapamil, MTS-verapamil. *J Biol Chem*, **276**, 14972-14979.

Luan, S., Kudla, J., Gruissem, W. and Schreiber, S.L. (1996) Molecular characterization of a FKBP-type immunophilin from higher plants. *Proc Natl Acad Sci U S A*, **93**, 6964-6969.

Luschnig, C. (2001) Auxin transport: why plants like to think BIG. *Curr Biol*, **11**, R831-833.

Luschnig, C., Gaxiola, R.A., Grisafi, P. and Fink, G.R. (1998) EIR1, a root-specific protein involved in auxin transport, is required for gravitropism in Arabidopsis thaliana. *Genes Dev*, **12**, 2175-2187.

M

Ma, J.F., Tamai, K., Yamaji, N., Mitani, N., Konishi, S., Katsuhara, M., Ishiguro, M., Murata, Y. and Yano, M. (2006) A silicon transporter in rice. *Nature*, **440**, 688-691.

Ma, J.F., Yamaji, N., Mitani, N., Tamai, K., Konishi, S., Fujiwara, T., Katsuhara, M. and Yano, M. (2007) An efflux transporter of silicon in rice. *Nature*, **448**, 209-212.

Maestre-Martinez, M., Edlich, F., Jarczowski, F., Weiwad, M., Fischer, G. and Lucke, C. (2006) Solution structure of the FK506-binding domain of human FKBP38. *J Biomol NMR*, **34**, 197-202.

Maher, E.P. and Martindale, S.J. (1980) Mutants of Arabidopsis thaliana with altered responses to auxins and gravity. *Biochem Genet*, **18**, 1041-1053.

Maisch, J. and Nick, P. (2007) Actin is involved in auxin-dependent patterning. *Plant Physiol*, **143**, 1695-1704.

Maki, N. and Dey, S. (2006) Biochemical and pharmacological properties of an allosteric modulator site of the human P-glycoprotein (ABCB1). *Biochem Pharmacol*, **72**, 145-155.

Maki, N., Moitra, K., Ghosh, P. and Dey, S. (2006a) Allosteric modulation bypasses the requirement for ATP hydrolysis in regenerating low affinity transition state conformation of human P-glycoprotein. *J Biol Chem*, **281**, 10769-10777.

Maki, N., Moitra, K., Silver, C., Ghosh, P., Chattopadhyay, A. and Dey, S. (2006b) Modulator-induced interference in functional cross talk between the substrate and the ATP sites of human P-glycoprotein. *Biochemistry*, **45**, 2739-2751.

Mancuso, S. and Marras, A.M. (2006) Adaptative response of Vitis root to anoxia. *Plant Cell Physiol*, **47**, 401-409.

Mancuso, S., Marras, A.M., Magnus, V. and Baluska, F. (2005) Noninvasive and continuous recordings of auxin fluxes in intact root apex with a carbon nanotube-modified and self-referencing microelectrode. *Anal Biochem*, **341**, 344-351.

Marchant, A., Kargul, J., May, S.T., Muller, P., Delbarre, A., Perrot-Rechenmann, C. and Bennett, M.J. (1999) AUX1 regulates root gravitropism in Arabidopsis by facilitating auxin uptake within root apical tissues. *Embo J*, **18**, 2066-2073.

Martin, C., Higgins, C.F. and Callaghan, R. (2001) The vinblastine binding site adopts high- and low-affinity conformations during a transport cycle of P-glycoprotein. *Biochemistry*, **40**, 15733-15742.

Martinoia, E., Klein, M., Geisler, M., Bovet, L., Forestier, C., Kolukisaoglu, U., Muller-Rober, B. and Schulz, B. (2002) Multifunctionality of plant ABC transporters--more than just detoxifiers. *Planta*, **214**, 345-355.

Matsuoka, S., Nicoll, D.A., Reilly, R.F., Hilgemann, D.W. and Philipson, K.D. (1993) Initial localization of regulatory regions of the cardiac sarcolemmal Na(+)-Ca2+ exchanger. *Proc Natl Acad Sci U S A*, **90**, 3870-3874.

Mealey, K.L., Barhoumi, R., Burghardt, R.C., McIntyre, B.S., Sylvester, P.W., Hosick, H.L. and Kochevar, D.T. (1999) Immunosuppressant inhibition of P-glycoprotein function is independent of drug-induced suppression of peptide-prolyl isomerase and calcineurin activity. *Cancer Chemother Pharmacol*, **44**, 152-158.

Meier, P.J. and Stieger, B. (2002) Bile salt transporters. *Annu Rev Physiol*, **64**, 635-661.

Menand, B., Desnos, T., Nussaume, L., Berger, F., Bouchez, D., Meyer, C. and Robaglia, C. (2002) Expression and disruption of the Arabidopsis TOR (target of rapamycin) gene. *Proc Natl Acad Sci U S A*, **99**, 6422-6427.

Mendoza, J.L. and Thomas, P.J. (2007) Building an understanding of cystic fibrosis on the foundation of ABC transporter

structures. *J Bioenerg Biomembr*, **39**, 499-505.

Michalke, W., Gerard, F.K. and Art, E.G. (1992) Phytotropin-binding sites and auxin transport in *Cucurbita pepo*: evidence for two recognition sites. *Planta*, **187**, 254-260.

Michniewicz, M., Zago, M.K., Abas, L., Weijers, D., Schweighofer, A., Meskiene, I., Heisler, M.G., Ohno, C., Zhang, J., Huang, F., Schwab, R., Weigel, D., Meyerowitz, E.M., Luschnig, C., Offringa, R. and Friml, J. (2007) Antagonistic regulation of PIN phosphorylation by PP2A and PINOID directs auxin flux. *Cell*, **130**, 1044-1056.

Miller, G. (2006) Scientific publishing. A scientist's nightmare: software problem leads to five retractions. *Science*, **314**, 1856-1857.

Mitchell, P. and Moyle, J. (1967) Acid-base titration across the membrane system of rat-liver mitochondria. Catalysis by uncouplers. *Biochem. J.*, **104**, 588-600.

Miwa, K., Takano, J., Omori, H., Seki, M., Shinozaki, K. and Fujiwara, T. (2007) Plants tolerant of high boron levels. *Science*, **318**, 1417.

Modok, S., Mellor, H.R. and Callaghan, R. (2006) Modulation of multidrug resistance efflux pump activity to overcome chemoresistance in cancer. *Curr Opin Pharmacol*, **6**, 350-354.

Moody, J.E. and Thomas, P.J. (2005) Nucleotide binding domain interactions during the mechanochemical reaction cycle of ATP-binding cassette transporters. *J Bioenerg Biomembr*, **37**, 475-479.

Moore, I. (2002) Gravitropism: lateral thinking in auxin transport. *Curr Biol*, **12**, R452-454.

Morris, D.A. (2000) Transmembrane auxin carrier systems--dynamic regulators of polar auxin transport. *Plant Growth Regul*, **32**, 161-172.

Morris, D.A. (2004) The tranport of auxins. In Davies, P.J. (ed.), *Plant Hormones: Biosynthesis, Signal Transduction, Action!* Kluwer Academics Publishers, pp. 437-470.

Morris, D.A., Rubery, P.H., Jarman, J. and Sabater, M. (1991) Effects of inhibitors of protein synthesis on transmembrane auxin transport in Cucurbita pepo L. hypocotyl segments. *J. Exp. Bot.*, **42**, 773-783.

Morris, M.E. and Zhang, S. (2006) Flavonoid-drug interactions: effects of flavonoids on ABC transporters. *Life Sci*, **78**, 2116-2130.

Motohashi, K., Koyama, F., Nakanishi, Y., Ueoka-Nakanishi, H. and Hisabori, T. (2003) Chloroplast cyclophilin is a target protein of thioredoxin. Thiol modulation of the peptidyl-prolyl cis-trans isomerase activity. *J Biol Chem*, **278**, 31848-31852.

Mouchel, C.F., Osmont, K.S. and Hardtke, C.S. (2006) BRX mediates feedback between brassinosteroid levels and auxin signalling in root growth. *Nature*, **443**, 458-461.

Mravec, J., Bailly, A., Hoyerová, K., Bielach, A., Skůpa, P., Petrášek, J., Gaykova, V., Stierhof, Y.D., Luschnig, C., Benková, E., Zažímalová, E., Geisler, M. and Friml, J. (2008) ER-localized PIN5 auxin transporter mediates cellular auxin homeostasis. *submitted to Science*.

Muday, G.K. (2000) Maintenance of asymmetric cellular localization of an auxin transport protein through interaction with the actin cytoskeleton. *J Plant Growth Regul*, **19**, 385-396.

Muday, G.K. and DeLong, A. (2001) Polar auxin transport: controlling where and how much. *Trends Plant Sci*, **6**, 535-542.

Muday, G.K. and Murphy, A.S. (2002) An emerging model of auxin transport regulation. *Plant Cell*, **14**, 293-299.

Muday, G.K., Peer, W.A. and Murphy, A.S. (2003) Vesicular cycling mechanisms that control auxin transport polarity. *Trends Plant Sci*, **8**, 301-304.

Muller, A., Guan, C., Galweiler, L., Tanzler, P., Huijser, P., Marchant, A., Parry, G., Bennett, M., Wisman, E. and Palme, K. (1998) AtPIN2 defines a locus of Arabidopsis for root gravitropism control. *Embo J*, **17**, 6903-6911.

Multani, D.S., Briggs, S.P., Chamberlin, M.A., Blakeslee, J.J., Murphy, A.S. and Johal, G.S. (2003) Loss of an MDR transporter in compact stalks of maize br2 and sorghum dw3 mutants. *Science*, **302**, 81-84.

Murphy, A., Peer, W.A. and Taiz, L. (2000) Regulation of auxin transport by aminopeptidases and endogenous flavonoids. *Planta*, **211**, 315-324.

Murphy, A.S., Bandyopadhyay, A., Holstein, S.E. and Peer, W.A. (2005) Endocytotic cycling of PM proteins. *Annu Rev Plant Biol*, **56**, 221-251.

Murphy, A.S., Hoogner, K.R., Peer, W.A. and Taiz, L. (2002) Identification, purification, and molecular cloning of N-1-naphthylphthalmic acid-binding plasma membrane-associated aminopeptidases from Arabidopsis. *Plant Physiol*, **128**, 935-950.

N

Nemhauser, J.L., Hong, F. and Chory, J. (2006) Different plant hormones regulate similar processes through largely nonoverlapping transcriptional responses. *Cell*, **126**, 467-475.

Nemhauser, J.L., Mockler, T.C. and Chory, J. (2004) Interdependency of brassinosteroid and auxin signaling in Arabidopsis. *PLoS Biol*, **2**, E258.

Nobel, P. (1991) *Physicochemical and Environmental Plant Physiology*. Academic Press, San Diego, CA, USA.

Noh, B., Bandyopadhyay, A., Peer, W.A., Spalding, E.P. and Murphy, A.S. (2003) Enhanced gravi- and phototropism in plant mdr mutants mislocalizing the auxin efflux protein PIN1. *Nature*, **423**, 999-1002.

Noh, B., Murphy, A.S. and Spalding, E.P. (2001) Multidrug resistance-like genes of Arabidopsis required for auxin transport and auxin-mediated development. *Plant Cell*, **13**, 2441-2454.

Nordstrom, A., Tarkowski, P., Tarkowska, D., Norbaek, R., Astot, C., Dolezal, K. and Sandberg, G. (2004) Auxin regulation of cytokinin biosynthesis in Arabidopsis thaliana: a factor of potential importance for auxin-cytokinin-regulated development. *Proc Natl Acad Sci U S A*, **101**, 8039-8044.

Nuhse, T.S., Stensballe, A., Jensen, O.N. and Peck, S.C. (2004) Phosphoproteomics of the Arabidopsis plasma membrane and a new phosphorylation site database. *Plant Cell*, **16**, 2394-2405.

O

O'Connor, R., Clynes, M., Dowling, P., O'Donovan, N. and O'Driscoll, L. (2007) Drug resistance in cancer - searching for mechanisms, markers and therapeutic agents. *Expert Opin Drug Metab Toxicol*, **3**, 805-817.

O'Mara, M.L. and Tieleman, D.P. (2007) P-glycoprotein models of the apo and ATP-bound states based on homology with Sav1866 and MalK. *FEBS Lett*, **581**, 4217-4222.

Okada, K., Ueda, J., Komaki, M.K., Bell, C.J. and Shimura, Y. (1991) Requirement of the Auxin Polar Transport System in Early Stages of Arabidopsis Floral Bud Formation. *Plant Cell*, **3**, 677-684.

Oldham, M.L., Khare, D., Quiocho, F.A., Davidson, A.L. and Chen, J. (2007) Crystal structure of a catalytic intermediate of the maltose transporter. *Nature*, **450**, 515-521.

Orlowski, S., Martin, S. and Escargueil, A. (2006) P-glycoprotein and 'lipid rafts': some ambiguous mutual relationships (floating on them, building them or meeting them by chance?). *Cell Mol Life Sci*, **63**, 1038-1059.

Oswald, C., Holland, I.B. and Schmitt, L. (2006) The motor domains of ABC-transporters. What can structures tell us? *Naunyn Schmiedebergs Arch Pharmacol*, **372**, 385-399.

Ottenschlager, I., Wolff, P., Wolverton, C., Bhalerao, R.P., Sandberg, G., Ishikawa, H., Evans, M. and Palme, K. (2003) Gravity-regulated differential auxin transport from columella to lateral root cap cells. *Proc Natl Acad Sci U S A*, **100**, 2987-2991.

P

Paciorek, T., Sauer, M., Balla, J., Wisniewska, J. and Friml, J. (2006) Immunocytochemical technique for protein localization in sections of plant tissues. *Nat Protoc*, **1**, 104-107.

Paciorek, T., Zazimalova, E., Ruthardt, N., Petrasek, J., Stierhof, Y.D., Kleine-Vehn, J., Morris, D.A., Emans, N., Jurgens, G., Geldner, N. and Friml, J. (2005) Auxin inhibits endocytosis and promotes its own efflux from cells. *Nature*, **435**, 1251-1256.

Palme, K. and Galweiler, L. (1999) PIN-pointing the molecular basis of auxin transport. *Curr Opin Plant Biol*, **2**, 375-381.

Panopoulou, E., Gillooly, D.J., Wrana, J.L., Zerial, M., Stenmark, H., Murphy, C. and Fotsis, T. (2002) Early endosomal regulation of Smad-dependent signaling in endothelial cells. *J Biol Chem*, **277**, 18046-18052.

Parry, G., Delbarre, A., Marchant, A., Swarup, R., Napier, R., Perrot-Rechenmann, C. and Bennett, M.J. (2001) Novel auxin transport inhibitors phenocopy the auxin influx carrier mutation aux1. *Plant J*, **25**, 399-406.

Parry, G. and Estelle, M. (2006) Auxin receptors: a new role for F-box proteins. *Curr Opin Cell Biol*, **18**, 152-156.

Peer, W.A., Bandyopadhyay, A., Blakeslee, J.J., Makam, S.N., Chen, R.J., Masson, P.H. and Murphy, A.S. (2004) Variation in expression and protein localization of the PIN family of auxin efflux facilitator proteins in flavonoid mutants with altered auxin transport in Arabidopsis thaliana. *Plant Cell*, **16**, 1898-1911.

Peer, W.A., Brown, D.E., Tague, B.W., Muday, G.K., Taiz, L. and Murphy, A.S. (2001) Flavonoid accumulation patterns of transparent testa mutants of arabidopsis. *Plant Physiol*, **126**, 536-548.

Peer, W.A. and Murphy, A.S. (2006) Flavonoids as signal molecules. Targets of flavonoid action. In Springer (ed.), *The Science of Flavonoids*. Grotewold, E., Berlin.

Peer, W.A. and Murphy, A.S. (2007) Flavonoids and auxin transport: modulators or regulators? *Trends Plant Sci*, **12**, 556-563.

Perez-Perez, J.M., Ponce, M.R. and Micol, J.L. (2004) The ULTRACURVATA2 gene of Arabidopsis encodes an FK506-binding protein involved in auxin and brassinosteroid signaling. *Plant Physiol*, **134**, 101-117.

Petrasek, J., Cerna, A., Schwarzerova, K., Elckner, M., Morris, D.A. and Zazimalova, E. (2003) Do phytotropins inhibit auxin efflux by impairing vesicle traffic? *Plant Physiol*, **131**, 254-263.

Petrasek, J., Mravec, J., Bouchard, R., Blakeslee, J.J., Abas, M., Seifertova, D., Wisniewska, J., Tadele, Z., Kubes, M., Covanova, M., Dhonukshe, P., Skupa, P., Benkova, E., Perry, L., Krecek, P., Lee, O.R., Fink, G.R., Geisler, M., Murphy, A.S., Luschnig, C., Zazimalova, E. and Friml, J. (2006) PIN proteins perform a rate-limiting function in cellular auxin efflux. *Science*, **312**, 914-918.

Pickett, F.B., Wilson, A.K. and Estelle, M. (1990) The aux1 Mutation of Arabidopsis Confers Both Auxin and Ethylene Resistance. *Plant Physiol*, **94**, 1462-1466.

Pleban, K., Kopp, S., Csaszar, E., Peer, M., Hrebicek, T., Rizzi, A., Ecker, G.F. and Chiba, P. (2005) P-glycoprotein substrate binding domains are located at the transmembrane domain/transmembrane domain interfaces: a combined photoaffinity labeling-protein homology modeling approach. *Mol Pharmacol*, **67**, 365-374.

Pohl, A., Devaux, P.F. and Herrmann, A. (2005) Function of prokaryotic and eukaryotic ABC proteins in lipid transport. *Biochim Biophys Acta*, **1733**, 29-52.

Polgar, O. and Bates, S.E. (2005) ABC transporters in the balance: is there a role in multidrug resistance? *Biochem Soc Trans*, **33**, 241-245.

Popescu, S.C., Popescu, G.V., Bachan, S., Zhang, Z., Seay, M., Gerstein, M., Snyder, M. and Dinesh-Kumar, S.P. (2007) Differential binding of calmodulin-related proteins to their targets revealed through high-density Arabidopsis protein microarrays. *Proc Natl Acad Sci U S A*, **104**, 4730-4735.

Prusty, R., Grisafi, P. and Fink, G.R. (2004) The plant hormone indoleacetic acid induces invasive growth in Saccharomyces cerevisiae. *Proc Natl Acad Sci U S A*, **101**, 4153-4157.

Q

Queitsch, C., Sangster, T.A. and Lindquist, S. (2002) Hsp90 as a capacitor of phenotypic variation. *Nature*, **417**, 618-624.

Quint, M. and Gray, W.M. (2006) Auxin signaling. *Curr Opin Plant Biol*, **9**, 448-453.

R

Ramaen, O., Sizun, C., Pamlard, O., Jacquet, E. and Lallemand,

J.Y. (2005) Attempts to characterize the NBD heterodimer of MRP1: transient complex formation involves Gly771 of the ABC signature sequence but does not enhance the intrinsic ATPase activity. *Biochem J*, **391**, 481-490.

Rashotte, A.M., Brady, S.R., Reed, R.C., Ante, S.J. and Muday, G.K. (2000) Basipetal auxin transport is required for gravitropism in roots of Arabidopsis. *Plant Physiol*, **122**, 481-490.

Raven, J.A. (1975) Transport of indole acetic acid in plant cells in relation to pH and electrical potential gradients, and its significance for polar IAA transport. *New Phytol.*, **74**, 163-172.

Ravna, A.W., Sylte, I. and Sager, G. (2008) A molecular model of a putative substrate releasing conformation of multidrug resistance protein 5 (MRP5). *Eur J Med Chem*.

Rea, P.A. (2007) Plant ATP-Binding Cassette Transporters. *Annu Rev Plant Biol*, **58**, 347-375.

Reddy, R.K., Kurek, I., Silverstein, A.M., Chinkers, M., Breiman, A. and Krishna, P. (1998) High-molecular-weight FK506-binding proteins are components of heat-shock protein 90 heterocomplexes in wheat germ lysate. *Plant Physiol*, **118**, 1395-1401.

Reinhardt, D., Mandel, T. and Kuhlemeier, C. (2000) Auxin regulates the initiation and radial position of plant lateral organs. *Plant Cell*, **12**, 507-518.

Reinhardt, D., Pesce, E.R., Stieger, P., Mandel, T., Baltensperger, K., Bennett, M., Traas, J., Friml, J. and Kuhlemeier, C. (2003) Regulation of phyllotaxis by polar auxin transport. *Nature*, **426**, 255-260.

Ren, X.Q., Furukawa, T., Yamamoto, M., Aoki, S., Kobayashi, M., Nakagawa, M. and Akiyama, S. (2006) A functional role of intracellular loops of human multidrug resistance protein 1. *J Biochem*, **140**, 313-318.

Rensing, S.A., Lang, D., Zimmer, A.D., Terry, A., Salamov, A., Shapiro, H., Nishiyama, T., Perroud, P.F., Lindquist, E.A., Kamisugi, Y., Tanahashi, T., Sakakibara, K., Fujita, T., Oishi, K., Shin, I.T., Kuroki, Y., Toyoda, A., Suzuki, Y., Hashimoto, S., Yamaguchi, K., Sugano, S., Kohara, Y., Fujiyama, A., Anterola, A., Aoki, S., Ashton, N., Barbazuk, W.B., Barker, E., Bennetzen, J.L., Blankenship, R., Cho, S.H., Dutcher, S.K., Estelle, M., Fawcett, J.A., Gundlach, H., Hanada, K., Heyl, A., Hicks, K.A., Hughes, J., Lohr, M., Mayer, K., Melkozernov, A., Murata, T., Nelson, D.R., Pils, B., Prigge, M., Reiss, B., Renner, T., Rombauts, S., Rushton, P.J., Sanderfoot, A., Schween, G., Shiu, S.H., Stueber, K., Theodoulou, F.L., Tu, H., Van de Peer, Y., Verrier, P.J., Waters, E., Wood, A., Yang, L., Cove, D., Cuming, A.C., Hasebe, M., Lucas, S., Mishler, B.D., Reski, R., Grigoriev, I.V., Quatrano, R.S. and Boore, J.L. (2008) The Physcomitrella genome reveals evolutionary insights into the conquest of land by plants. *Science*, **319**, 64-69.

Reyes, C.L., Ward, A., Yu, J. and Chang, G. (2006) The structures of MsbA: Insight into ABC transporter-mediated multidrug efflux. *FEBS Lett*, **580**, 1042-1048.

Robinson, J.S., Albert, A.C. and Morris, D.A. (1999) Differential effects of brefeldin A and cycloheximide on the activity of auxin carriers in Cucurbita pepo L. *J. Plant Physiol.*, **155**, 678-684.

Romano, P., Gray, J., Horton, P. and Luan, S. (2005) Plant immunophilins: functional versatility beyond protein maturation. *New Phytol*, **166**, 753-769.

Rosado, A., Schapire, A.L., Bressan, R.A., Harfouche, A.L., Hasegawa, P.M., Valpuesta, V. and Botella, M.A. (2006) The Arabidopsis tetratricopeptide repeat-containing protein TTL1 is required for osmotic stress responses and abscisic acid sensitivity. *Plant Physiol*, **142**, 1113-1126.

Rosenberg, M.F., Callaghan, R., Modok, S., Higgins, C.F. and Ford, R.C. (2005) Three-dimensional structure of P-glycoprotein: the transmembrane regions adopt an asymmetric configuration in the nucleotide-bound state. *J Biol Chem*, **280**, 2857-2862.

Rosenberg, M.F., Kamis, A.B., Callaghan, R., Higgins, C.F. and Ford, R.C. (2003) Three-dimensional structures of the mammalian multidrug resistance P-glycoprotein demonstrate major conformational changes in the transmembrane domains upon nucleotide binding. *J Biol Chem*, **278**, 8294-8299.

Rosenberg, M.F., Velarde, G., Ford, R.C., Martin, C., Berridge, G., Kerr, I.D., Callaghan, R., Schmidlin, A., Wooding, C., Linton, K.J. and Higgins, C.F. (2001) Repacking of the transmembrane domains of P-glycoprotein during the transport ATPase cycle. *Embo J*, **20**, 5615-5625.

Routaboul, J.M., Kerhoas, L., Debeaujon, I., Pourcel, L., Caboche, M., Einhorn, J. and Lepiniec, L. (2006) Flavonoid diversity and biosynthesis in seed of Arabidopsis thaliana. *Planta*, **224**, 96-107.

Rubery, P.H. (1990) Phytotropins: receptors and endogenous ligands. *Symp Soc Exp Biol*, **44**, 119-146.

Rubery, P.H. and Sheldrake, A.R. (1973) Effect of pH and surface charge on cell uptake of auxin. *Nat New Biol*, **244**, 285-288.

Rubery, P.H. and Sheldrake, A.R. (1974) Carrier-mediated auxin transport. *Planta*, **188**, 101-121.

Ruzicka, K., Nejedla, E., Murphy, A., Kleine-Vehn, J., Bailly, A., Gaykova, V., Fujita, H., Ito, H., Syono, K., Hejatko, J., Gray, W.M., Martinoia, E., Geisler, M. and Friml, J. (2008) PIS1 exporter for auxinic compounds defines outer polar domain in plants. *Nature*, in preparation.

S

Sabatini, S., Beis, D., Wolkenfelt, H., Murfett, J., Guilfoyle, T., Malamy, J., Benfey, P., Leyser, O., Bechtold, N., Weisbeek, P. and Scheres, B. (1999) An auxin-dependent distal organizer of pattern and polarity in the Arabidopsis root. *Cell*, **99**, 463-472.

Sachs, J. (1865) *Handbuch der Experimentalphysiologie des Pflanzen*.

Sanchez-Fernandez, R., Davies, T.G., Coleman, J.O. and Rea, P.A. (2001a) The Arabidopsis thaliana ABC protein superfamily, a complete inventory. *J Biol Chem*, **276**, 30231-30244.

Sanchez-Fernandez, R., Rea, P.A., Davies, T.G. and Coleman, J.O. (2001b) Do plants have more genes than humans? Yes, when it comes to ABC proteins. *Trends Plant Sci*, **6**, 347-348.

Sangster, T.A. and Queitsch, C. (2005) The HSP90 chaperone

complex, an emerging force in plant development and phenotypic plasticity. *Curr Opin Plant Biol*, **8**, 86-92.

Santelia, D., Vincenzetti, V., Azzarello, E., Bovet, L., Fukao, Y., Duchtig, P., Mancuso, S., Martinoia, E. and Geisler, M. (2005) MDR-like ABC transporter AtPGP4 is involved in auxin-mediated lateral root and root hair development. *FEBS Lett*, **579**, 5399-5406.

Santelia, D., Henrichs, S., Vincenzetti, V., Sauer, M., Bigler, L., Klein, M., Bailly, A., Lee, Y., Friml, J., Geisler, M. and Martinoia, E. (2008) Flavonoids redirect polar auxin fluxes during gravitropic responses. *J. Biol. Chem.*, ms. M7:09655, resubmission.

Santner, A.A. and Watson, J.C. (2006) The WAG1 and WAG2 protein kinases negatively regulate root waving in Arabidopsis. *Plant J*, **45**, 752-764.

Sapay, N., Guermeur, Y. and Deleage, G. (2006) Prediction of amphipathic in-plane membrane anchors in monotopic proteins using a SVM classifier. *BMC Bioinformatics*, **7**, 255.

Sauer, M., Balla, J., Luschnig, C., Wisniewska, J., Reinohl, V., Friml, J. and Benkova, E. (2006a) Canalization of auxin flow by Aux/IAA-ARF-dependent feedback regulation of PIN polarity. *Genes Dev*, **20**, 2902-2911.

Sauer, M., Paciorek, T., Benkova, E. and Friml, J. (2006b) Immunocytochemical techniques for whole-mount in situ protein localization in plants. *Nat Protoc*, **1**, 98-103.

Scarpella, E., Marcos, D., Friml, J. and Berleth, T. (2006) Control of leaf vascular patterning by polar auxin transport. *Genes Dev*, **20**, 1015-1027.

Schapire, A.L., Valpuesta, V. and Botella, M.A. (2006) TPR proteins in plant hormone signaling. *Plant Signaling and Behavior*, **1:5**, 229-230.

Scheidt, H.A., Vogel, A., Eckhoff, A., Koenig, B.W. and Huster, D. (2007) Solid-state NMR characterization of the putative membrane anchor of TWD1 from Arabidopsis thaliana. *Eur Biophys J*, **36**, 393-404.

Scherer, G.F. (2002) Secondary messengers and phospholipase A2 in auxin signal transduction. *Plant Mol Biol*, **49**, 357-372.

Scheres, B. and Xu, J. (2006) Polar auxin transport and patterning: grow with the flow. *Genes Dev*, **20**, 922-926.

Schiene, C. and Fischer, G. (2000) Enzymes that catalyse the restructuring of proteins. *Curr Opin Struct Biol*, **10**, 40-45.

Schlicht, M., Strnad, M., Scanlon, M.J., Mancuso, S., Hochholdinger, F., Palme, K., Volkmann, D., Menzel, D. and Baluska, F. (2006) Auxin Immunolocalization Implicates Vesicular Neurotransmitter-Like Mode of Polar Auxin Transport in Root Apices. *Plant Signal. Behav.*, **1**, 122-133.

Schoonheim, P.J., Veiga, H., Pereira Dda, C., Friso, G., van Wijk, K.J. and de Boer, A.H. (2007) A comprehensive analysis of the 14-3-3 interactome in barley leaves using a complementary proteomics and two-hybrid approach. *Plant Physiol*, **143**, 670-683.

Schwede, T., Kopp, J., Guex, N. and Peitsch, M.C. (2003) SWISS-MODEL: An automated protein homology-modeling server. *Nucleic Acids Res*, **31**, 3381-3385.

Seidel, C., Walz, A., Park, S., Cohen, J.D. and Ludwig-Muller, J. (2006) Indole-3-acetic acid protein conjugates: novel players in auxin homeostasis. *Plant Biol (Stuttg)*, **8**, 340-345.

Shapiguzov, A., Edvardsson, A. and Vener, A.V. (2006) Profound redox sensitivity of peptidyl-prolyl isomerase activity in Arabidopsis thylakoid lumen. *FEBS Lett*, **580**, 3671-3676.

Shapiro, A.B. and Ling, V. (1997a) Extraction of Hoechst 33342 from the cytoplasmic leaflet of the plasma membrane by P-glycoprotein. *Eur J Biochem*, **250**, 122-129.

Shapiro, A.B. and Ling, V. (1997b) Positively cooperative sites for drug transport by P-glycoprotein with distinct drug specificities. *Eur J Biochem*, **250**, 130-137.

Shapiro, A.B. and Ling, V. (1998) Stoichiometry of coupling of rhodamine 123 transport to ATP hydrolysis by P-glycoprotein. *Eur J Biochem*, **254**, 189-193.

Shirane, M. and Nakayama, K.I. (2003) Inherent calcineurin inhibitor FKBP38 targets Bcl-2 to mitochondria and inhibits apoptosis. *Nat Cell Biol*, **5**, 28-37.

Shirley, B.W., Kubasek, W.L., Storz, G., Bruggemann, E., Koornneef, M., Ausubel, F.M. and Goodman, H.M. (1995) Analysis of Arabidopsis mutants deficient in flavonoid biosynthesis. *Plant J*, **8**, 659-671.

Shitan, N., Bazin, I., Dan, K., Obata, K., Kigawa, K., Ueda, K., Sato, F., Forestier, C. and Yazaki, K. (2003) Involvement of CjMDR1, a plant multidrug-resistance-type ATP-binding cassette protein, in alkaloid transport in Coptis japonica. *Proc Natl Acad Sci U S A*, **100**, 751-756.

Siarheyeva, A., Lopez, J.J. and Glaubitz, C. (2006) Localization of multidrug transporter substrates within model membranes. *Biochemistry*, **45**, 6203-6211.

Sidler, M., Hassa, P., Hasan, S., Ringli, C. and Dudler, R. (1998) Involvement of an ABC transporter in a developmental pathway regulating hypocotyl cell elongation in the light. *Plant Cell*, **10**, 1623-1636.

Sinars, C.R., Cheung-Flynn, J., Rimerman, R.A., Scammell, J.G., Smith, D.F. and Clardy, J. (2003) Structure of the large FK506-binding protein FKBP51, an Hsp90-binding protein and a component of steroid receptor complexes. *Proc Natl Acad Sci U S A*, **100**, 868-873.

Sitbon, F., Ostin, A., Sundberg, B., Olsson, O. and Sandberg, G. (1993) Conjugation of Indole-3-Acetic Acid (IAA) in Wild-Type and IAA-Overprodcing Transgenic Tobacco Plants, and Identification of the Main Conjugates by Frit-Fast Atom Bombardment Liquid Chromatography-Mass Spectrometry. *Plant Physiol*, **101**, 313-320.

Smyczynski, C., Roudier, F., Gissot, L., Vaillant, E., Grandjean, O., Morin, H., Masson, T., Bellec, Y., Geelen, D. and Faure, J.D. (2006) The C terminus of the immunophilin PASTICCINO1 is required for plant development and for interaction with a NAC-like transcription factor. *J Biol Chem*, **281**, 25475-25484.

Stamnes, M.A., Shieh, B.H., Chuman, L., Harris, G.L. and Zuker, C.S. (1991) The cyclophilin homolog ninaA is a tissue-specific integral membrane protein required for the proper synthesis of a subset of Drosophila rhodopsins. *Cell*, **65**, 219-227.

Stieger, B., Meier, Y. and Meier, P.J. (2007) The bile salt export pump. *Pflugers Arch*, **453**, 611-620.

Stieger, P.A., Reinhardt, D. and Kuhlemeier, C. (2002) The auxin

influx carrier is essential for correct leaf positioning. *Plant J*, **32**, 509-517.

Sussman, M.R. and Gardner, G. (1980) Solubilization of the Receptor for N-1-Naphthylphthalamic Acid. *Plant Physiol*, **66**, 1074-1078.

Swarup, R. and Bennett, M. (2003) Auxin transport: the fountain of life in plants? *Dev Cell*, **5**, 824-826.

Swarup, R., Friml, J., Marchant, A., Ljung, K., Sandberg, G., Palme, K. and Bennett, M. (2001) Localization of the auxin permease AUX1 suggests two functionally distinct hormone transport pathways operate in the Arabidopsis root apex. *Genes Dev*, **15**, 2648-2653.

Swarup, R., Kargul, J., Marchant, A., Zadik, D., Rahman, A., Mills, R., Yemm, A., May, S., Williams, L., Millner, P., Tsurumi, S., Moore, I., Napier, R., Kerr, I.D. and Bennett, M.J. (2004) Structure-function analysis of the presumptive Arabidopsis auxin permease AUX1. *Plant Cell*, **16**, 3069-3083.

Swarup, R., Marchant, A. and Bennett, M.J. (2000) Auxin transport: providing a sense of direction during plant development. *Biochem Soc Trans*, **28**, 481-485.

Swarup, R., Parry, G., Graham, N., Allen, T. and Bennett, M. (2002) Auxin cross-talk: integration of signalling pathways to control plant development. *Plant Mol Biol*, **49**, 411-426.

T

Taiz, L. and Zeiger, E. (2006a) Auxin: The Growth Hormone. In Sinauer (ed.), *Plant Physiology*.

Taiz, L. and Zeiger, E. (2006b) *Plant Physiology*. Sinauer Associates, Inc.

Takano, J., Miwa, K., Yuan, L., von Wiren, N. and Fujiwara, T. (2005) Endocytosis and degradation of BOR1, a boron transporter of Arabidopsis thaliana, regulated by boron availability. *Proc Natl Acad Sci U S A*, **102**, 12276-12281.

Tan, X., Calderon-Villalobos, L.I., Sharon, M., Zheng, C., Robinson, C.V., Estelle, M. and Zheng, N. (2007) Mechanism of auxin perception by the TIR1 ubiquitin ligase. *Nature*, **446**, 640-645.

Tanaka, H., Dhonukshe, P., Brewer, P.B. and Friml, J. (2006) Spatiotemporal asymmetric auxin distribution: a means to coordinate plant development. *Cell Mol Life Sci*, **63**, 2738-2754.

Taylor, L.P. and Grotewold, E. (2005) Flavonoids as developmental regulators. *Curr Opin Plant Biol*, **8**, 317-323.

Teale, W.D., Paponov, I.A. and Palme, K. (2006) Auxin in action: signalling, transport and the control of plant growth and development. *Nat Rev Mol Cell Biol*, **7**, 847-859.

Terasaka, K., Blakeslee, J.J., Titapiwatanakun, B., Peer, W.A., Bandyopadhyay, A., Makam, S.N., Lee, O.R., Richards, E.L., Murphy, A.S., Sato, F. and Yazaki, K. (2005) PGP4, an ATP binding cassette P-glycoprotein, catalyzes auxin transport in Arabidopsis thaliana roots. *Plant Cell*, **17**, 2922-2939.

Theodoulou, F.L. (2000) Plant ABC transporters. *Biochim Biophys Acta*, **1465**, 79-103.

Thompson, J.D., Gibson, T.J., Plewniak, F., Jeanmougin, F. and Higgins, D.G. (1997) The CLUSTAL_X windows interface: flexible strategies for multiple sequence alignment aided by quality analysis tools. *Nucleic Acids Res*, **25**, 4876-4882.

Timerman, A.P., Wiederrecht, G., Marcy, A. and Fleischer, S. (1995) Characterization of an exchange reaction between soluble FKBP-12 and the FKBP.ryanodine receptor complex. Modulation by FKBP mutants deficient in peptidyl-prolyl isomerase activity. *J Biol Chem*, **270**, 2451-2459.

Tsui, L.C. (1992) The spectrum of cystic fibrosis mutations. *Trends Genet*, **8**, 392-398.

U

Ueda, M., Matsui, K., Ishiguro, S., Sano, R., Wada, T., Paponov, I., Palme, K. and Okada, K. (2004) The HALTED ROOT gene encoding the 26S proteasome subunit RPT2a is essential for the maintenance of Arabidopsis meristems. *Development*, **131**, 2101-2111.

Ulmasov, T., Hagen, G. and Guilfoyle, T.J. (1999) Activation and repression of transcription by auxin-response factors. *Proc Natl Acad Sci U S A*, **96**, 5844-5849.

Utsuno, K., Shikanai, T., Yamada, Y. and Hashimoto, T. (1998) Agr, an Agravitropic locus of Arabidopsis thaliana, encodes a novel membrane-protein family member. *Plant Cell Physiol*, **39**, 1111-1118.

V

Veit, M. and Pauli, G.F. (1999) Major flavonoids from Arabidopsis thaliana leaves. *J Nat Prod*, **62**, 1301-1303.

Verrier, P.J., Bird, D., Burla, B., Dassa, E., Forestier, C., Geisler, M., Klein, M., Kolukisaoglu, U., Lee, Y., Martinoia, E., Murphy, A., Rea, P.A., Samuels, L., Schulz, B., Spalding, E.J., Yazaki, K. and Theodoulou, F.L. (2008) Plant ABC proteins - a unified nomenclature and updated inventory. *Trends Plant Sci*.

Vespa, L., Vachon, G., Berger, F., Perazza, D., Faure, J.D. and Herzog, M. (2004) The immunophilin-interacting protein AtFIP37 from Arabidopsis is essential for plant development and is involved in trichome endoreduplication. *Plant Physiol*, **134**, 1283-1292.

Vieten, A., Sauer, M., Brewer, P.B. and Friml, J. (2007) Molecular and cellular aspects of auxin-transport-mediated development. *Trends Plant Sci*, **12**, 160-168.

Vittorioso, P., Cowling, R., Faure, J.D., Caboche, M. and Bellini, C. (1998) Mutation in the Arabidopsis PASTICCINO1 gene, which encodes a new FK506-binding protein-like protein, has a dramatic effect on plant development. *Mol Cell Biol*, **18**, 3034-3043.

Vucich, V.A. and Gasser, C.S. (1996) Novel structure of a high molecular weight FK506 binding protein from Arabidopsis thaliana. *Mol Gen Genet*, **252**, 510-517.

W

Weber, H., Chetelat, A., Reymond, P. and Farmer, E.E. (2004) Selective and powerful stress gene expression in Arabidopsis in response to malondialdehyde. *Plant J*, **37**, 877-888.

Weiergraber, O.H., Eckhoff, A. and Granzin, J. (2006) Crystal

structure of a plant immunophilin domain involved in regulation of MDR-type ABC transporters. *FEBS Lett*, **580**, 251-255.

Weijers, D., Van Hamburg, J.P., Van Rijn, E., Hooykaas, P.J. and Offringa, R. (2003) Diphtheria toxin-mediated cell ablation reveals interregional communication during Arabidopsis seed development. *Plant Physiol*, **133**, 1882-1892.

Went, F. (1926) On growth-accelerating substances in the coleoptile of Avena sativa. *Proc K Ned Akad Wet*, **30**, 10–19.

Wilkins, M.B. and Martin, M. (1967) Dependence of Basipetal Polar Transport of Auxin upon Aerobic Metabolism. *Plant Physiol*, **42**, 831-839.

Wisniewska, J., Xu, J., Seifertova, D., Brewer, P.B., Ruzicka, K., Blilou, I., Rouquie, D., Benkova, E., Scheres, B. and Friml, J. (2006) Polar PIN localization directs auxin flow in plants. *Science*, **312**, 883.

Woodward, A.W. and Bartel, B. (2005) Auxin: regulation, action, and interaction. *Ann Bot (Lond)*, **95**, 707-735.

Wu, G., Lewis, D.R. and Spalding, E.P. (2007) Mutations in Arabidopsis multidrug resistance-like ABC transporters separate the roles of acropetal and basipetal auxin transport in lateral root development. *Plant Cell*, **19**, 1826-1837.

X

Xu, J., Hofhuis, H., Heidstra, R., Sauer, M., Friml, J. and Scheres, B. (2006) A molecular framework for plant regeneration. *Science*, **311**, 385-388.

Xu, Q., Liang, S., Kudla, J. and Luan, S. (1998) Molecular characterization of a plant FKBP12 that does not mediate action of FK506 and rapamycin. *Plant J*, **15**, 511-519.

Y

Yamamoto, M. and Yamamoto, K.T. (1998) Differential effects of 1-naphthaleneacetic acid, indole-3-acetic acid and 2,4-dichlorophenoxyacetic acid on the gravitropic response of roots in an auxin-resistant mutant of arabidopsis, aux1. *Plant Cell Physiol*, **39**, 660-664.

Yang, T. and Poovaiah, B.W. (2003) Calcium/calmodulin-mediated signal network in plants. *Trends Plant Sci*, **8**, 505-512.

Yang, Y., Hammes, U.Z., Taylor, C.G., Schachtman, D.P. and Nielsen, E. (2006) High-affinity auxin transport by the AUX1 influx carrier protein. *Curr Biol*, **16**, 1123-1127.

Yuan, Y.R., Blecker, S., Martsinkevich, O., Millen, L., Thomas, P.J. and Hunt, J.F. (2001) The crystal structure of the MJ0796 ATP-binding cassette. Implications for the structural consequences of ATP hydrolysis in the active site of an ABC transporter. *J Biol Chem*, **276**, 32313-32321.

Z

Zaitseva, J., Oswald, C., Jumpertz, T., Jenewein, S., Wiedenmann, A., Holland, I.B. and Schmitt, L. (2006) A structural analysis of asymmetry required for catalytic activity of an ABC-ATPase domain dimer. *Embo J*, **25**, 3432-3443.

Zazimalova, E., Krecek, P., Skupa, P., Hoyerova, K. and Petrasek, J. (2007) Polar transport of the plant hormone auxin - the role of PIN-FORMED (PIN) proteins. *Cell Mol Life Sci*, **64**, 1621-1637.

Zhang, S., Yang, X., Coburn, R.A. and Morris, M.E. (2005) Structure activity relationships and quantitative structure activity relationships for the flavonoid-mediated inhibition of breast cancer resistance protein. *Biochem Pharmacol*, **70**, 627-639.

Zhao, Y., Christensen, S.K., Fankhauser, C., Cashman, J.R., Cohen, J.D., Weigel, D. and Chory, J. (2001) A role for flavin monooxygenase-like enzymes in auxin biosynthesis. *Science*, **291**, 306-309.

Zimmermann, P., Hirsch-Hoffmann, M., Hennig, L. and Gruissem, W. (2004) GENEVESTIGATOR. Arabidopsis microarray database and analysis toolbox. *Plant Physiol*, **136**, 2621-2632.

Zolnerciks, J.K., Wooding, C. and Linton, K.J. (2007) Evidence for a Sav1866-like architecture for the human multidrug transporter P-glycoprotein. *Faseb J*, **21**, 3937-3948.

NAME: BAILLY
SURNAME: Aurélien
Date of birth: 31.07.1979
Nationality: French

Laboratory of Molecular Plant Physiology
Institute of Plant Biology
University of Zürich
Zollikerstrasse 107
CH-8008 Zürich SWITZERLAND
+41-0-44 634 82 76
+41-0-78 829 26 29
abailly@botinst.uzh.ch

EDUCATION

2008 **Employed as PhD student at the University of Zurich since 09/04**
Current position at the laboratory of Molecular Plant Physiology, University of Zurich
Doctorate thesis : *Cellular Auxin Transport and its Regulation in Arabidopsis.*
Supervisors : Dr. M. GEISLER and Prof. E. MARTINOIA.

2004 **Master 2nd – Biochemistry, Cellular and Molecular Biology**
Diplôme d'études approfondies – Biochimie, Biologie Cellulaire et Moléculaire. Ecole Doctorale des Sciences de la Vie et de la Santé – Université de Bourgogne – France.
Diploma thesis : *Etudes des interactions entre le transporteur ABC AtPGP1 et l'immunophiline TWD1 chez Arabidopsis thaliana : une possible régulation par les flavonoïdes.*
Laboratory of Molecular Plant Physiology - University of Zürich
Supervisors : Dr. M. GEISLER and Prof. E. MARTINOIA.

2003 **Master 1st – Biochemistry, Cellular and Molecular Biology**
Maitrîse de Biochimie – Option Génétique. UFR Sciences de la Vie – Université de Bourgogne – France.
Diploma thesis : *Analyse fonctionnelle des variations de la concentration en calcium libre dans le cytoplasme des cellules de tabac en réponse au monoxyde d'azote (NO).*
UMR1088 INRA-CNRS-Université de Bourgogne – Plante-microbe environnement, biochimie, biologie cellulaire et écologie.
Supervisors : Dr. D. WENDEHENNE, Dr. O. LAMOTTE and Prof. A. PUGIN.

2002 **Bachelor degree – Biochemistry, Genetics**
Licence de Biochimie – Option Génétique. UFR Sciences de la Vie – Université de Bourgogne – France.

2001 **Bachelor 2nd – Biology, Biochemistry**
DEUG2 Sciences de la Vie – Option Biochimie. UFR Sciences de la Vie – Université de Bourgogne – France.

2000 **Bachelor 1st – General Biology, Geology**
DEUG1 Sciences de la Vie et de la Terre. UFR Sciences de la Vie – Université de Bourgogne – France.

1997 **Baccalauréat (A-levels) Mathematics, Physics, Biology**
Lycée Jeanne d'Arc - France

For having been the firsts to support me during all these years, I want to thank my parents. My sister, my brother and my family have always been of an essential value for me.

I am grateful to Dr. Prof. Alain Pugin and his team, their confidence in me brought me to this work.

At the outset, I would like to express my sincere gratitude to my thesis advisors.

I am very grateful to Dr. Prof. Enrico Martinoia for his trust and his humanity. It was a pleasure to work with him during my PhD.

I want to especially thank Dr. Markus Geisler for his friendship, for his outstanding competence, for having had the chance to collaborate with him, for his daily humor at work, his trust and for his taste in the French *Cuisine* and wine. This last trait reveals the high degree of sophistication of his personality. Meeting him was a milestone in my professional and personal life.

I also thank the honorable members of the jury – Prof. Dr. Enrico Martinoia, Dr. Markus Geisler, Prof. Dr. Ueli Grossniklaus, and Dr. Jean-Denis Faure – for their evaluation of this work.

Many many thanks to Vincent Vincenzetti, our excellent technician and my excellent friend. Without him our lab would have gone *twisted* in few days. It was always a pain when he was away for holidays! Many kisses to Christine for her friendship, her kindness, and her incredible strength in her PhD. Mine appeared to be really easy compared to hers. I am proud to have friends like them.

Many thanks to the *old guard* from the Geisler's Lab. Dr. Rodolphe Bouchard, Dr. Diana Santelia, Dr. Michal Jasinski and Prof. Dr. Katsuhiro Shiratake for their inestimable friendship, their competent help at the work bench and the good time we spent together inside and outside the lab.

My sincere sympathy to the current students of the Geisler Lab. Sina, Valpuri, Simona and Bangjun shared a very good time together. My best wishes for their future work.

I would like to thank all past and present members of the Martinoia Lab for their kindness and their support. Without naming them all: Bo Burla, for his patient sympathy, for the PolarBar software he designed for us, Hanne Grob for her vivid daily humor, Krasimira, Barbara, Magali, Shaun, for his style and friendship, and all present and past members of the laboratory. I will not forget the good moments we spent together.

I am very gateful to Dr. Christian Fankhauser and his team for their time, their expertise and their kindness.

Last, but definitely not least, I express my deepest love and respect to my dear Anne. Her, and our growing family, were all these years the best support and motivation for my work and life in Zürich. When she smiles, I am the happiest man in the whole world, I love her.